Oxford Brookes University
School of Engineering, Computing, and Mathematics
Department of Computing and Communication Technologies

Criticality control of insulin release: a novel alternative for detailed modelling of insulin secretion

Mireya Muñoz-Balbontín

Submitted in part fulfilment of the requirements of the award of
Doctor of Philosophy in Computing and Mathematics
of Oxford Brookes University, March 2020

Abstract

Representation of the dynamic components of the glucose-insulin system has posed a major challenge in the field of physiological modelling for the past six decades. Early stages in development focused on a descriptive approach where mathematical complexity was usually compromised, causing misrepresentation of the system. The use of such models allowed the study of the system under extremely specific circumstances, and although it aided in the development of devices to manage type 1 Diabetes, it allowed little opportunity to study the system under normal circumstances. In the early 1990's, evidence of insulin oscillations in the system motivated a more detailed approach, with the analysis and representation of the molecular interactions involved.

This work presents a novel modelling methodology which aligns with the aforementioned focus. The methodology focuses on representing a network of cells represented by systems which are inherently non-linear. In order to develop it, a review of reaction-diffusion systems was conducted, where four models were chosen as candidates to represent the building blocks for the resulting model. These were chosen due to their biological relevance and capability of generating a wide range of dynamics using a relatively simple formulation. The resulting model is comprised of a set of sixteen coupled oscillators organized into four clusters. It successfully incorporates characteristics that have been observed in the glucose-insulin system, such as non-linear dynamics, coupling, and response to external influences.

In order to tune the system and achieve multiple stable states, a biologically inspired control method (Rate Control of Chaos) was implemented. The overall structure will allow the study of the mechanisms that keep the system from reaching a chaotic state (diabetes), based on the property of self-organized criticality. The results show that the chosen candidate models are capable of representing the desired structure whilst maintaining the desired dynamics; achieved through the variation of system parameters and initial conditions. They are responsive to the controller and are tolerant to modifications in the system such as the increment of the control signal and coupling strength. The behaviour observed differs among the models and was instrumental in assessing biological relevance.

Acknowledgements

I would like to express my deepest gratitude to:

- My supervisors, Dr. Tjeerd olde Scheper and Dr. Arantza Aldea for giving me the freedom to choose this topic, for all their support, and for making such a great team.

- Oxford Brookes University and CONACyT, for awarding the financial support needed to complete this degree.

- My parents and sisters, for your support and motivation, and for believing in me.

- My husband, for your patience and endless support in this journey.

Contents

Chapter 1

Terminology

- Homeostasis: refers to any self-regulating process present in biological systems to maintain stability and adapt to the conditions necessary for survival. Homeostasis is required for life to continue

- Hormone: substance synthesized and released by the human body to regulate processes and maintain homeostasis.

- Glucose: a type of simple sugar. In the human body it is the main source of energy in cell function, making it's regulation one of the most important processes.

- Pancreas: organ of the human body, it is part of the digestive system and specializes in the secretion of enzymes and hormones required for the digestion of food. It is in charge of the controlled secretion of two hormones, insulin and glucagon.

- Insulin: hormone involved in the regulation of glucose. It will be released from the β-cells when glucose levels are high in order to facilitate it's transport across the cellular membrane.

- Glucagon: hormone involved in the regulation of glucose. When blood glucose is low, glucagon will be released by the α-cells in the pancreas in order for the liver to release glucose into the blood

- Pancreatic islets: units in the pancreas which contain the hormone-producing cells. According to [24] there are between 200,000 and 2,000,000 islets in the pancreas, and they are also known as the islets of Langerhans.

- β-cell: most common cell in pancreatic islets. It is in charge of the synthesis and release of insulin.

- α-cell: cell in the islets of Langerhans which produces and releases the hormone glucagon.

- Compartmental model: a model where the transport of a substance (glucose or insulin) from one compartment to another is represented. The compartments can either represent a space (pancreas, liver, brain, etc.), or the amount of a substance in a space (glucose in blood, glucose in the liver, etc.). Compartmental modeling is a special type of physiological modeling, and it is mainly concerned with representing the mechanisms required to maintain correct chemical levels.

- Minimal model: in physiological modeling of the glucose-insulin system, these models focus on describing the key components of the system. They are characterized for not being large-scale and it is desired that the greater number of system dynamics are represented using the minimum number of identifiable parameters. They are also known as coarse models

- Maximal model: in physiological modeling of the glucose-insulin system, these models focus on representing all available knowledge on the system functionality. This focus makes them capable of simulating the system in diabetes and simulating specific scenarios. These are also known as fine-grain models.

- Oral Glucose Tolerance Test: clinical method used to determine whether the body has any difficulties when processing sugars/carbohydrates. It can assist in the diagnosis of diabetes and insulin resistance. In physiological modelling, the data obtained from these tests has been used to fit models and obtain information on the properties of the system.

- Criticality: property of dynamical systems, occurs either when there is a shift from one stable state to another () or when the system finds itself in a state with high fluctuation

and becomes highly sensitive to small shifts in behaviour.

- Reaction-Diffusion system: systems which, under ideal circumstances, achieve chemical equilibrium exhibiting characteristics such as wave-like patterns or damped oscillations. These are also capable of generating Turing patterns, a type of pattern present in nature.

- Hopf Bifurcation: it is the simplest bifurcation in dynamic bifurcation theory, referring to the local birth or death of a periodic solution from an equilibrium when the parameter crosses a critical value.

- Turing Patterns: self-organized patterns, such as stripes, hexagons, or more intricate structures, which arise from the solution of reaction-diffusion equations. These patterns have been observed widely in nature.

Chapter 2

Introduction

The regulation of glucose in the bloodstream by pancreatic islets (clusters of β-cells), is an example of a negative feedback mechanism in the human body. β-cells in the pancreas sense the concentration of glucose in circulating blood levels and release insulin accordingly. When the concentration of glucose falls below 70-110 mg/dl, the counter-regulatory hormone known as glucagon is produced by the α-cells which triggers the release of glucose by the liver. Failure in these mechanisms can eventually lead to the development of diabetes, a disease where the pancreas is incapable of meeting the demand of insulin necessary to adequately control the levels of glucose in the blood.

The earliest discovery documented dates back to the year 1920, when Frederick Banting discovered insulin. This discovery changed the lives of many patients with type 1 diabetes and triggered the research and development of further treatments and technologies to assist with the management of this condition. The research has advanced fast and current Continuous Glucose Monitoring (CGM) technologies significantly increase the quality of life of patients. The motivation behind the development of this work relates to the aspects surrounding the physiological representation of the glucose insulin release system. The development of physiological models of this system started in the 1960's and have assisted in identifying important characteristics. However, when studying the most widely used models of the system it was identified that much

work remains to be done in terms of detailed modelling of insulin-secretion. With this in mind, this research project focused on answering the following question:

Can we simulate the relationship between glucose and insulin secretion at cellular level by developing a dynamical, biologically-inspired phenomenological model?

To answer this question, the most relevant characteristics of the insulin-release phenomenon were used to develop a modelling methodology and apply it to four different base models. This work presents the information pertinent to the development of the project and the results which contributed to achieving the specified objectives. This first chapter introduces the motivation behind the development of the methodology, the objectives of the project, and the structure of this work, which is divided into six chapters and two appendices.

2.1 Motivation

One of the most challenging tasks in modelling the glucose-insulin system is the representation of its dynamic components (non-linearities and disturbances). In physiological models, these properties are commonly reduced by linearising the system, neglecting the disturbances, or by making assumptions. An example of this was the initial trend of modelling the system to represent a normal 70 kg unstressed adult [67]. This in turn affects the overall performance and accuracy of the model. During the background research development stage of this project, it was identified that the limitations are mostly associated with the top-down approach followed in the development of these models. It was common practise to develop models with significantly reduced mathematical complexity to simplify the modelled physical interactions, although the literature mentions how it is difficult to represent physiological systems of this type solely from physical interactions.

The hypothesis postulated in this research states that it is possible to model the insulin release system using a bottom-up approach, where the dynamic components of the system are taken into account. This will be achieved using computational models to include specific properties such as: Turing patterns, travelling-wave phenomena, reaction-diffusion systems, and self - organised criticality. These models and properties have been identified in biological systems and are capable of representing highly complex systems using a straightforward mathematical approach. The construction of this new model uses a bottom-up approach, where the building blocks will be coupled oscillators that represent the dynamics of insulin release in beta cell clusters.

The existing literature on the topic has started to consider the inclusion of non-linear dynamics, and further the understanding of detailed modelling of insulin secretion. The presence of oscillations in the glucose-insulin release system in the pancreas [63] supports the approach of non-linear local dynamic states contributing to a globally stable glucose function. This control of the local non-linear behaviour that is cardinal to control the global system can be modelled using oscillators that exhibit criticality. This is a property of rate controlled chaotic systems allowing near scale-free dynamics. The main consideration for any given non-linear critical model is to represent the system as a network of weakly coupled oscillators arranged in clusters, where the connectivity strength will be varied in order to observe the response of the system in terms of global and local feedback (see [48] and [49]). Further to this, in order to represent a structure similar to the pancreas, the oscillators must be divided into clusters.

Knowing that certain computational models, such as reaction-diffusion systems, are capable are of generating the desired behaviour, motivated the development of the methodology used in this project. These types of models were studied and four of them were selected to evaluate the model structure discussed in this work. The following section lists the characteristics desired for the model and the models used will be discussed in the following chapters (section 3.1).

2.2 Aim and objectives

To answer the research question previously mentioned, the objective of this project was to develop a model which adheres to the following characteristics:

- The dynamical behaviour which has been observed and studied in the pancreas is represented using models which are known for being capable of providing a wide range of dynamics given their parameter values.
- The system is represented as a network of coupled oscillators that exhibit criticality: this structure provides biological relevance and facilitates modelling the control of the non-linear local dynamic states that contribute to a globally stable glucose function.
- The coupling strength of the network acts as local feedback and has an effect on the global stability of the system: this makes up the communication among the cells and the clusters.
- The model integrates aspects that allow the evaluation of real-world conditions such as meal and exercise, this is necessary in order to keep the system robust, and as close to the actual behaviour of a human being.
- The units are recruited in accordance with the surrounding concentration of glucose: this is to take into account the threshold of the cells and clusters, which are not assumed to be the same throughout the pancreas.
- Insulin secretion propagates as a wave function: meaning that the cluster is in communication with its neighbours and alerts them when they are needed, and thus spreads the communication.

This architecture will allow the study of the different states of operation present in the pancreas, according to the sensed concentration of glucose. The construction of this model will introduce the use of the computational models and systems used in this research project and motivate their use in representing other physiological systems more effectively, as well as other

possible applications. The resulting models were evaluated in terms of biological and dynamical relevance. The main considerations used for this was the capability of the model to support the structure with sufficient singularity for each cluster using the parameters of the system. It is important to represent this characteristic as it is known that physiological processes operate in ranges of behaviour depending on the globally-stable state which is observed at a determined point in time.

2.3 Considerations for bibliographical resources

The following criteria was used to identify the appropriate sources for the review:

- Sources on computational models: an appropriate source will include a detailed description of the model and/or property or mention of an additional source where it can be found, the biological system it has been identified in, the way it assists in representing dynamic components, and how it reflects or assists in observing the global state of stability.
- It is also preferred that these sources are as recent as possible in order to validate the originality of the contribution of the research project, and to evaluate the state of the art as accurately as possible.
- IEEExplore was the initial database used. The same methodology was followed, where if the original source did not contain the complete formulation of a model, the references would be used as a starting point to find the actual ones through an on-line search. The main keywords used for this search were: reaction-diffusion model, oscillators, Turing patterns, activator-inhibitor systems.
- Should the main source not include the complete formulation required, the references available assist in the search and lead to additional repositories, i.e. NCBI, PubMed, Springer, or ScienceDirect.

2.4 Structure of this work

This chapter introduced the research project associated with this thesis. The necessary terminology was listed along with the motivation and objectives of the project. The rest of this work is organised in the following chapters:

1. **Chapter 1 - Terminology:** Due to the cross-disciplinary nature of this research, it was necessary to include a chapter which defines the required terminology in order to familiarize the reader with relevant terminology. This terminology is presented in this chapter .

2. **Chapter 3 - Modelling the glucose-insulin system:** This chapter presents the background theory associated with physiological modelling of the glucose-insulin system. It focuses on presenting an overview of some of the most notable milestones since the start of the artificial pancreas project, which started around the 1960's. The chapter begins by introducing the information pertinent to the regulatory system of glucose and the artificial pancreas project, including a description of the early models of insulin release. The chapter then continues to present the literature review conducted during early stages of development of the project. This review focused on studying the physiological models of insulin release which provide key findings on the properties of the system that must be represented in the model. Additionally, studying these models and their formulations aided in identifying certain shortcomings that must be avoided in the development of the model presented in this work. The chapter concludes by providing the information pertinent to oscillations in the glucose-insulin system, which is a key property to be represented in the model.

3. **Chapter 4 - Computational Modelling Background:** This chapter presents the background research and information obtained to design the methodology used to carry out this research project from a computational modelling perspective. The computational models presented in this literature review were studied to determine the appropriate candidates to represent the system in question and the properties desired. The chapter begins

by defining how the review was performed, and which type of models were of interest to define the methodology. The models are then presented and the chapter ends with a brief discussion of the advantages of using these models and how they assist in representing the desired structure.

4. **Chapter 5 - Model Development:** This chapter details the methodology followed to develop the model. It begins by outlining the characteristics to be represented in the model, and expand them to describe how their representation will be achieved. The function of the base models and the stability analysis are presented. Another section is dedicated to introduce the rate control of chaos method (RCC) which is incorporated in the structure of the model. An example using the Lorenz oscillator is shown to demonstrate the capacity of the controller. The last part of the chapter defines the model structure that will be followed for all four candidate models.

5. **Chapter 6 - The Lengyel-Epstein System:** This chapter presents all information pertinent to the development of the model using the Lengyel-Epstein system as a candidate. The formulations are presented along with an introduction to the parameters that will be used to establish the desired behaviour. The control equations for each model are presented as well, specifying where they will be applied on the model. The first section presents the structure of the model, the formulation, and the stability analysis performed. The second section presents the results, and the third and last section presents a discussion of the results.

6. **Chapter 7 - The Brusselator:** This chapter presents all information pertinent to the development of the model using the Brusselator as a candidate. The formulations are presented along with an introduction to the parameters that will be used to establish the desired behaviour. The control equations for each model are presented as well, specifying where they will be applied on the model. The first section presents the structure of the model, the formulation, and the stability analysis performed. The second section presents

the results, and the third and last section presents a discussion of the results.

7. **Chapter 8 - The Gray-Scott System:** This chapter presents all information pertinent to the development of the model using the Gray-Scott system as a candidate. The formulations are presented along with an introduction to the parameters that will be used to establish the desired behaviour. The control equations for each model are presented as well, specifying where they will be applied on the model. The first section presents the structure of the model, the formulation, and the stability analysis performed. The second section presents the results, and the third and last section presents a discussion of the results.

8. **Chapter 9 - The Berry Model:** This chapter presents all information pertinent to the development of the model using the Berry Model as a candidate. The first section presents the structure of the model, the formulation, and the stability analysis performed. The formulations are presented along with an introduction to the parameters that will be used to establish the desired behaviour. The control equations for each model are presented as well, specifying where they will be applied on the model. The second section presents the results, and the third and last section presents a discussion of the results.

9. **Chapter 10 - Discussion:** This chapter discusses the outcomes from the research work, focusing on the performance of the candidate models. The final formulation of the model is presented and discussed in terms of the research and modelling objectives.

10. **Chapter 11 - Conclusion:** This is the final chapter of this work and it presents the results of this research project. The chapter is organized to present the results in relation to the key aspects that contributed to the results obtained. This chapter also presents the possible applications and future work associated with this research project, as well as a final statement of originality of this research project.

11. **Appendix - EuNeurone Scripts:** This appendix includes the EuNeurone scripts used to run the models and obtain the results presented in this work. The appendix is separated into four section where each section corresponds to a model.

Chapter 3

Modelling the Glucose-Insulin System

This chapter identifies and describes the biological background and models necessary for the development of this project. As can be inferred from the previous chapter, the essence of this project is to provide an alternative methodology to represent the phenomenon of Insulin release. Due to the nature of this project it was necessary to explore the background of three main areas, all of which are presented in this work. The first area to consider was the biological background, which defines the operation of the pancreas under normal conditions and the circumstances which can lead to the development of Diabetes. The second area to consider was the background related to physiological modelling of the system, which ranges from the early models used to represent the behaviour of the glucose-insulin system to the most recent ones used to simulate patient behaviour under specific circumstances. The third area considered is the computational modelling background, which is related to the study of models which are capable of generating dynamic behaviour and patterns, and in this case are also biologically relevant. The first two areas are presented in this chapter, and the third is explored in chapter 4. The aim of conducting this review was to identify the main physiological models considered for Continuous Glucose Monitoring (CGM) devices, and extract the key components required to modify the modelling methodology to incorporate the dynamic aspects of the glucose-insulin system. The chapter concludes with a brief mention of one of the main aspect to consider for the modelling methodology, which is oscillations in the glucose - insulin system.

3.1 An introduction to the regulatory system of glucose

Regulation of glucose in the pancreas is a complex process, whose understanding and study is highly relevant for the management of diabetes. This system is in turn influenced by factors such as meal intake, heart rate, exercise, sleep, and other factors. The system is dependant on the release of two regulatory hormones, insulin and glucagon. The state where a stable concentration of glucose is present, which ranges from 70 - 180 mg/dl, is known as normoglycemia. There are two negative feedback mechanisms that are in charge of maintaining these blood glucose levels. When blood glucose drops below 70 mg/dl of glucose, the body enters the state of hypoglycemia, alpha cells in the pancreas will release glucagon, which triggers the release of glucose from the liver and back into the blood flow, bringing it back to a stable concentration. On the contrary, when blood glucose rises above 180 mg/dl, the body enters hyperglycemia, beta cells in the pancreas will release insulin, which will trigger the uptake of glucose by fatty tissue, thus bringing the level of glucose back to normal. A schematic representation of this process is depicted in figure 3.1.

Disruptions in these mechanisms can lead to the development of the pathological state known as Diabetes, which is typically classified into two types. Diabetes type 1 is known for being autoimmune, where the body attacks the cells in the pancreas and disables them from producing insulin. Diabetes type 2 is the state were the pancreas is capable of producing insulin, but it either does not produce enough to meet its demand, or the tissues become resistant to it. Patients with type 1 diabetes are dependent on exogenous insulin, and can manage their condition with devices such as blood glucose monitors and insulin pumps. Patients with type 2 diabetes manage their condition with lifestyle changes, and medication depending on their specific circumstances.

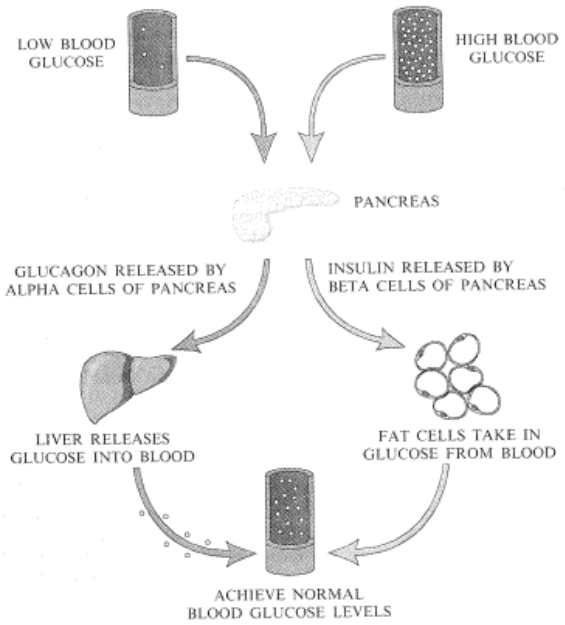

Figure 3.1: Negative feedback mechanisms for blood glucose control [24]

3.2 The Artificial Pancreas Project

The study of the Glucose-Insulin system can be dated back as far as 1855 when physiologist Claude Bernard isolated glycogen. In relation to the control and management of diabetes, the first breakthrough was achieved by Banting and Best in the year 1922, with the the discovery of insulin. This discovery saved the lives of many type 1 diabetic patients, and would represent the second major advancement in understanding the regulatory system of glucose. Counter-regulatory hormones, glucagon and epinephrine, would be discovered not long after, in 1923 and 1924 respectively. It would take approximately 40 years after this for insulin concentration to be measured successfully using radioimmunoassay, and thus start the development of what is known as the Artificial Pancreas Project. Since it's beginning, the aim of the Artificial Pancreas project has been to advance research on the glucose-insulin system in order to develop an automated delivery system for diabetic patients. These devices are comprised of a system which combines a glucose sensor, a control algorithm, and an insulin infusion device. Many milestones would follow in the development of this system, a summary of these can be seen in the time-line presented in figure 3.2. The time-line presents the Minimal model of glucose kinetics, and the UVA/Padova Simulator, the study of these was relevant to the development of this project, therefore they will be detailed further in this chapter (section 3.4).

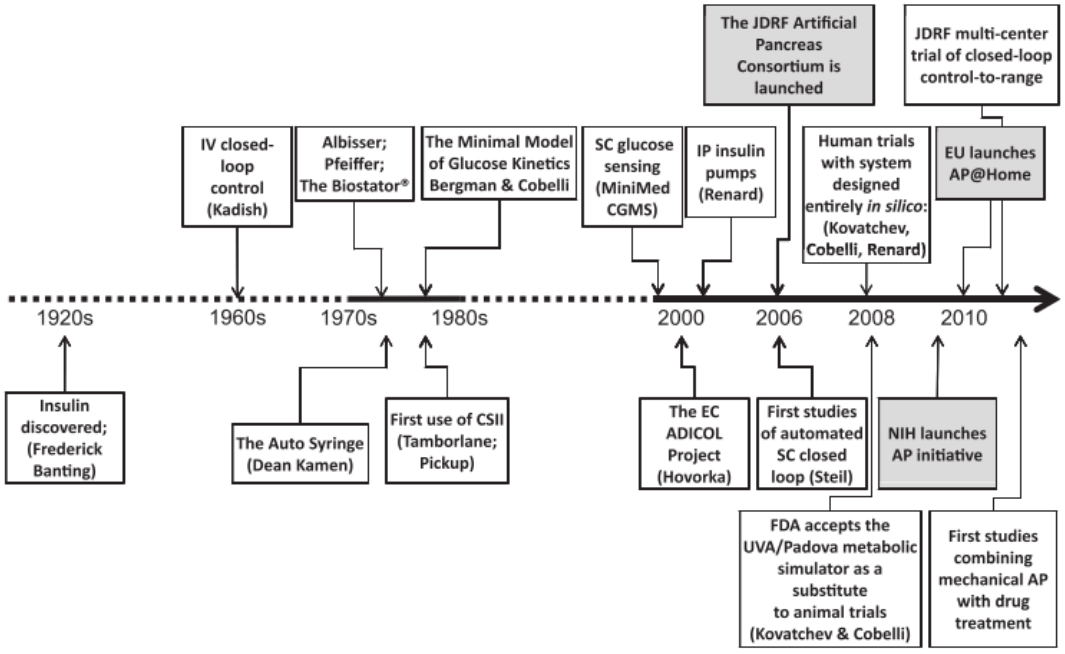

Figure 3.2: Timeline of milestones in the Artificial Pancreas Project [15]

Models, signals, and control algorithms involved in the design of these devices are the three most relevant areas of study in this field. Significant improvements have been made in continuous glucose monitoring technologies; advancements in 1977 produced the first commercial device (Biostator), followed by the Nikkiso inpatient system. After observing the feasibility of subcutaneous insulin delivery, an implantable system was introduced in the late 80's, which was developed further despite its limitations caused by surgical requirements. The use of controllers has also evolved from the use of PD and P-I-D to the use of advanced model predictive controllers. Many of these M-P-C controllers used in the artificial pancreas system are based on the Minimal Model of Glucose Kinetics (detailed in section 3.4.1), and are still in use today. Advancements have also been made in relation to testing and validation, with the acceptance of the UVA/Padova Simulator [16] [17] by the FDA to be used instead of animal trials.

Studying all available physiological models is a complex task due to the amount of work that has been done since it's beginning in the 1960's. Studying the work by Cobelli and Renard [15] assisted in defining the most notorious stages of development to narrow down the most notorious models. This article presents a detailed time-line of the evolution of the artificial

pancreas and technologies associated with it (see figure 3.2). In terms of the models a few key milestones are mentioned, such as the closed-loop control developed by Kadish in the 1960's, the minimal model of glucose kinetics by Bergman and Cobelli around the 1980's, and the development and FDA approval of the UVA/Padova Diabetes simulator, which has substituted animal trials. This article references valuable sources where the aforementioned models are available in complete description.

Cobelli et.al. have published more work on physiological models of the glucose insulin system. An important one considered for this work is the review of models presented in [14]. The focus of this article is to review the state of the art in modelling, signals, and control of diabetes. The section of the article which includes the greatest interest for the purpose of this research project is the section on the models, where minimal and maximal models are discussed. The concept of compartmental structure, and the models used to understand and/or measure glucose metabolism and insulin control are discussed in the minimal models section. The section on maximal models describes the glucose-insulin meal simulation model that assisted in the development of the type-1 diabetes simulator approved by the FDA to substitute pre-clinical animal trials. This article proved useful to extract the most relevant models for the purpose of this study, and their properties; most of the models are detailed and/or referenced. In this chapter, the following sections summarize the main stages of development of physiological modelling of the system in question, where each section presents a representative example.

3.3 Early models of insulin release

The possibility of measuring insulin concentration by radioimmunoassay in the early 1960s prompted the development of the first models of glucose metabolism. The model of ordinary differential equations developed by Bolie in 1961 would mark the start of the 5 decades where scientists have been developing models. Between the 1960's and the 1970's the main focus of

the models was to provide a descriptive approach of the system and the tendency was compartmental modelling. The basic structure accounted for compartments of glucose in the blood, and insulin in the blood, such as the one developed by Ackerman et. al. in 1965.

3.3.1 Ackerman Glucose Metabolism Model

The first known formulation of the glucose metabolism model was given by Bolie in 1960. Given that this formulation is not easily accessible, the formulation by Ackerman is included and was studied for this project. Just like Bolies' model, Ackerman uses a linearised, two-compartment formulation to define the system. Figure 3.3 shows a diagram of the model, and the mass-balance equations for the blood compartments are expressed as follows:

$$V_B \frac{dG}{dt} = -m_1(G - G_{Basal}) - m_2(I - I_{Basal}) + J(t) \tag{3.1}$$

$$V_B \frac{dI}{dt} = -m_3(I - I_{Basal}) + m_4(G - G_{Basal}) \tag{3.2}$$

Where:

- V_B represents the volume of blood compartments. It is not specified in the literature what it's value is or how to obtain it.
- $J(t)$ is the gut glucose input rate.
- m_i are rate constants for the corresponding metabolic sources and sinks depicted in 3.3. The exact values of these coefficients are not reported in the literature but it is mentioned that these were estimated by assuming a functional relationship for $J(t)$ and matched predictions from equations 3.1 and 3.2 with experimental data for the time courses of glucose and insulin during oral glucose tolerance tests [67].

Other authors extended the original formulation postulated by Bolie to include compartments

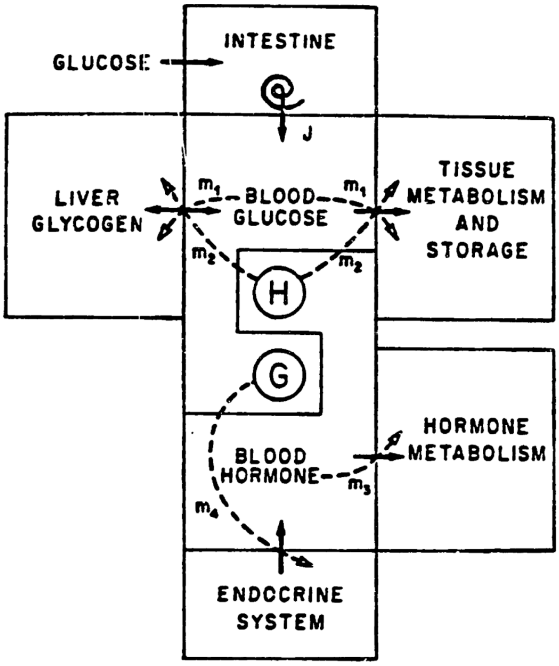

Figure 3.3: Ackerman model. Available in [67]

of liver glycogen and muscle glycogen (Foster et al. 1973, found in [67]), some considered hypothetical compartments for insulin distribution (Silvers et al. 1969, found in [67]), and one of the first to incorporate non-linear representations and multi hormonal control the model developed by Charette et al in 1967.

Due to the antiquity of the aforementioned models, their formulations are not easily accessible but they were found in Sorensen's thesis [67]. This work, published in 1985, was of great importance to evaluate early models of Insulin release given that it is one of the few sources found which both introduces and details the formulation of the models. More importantly, this work details the considerations used for the developments of the model which create misrepresentations in the system. The study of these models is relevant in order to understand how the research of this system has shifted from a descriptive approach to an approach focused on intervention and automated delivery of Insulin. The model developed by Sorensen is a solid example of this. It was developed after the Minimal Model was published, and became useful for the design and assessment of Insulin therapies. The model itself is not detailed in this work as it is contemporary to the Minimal model of glucose, which represented a more simplistic

approach for the time, thus it provided opening for a wider range of applications. Modifications of Sorensen's model have been useful to evaluate effects of exercise, such as the one presented in [11].

It has now been acknowledged that these early models represented the glucose regulatory system in an extremely simplified way by methods such as considering a single input to the system and linearising relevant metabolic rate functions [2]. Additionally, parameter estimation was calculated by either assuming multiple insulin absorption pathways or through interpretation of the literature. An additional finding in Sorensen's thesis [67] revealed how some of the models were developed to represent a normal, 70 kg unstressed adult, which renders bias in the representation. More information on these early models is available in [67].

3.4 Minimal and Maximal Models

Minimal models focus on explaining the key components of the system and measuring essential processes involved in healthy state and diabetes. One of the earliest models documented is the one developed by Bergman and colleagues back in the 70s [15], several extensions of this model have been performed to include disturbances such as meal and exercise. In 1979, the 'minimal model' [6] developed by Bergman, Ider, Bowden, and Cobelli was published and is considered one of the most influential to date. Improvements to this model followed shortly [72], along with further testing and validation by Bergman, Philips and Cobelli [7]. Other examples of minimal models include the compartmental approaches proposed by Insel, et. al. and Cobelli et. al. which attempt to measure and understand glucose metabolism and its regulation by insulin.

3.4.1 Minimal Model

This model is one of the most influential given its reduced complexity and ability to provide reliable solutions in the short-term spectrum. The equations of this model are as follow:

$$\frac{dI}{dt} = -nI(t) + p_4 u_1(t); \qquad I(0) = I_b = \frac{p_4}{n} u_{1b} \tag{3.3}$$

$$\frac{dX}{dt} = -p_2 X(t) + p_3[I(t) - I_b]; \qquad X(0) = 0 \tag{3.4}$$

$$\frac{dG}{dt} = -p_1 G(t) - X(t)G(t) + p_1 G_b + \frac{u_2(t)}{Vol_G}; \qquad G(0) = G_b \tag{3.5}$$

Where:

Parameter	Value	Unit
p_1	0.035	$\frac{1}{min}$
p_2	0.05	$\frac{1}{min}$
p_3	0.000028	$\frac{ml}{\mu U \cdot min^2}$
p_4	0.098	$\frac{1}{ml}$
n	0.142	$\frac{1}{min}$
Vol_G	117.0	dl
G_b	80.0	$\frac{mg}{dl}$

Table 3.1: Bergman Minimal Model Parameters

- I_b and G_b: concentrations of basal insulin and glucose respectively. The initial value for these concentrations were obtained from the study by Bergman et. al. in 1981, found in [7].

- U_{1b}: exogenous insulin infusion rate to maintain I_b. A specific value for it is not provided in the literature, but it is believed this parameter was estimated, given it being an exogenous input.

- n: rate constant for clearance of plasma insulin, see table 3.1 for its value.

- p_3: rate of appearance of insulin in the remote insulin compartment, see table 3.1 for its value.
- p_2 rate of disappearance of insulin from the remote insulin compartment, see table 3.1 for its value.
- $u_2(t)$: dietary absorption or external infusion of glucose, see table 3.1 for its value.
- Vol_G: glucose distribution space, see table 3.1 for its value.
- p_1: removal rate of glucose from plasma space, independent of the influence of insulin, see table 3.1 for its value.

Table 3.1 shows the parameters used for the formulation obtained from Parker and Roy in [60]. These were first derived from the study of human subjects performed by Bergman et. al. in 1981, more details and values pertaining to the study can be found in [7].

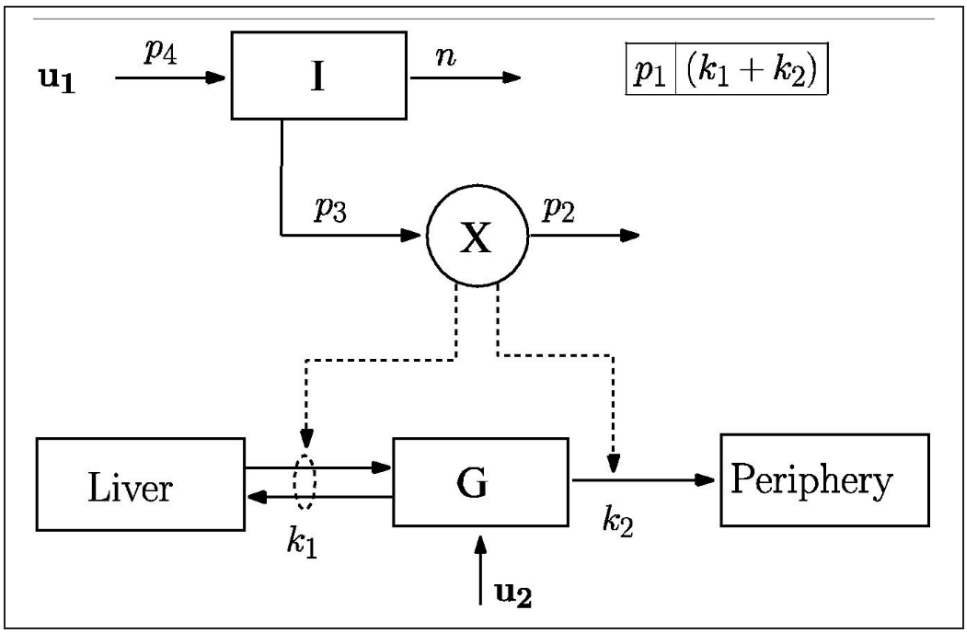

Figure 3.4: Minimal model developed by Bergman et. al. Available in [60]

The usefulness of the minimal model relies on the fact that it provides the minimal number of equations and parameters necessary to provide short-term solutions, with the capability to tune the system to each individual experiment, this meaning that the basic definition of the model makes it inherently simplistic in its ability to generate long-term solutions. The publication of

this model provided inspiration for authors to adapt the model to external disturbances, such as the presence of exercise and the study of the system during this time-period. An example of this is the adaptation proposed by Derouich and Boutayeb in the year 2002, where the influence of exercise in the system was studied to determine it's effect on glucose dynamics [22]. The results of this model might me considered inaccurate as the parameters were derived off of data from healthy subjects.

As mentioned in [15] the Bergman three-compartment minimal model was one of the first to be developed around the 1980's, consisting of 3 differential equations, and 7 parameters. It has since been revised and extended for several situations to refine the insulin-glucose descriptions. The work by Parker and Roy in 2007 [60] presents the contribution of the authors to this advancement, which focuses on capturing the changes in glucose and insulin dynamics caused by exercise. This model is one of the most recent developments which, similar to the model developed by Derouich and Boutayeb, focuses on studying the effects of exercise, with the addition of exploring short and long term effects of the same during the stage of recovery. The development of these last models opened up avenues to continue exploring the influence of other disturbances to the system, exercise and meal intake being some of the most widely explored.

The resulting model is comprised of 10 differential equations and 8 parameters. The results show that the extended model is capable of predicting plasma glucose and insulin concentrations in response to exercise (mild to moderate). The model developed was also successful in capturing fluctuations in glucose dynamics during the relaxation period after exercise. Relevant information on these (and other dynamics) can be found in the article.

Minimal Exercise Model

Shortly after the development of the minimal model, and given its known advantages, many scientists began developing extensions to it. The model developed by Parker and Roy in 2007 is a good example of this. It is defined as follows:

$$\frac{dI}{dt} = -nI(t) + p_4 u_1(t) - I_e(t); \qquad I(0) = I_b = \frac{p_4}{n} u_{1b} \tag{3.6}$$

$$\frac{dX}{dt} = -p_2 X(t) + p_3[I(t) - I_b]; \qquad X(0) = 0 \tag{3.7}$$

$$\frac{dG}{dt} = -p_1[G(t) - G_b] - X(t)G(t) + \frac{W}{Vol_G}[G_{prod}(t) - G_{gly}(t)] - \frac{W}{Vol_G} G_{up}(t) + \frac{u_2(t)}{Vol_G}; \qquad G(0) = G_b \tag{3.8}$$

$$\frac{dG_{prod}}{dt} = a_1 PVO_2^{max}(t) - a_2 G_{prod}(t); \qquad G_{prod}(0) = 0 \tag{3.9}$$

$$\frac{dG_{up}}{dt} = a_3 PVO_2^{max}(t) - a_4 G_{up}(t); \qquad G_{up}(0) = 0 \tag{3.10}$$

$$\frac{dI_e}{dt} = a_5 PVO_2^{max}(t) - a_6 I_e(t); \qquad I_e(0) = 0 \tag{3.11}$$

$$\frac{dG_{gly}}{dt} = \begin{cases} 0 & A(t) < A_{TH} \\ k & A(t) \geq A_{TH} \\ -\frac{G_{gly}(t)}{T_1} & u_3(t) = 0 \end{cases}$$

$$\frac{dA}{dt} = \begin{cases} u_3(t) & u_3(t) > 0 \\ -\frac{A(t)}{0.001} & u_3(t) = 0 \end{cases}$$

This is an adaptation of Bergman's model, the original formulation has been modified to include terms $I_e(t)$ in the first equation, and $\frac{W}{Vol_G}[G_{prod}(t) - G_{gly}(t)] - \frac{W}{Vol_G} G_{up}(t)$ has been added to the third. Aside from this, the system considers the weight of the patient and also includes the addition of 5 differential equations to define the dynamics of the following:

- $G_{prod}(t)$: Rate of hepatic glucose production
- $G_{up}(t)$: Rate of glucose uptake
- $I_e(t)$: Rate of insulin removal from the circulatory system due to exercise-induced physiological changes
- $G_{gly}(t)$: Decline of the glycogenolysis rate during prolonged exercise due to depletion of liver glycogen stores
- $A(t)$: Integrated exercise intensity

In addition to the parameters of the original model developed by Bergman et. al, Parker and Roy used the parameters presented in table 3.2 for their model. Where the value of ${PVO_2}^{max}$ was varied to establish the intensity of exercise, the main motivation behind the development of the model. More information on the development of the model andparameters used are available in [60].

Parameter	Value	Unit
a_1	0.00158	$\frac{mg}{kg \cdot min^2}$
a_2	0.056	$\frac{1}{min}$
a_3	0.00195	$\frac{mg}{kg \cdot min^2}$
a_4	0.0485	$\frac{1}{min}$
a_5	0.00125	$\frac{\mu U}{ml \cdot min}$
a_6	0.075	$\frac{1}{min}$
k	0.0108	$\frac{mg}{kg \cdot min^2}$
T_1	6.0	min

Table 3.2: Minimal Exercise Model Parameters

3.4.2 Glucose Insulin Control System

Maximal models attempt to simulate the glucose insulin system using all available knowledge of functionality, thus allowing the researcher to carry out experiments in particular scenarios [16]. Useful information on the general functions of the system has been collected. One of the

most representative examples is that of the GIM (Glucose Insulin Model) simulation software, which was designed based on the model proposed by Chiara Dalla Man, Robert A. Rizza, and Claudio Cobelli, consisting of 12 differential equations and 35 parameters. This software has been useful to simulate healthy state subjects, type 2 diabetic subjects, and impaired glucose-tolerant subjects in two main scenarios: meal and daily life.

The software facilitates the simulation under normal conditions, and pathological conditions such as type 2 diabetes and closed-loop insulin infusions in type 1 diabetes. The model implemented by this software is a variation of a model described in [47]. The system uses a subcutaneous insulin infusion module to simulate a type 1 diabetic subject. The main equations and parameters for the aforementioned module are presented, including the P-I-D controller which is used for the system, described in [68]. The remainder of the article describes the procedure to run a few case scenarios to illustrate the potential of the software, concluding this could be a useful tool to study the patho-physiology of the condition.

In [17] a detailed description of the model which inspired the development of the simulators mentioned in [16] and [34] is presented. From [14] it is shown that this maximal model was developed on the average data acquired from 204 healthy subjects. The study is comprised of a triple tracer meal protocol which all subjects underwent. The model contains a glucose subsystem described by a two compartment model, an insulin subsystem described by a two compartment model, and four subsystems of unit processes of glucose and insulin: endogenous glucose production, glucose rate of appearance, glucose utilization, and glucose renal excretion. The final model consists of 12 differential equations and 35 parameters (9 of these derived from steady state).

The mode made it possible to simulate a mixed meal scenario in a normal, and a type 2 diabetic subject, as well as a daily life scenario[1] in normal, and impaired glucose-tolerant subject. One of the most important limitations of the model is that it does not consider counter-regulatory

[1]Typical day life: 24 h with breakfast at 8 a.m. (45 g), lunch at 12 p.m. (70 g), and dinner at 8 p.m. (70 g)[17]

hormones (glucagon, epinephrine, growth hormone).

This model is a representative example of the era of maximal models, given it's inclusion of subsystems for the main components involved in glucose and insulin absorption, as can be seen in the block diagram below. This model is the foundation for the GIM (Glucose Insulin Model) simulation software, an FDA approved MATLAB based application used to simulate healthy state, type 2, and impaired glucose-tolerant subjects. It's acceptance by the FDA represented a major milestone in the artificial pancreas project, and provided researchers with the opportunity to generate useful data to substitute clinical trials. The full formulation of the model and its parameters is not included in this thesis given its size. A detailed description of it as well as the parameters used can be found in [16] and [17].

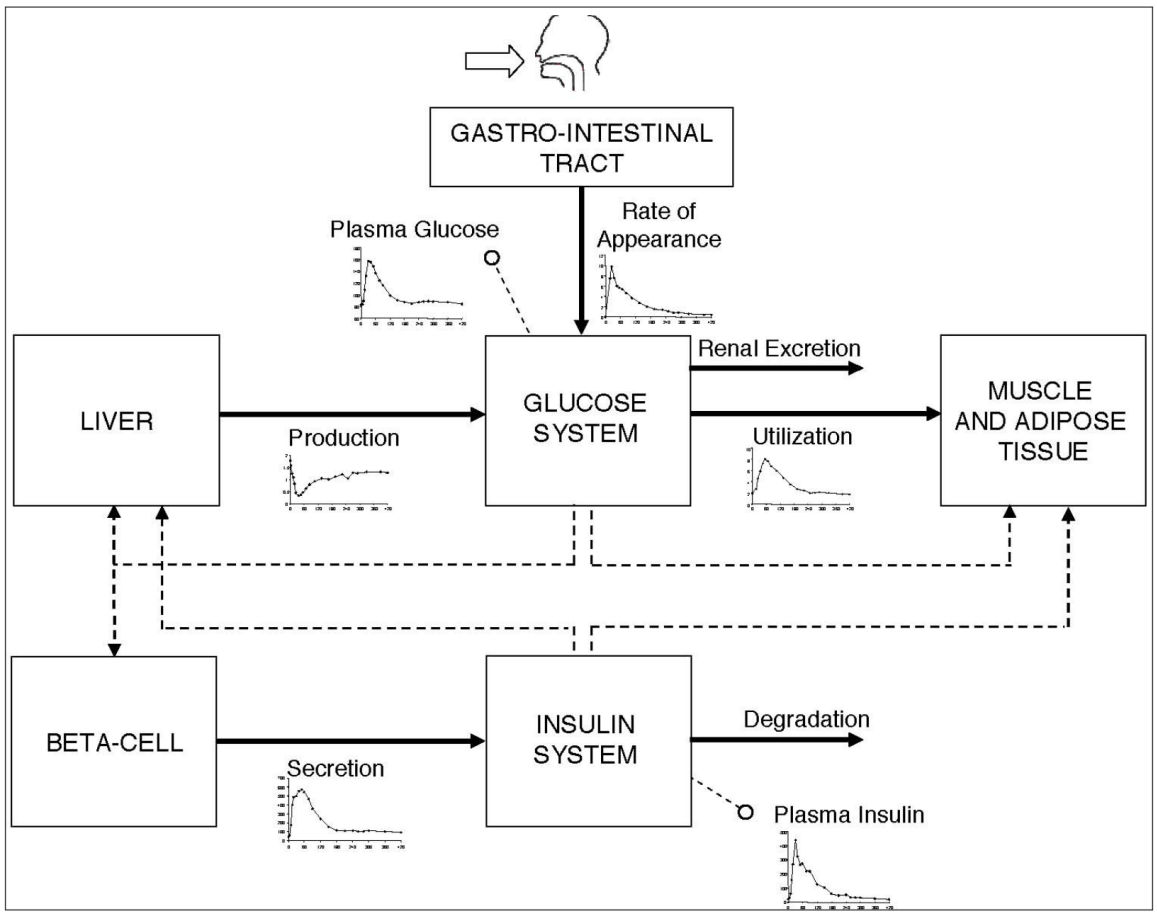

Figure 3.5: Block diagram of the GIM developed by Dalla Man, Rizza, and Cobelli. Available in [17]

Minimal and maximal models were identified as the main physiological models considered for CGM technology development. For the purpose of the proposed research project, further study-

ing of the phenomenological aspects of insulin-release using mathematical properties was conducted. This was decided given a few misrepresentations found in physiological models.

3.5 Oscillations in the Glucose-Insulin system

One of the most important outcomes of this background research was the information pertinent to the presence of oscillations in the system. This was not covered in the scope of the review as oscillating behaviour has not been successfully incorporated in the field of physiological modelling. One of the earliest attempts at representing this oscillatory behaviour was the one developed by Sturis et. al in 1991. The development of this model intended to reproduce the oscillations present in the system and considered the biphasic nature. The experiment concluded with differences between the simulations and the experimental data, and it was stated that the origin of the oscillations was unknown; a full description of the model is available in [2].
Although it has been known that oscillations are present in the system since the 1990s, the study of these took a few years to begin, with observations provided by Nan-Kuang Yao and Liang-Wey Chang in 1997 [76]. In 2002, Gilon et.al continued investigating the oscillating behaviour in β cells, focusing on the close relationship between calcium oscillations and insulin secretion [26]. That same year, Simon and Brandenberger published their findings on the ultradian rhythmicity of insulin oscillations [63]. Both of these papers aided to consolidate the methodology for developing the model in this research project, as they elaborate on the close relation between low level metabolic processes and insulin secretion. Work on the influence of calcium and other metabolites on insulin secretion has continued to be studied and validated since ([53], [71], [9], [39]).

In respect to the characteristics of the oscillations, two different modes have been observed: high frequency, and low frequency. High frequency oscillations are characterized as pulsatile variations of glycaemia and insulinemia, with intervals of about 5-15 min. Low frequency oscillations are known as ultradian oscillations and can be associated with the circadian rhythm, their frequency varies between 50-150 min. These are depicted in figure 3.6

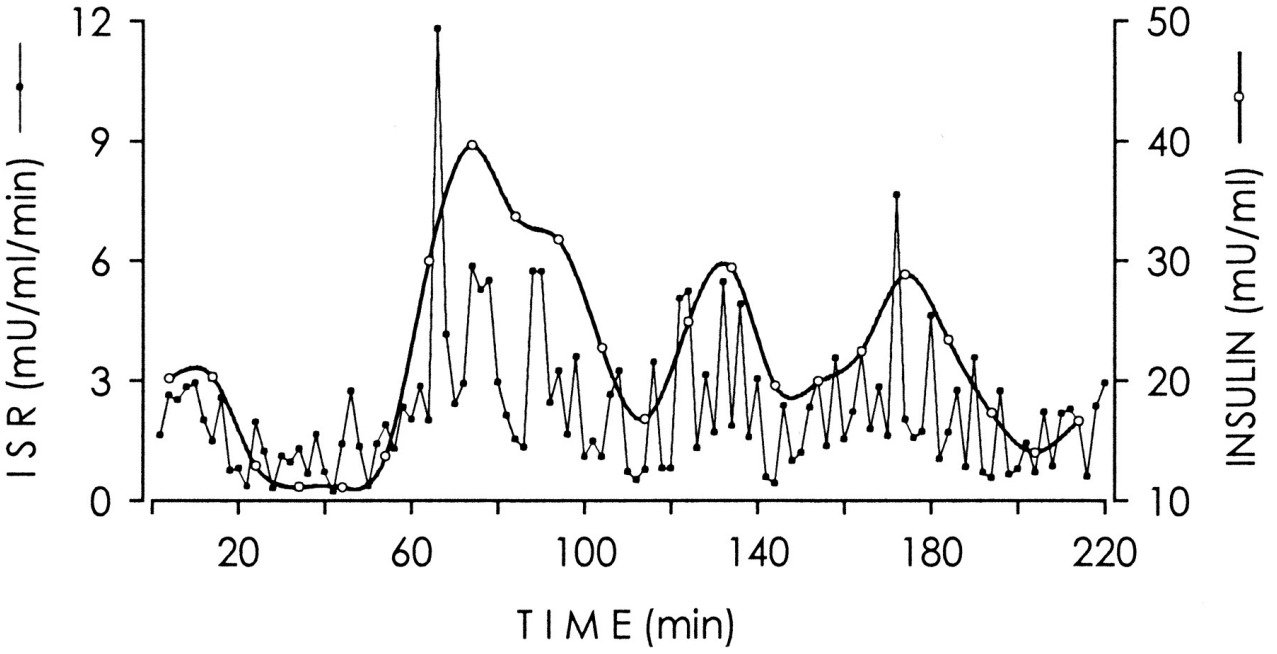

Figure 3.6: Plasma insulin concentration and corresponding ISR profile [63].

Behaviour of the secretory units, or beta cells, was also studied. Cellular modelling is a relatively recent and unexplored area. The work published by Pedersen et. al [54] is an example of a model that attempts to bridge the gap between minimal models, which are important for parameter estimation from in-vivo data, and mechanistic models, which focus on expanding the knowledge of the underlying physiological mechanisms. This model is known as the β cell model; it's development has assisted in observing that the cells react to the circulating level of glucose, and will release a packet of insulin when the cell's threshold is surpassed. This indicates the existence of at least three different states the cell can be in. A cell is active when it is releasing the packet of insulin, it enters a refractory state right after, which can be referred to as a recuperation period, and after this state it enters a state of latency, where it is ready to release insulin but is waiting for the appropriate conditions to be met in order to enter an active state again. This model is one of the few that considers the presence of metabolites such as calcium, although no further work has been done on the effect of the calcium oscillations on the model.

Some work has been done on the influence of calcium oscillations on the glucose-insulin system.

One example is the Morris-Lecar-like model developed by Tsaneva - Atanasova et al in [71], which is used to study the diffusion of calcium. Another example is the work developed by Pu et al [57], which is one of the few models found which uses a structure of coupled oscillators to analyse the system, although the scope of the article does not cover the simulation of an artificial pancreas or a controlled system, it rather focuses on evaluating the response of the structure to analyse the effect of unhealthy β-cells on the pulsatile secretion of insulin. These two models were not considered as candidates for the development of this model given the limitations in their structure. The models are of large scale and developed on experimental data which does not yield flexible parameter values for tuning the system with the controller implemented. In order to incorporate the effects of calcium oscillations into the system, their relationship must be studied using an in-depth approach as these are dependant on low-level enzymatic reactions. This analysis is not covered in the scope of this work.

3.6 Closing Statement

This chapter provided the relevant background research associated with the requirements needed to develop this research project. Physiological models were explored in three separate stages. Early models were presented in section 3.3 to introduce the Artificial Pancreas project and provide an overview of the aims of said project in terms of modelling. A review was conducted where the key milestone models were identified, the outcome of the review presented the main characteristics of the models that need to be represented, and the misrepresentations that must be assessed. Finally, the most recent work done on the representation of insulin oscillations was introduced. This served to gain insight into the current work done and gain more knowledge on the properties that must be represented.

3.6.1 Outcomes

This section will present the key findings from the literature review that led to the development of the methodology, the desired characteristics to represent in the model will also be presented along with the approach that will be taken in order to address them. Modelling of the glucose-insulin system has been around for almost 6 decades and still remains as one of the most complex problems to solve in biomedical engineering. Performing a systematic review of all the models would prove a very difficult task since many of the formulations are not easily accessible given their antiquity, and a lot of others have undergone modification, meaning that their formulations will differ depending on the author. Through revision of the literature and the available reviews, it was possible to identify three main stages in the context of physiological modelling of the system.

1. **Early modelling (1960 1985):** Models developed in this stage followed a compartmental approach and focused on furthering the understanding of the transport of glucose. The earliest formulation found in the literature was Ackerman's model (see section 3.3). During this stage, it was common to model the system to represent a 70 kg unstressed adult male, and to estimate parameters through interpretation of the literature.

2. **Minimal and Maximal models (1979 2008):**

   - Minimal models focus on representing key components of system behaviour, they became useful to analyse the results of oral glucose tolerance tests and to simulate the system after a dose of glucose, both of these applications mean that these models are optimal for analysis in the short-term. Their introduction opened up avenues to consider the influence of external disturbances such as meal and exercise. During this stage it was common to develop these models to represent an insulin-dependent subject by assuming exogenous inputs of insulin.

   - Maximal models focus on representing all available system knowledge, meaning that these would not be useful to represent the low-level mechanisms involved in insulin-

release, but would rather be useful to simulate behaviour and scenarios at higher levels. For their development it was common to use average data obtained from healthy subjects. The formulation of these models is complex given the high number of equations and parameters involved, which limits the possibilities of the model to simulation only.

3. **Oscillating behaviour in the system (1990- present day):** The identification and study of oscillations in the system began in the 1990's, raising a lot of questions on what generates and controls them. It can be concluded that their discovery caused a shift in the field, from the representation of all available knowledge to a focus on modelling at a molecular level. A lot of work has been documented on the influence of calcium oscillations on insulin release, and has been validated by recent studies. More work remains to be done on modelling the system at a low-scale level, which motivated the development of the methodology presented in this chapter.

From the identification of these stages and the study of the models from them, it was found that although these are useful at collecting relevant information on the behaviour of the system, their development contains certain limitations that must be addressed to develop a model capable of representing the oscillating behaviour present in the system. Given the complexity of the system, it can only be considered as highly non-linear and dynamic in mathematical terms. However, a pattern of reduction of this mathematical complexity was observed, where important dynamical components of the system are discarded, and/or linearised. In some of the models insulin is assumed exogenous, which tailors the model to the behaviour of a type 1 diabetic patient. It was also found that the tendency in physiological modelling of this system is to follow a top-down approach, where it is fitted from average data. It is also important to focus on developing a model capable of representing highly complex dynamics, using relatively simple formulation which is not constricted by its parameters.

Several other studies have been conducted in an attempt to understand the insulin release phenomenon in the human pancreas, these include glucose tolerance tests and in-vitro studies.

Minimal models are commonly used to analyse the data obtained from glucose tolerance tests. Although the results obtained prove useful, they tend to misrepresent the actual dynamics of the glucose-insulin system given that they are modelled in steady state. Some misrepresentation is also observed in maximal models, given that several of the parameters used in the system are derived from steady-state conditions. The model developed by Grodzky, Jonkers and Henquin, was able to demonstrate the number of active cells is a sigmoidal function of glucose concentration, and suggest that insulin release is subject to different thresholds [14].

Physiological models were explored in three separate stages. Early models were presented in section 3.4 to introduce the Artificial Pancreas project and provide an overview of the aims of said project in terms of modelling. A review was conducted where the key milestone models were identified, the outcome of the review presented the main characteristics of the models that need to be represented, and the misrepresentations that must be assessed. Finally, the most recent work done on the representation of insulin oscillations was introduced. This served to gain insight into the current work done and gain more knowledge on the properties that must be represented. Table 3.3 provides a summary the models that were studied in this section. These were chosen given that they exemplify progression of the modelling methodology in the field.

Table 3.3: Physiological models

Model	Available	Authors	Details	Description
Ackerman glucose metabolism model	[67]	Ackerman et. al. (1965)	2 differential equations used to represent the mass balances for each compartment.	One of the very first minimal models to follow the original formulation proposed by Bolie in 1960. Linearised two-compartment model of glucose metabolism; one compartment representing glucose and the other representing insulin. The model assumes glucose enters the blood from the gut at a rate J(t) following an oral dose (input to the model). Metabolic processes were assumed to add/remove insulin and glucose in proportion to the compartmental concentration to reduce mathematical complexity.
Bergman minimal model	[60]	Bergman, Philips, Cobelli (1981)	3 differential equations. 7 parameters, estimated using non-linear squares technique.	Three compartment minimal model; used to represent plasma insulin(I), remote insulin(X), and plasma glucose(G) concentrations. Useful to analyse glucose disappearance and insulin sensitivity during an Intra-Venous Glucose Tolerance Test (IVGTT). The model assumes all necessary insulin is exogenous, thereby representing an insulin-dependent diabetic patient.
Minimal exercise model	[60]	Parker & Roy (2007)	10 differential equations. 8 parameters.	Extension of the Bergman minimal model to incorporate the effects of physiological exercise. This is one of the most recent modifications to the original Bergman model which represents changes in glucose and insulin dynamics during exercise.
Glucose-insulin control system	[17]	Dalla Man, Rizza, Cobelli (2007)	12 differential equations; 35 parameters, of which 26 were derived from steady state.	Developed on average data obtained from each of 204 non-diabetic individuals. Contains a glucose subsystem described by a two compartment model, an insulin subsystem described by a two-compartment model, and four unit processes of the glucose and insulin subsystem: endogenous glucose production, glucose rate of appearance, glucose utilization, and insulin secretion. The models were identified from average data, using a forcing function strategy.

Chapter 4

Computational Modelling Background

This chapter presents the literature review conducted in order to develop the methodology for the model from a computational modelling standpoint. The previous chapter presented the key components required to develop the model. The aim of the review presented in this chapter was to identify the computational models and/or formulations and properties that can assist in represent these components. The characteristics to be followed for the development of the model were introduced in chapter 2, section 2.2 of this thesis, where the motivation and objectives of this project were presented.

In the context of physiological modelling, a notable challenge is the representation of the dynamic components of the glucose-insulin system. These components tend to be reduced in some cases by linearising the equations of the model, deriving the parameters in steady-state, and over-fitting the data. The literature indicates that there is still plenty of work to be done on detailed modelling of insulin-release. This justifies the study of computational models capable of assisting the representation of this behaviour, as these will provide the foundation to assess the inclusion of the dynamic components of the system. An outcome of the review presented in this section was the selection of the base models for the project. These models are introduced in this chapter and their complete formulation is available in chapters 5 through 8, where the experimental work and results on these is presented.

Turing patterns are studied and considered for this research project given their identification

and presence in biological systems. For this research project, Turing patterns could be the factor that allows protein producing organs to control release due to refractory periods of a proportion of the cells. The sources studied include the reaction-diffusion models capable of generating the patterns of interest, which is why they were selected. These models are: The Gray-Scott model, the Lengyel-Epstein system, and the Brusselator. Additionally, the Berry model was also considered for the study as it has been proven to work with the controller used for the model. More information on this controller is detailed in chapter 4.

It is known that Turing patterns are present in nature, and Turing mechanisms have been used to investigate the formation of biological patterns. These have been particularly useful in research related to pattern formation in biological patterns such as the scales of fish, the formation of a foetus, and at a more molecular level, pattern formation in cellular slime mould and calcium activity [31]. The scope of this thesis does not cover the definition of Turing patterns in the Glucose-Insulin system however, using models capable of generating said patterns increases the biological relevance of the model given the evidence of their existence in nature.

The study presented in [32] was motivated by the demonstration that local feedback can control the formation of such patterns and their dynamic behaviour. In biological systems, the instances of local feedback that can influence the system include metabolic and biophysical processes which are involved in chemical transmission. In the glucose-insulin system, this biophysical process would be the release of insulin caused by the sensed concentration of glucose, which represents the local feedback in question. A two-variable Lengyel-Epstein model was used to demonstrate how Turing pattern formation is influenced by local feedback. The results show that differently oriented Turing patterns are present when adding local feedback to a given area, which only represents a small part of the system ($\sim$4%). Different types of oriented Turing patters were obtained by varying the intensity of the feedback. Delay times were also explored an found that three different types of dynamic behaviour were exhibited in the system. The results found could be of great significance for biological systems, given the properties they exhibit.

The authors performed an extension to the study [31] using the same considerations; the Lengyel-Epstein system is also used, with modifications. The system is now a two-layer-coupled reaction-diffusion system, and the effects of sub-environment and external influence on Turing pattern generation are studied. Results are shown for the case with two layers in different sub-environments, and one of the layers under external influence. The factors found to have significant influence on the formation of Turing patterns are: coupling strength, external light intensity, coupling medium, and the original stable states of the two layers. It was also found that under strong external influence Turing patterns survive in coupled systems (this does not happen in single-layer systems), which motivated the continuation of the study. The results from these studies motivate the use of the Lengyel-Epstein system as a candidate to develop the model defined in this thesis.

Two main outcomes can be drawn from these studies. The first being how local feedback has a direct effect on the orientation of the Turing pattern in a system, and can change the global or local dynamics in it. For the application proposed in this research the concept of local feedback defines the operational states of the pancreatic islets. It is known that the behaviour will change in accordance to the sensed concentration of glucose, providing at least three possible states the cells/islets can be in: active, in recovery, or on stand-by. The active state refers to the state where the sensed concentration of glucose has surpassed the release threshold which triggers the release of insulin. The in-recovery state refers to the state where the cell is recovering after releasing the insulin packet. The stand-by state, refers to the state where the cell is ready to release insulin but is waiting for the threshold to be met in order to do so.

The second outcome relates to the formation and preservation of Turing patterns with the use of coupling in the system. For the purpose of this research, these findings can assist in understanding and defining the communication mechanisms followed by beta cells which lead to the release of insulin. In the Lengyel-Epstein system, as well as other reaction-diffusion systems, the coupling strength is the element that will act as cellular communication. This can be achieved by adding constraints to the insulin-release system, such as thresholds and external

stimuli (e.g. meal and exercise). By adding these disturbances to the system, it will be possible to observe the effect on the insulin-release pattern, and whether or not it converges to a critical point. The form these disturbances take can also be defined by changes made to the internal structure of the model itself.

When modelling physical, biological, chemical, and engineering phenomena, spatially extended systems tend to arise. Understanding and studying these systems becomes important in order to understand how to control them in order to achieve specific behaviour. In [33] it was demonstrated how beta cells are recruited in accordance with the sensed concentration of glucose, given that they have different threshold sensitivities to it, leading to the states of operation previously mentioned. The study also shows how the behaviour of a single cell can be extrapolated to the behaviour of the islet (cluster) it is associated with. This property can indicate that the propagation of insulin secretion behaves as a wave function.

Knowing that the addition of external perturbations to a dynamical system is usually required to control it, motivates the study of methods and techniques that can assist. Time-Delayed feedback control has proven useful to stabilize unstable periodic orbits in biological systems and most recently, in chemical reactions, used to control spatio-temporal chaos and pattern formation.

The control of such a system has been studied by Y. N. Kyrychko et. al [36] where the Gray-Scott system is used in order to analyse the effects of time delayed feedback control on the dynamics in reaction-diffusion systems. One of the dynamics being the development of spatio-temporal patterns which can be involved in the release control. Single-species, diagonal, and mixed control schemes are studied. The results show that stable states can be reached using single-species, and mixed control schemes. Convergence to stability was achieved regardless of the chaotic nature of the system. The equations and parameters that allow such states are described in [36].

This study further demonstrates the advantages of using reaction-diffusion systems, such the as Lengyel-Epstein and Gray-Scott systems, to describe pattern formation phenomena (including Turing patterns), particularly in systems that involve the interaction of many components. This, and the wide range of spatio-temporal dynamics it supports, make it one of the models of interest for the research project.

Non-linearly coupled systems generate numerous regular patterns that differ to those that are generated in linearly coupled systems. In [37], a model of two non-linearly coupled Turing systems is proposed to further study pattern formation, specifically in layered membrane-like structures. The Brusselator model is exclusively used to examine all the coupling possibilities in layered systems. After reproducing the results obtained with linear coupling in previous studies, non-linear coupling is activated in the system and studied. It is observed that coupling strength plays a role in defining the complexity of the patterns exhibited. When the coupling is strong only the pattern with the largest wavelength survives and thus simplifies the output. Weak non-linear coupling shows more complicated patterns whose formation is studied in function of coupling strength, dramatic changes are found in the topology and overall symmetry of the patterns.

In nature, systems tend to organize in a specific way that becomes essential to the proper functioning of the system as a whole. This organization becomes difficult to represent parting solely from physical interactions, hinting that there must exist a simple mechanism to break the symmetry and generate a spatially stationary pattern. The specific organization of the glucose-insulin release system is no exception to this observation. The low-level mechanisms that contribute to the general stability of the system have to be studied further, and represented in a way that tolerates the external disturbances, non-linearities, and dynamic aspects characteristic to the system. The key to representing the system relies on the focus on the low-level structure and interactions that render global stability.

This precedent motivates the study and representation of self-organized criticality in our system. This is a property which is particular to dynamical systems that are attracted to a critical point; for the past decade it has been identified and studied in biological systems. It has proven useful in defining and understanding neuronal communication, the functionality of protein families, pattern formation in biological systems, among others [45].

The review of historic and current physiological models revealed characteristics of the system that indicate the presence of this property in the system. An example is the prior knowledge that the glucose insulin system operates in ranges, which in turn define the global and local states expressed in the system. By studying this property it will be possible to gather a wider knowledge on the phenomenological aspects of the system and the effect these have over the global state of stability [48].

Reviewing the background literature presented in this chapter indicates that the characteristics of the can be represented computational models and properties. More specifically, the system and its behaviour can be represented when building a structure of coupled reaction diffusion systems (oscillators). This structure allows the representation of the low level mechanisms of insulin release, to observe their influence on stability at a global level. Each coupled element is an oscillator which in turn represents a pancreatic β-cell.

The desired behaviour can be achieved by the implementation of a controller which allows the system to stabilize periodically. Such a controller has been developed by olde Scheper T [48]; it is known as the rate control of chaos controller (RCC) and it has been implemented on the Berry auto-catalytic system. The controller is biologically inspired and is efficient in stabilizing chaotic systems into periodically stable states. A detailed description of this controller and its implementation is presented in the following chapter, where the methodology followed to construct the model is outlined.

4.1 Closing Statement

This chapter provided the relevant background research associated with the requirements needed to develop this research project from a computational modelling standpoint. Models capable of representing the required behaviour were studied and introduced as the base for the development of the resulting model. Given their role in the modelling methodology, their complete formulation and development is presented in chapters 6 through 9.

The main outcome from this chapter was the identification of the type of models which are capable of representing the desired properties of the glucose-insulin system which were identified in chapter 3. Reaction-diffusion systems capable of stabilizing into periodic orbits are considered the best fit to make up the building blocks of the system. This is because these types of models are capable of generating and sustaining Turing patterns under the effects of coupling and the influence of local feedback, two considerations of relevance to the glucose-insulin system. The following chapter outlines the structure of the proposed model in this research work and elaborates on the relevant considerations for it.

Chapter 5

Model development

This chapter focuses on the description of the method chosen to develop the model associated with this project. In order to develop the proposed method, the outcomes of the literature review were taken into account to choose the relevant candidate models. An important outcome of the review to consider was the presence of oscillations in the system, therefore, once the candidate models were selected. This chapter introduces the candidate models and defines how these will be implemented to develop the model. The resulting model is homogeneous, meaning only one candidate model is used to construct it at a time, in order to determine which base model performs best. The methodology followed to perform the stability analysis is also introduced in this chapter,as well as the RCC controller implemented on the system. This is a control method patented by olde Scheper, T. used to limit the non-linear dynamics of complex control problems into stable control domains, this method and its implementation is discussed further in section 5.3 of this chapter.

5.1 Characteristics of the proposed model

Taking into consideration the limitations identified in the literature review, it was decided to study the key properties of the system, and focus on building a bottom-up approach. This

assisted in establishing the characteristics desired for the model, which were introduced in the first chapter of this work in section 2.2. These characteristics will now be revisited and justified in order to provide more insight on their importance to the development of the model.

1. **The dynamic behaviour which has been observed and studied in the pancreas is represented using models which are known for being capable of providing a wide range of dynamics given their parameter values:** This was achieved by using reaction-diffusion systems as the building blocks for the model. The behaviour of these systems is inherently dynamic and can be modified using the system parameters.

2. **The system is represented as a network of coupled oscillators that exhibit criticality: this will allow to model the control of the non-linear local dynamic states that contribute to a globally stable glucose function.**
   This representation is consistent with the bottom-up approach to model the system. It is justified by the recent tendency in physiological modelling of the system where the low level mechanisms that influence insulin release are studied, as shown in section 3.5. To achieve this behaviour in the system, the units are simulated using reaction-diffusion systems under conditions where oscillating behaviour is exhibited.

3. **The coupling strength of the network acts as local feedback and has an effect on the global stability of the system: this makes up the communication among the cells and the clusters.**
   Coupling of the system will serve two main functions, to represent the communication of the cells among themselves, and the communication among clusters. This is justified given the structure of the pancreas, where β-cells are clustered in the islets of Langerhans in the pancreas. The coupling strength was modified to simulate states of strong and weak communication among the units/clusters of the system

4. **The system will need to be evaluated under real-world conditions such as meal and exercise, this is necessary in order to keep the system as accurate as possible, and close to the actual behaviour of a human being.**

This is a necessary characteristic to represent, and it is one which was also taken into consideration throughout the development of minimal and maximal models. This is achieved by modifying parameters of the system throughout the simulation or by the introduction of a pulse or a step signal at a given point in time.

5. **The units are recruited in accordance with the surrounding concentration of glucose: this is to take into account the threshold of the cells and clusters, which are not assumed to be the same throughout the pancreas.**

   This can be represented by controlling the model in a way that it shifts from one stable state to the other using the Rate Control of Chaos (RCC) method. In section 3.5 of this work, the stable states that β cells are governed by were introduced.

6. **Insulin secretion propagates as a wave function: meaning that the cluster is in communication with its neighbours and alerts them when they are needed, and thus spreads the communication.**

   This is another characteristic that can be represented by the incorporation of coupling, and the modification of its strength in the network and the clusters. It can also be achieved by selecting models capable of naturally generating said behaviour, in which case what would need to be done would be to focus on the parameters of the controller to observe their behaviour

Once these characteristics and the approach to represent them were developed, a second review was conducted in order to determine which models/systems would be the most appropriate to represent the desired behaviour. Four different models were considered as candidates to establish the base for the system, these are presented in the following section.

5.2 Base models for comparison

This section presents the models that were considered as the basis to develop the outcome of this research project, these were selected given their capability to generate the desired oscil-

lating behaviour that characterizes the glucose-insulin system. Chapter 4 detailed the studies that were performed on these models in order to explore their behaviour and capacity of generating and sustaining the desired behaviour. Table 5.1 provides a brief description of the four candidates considered for the development of this research work.

Table 5.1: Candidate models

Model	Available	Authors	Details	Description
Two-variable Lengyel-Epstein model	[31] and [32]	Lengyel & Epstein (1991)	2 differential equations, and 3 parameters.	Model for the photosensitive chlorine dioxide-iodine-malonic acid reaction (CDIMA). Has proven useful for investigating the continuous effect of external influence on Turing pattern formation.
Gray-Scott system	[36]	P. Gray & S.K. Scott	2 differential equations. 2 kinetic parameters, and 2 system parameters	Describes auto-catalytic chemical reactions of type: $A + 2B \rightarrow 3B$; $B \rightarrow C$, where the first equation represents an auto-catalytic process. It is possible to observe a wide range of dynamics when the input to the reactor is a continuous uniform flow of species A. The system can have up to three homogeneous steady-states: one trivial, and two non-trivial.
Brusselator autocatalytic system	[37]	Prigogine et. al. (late 1960's)	2 differential equations, including 2 diffusion coefficients, concentrations for the reactor and inhibitor, and 2 rate constants	Reaction-diffusion model developed to prove Turing's theory, and show that Turing patterns which follow the rules of chemical kinetics exist. The model represents the interaction between a reactor and an inhibitor, and is nowadays considered one of the simplest reaction-diffusion systems capable of generating complex spatial patterns [74]. The proposed activator-inhibitor interaction is a well-known principle to explain pattern formation in chemical, ecological, physical, and biological systems.
Berry model	[8]	Berry, H. (2003)	4 differential equations, including 12 parameters	Based on the classical Michaelis-Menten formalism for three out of the four reactions. The model represents an enzymatic system consisting of two cyclically-organized enzyme reactions, which are the generation and degradation of extracellular matrix proteins. This model has been studied with the use of the RCC controller.

5.2.1 Stability analysis

For each one of the candidate models in table 5.1, a stability analysis was conducted on the kinetic equations of each system. Regularly, the aim of said analysis is to find the set of parameters that allow the system to reach stability. Given the dynamical properties of the system, the analysis focused on determining the parameters that would result in periodically stable oscillating behaviour. This was both an important requirement to represent the behaviour of the system in question and an initial experiment on the candidate models to evaluate the behaviour of the system parameters. Chapters 6 through 9 present the system equations, parameters, and initial conditions established to complete the stability analysis for each candidate model. The parameter values used for the stability analysis were taken from the literature. Further analysis of system stability was performed when the final models were constructed, which was necessary given the desired structure of the model. This is considered as the second experiment on the candidate models to validate their capacity to support the structure.
These models are capable of generating a wide range of dynamic behaviours and states, meaning that each author will have a different approach depending on what their aim is. The sources used as reference to establish the parameters and initial conditions are: [46], [61], [3], [37], [74], [36], [56], [8]. These served as reference and were modified accordingly to obtain the desired results in the model when possible. More specific details on how these were modified are available in the following chapters, where the results are presented and discussed.

5.3 Rate Control of Chaos Method

This section introduces the control method that was implemented in the model. The method is relatively novel and was formulated and patented by olde Scheper, T [48] [49]. The development of this control method was inspired by the observation that biological systems rarely exhibit chaotic behaviour under non-pathological circumstances. This observation indicated that said systems are probably governed by multiple states controlled by interactions that are happening

at a very low (molecular) level, and the system will only reach a chaotic state if control of these mechanisms is affected in some way.

To define a way to achieve control of these mechanisms, enzymatic control was studied as (arguably) all chemical reaction steps present in biological systems are subject to enzymatic control of one form or another. The Michaelis-Menten model was employed to formulate this control method as it is known to account for the kinetic properties of many enzymes using a simple approach. The formulation is defined in equation 5.1 and describes the dynamics depicted in figure 5.1, where it can be seen that the maximal velocity is approached in an asymptotic manner.

$$V_0 = V_{max} \frac{[S]}{[S] + K_M} \tag{5.1}$$

Where

- V_0 = Reaction Velocity, or rate curve
- V_{max} = Maximum velocity, or limiting rate
- $[S]$ = Substrate concentration
- K_M = Michaelis constant

This model represents a rate of reaction which depends on the concentration of a substrate in a non-linear manner. Rate saturation is exhibited as the concentration of a substrate increases, which is the foundation for this control method.

An advantage of this method is that it is not dependent on *a priori* knowledge of the presence of unstable periodic orbits in the system. It is applied directly on the growth terms of the system equations and the following is applied:

For

$$\sigma(n) = f e^{\xi q_n + \theta} \tag{5.2}$$

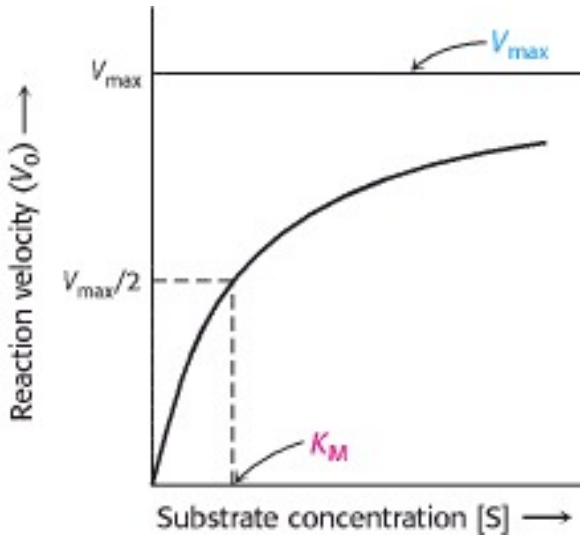

Figure 5.1: Michaelis-Menten Kinetics. Taken from [5]

where

$$q_n = \frac{n}{n + \mu_n} \tag{5.3}$$

The following is true of the implementation of this method:

- The method is used to stabilize the system into periodic orbits by limiting the selected incremental term in proportion to the divergence rate.
- n refers to the system variable on which the controller is applied
- q_n is a quotient used as the argument in an exponential function (σ_n). It determines the appropriate increase or decrease in the rate of growth a shown in 5.2.
- $\sigma(n)$ is the control function, applied as a multiplier on selected incremental terms of the system of equations. An example of this is $\sigma(x_y)$ in equation 5.5, which indicates the control function is being applied on incremental term x, and the y subindex is used to indicate it is being applied on the differential equation of y.
- Parameter ξ is the rate control parameter.It is a variable scalar set to -1 by default and is modified to tune the control strength, it's effect will be seen in the amplitude of the controlled orbits (see [48]).

- μ is a constant obtained from the uncontrolled system dynamics, obtained by observing the phase-space plot of the system and calculating the amplitude of the variable to be controlled. This value establishes the maximum capacity of the variable in the controller.
- θ is an optional bias usually set to 0.
- f is a variable scalar which serves to stabilise different orbits, by default it is set to 1.

5.3.1 The Lorenz attractor

In this section, the Lorenz attractor is used to demonstrate the capabilities of the control method. This system is a good example of a chaotic system with multiple modes where small modifications in the parameters and initial conditions can generate a wide range of dynamics. The rate control of chaos method (RCC) is applied to the system equations as shown in equations 5.4 to 5.6.

$$\frac{dx}{dt} = \gamma(\sigma(y_x)y - \sigma(x_x)x) \tag{5.4}$$

$$\frac{dy}{dt} = -xz + \sigma(x_y)\rho x - y \tag{5.5}$$

$$\frac{dz}{dt} = xy - \beta z \tag{5.6}$$

Where:

$$\sigma(y_x) = f \ \ exp\left\{\frac{\xi_y(y+\theta_y)}{y+\mu_y}\right\} \tag{5.7}$$

$$\sigma(x_x) = f \ \ exp\left\{\frac{\xi_x(x+\theta_x)}{x+\mu_x}\right\} \tag{5.8}$$

$$\sigma(x_y) = f \ \ exp\left\{\frac{\xi_x(x+\theta_x)}{x+\mu_x}\right\} \tag{5.9}$$

Figure 5.2 shows the results of applying RCC to the Lorenz attractor. It can be observed how control is achieved although it is not applied on all the incremental terms of the system equations. The control is initialized at $t = 250$, and the difference is noticeable in all the

variables (see figures 5.3.1, 5.3.1, and 5.3.1), although it is only directly applied on incremental terms which contain only variables x and y individually. This proves the efficacy of the method on the overall system response. Figure 5.3.1 shows the system response for variables x and y before the control is applied on $t < 250$, shown in blue, and after it is applied on $t > 250$ shown in red. It is evident from this that the control method manages to stabilize the chaotic orbits which characterize this system. This is just one example of the application of this control method on the Lorenz attractor, more work on this is available in [48] and [49].

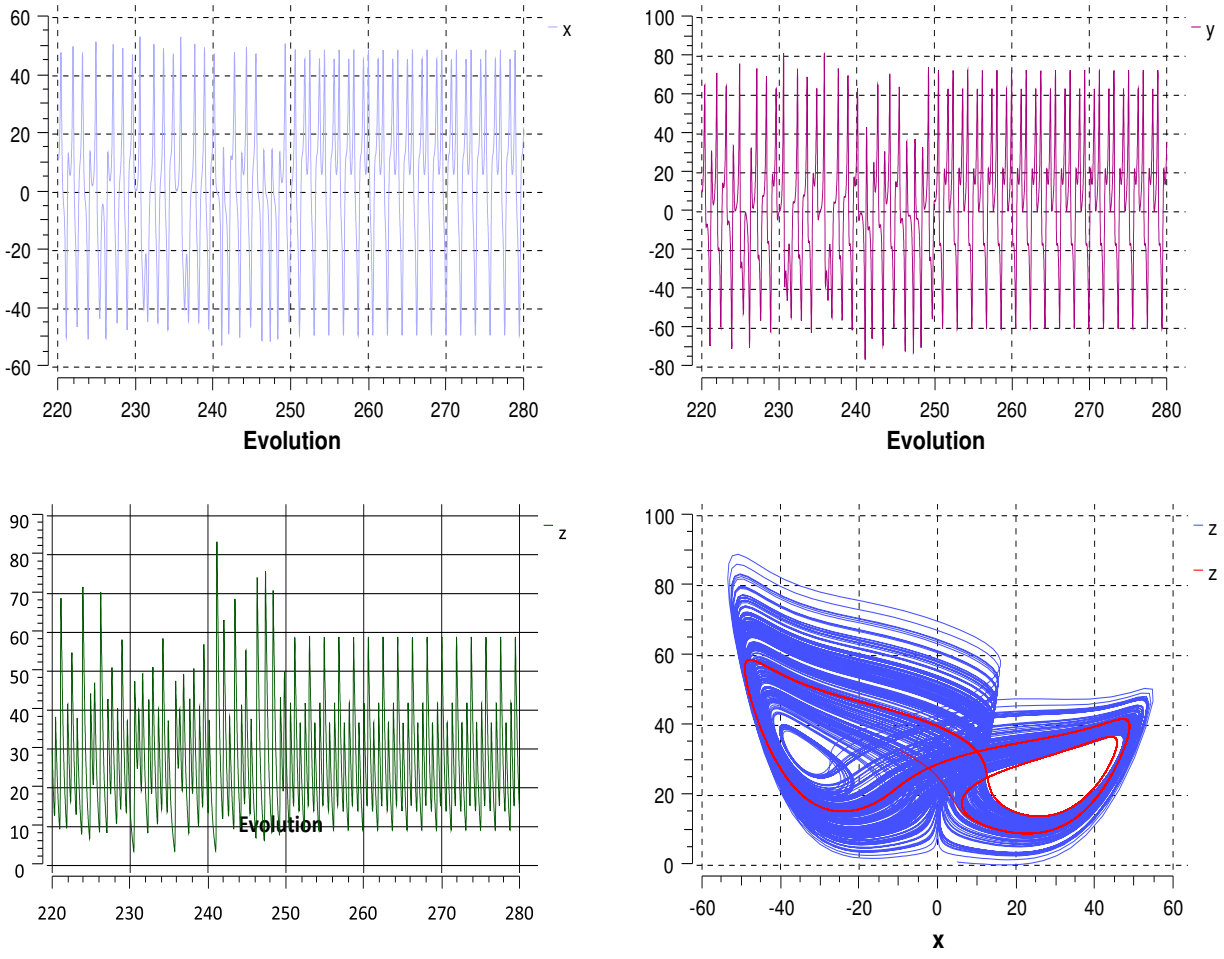

Figure 5.2: Results of Lorenz Model with RCC. The figures labelled 'Evolution' show the evolution of variables x, y and z respectively. The bottom-right figure shows the system response for x and y before applying control (blue) and after (red)

5.4 Model Structure

The final structure consist of 16 oscillators separated into 4 clusters by means of modifying the coupling strength and selected parameters. The main reason for choosing to use 16 oscillator is as this structure has already been used previously by olde Scheper, T with the Berry model [48], [49]. This number of oscillators also allows the possibility of representing 4 clusters, where each cluster is made up of 4 oscillators. Structurally, the oscillators are coupled with their immediate neighbours, meaning oscillator 1 is coupled with oscillators 2 and 16, oscillator 2 is coupled with oscillator 1 and 3 etc. The parameter values and initial conditions of the system were used to separate the system into clusters and add singularity to the system when possible. In order to establish coupling, it was required that each model included a term which facilitates this. It was possible to use a step function to modify the coupling strength throughout the simulation and trigger the shifting of states in the system. Biologically, this shift in state represents the shift in state for the islets to adapt to the surrounding level of glucose. For each experiment, the shape of the function is shown and the increase for each candidate model is as follows.

- **Lengyel-Epstein System:** 0.1 increase for step function.
- **Brusselator:** 0.1 increase for step function.
- **Gray-Scott System:** 0.1 increase for step function.
- **Berry Model:** 0.05 increase for step function.

The control equations will also be involved in evaluating the system response. The specific parameter values used are discussed in the following four chapters as these differ for each candidate model and the development of these was crucial to obtain the results. To select the parameter values, the results from the stability analysis were considered, and the values used in the literature were also taken into account. In some cases, these values were tuned as the structure of the model grew and modifications were implemented, such as the incorporation of the controller and modifications to the coupling strength. For this same reason, the values are reported for each experiment in the results. The experiments focus on finding the right set of

parameters to achieve the representation of the structure as well as the adaptability to modifications in the system. An extract from the script used for the Gray-Scott system is presented up next in order to exemplify how the model is built. The terms No_i refer to the step functions used to modify the coupling strength. The terms sa_i and sb_i refer to the control functions, and the sub-indices indicate the number of oscillators:

$$a'_1 = \delta * (No_1 * (a_{16} - a_1) + No_1 * (a_2 - a_1)) + sa_1 * (1 - a_1)/T_{res}1 - a_1 * b_1 * b_1$$
$$b'_1 = (No_1 * (b_{16} - b_1) + No_1 * (b_2 - b_1)) + sb_1 * (b_0 - b_1)/T_{res}1 + a_1 * b_1 * b_1 - k * b_1$$
$$a'_2 = \delta * (No_1 * (a_1 - a_2) + No_1 * (a_3 - a_2)) + sa_2 * (1 - a_2)/T_{res}1 - a_2 * b_2 * b_2$$
$$b'_2 = (No_1 * (b_1 - b_2) + No_1 * (b_3 - b_2)) + sb_2 * (b_0 - b_2)/T_{res}1 + a_2 * b_2 * b_2 - k * b_2$$
$$\ldots\ldots\ldots\ldots$$
$$a'_{16} = \delta * (No_4 * (a_{15} - a_{16}) + No_4 * (a_1 - a_{16})) + sa_{16} * (1 - a_{16})/T_{res}2 - a_{16} * b_{16} * b_{16}$$
$$b'_{16} = (No_4 * (b_{15} - b_{16}) + No_4 * (b_1 - b_{16})) + sb_{16} * (b_0 - b_{16})/T_{res}2 + a16 * b_{16} * b_{16} - k * b_{16}$$

A complete description of each candidate model, including the simulation parameters, is provided in the appendix.

Chapter 6

The Lengyel-Epstein System

6.1 Model Development

This model represents the chlorine-iodide-malonic acid (CIMA) reaction, which has been studied widely given how its non-linear kinetics give rise to Turing patterns in a non-homogeneous environment [1]. De Kepper [19] was the first to observe this in 1991, and it would represent the first observation of a Turing-type pattern in a chemical reactor. Shortly after, in 1992, Istvan Lengyel and Irving Epstein developed their own model for the CIMA reaction [41]. Their work has since been extensively studied to explore dynamics such as global asymptotical behaviour, presence of Hopf bifurcations, existence of multiple periodic solutions, and other experiments centred on the modification of system parameters. The model is comprised of two differential equations and parameters a, b, and σ as follows:

$$\frac{du}{dt} = a - u - \frac{4uv}{1+u^2} + d_1(u_2 - u_1) \tag{6.1}$$

$$\frac{dv}{dt} = \sigma[b(u - \frac{uv}{1+u^2})] + d_2(v_2 - v_1) \tag{6.2}$$

6.1.1 Stability Analysis

The Lengyel-Epstein system gives us two sets of initial conditions that can achieve it, in both cases the system evolves into stable oscillations of similar morphology (see figure 6.1). For the development of the model it is also desired to modify the parameter values in order to adjust the conditions for every cluster simulated. The works published by Kytta [37] and Ji et al [31] [32] were instrumental in defining the parameter values for the experiments presented in this chapter. The complete formulation of the system which was implemented for the final model also includes a couple parameters more, in addition to the ones included to establish the coupling.

Behaviour	Parameters and Initial Conditions
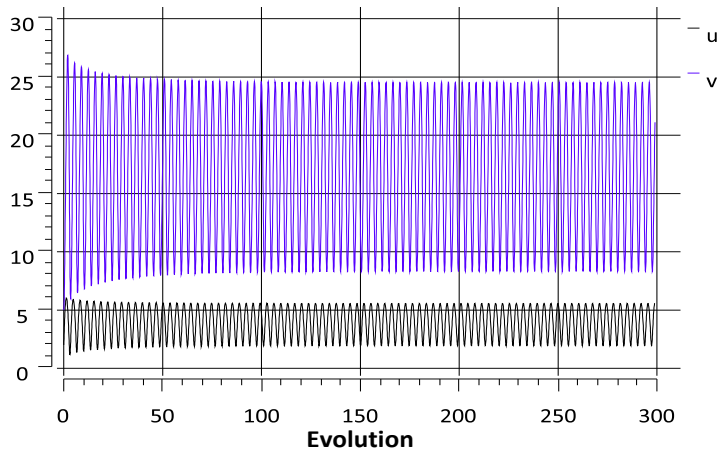	Initial Conditions • u = 2 • v = 5 Parameters • a = 20 • b = 1.3375
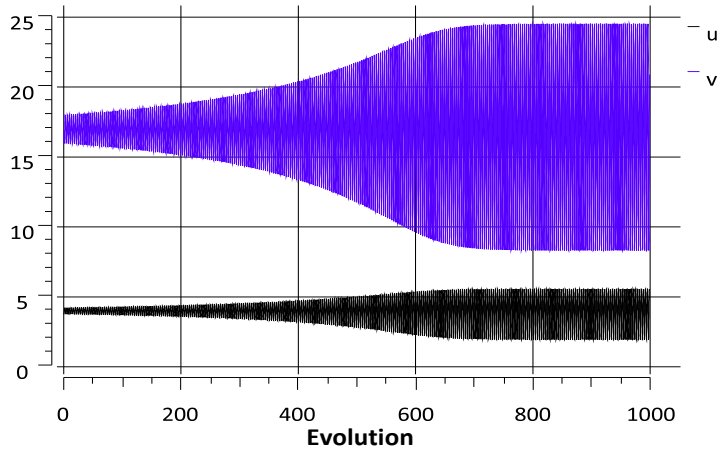	Initial Conditions • u = 3.8 • v = 16.8 Parameters • a = 20 • b = 1.3375

Figure 6.1: Stability Analysis - Lengyel-Epstein System

6.1.2 Model Structure

This system was obtained from [31], this formulation was used in all experiments which focused on modifications to control strength and is defined as follows:

$$\frac{\partial u}{\partial t} = a_i - u_i - \frac{4u_i v_i}{1+u_i^2} - \Phi_i + \nabla^2 u_i + D_i(u_{i+1} - u_i) \tag{6.3}$$

$$\frac{\partial v}{\partial t} = \sigma[b(\sigma_v^{RCC}(u)u_i - \frac{u_i v_i}{1+u_i^2} + \Phi_i) + e_i\nabla^2 v_i] + D_i(v_{i+1} - v_i) \tag{6.4}$$

Where $\nabla^2 = \frac{\partial^2}{\partial x^2}$. In order to differentiate the clusters we have parameters a, b, Φ, D, σ and e. The specific values for these are listed in the following section, these will differ for each experiment. RCC is applied on the incremental term u_i in equation 6.4, denoted as $\sigma^{RCC}(u)$ in order to differentiate it from system parameter σ. Coupling is given by terms $\nabla^2 u_i$ and $D_i(u_{i+1} - u_i)$ in equation 6.3, and terms $e_i\nabla^2 v_i$ and $D_i(v_{i+1} - v_i)$ in equation 6.4, parameters D_i, and e_i will therefore be useful to control the coupling strength.

6.2 Results

6.2.1 Parameter tuning to support model structure

As previously mentioned, this model was developed by Lengyel and Epstein in 1991 [42]. This model was chosen as it has proven useful for investigating the continuous effect of external influences on the formation of Turing pattern. This was useful as external disturbances (meal, exercise, etc.) are some of the important factors to consider when modelling the glucose-insulin system. For the case of this project, it was necessary for the system to maintain oscillating behaviour, which was achieved by the stability analysis in section 6.1.1. The selection of the parameters and initial conditions was based on studies where the system was evaluated under the effects of coupling. This approach is not as common as the exploration of the reaction kinetics, which made it all the more relevant to choose the appropriate sources.

The experiments presented in this section were designed to evaluate the system's capability to represent the structure of sixteen coupled oscillators subdivided into four clusters. Four experiments were performed in order to observe the effects of modifying the system's coupling strength. At this stage, only one of the coupling terms is being considered is being considered for each equation: $D_i(u_{i+1}-u_i)$ and $D_i(v_{i+1}-v_i)$. The terms $\nabla^2 u_i$ and $e_i\nabla^2 v_i$ were implemented alongside the controller and the results are presented in the following section. The parameters for each experiment are presented in tables 6.1 - 6.8. For each experiment, the response of the system is shown in the form of phase space plots and evolution in time, the same is shown for a member of each cluster. Parameters a and b were instrumental in separating the system into clusters, their values remain constant throughout the experiments presented in this section, the same is true for the initial conditions. Taking into account all these considerations, the division of the clusters is as follows:

- Cluster 1:
  - Parameters: a1, b1, D1
  - Oscillators: [u1,v1], [u2,v2], [u3,v3], [u4,v4].
- Cluster 2:
  - Parameters: a2, b2, D2
  - Oscillators: [u5,v5], [u6,v6], [u7,v7], [u8,v8].
- Cluster 3:
  - Parameters: a3, b3, D3
  - Oscillators: [u9,v9], [u10,v10], [u11,v11], [u12,v12].
- Cluster 4:
  - Parameters: a4, b4, D4
  - Oscillators: [u13,v13], [u14,v14], [u15,v15], [u16,v16].

Tables 6.1 and 6.2 show the parameters and initial conditions for the first experiment conducted, and the results are presented in figures 6.2, 6.3, and 6.4. The aim of this experiment was to demonstrate the structure can be supported with unique values of coupling with high variability. Each cluster behaves as expected by depicting four different types of behaviour. The evolution of the variables, shown in figure 6.2 shows how the system achieves periodic stability quickly and at different amplitudes. The global response of the system is given by figures 6.3 and 6.4, where it is seen that the system also stabilizes to a state of stable oscillations. This combination of parameters and initial conditions satisfies the requirements of the structure of the system, and were chosen to continue the development of the system for this candidate.

Three further experiments were conducted in order to observe how the system would behave under conditions where the RCC controller is implemented, and coupling is set at the same value for the system, or turned off altogether. The significance of these experiments was to observe which parameter values and initial conditions react better (or worse), to changes in coupling strength. Performing these experiments was relevant in order to observe how the parameter value would need to be modified further with the implementation of the RCC controller and the use of the second formulation.

Parameter	Value
a1	21
a2	16
a3	20
a4	15
b1	1.3375
b2	1.3475
b3	1.3375
b4	1.3475
D1	0.005
D2	0.05
D3	0.5
D4	0.0005
σ	8

Table 6.1: Lengyel-Epstein Experiment 1 - Parameter Values

Variable	Initial Value
u_1, u_5, u_9, u_{13}	3.3
v_1, v_5, v_9, v_{13}	2
u_2, u_6, u_{10}, u_{14}	3.3
v_2, v_6, v_{10}, v_{14}	3.8
u_3, u_7, u_{11}, u_{15}	10.5
v_3, v_7, v_{11}, v_{15}	5
u_4, u_8, u_{12}, u_{16}	5
v_4, v_8, v_{12}, v_{16}	16.8

Table 6.2: Lengyel-Epstein Experiment 1 - Initial Conditions

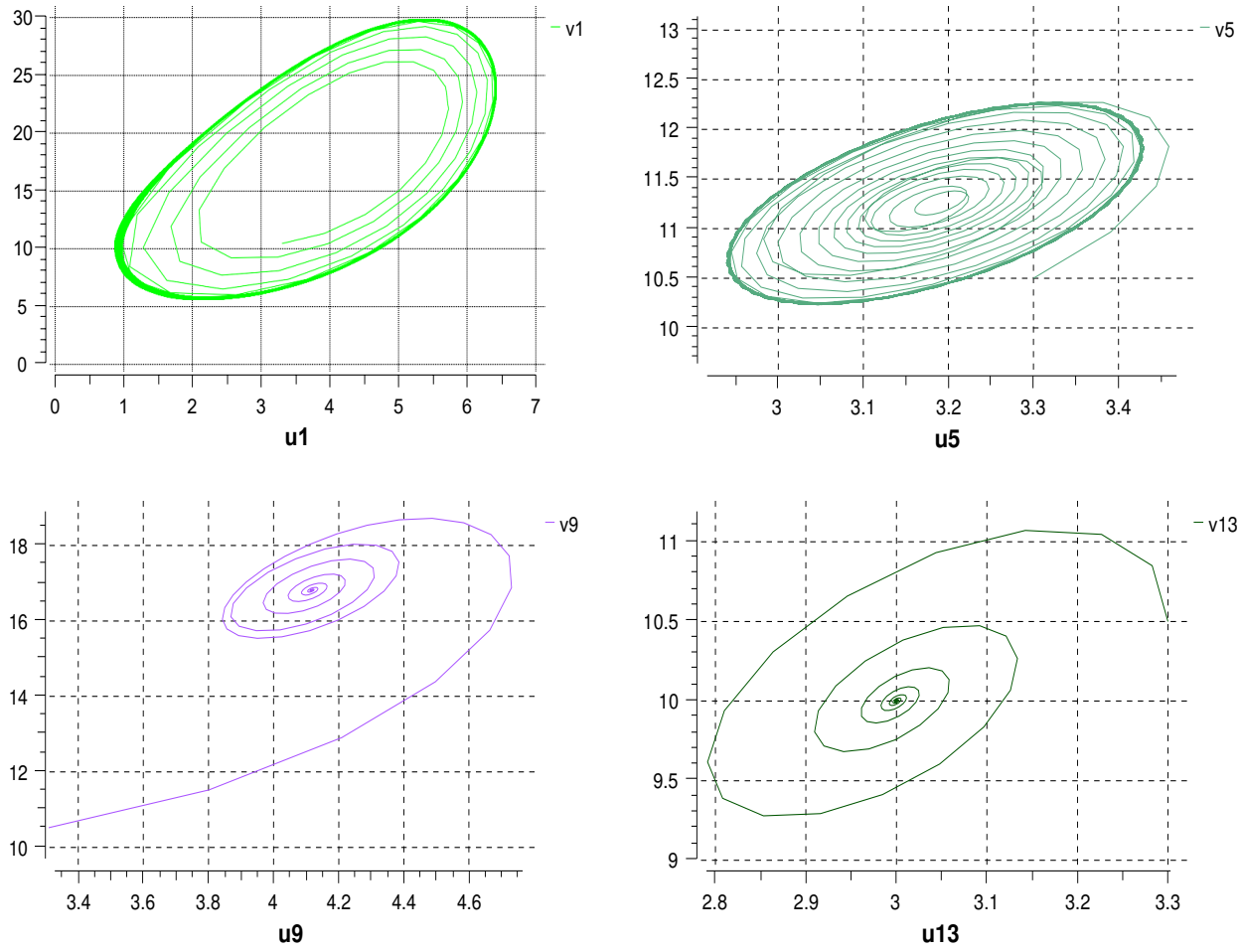

Figure 6.2: Phase space plots for oscillators [u1,v1], [u5,v5], [u9,v9], [u13,v13] of the Lengyel-Epstein system. This experiment considered different coupling strengths and values for each cluster, the RCC controller was not implemented at this stage. The parameters for this experiment are available in tables 6.1 and 6.2. Oscillator [u9,v9] stabilizes periodically at [4.117,16.81] and oscillator [u13,v13] at [3,10].

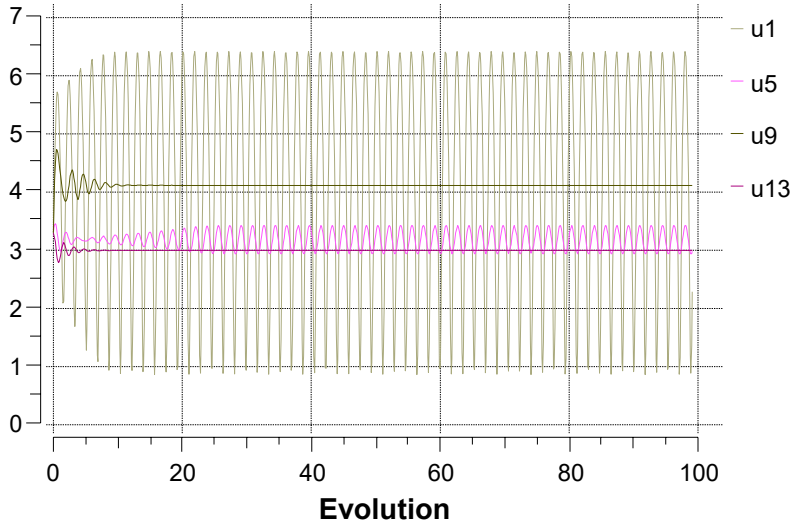

Figure 6.3: Evolution in time for oscillators [u1,v1], [u5,v5], [u9,v9], [u13,v13] of the Lengyel-Epstein system. All oscillators achieve periodic stability at t=20.

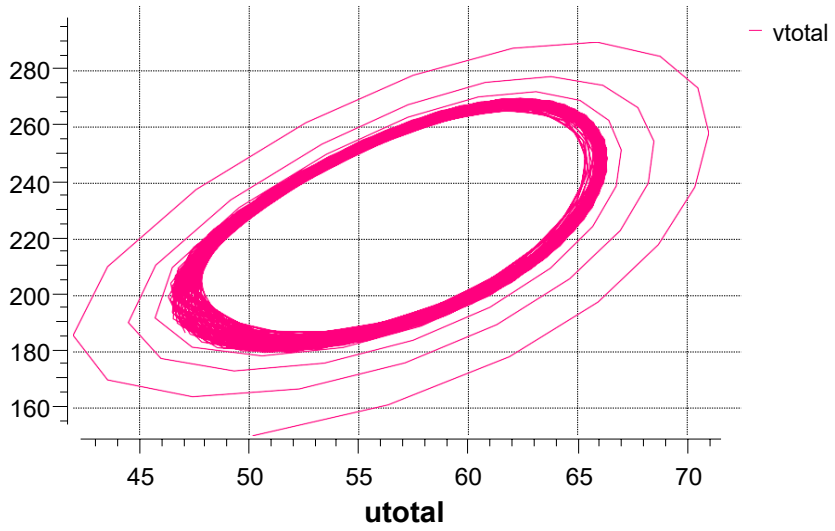

Figure 6.4: Phase space plot for system response of the first experiment

Tables 6.3 and 6.4 show the parameters and initial conditions for the second experiment conducted using the Lengyel-Epstein system. For this experiment, the values remained the same as for the first experiment, and the RCC controller was implemented throughout. The aim of this experiment was to observe the response of the system to the controller before continuing any further experimental work, proving the structure can support the controller. Figures 6.5 and 6.6 show the response of the individual oscillators where slight changes are visible. A change in frequency is evident, and a delay in oscillator [u9,v9] to reach periodic stability can also be observed. The changes are also visible in the total response of the system in figure 6.7, as it takes longer for the system to reach periodic stability, the system stabilizes around a different point in space and the amplitude decreases in both u and v, as well as the total response of the system. These results are expected given the function of the controller. By completing this experiment it is observed that the structure can be supported with high variation of the coupling strength and the implementation of the controller. Subsequent experiments focused on observing the effects of modifying the coupling strength.

Parameter	Value
a1	21
a2	16
a3	20
a4	15
b1	1.3375
b2	1.3475
b3	1.3375
b4	1.3475
D1	0.005
D2	0.05
D3	0.5
D4	0.0005
σ	8
f (RCC)	1.5
ξ(RCC)	1.5
μ (RCC)	6

Table 6.3: Lengyel-Epstein Experiment 2 - Parameters

Variable	Initial Value
u_1, u_5, u_9, u_{13}	3.3
v_1, v_5, v_9, v_{13}	2
u_2, u_6, u_{10}, u_{14}	3.3
v_2, v_6, v_{10}, v_{14}	3.8
u_3, u_7, u_{11}, u_{15}	10.5
v_3, v_7, v_{11}, v_{15}	5
u_4, u_8, u_{12}, u_{16}	5
v_4, v_8, v_{12}, v_{16}	16.8

Table 6.4: Lengyel-Epstein Experiment 2 - Initial Conditions

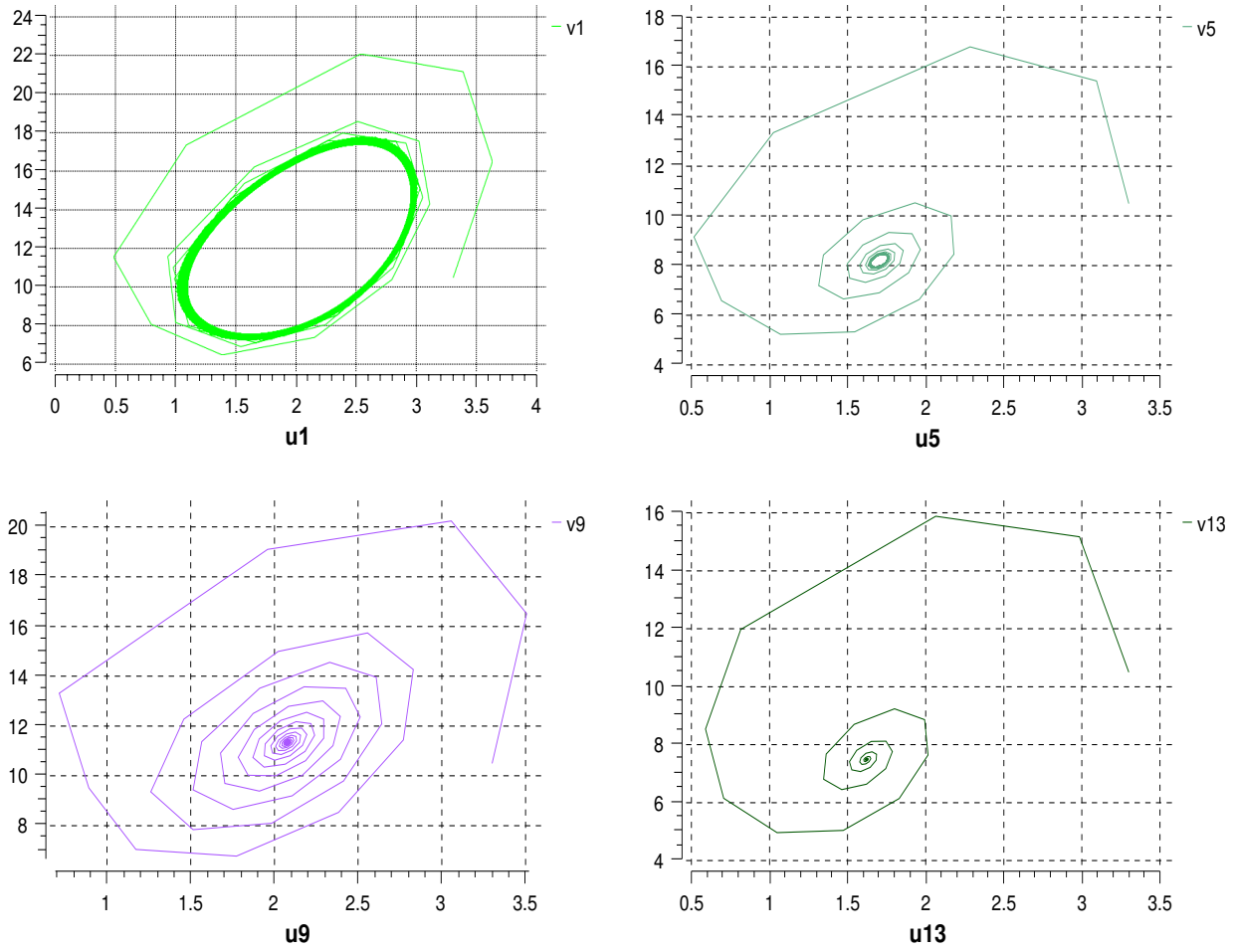

Figure 6.5: Phase space plots for oscillators [u1,v1], [u5,v5], [u9,v9], [u13,v13] of the Lengyel-Epstein system. This experiment considered different coupling strengths and values for each cluster and the RCC controller was implemented throughout the simulation. The parameters for this experiment are available in tables 6.3 and 6.4.

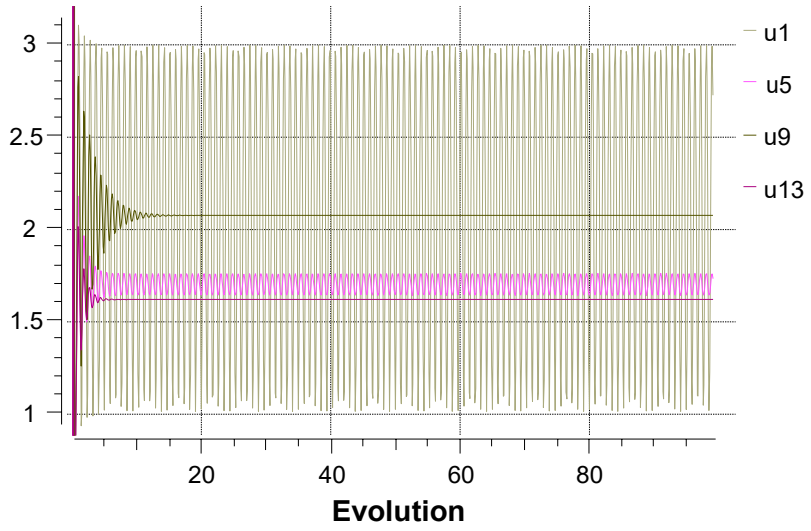

Figure 6.6: Evolution in time of variables u1, u5, u9, and u13, all of which reach periodic stability after t=18

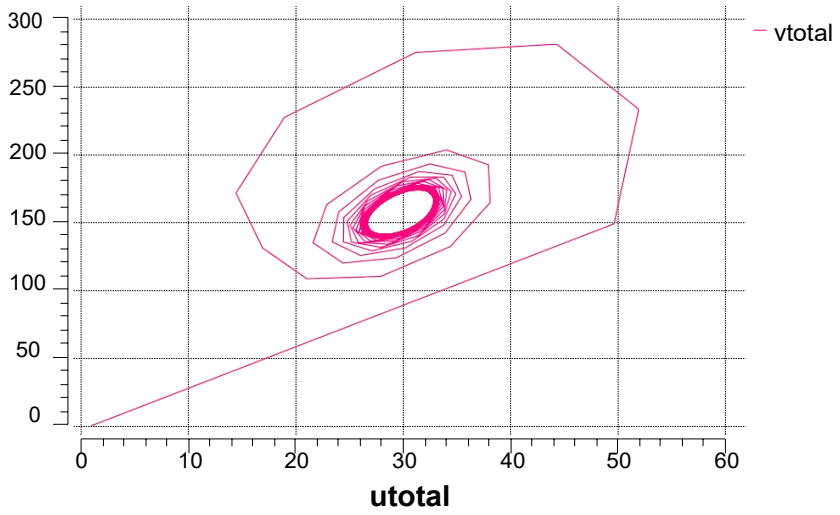

Figure 6.7: Phase space plot for total system response of the second experiment using the Lengyel-Epstein system.

Tables 6.5 and 6.6 show the parameters and initial conditions for the third experiment conducted using the Lengyel-Epstein system. The RCC controller remained the same and values were only changed for the coupling strength, by setting it to 0, in order to continue evaluating the effects of modifications to the coupling strength on individual clusters. In figure 6.8 it can be observed that the response of the individual oscillators is modified slightly, although the modifications are more noticeable for [u5,v5], where it takes longer for the cluster to reach periodic stability. The opposite effect is seen in the response of oscillator [u9,v9], where periodical stability is reached faster than in the prior experiments. These modifications can also be observed

by taking a look at the evolution of the variables in figure 6.9, and more importantly in the total response of the system in figure 6.10, as it takes longer for the system to reach periodic stability.

Parameter	Value
a1	21
a2	16
a3	20
a4	15
b1	1.3375
b2	1.3475
b3	1.3375
b4	1.3475
D1	0
D2	0
D3	0
D4	0
σ	8
f (RCC)	1.5
ξ(RCC)	1.5
μ (RCC)	6

Table 6.5: Lengyel-Epstein Experiment 3 - Parameters

Variable	Initial Value
u_1, u_5, u_9, u_{13}	3.3
v_1, v_5, v_9, v_{13}	2
u_2, u_6, u_{10}, u_{14}	3.3
v_2, v_6, v_{10}, v_{14}	3.8
u_3, u_7, u_{11}, u_{15}	10.5
v_3, v_7, v_{11}, v_{15}	5
u_4, u_8, u_{12}, u_{16}	5
v_4, v_8, v_{12}, v_{16}	16.8

Table 6.6: Lengyel-Epstein Experiment 3 - Initial Conditions

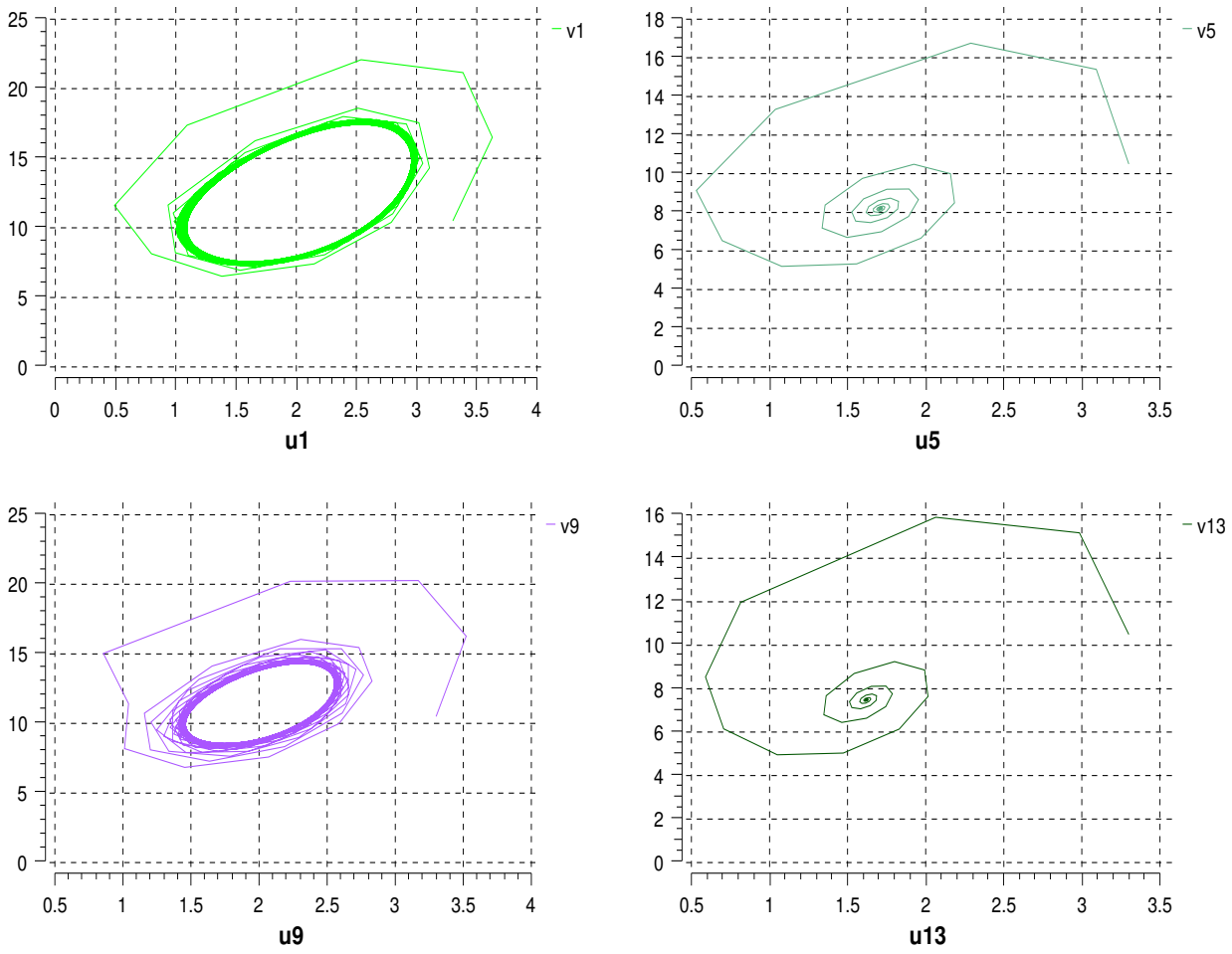

Figure 6.8: Phase space plots for oscillators [u1,v1], [u5,v15], [u9,v9], [u13,v13] of the Lengyel-Epstein system. This experiment consisted in setting the values for the coupling strength variables to 0. The parameters for this experiment are available in tables 6.5 and 6.6. Each oscillator shown is a member of each of the four clusters.

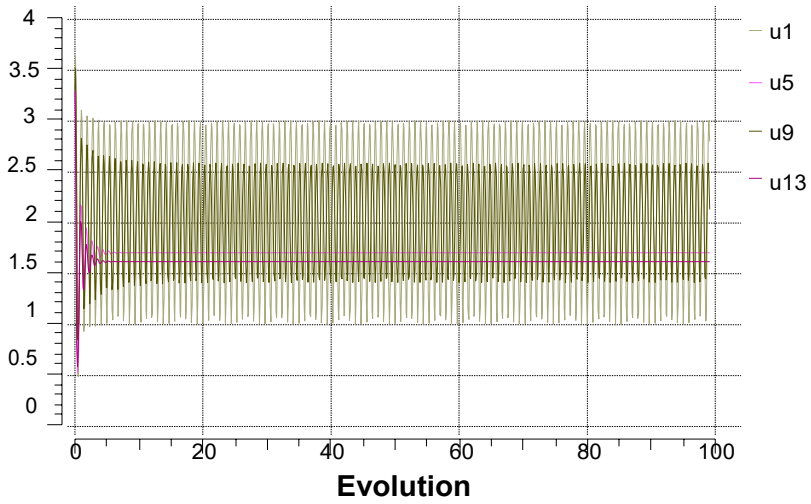

Figure 6.9: Evolution in time of variables u1, u5, u9, and u13, all of which reach periodic stability after t=10 approximately.

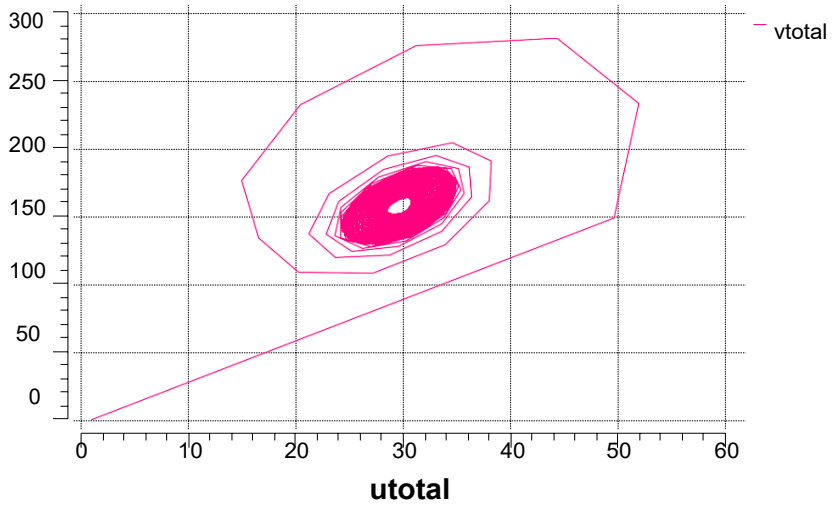

Figure 6.10: Phase space plot of the total response of the system for the third experiment Using the Lengyel-Epstein System.

The outcome of the previous experiment was successful in demonstrating the structure supports the change in coupling from prior experiments, and it supports the case where the coupling strength is set to 0, which biologically represents the case where there is no cellular communication. Tables 6.7 and 6.8 show the parameter and initial condition values used to conduct the fourth experiment for the Lengyel-Epstein system. In this case, the coupling strength was set to 0.1 for all the oscillators, in order to test the response of the controlled system when coupling is low and uniform throughout the clusters, representing weak communication among the cells

and clusters, which is the case for specific biological states where cellular communication is weak when local feedback has little effect on the systemd ynamics. The individual responses did not differ greatly but it can be seen by the evolution of the variables in figure 6.11. For the two other experiments, this would be achieved at around t=20, but for this case it is achieved at t = 1750. The total response of the system is shown in figure 6.12 and it can be seen that it also reaches periodic stability.

Parameter	Value
a1	21
a2	16
a3	20
a4	15
b1	1.3375
b2	1.3475
b3	1.3375
b4	1.3475
D1	0.1
D2	0.1
D3	0.1
D4	0.1
σ	8
f (RCC)	1.5
ξ(RCC)	1.5
μ (RCC)	6

Table 6.7: Lengyel-Epstein Experiment 4 - Parameters

Variable	Initial Value
u_1, u_5, u_9, u_{13}	3.3
v_1, v_5, v_9, v_{13}	2
u_2, u_6, u_{10}, u_{14}	3.3
v_2, v_6, v_{10}, v_{14}	3.8
u_3, u_7, u_{11}, u_{15}	10.5
v_3, v_7, v_{11}, v_{15}	5
u_4, u_8, u_{12}, u_{16}	5
v_4, v_8, v_{12}, v_{16}	16.8

Table 6.8: Lengyel-Epstein Experiment 4 - Initial Conditions

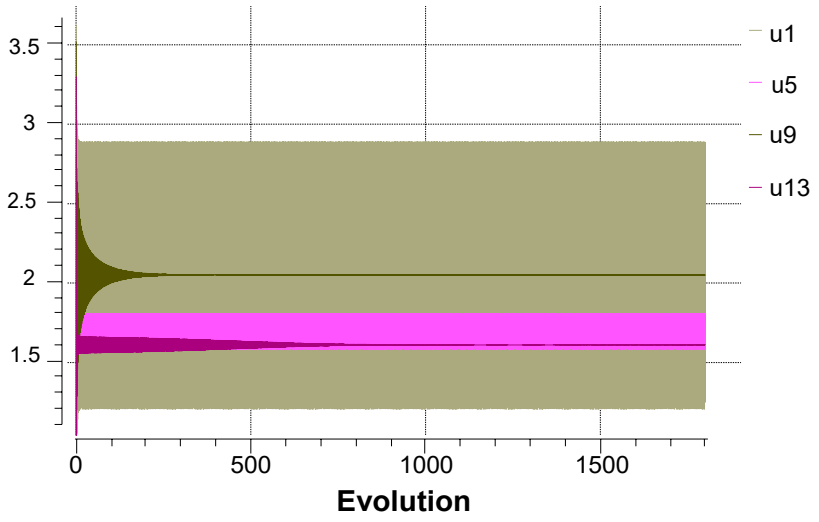

Figure 6.11: Evolution in time of variables u1, u5, u9, and u13. For this experiment the coupling strength was increased for all the clusters and set to 0.1. This significantly changes the results as it takes the variables much longer to achieve periodic stability at point t = 1750.

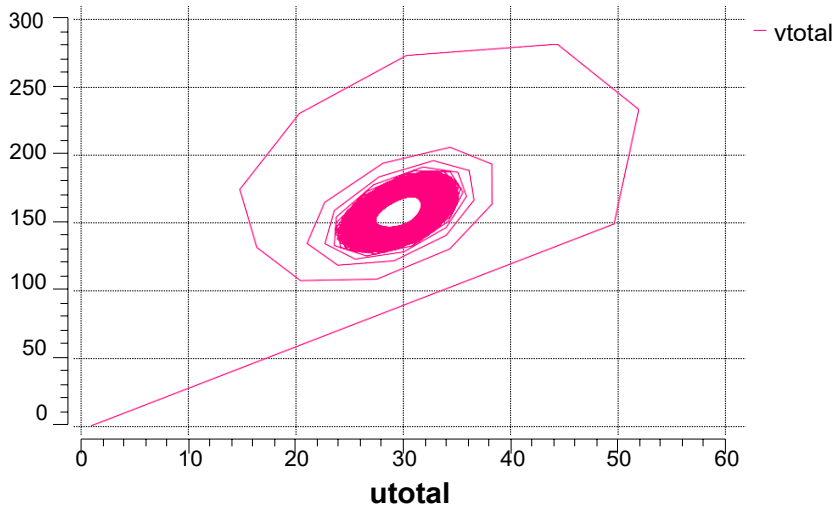

Figure 6.12: Phase space plot of the total evolution of the system for the fourth experiment with the Lengyel-Epstein system.

6.2.2 Response to changes in coupling and control strength in the system

From the experiments presented in the previous section, we learn that the structure is supported but without sufficient singularity in the clusters. To improve this the final form of the Lengyel-Epstein system is implemented. Including the RCC controller used to conduct the experiments in this section, the formulation ofthe system is described by equations 6.5, 6.6, 6.7, and 6.8 where i = 1....16.

$$\frac{\partial u}{\partial t} = a_i - u_i - \frac{4u_i v_i}{1+u_i^2} - \Phi_i + \nabla^2 u_i + D_i(u_{i+1} - u_i) \tag{6.5}$$

$$\frac{\partial v}{\partial t} = \sigma[b(\sigma_v^{RCC}(u)u_i - \frac{u_i v_i}{1+u_i^2} + \Phi_i) + e_i\nabla^2 v_i] + D_i(v_{i+1} - v_i) \tag{6.6}$$

Where the RCC control equations are given by:

$$\sigma(v) = fe^{\xi q_u + \theta} \tag{6.7}$$

And

$$q_u = \frac{u}{u+\mu_u} \tag{6.8}$$

Certain modifications were implemented upon the incorporation of the second formulation of the model, given in the above equations. Parameter b could no longer be used to differentiate the clusters, and the value of parameter a had to be modified. The incorporation of the RCC provided the advantage of exploring the use of control strength to add singularity to the clusters. Ultimately, the coupling strength was able to be modified to establish the clusters, along with parameter a. Parameter D_i was implemented as a step function for the experiments presented in this section, denoted as No_i. The initial value for the step function is unique to each cluster and is presented in the parameter value tables for each experiment. It aided in evaluating the system response to modification in coupling strength. The form of this step function is shown for each experiment. With all these considerations, the cluster structure for the experiments presented in this section is as follows:

- Cluster 1:
  - Parameters: a1, No_1
  - Oscillators: [u1,v1], [u2,v2], [u3,v3], [u4,v4].
- Cluster 2:
  - Parameters: a2, No_2
  - Oscillators: [u5,v5], [u6,v6], [u7,v7], [u8,v8].
- Cluster 3:
  - Parameters: a3, No_3
  - Oscillators: [u9,v9], [u10,v10], [u11,v11], [u12,v12].
- Cluster 4:
  - Parameters: a4, No_4
  - Oscillators: [u13,v13], [u14,v14], [u15,v15], [u16,v16].

The parameter values for the RCC controller will differ for each model, these are presented in the parameter tables for each experiments and have assigned sub-indices (1-4) depending

on which cluster they belong to. Tables 6.9 and 6.10 show the parameter values used for the first experiment presented in this section. The results are shown in figures 6.13, 6.14, and 6.15. Figure 6.13 shows the responses of a member from each cluster. Chaotic behaviour is observed before the controller is activated by the step function. The periodically stable states for each oscillator are colour coded and can be observed better in figures 6.14 and 6.15, where the evolution in time of the oscillators is also shown. The system response is available in figure 6.15, along with the step functions used to modify the coupling strength. This first experiment was useful to evaluate the formulation with the implementation of the controller and the step function that modifies the coupling strength. The outcome shows a wide range of behaviour in each cluster, and the system is capable of adapting to all the states provided by the change in coupling. This is a relevant feature of the model as it demonstrates the system is capable of switching between periodically stable states, a biologically relevant feature of the glucose-insulin system.

Parameter	Value
a_1, a_3	50
a_2, a_4	33
b	2.5
No_1(step)	0.05
No_2(step)	0.0005
No_3(step)	0.005
No_4(step)	0.00005
σ	8
e_i	1.2
Φ_i	5
f (RCC)	1
ξ (RCC)	-0.6
μ (RCC)	16
θ (RCC)	1.9

Table 6.9: Lengyel-Epstein Experiment 1 - Parameters

Variable	Initial Value
u_1, u_3, u_5, u_7	3.8
v_1, v_3, v_5, v_7	15.44
u_2, u_4, u_6, u_8	2
v_2, v_4, v_6, v_8	5
u_9, u_{11}, u_{13}, u_{15}	3.8
v_9, v_{11}, v_{13}, v_{15}	15.44
u_{10}, u_{12}, u_{14}, u_{16}	2
v_{10}, v_{12}, v_{14}, v_{16}	5

Table 6.10: Lengyel-Epstein Experiment 1 - Initial Conditions

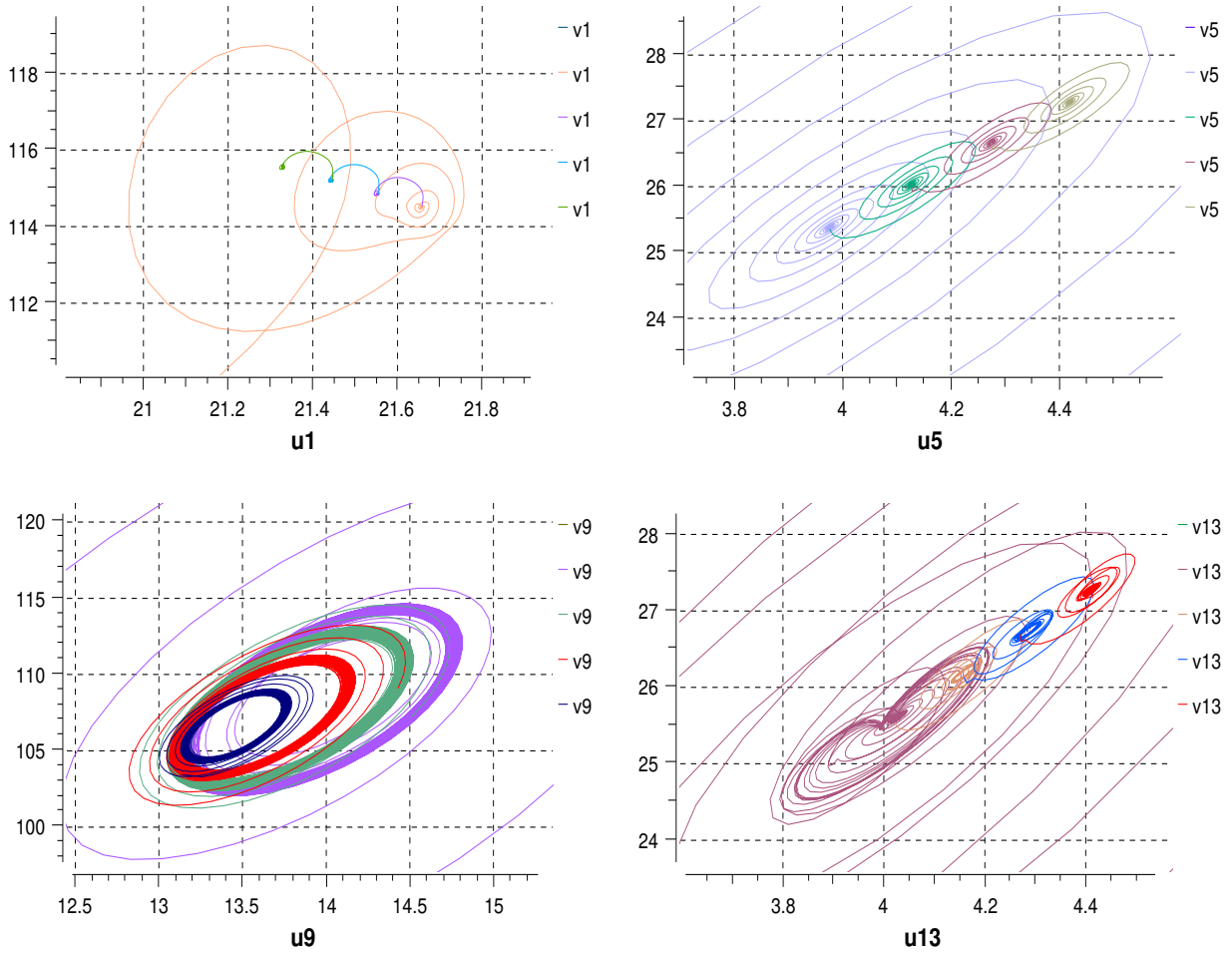

Figure 6.13: Response of oscillators [u1,v1], [u5,v5], [u9,v9], and [u13,v13], the image has been modified to show the different states the oscillators stabilize into. The parameters for this experiment are shown in tables 6.9 and 6.10. Oscillators [u1,v1] and [u5,v5] stabilize periodically around the point [21.33,115.5] and [4.419,27.29] respectively.

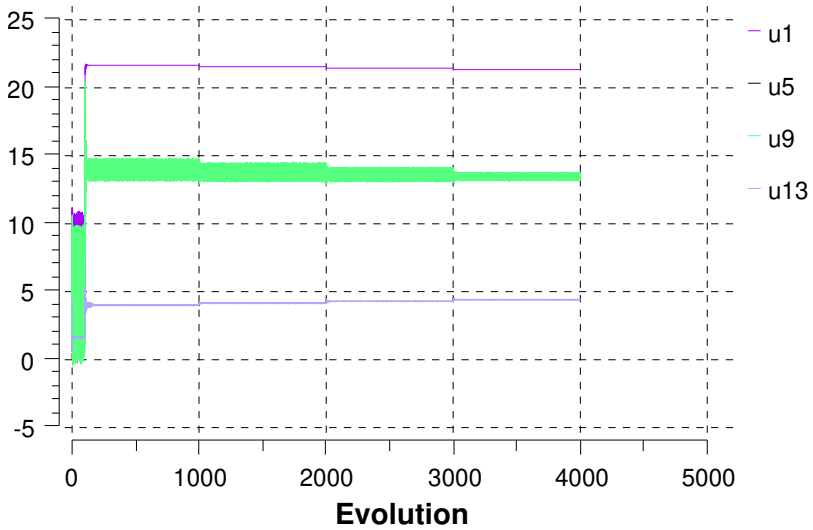

Figure 6.14: Evolution in time of oscillators. The parameters for this experiment are shown in tables 6.9 and 6.10.

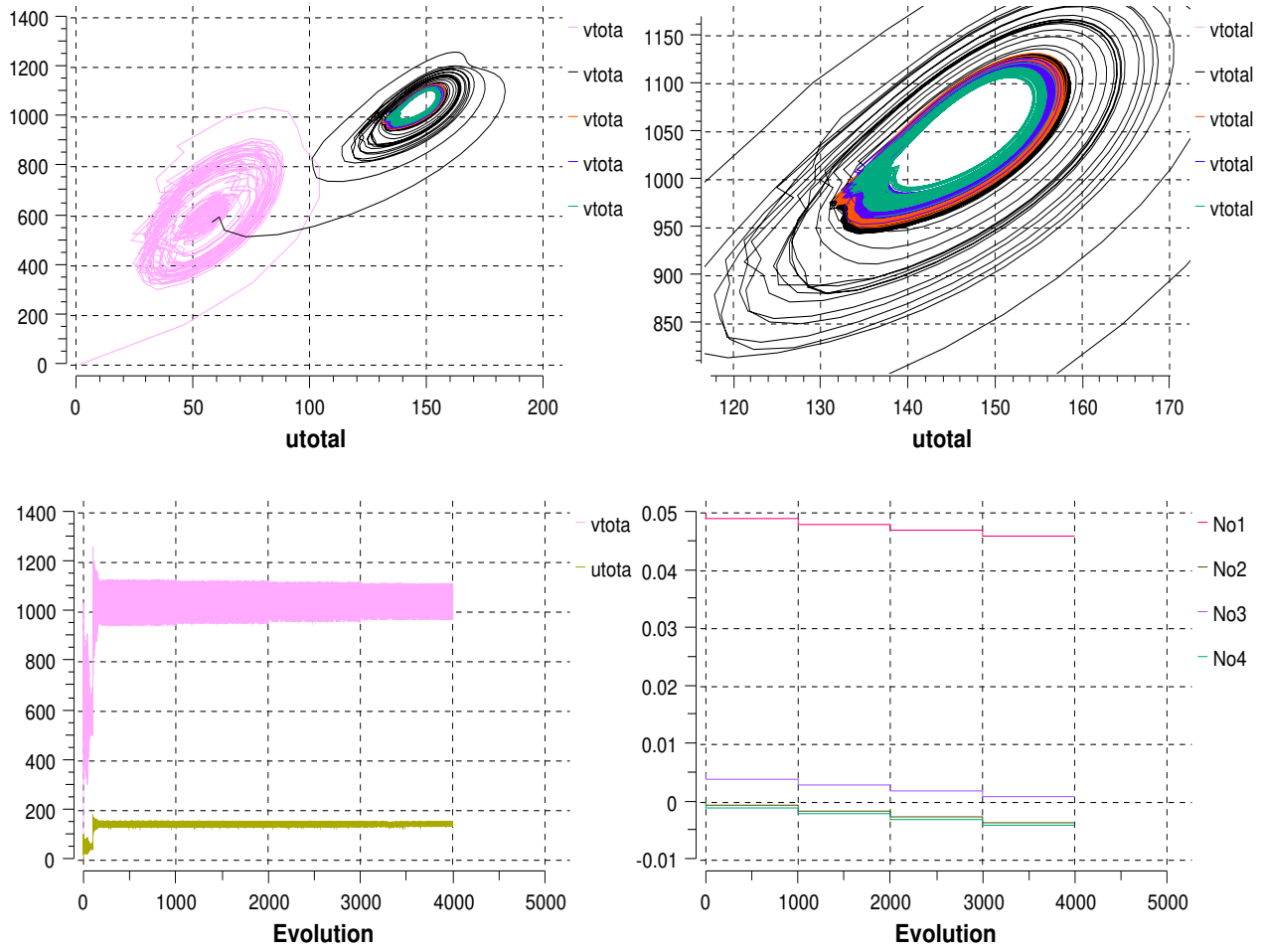

Figure 6.15: Phase space plots showing response of the system and amplification to show the different periodically stable states [top]. Evolution of system response variables and step functions used to modify the coupling strength [bottom]

Tables 6.11 and 6.12 show the parameter values used for the second experiment presented in this section. The results are shown in figures 6.16, 6.17, and 6.18. Figure 6.16 shows the responses of a member from each cluster. Chaotic behaviour is observed before the controller is activated by the step function. The periodically stable states for each oscillator are colour coded and can be observed better in figures 6.17 and 6.18, where the evolution in time of the oscillators is also shown. The system response is available in figure 6.18, along with the step functions used to modify the coupling strength. For this experiment, control parameter ξ_i was modified for clusters 2 and 4 to continue providing singularity to the clusters, which in turn evaluates the capability of the model to support the structure. The changes in the model can be seen in oscillators [u5,v5] and [u13,v13], where periodical stability is reached much faster.

Parameter	Value
a_1, a_3	50
a_2, a_4	33
b	2.5
No_1(step)	0.05
No_2(step)	0.0005
No_3(step)	0.005
No_4(step)	0.00005
σ	8.25
e_i	1.2
Φ_i	5
f (RCC)	1
ξ_1, ξ_3 (RCC)	-0.6
ξ_2, ξ_4 (RCC)	-0.5
μ (RCC)	16
θ (RCC)	1.9

Table 6.11: Lengyel-Epstein Experiment 2 - Parameters

Variable	Initial Value
u_1, u_3, u_5, u_7	3.8
v_1, v_3, v_5, v_7	15.44
u_2, u_4, u_6, u_8	2
v_2, v_4, v_6, v_8	5
u_9, u_{11}, u_{13}, u_{15}	3.8
v_9, v_{11}, v_{13}, v_{15}	15.44
u_{10}, u_{12}, u_{14}, u_{16}	2
v_{10}, v_{12}, v_{14}, v_{16}	5

Table 6.12: Lengyel-Epstein Experiment 2 - Initial Conditions

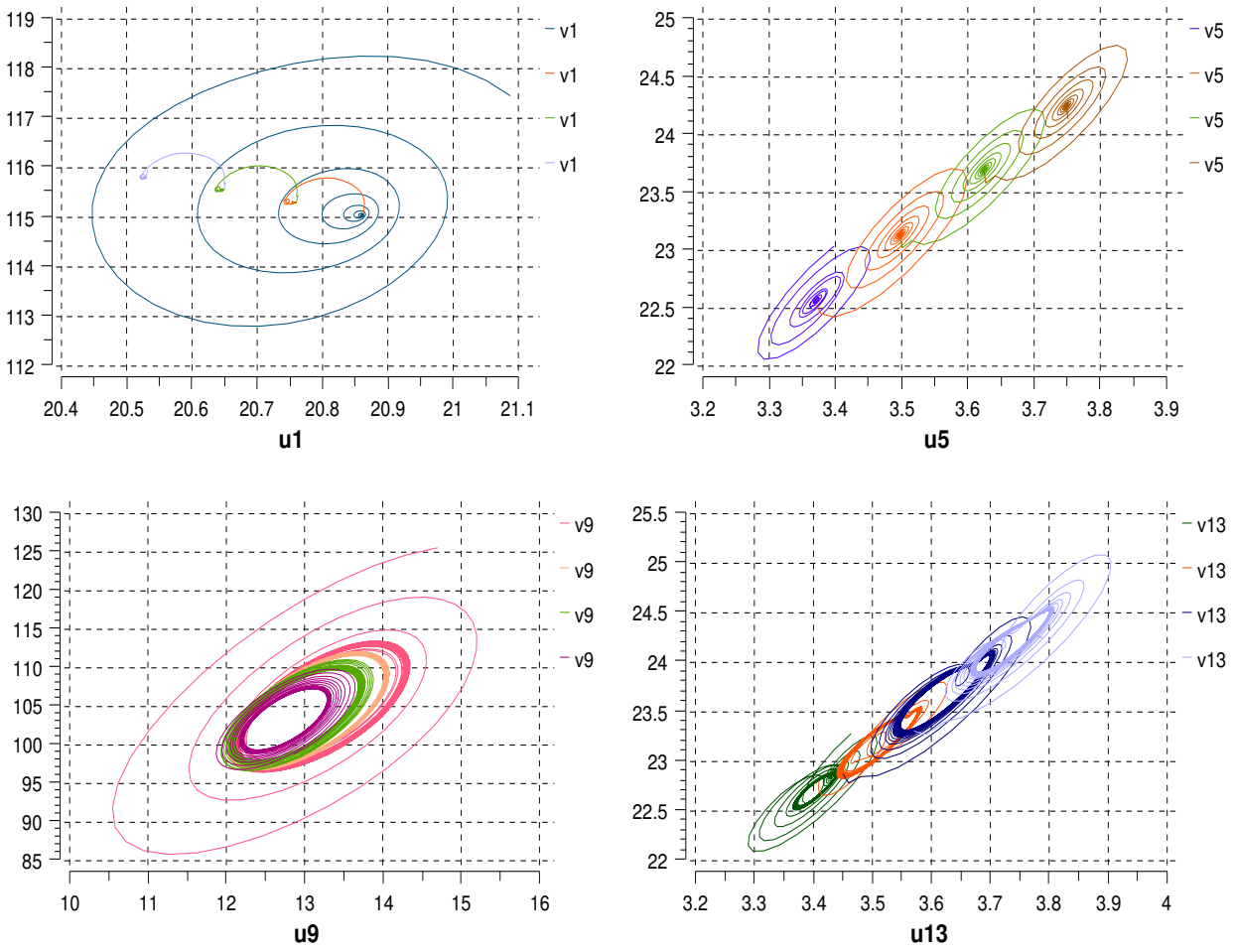

Figure 6.16: Response of oscillators [u1,v1], [u5,v5], [u9,v9], and [u13,v13]. The parameters for this experiment are shown in tables 6.11 and 6.12. The coupling strength has been decreased using the step functions shown in figure 6.15. Oscillators [u1,v1] and [u5,v5] stabilize periodically around point [20.53,115.8] and [3.749,24.25] respectively.

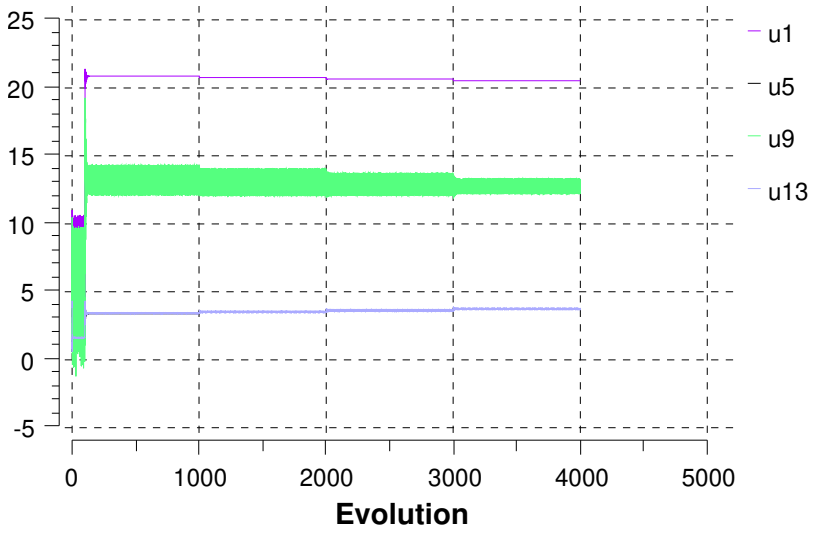

Figure 6.17: Evolution in time of oscillators. The parameters for this experiment are shown in tables 6.11 and 6.12.

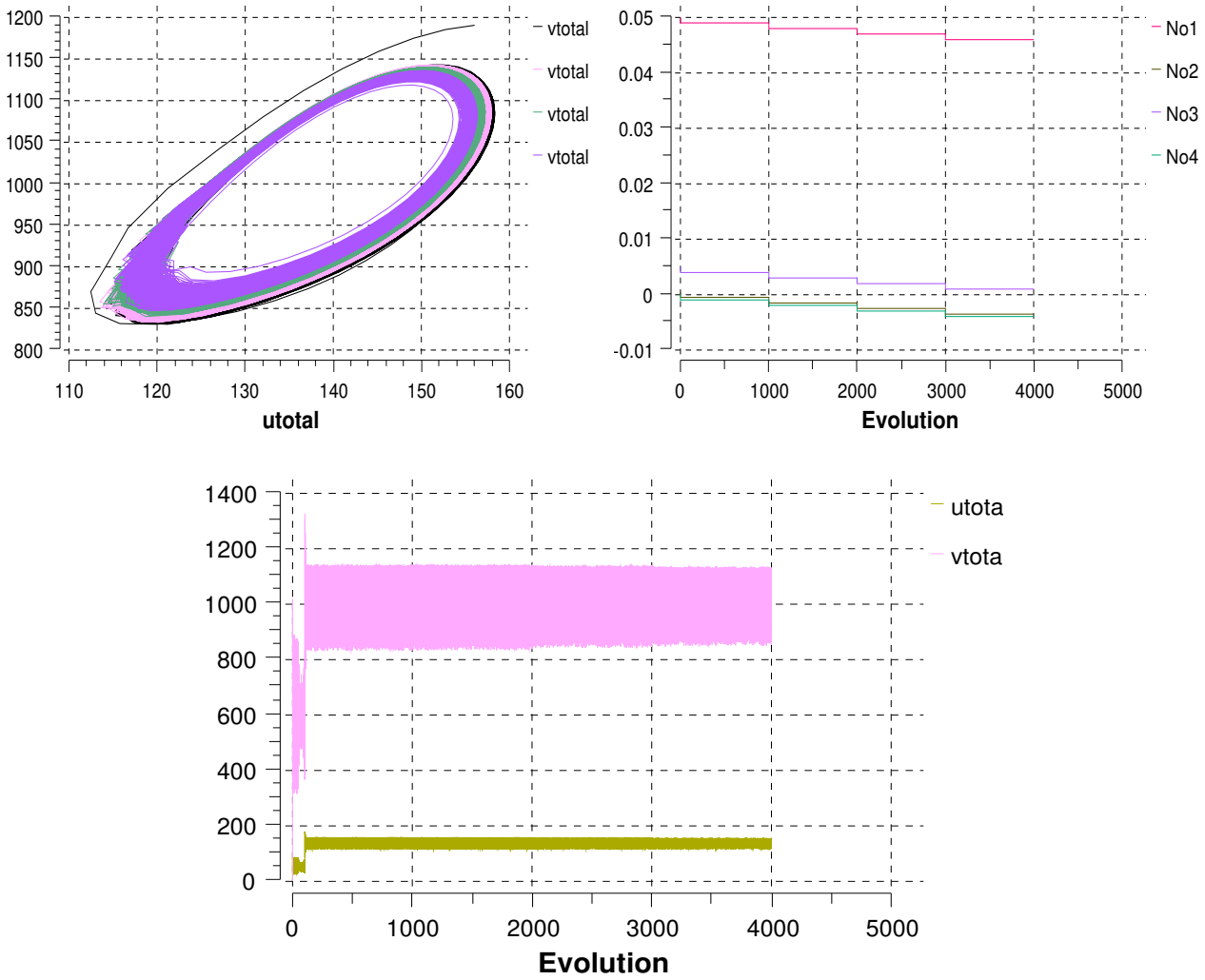

Figure 6.18: Phase space plots showing response of the system and amplification to show the different periodically stable states [top]. Evolution of system response variables and step functions used to modify the coupling strength [bottom]

Tables 6.13 and 6.14 show the parameter values used for the third experiment presented in this section. The results are shown in figures 6.19, 6.20, and 6.21. Figure 6.19 shows the responses of a member from each cluster. Chaotic behaviour is observed before the controller is activated by the step function. The periodically stable states for each oscillator are colour coded and can be observed better in figures 6.20 and 6.21, where the evolution in time of the oscillators is also shown. The system response is available in figure 6.21, along with the step functions used to modify the coupling strength.

The prior two experiments showed positive results at the cluster level, but when the total response of the system was evaluated, the same was not true, as the controlled states are not easily distinguishable and the phase space response appears irregular, meaning the total response of the system is not adapting well to the structure provided by each cluster, even with the implementation of the controller. To attempt to improve this, the value of μ_i was modified for each cluster in order to tune the controller, given the differences in the clusters observed in the stability analysis. The most notable change observed with these modifications was in the amplitude of the outputs, which was due to the increase in the control strength.

Parameter	Value
a_1, a_3	50
a_2, a_4	33
b	2.5
No_1(step)	0.05
No_2(step)	0.0005
No_3(step)	0.005
No_4(step)	0.00005
σ	8.25
e_i	1.2
Φ_i	5
f (RCC)	1
ξ(RCC)	-0.55
μ_1 (RCC)	10
μ_2 (RCC)	0.2
μ_3 (RCC)	12
μ_4 (RCC)	0.1
θ (RCC)	1.9

Table 6.13: Lengyel-Epstein Experiment 3 - Parameters

Variable	Initial Value
u_1, u_3, u_5, u_7	3.8
v_1, v_3, v_5, v_7	15.44
u_2, u_4, u_6, u_8	2
v_2, v_4, v_6, v_8	5
u_9, u_{11}, u_{13}, u_{15}	3.8
v_9, v_{11}, v_{13}, v_{15}	15.44
u_{10}, u_{12}, u_{14}, u_{16}	2
v_{10}, v_{12}, v_{14}, v_{16}	5

Table 6.14: Lengyel-Epstein Experiment 3 - Initial Conditions

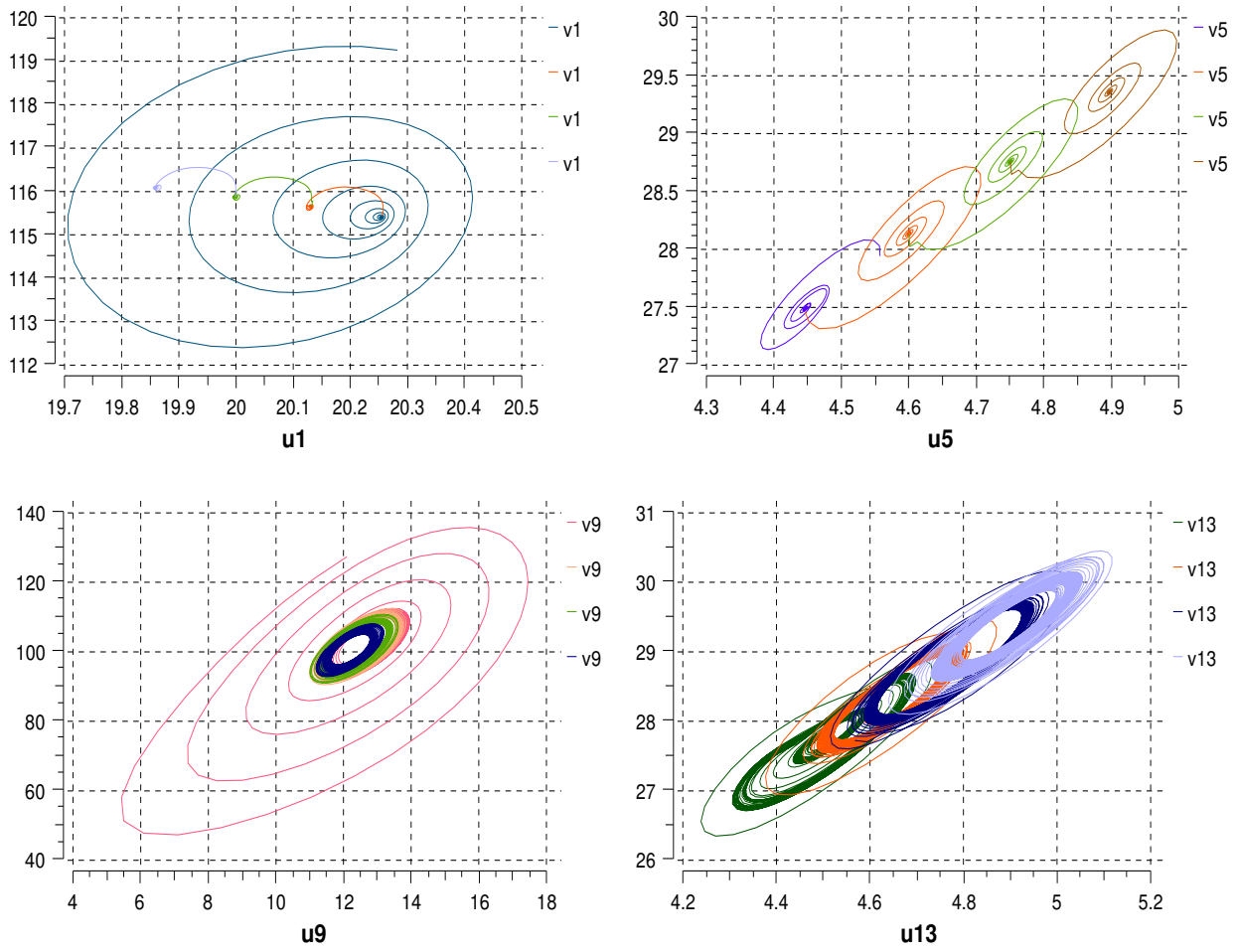

Figure 6.19: Response of oscillators [u1,v1], [u5,v5], [u9,v9], and [u13,v13]. The parameters for this experiment are shown in tables 6.13 and 6.14. The coupling strength has been decreased using the step functions shown in figure 6.15. Oscillators [u1,v1] and [u5,v5] stabilize periodically around points [19.86,116.1] and [4.898,29.36] respectively.

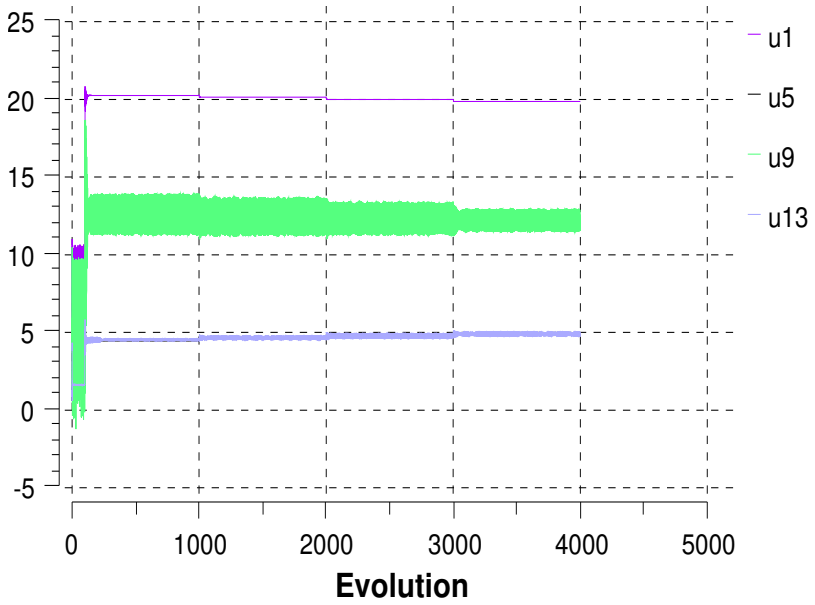

Figure 6.20: Evolution in time of oscillators. The parameters for this experiment are shown in tables 6.13 and 6.14.

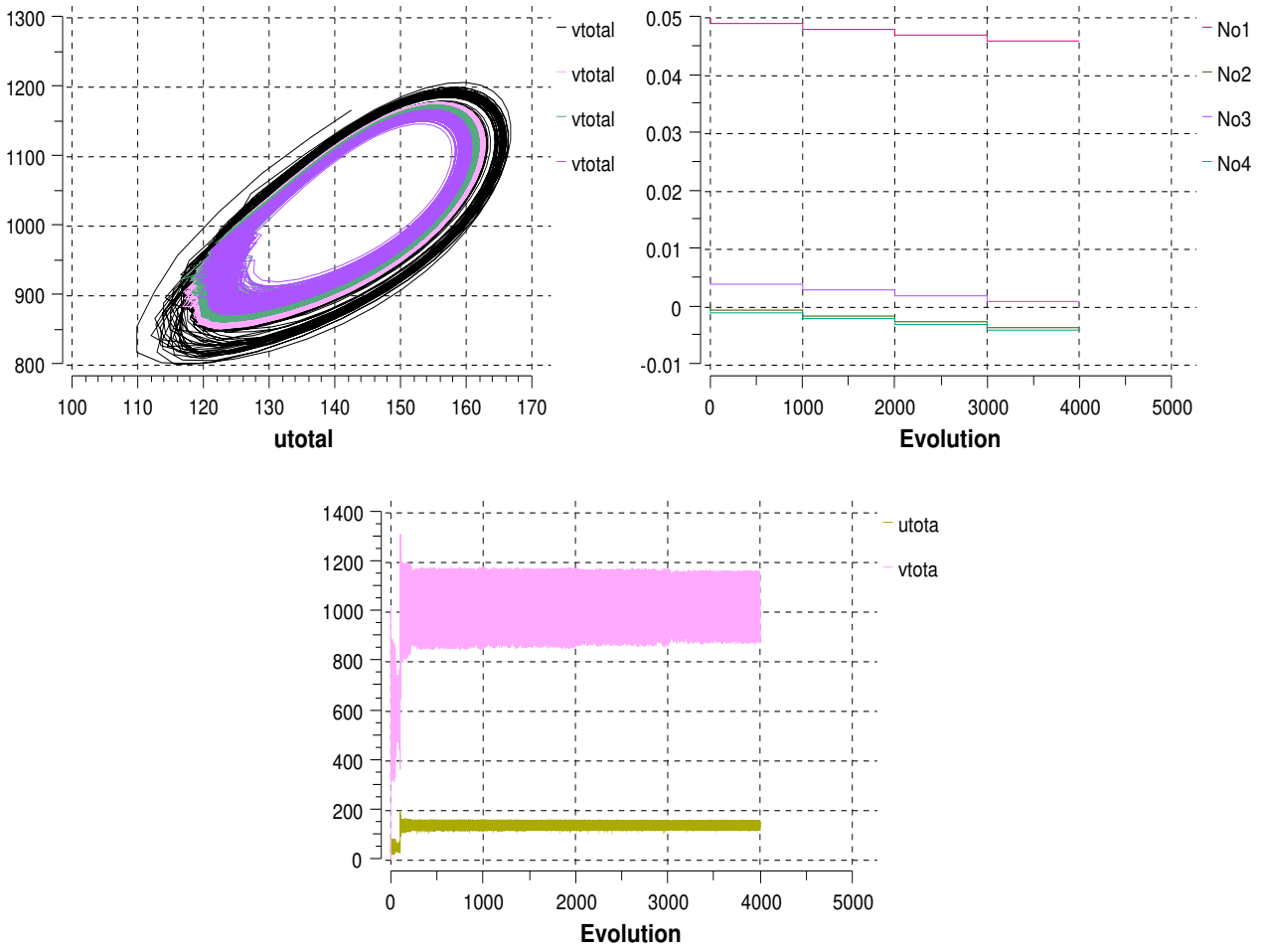

Figure 6.21: Phase space plots showing response of the system and amplification to show the different periodically stable states [top]. Evolution of system response variables and step functions used to modify the coupling strength [bottom]

6.3 Discussion

Two formulations were selected for the development of the model, both of which were presented in this chapter. The first one was taken from [3] and it was used for the first set of experiments in order to build the model and observe how it adapted to the structure required. It was observed that the model was limited in terms of the values that the parameters could accept. For the remaining experiments the formulation presented in [32] was used instead, this particular formulation was chosen as it is an extension of the previous, and it provided 3 additional parameters, including an additional term for coupling. Although this formulation provided better results it still had some limitations which will be discussed in the following sections.

6.3.1 Response to modifications to support model structure and implementation of RCC controller

The model was first tested without the influence of the controller to observe if the structure could be supported. The work by Aly, Shaban was used as reference in order to perform both the stability analysis and the initial experiments for the model. The article considers two linearly coupled systems, where it is assumed that parameters a, b, and σ are all positive and their values are established in the ranges $0 < a < 35$, $0 < b < 8$ and $\sigma = 8$. Another advantage of this formulation, is the range of values that can be used for the coupling strength and the wide rage of dynamics it provided, however, for the purpose of this project, it is preferred to keep the coupling parameter low and to use it to separate the clusters. Taking all this into account, the parameters were selected as presented in tables 6.1 and 6.2. The outcome was successful in representing the structure, where small modifications in the parameters achieved visible differences between the clusters. This can be seen in figures 6.2, 6.3, and 6.4.

Once this was finalized, the controller was implemented on the incremental term u_i of equation 6.6. The values chosen for the controller are available in tables 6.3 and 6.4. At this stage in the process it was only desired to evaluate if the structure supported the controller, therefore the values were assigned according to the recommendations established in [3]. Once the controller was implemented and it was seen that it could be supported by the structure, three experiments were conducted where the main focus was to modify the coupling strength in order to observe the best ranges to consider in order to continue developing the model using the other formulation. It was observed that the best response of the system was obtained when the coupling strength had high variation among the clusters. This corresponds to the results of experiment 2. The model performed well in terms of supporting the structure and the controller. It was possible to separate the system into clusters using the initial conditions and parameters a, b, and d. The established values were taken as reference to implement the formulation presented in [3] for the remaining experiments.

Experiments 3 and 4 of section 6.2.1 considered coupling strengths in all clusters of 0 and 0.1 respectively where the outcome showed a delay in the system's capability to stabilise into periodic orbits. This delay was greater for experiment 3 where periodic stability was reached around t = 1800 for cluster 4 (u_{13} in figure 6.11). These experiments show the model is capable to sustain major differences among the coupling strengths in the clusters, and that the response is better at lower values of coupling strength. These features represent the possibility of tailoring the response of the system to specific cases i.e. cases where delay is acceptable or even required. The desired behaviour for the structure of the system corresponds to the results obtained for experiment 2, where the coupling strength is different for each cluster and parameter a is used to provide singularity as well. It was observed that the parameters chosen for this experiment provide sufficient singularity to each of the clusters. These were taken as reference for further experiments where the control strength and the coupling strength were modified to achieve multiple periodically stable states.

6.3.2 Response to modifications of coupling strength

To continue the experiments with this model, the formulation by Ji, Lin and Li, Qian Shu available in [31] was implemented. Initially, the parameters used for the prior experiments were also implemented and it was found that they were no longer viable using this new formulation. The article by Ji et. al experiments the model with higher values for parameters a and b. Additionally, the article proposes several values of ϕ which can work with the formulation in the form of a phase diagram. This diagram was taken into consideration but ultimately, only a few worked given the sixteen coupled oscillator structure. The initial conditions were also modified as this formulation no longer accepted the ones used for the experiments discussed in section 6.3.1. The value of σ was also increased slightly to improve the response, and the control strength was modified for two of the clusters. These modifications were implemented for the experiment discussed in this section and are available in tables 6.9 - 6.14.

All three experiments show the system is capable of stabilizing into multiple states at the lower level. However, when the general response of the system is analysed, it is difficult to observe the changes in state. For this reason, three experiments were carried out in order to observe which parameters could be modified to provide a better response of the system, where these changes in state would be observable. Parameters σ, ξ, and μ were modified. It was thus seen that the best response is obtained with the parameters established in experiment 2. The parameter values are available in tables 6.11 and 6.4, where it is shown that control parameter ξ is assigned different values to create two sets of clusters, a unique value of μ is used for all clusters, and the value of σ is increased to 8.25.

Overall the parameter values for contributed to differentiate the cluster and system states in similar measures, although not as effectively as seen for the other candidate models. The best results achieved were those corresponding to experiment 1. Figure 6.22 show the response of clusters 3 and 4 and the total system, as well as the step function which was used to modify the coupling strength. The multiple periodically stable states can be clearly distinguished in the clusters, but the same is not true for the total response of the system. It can be said that this model formulation is restricted by its parameter values, especially once the controller is implemented. One of the possible causes for this could be that there is only one incremental term where the controller can be implemented.

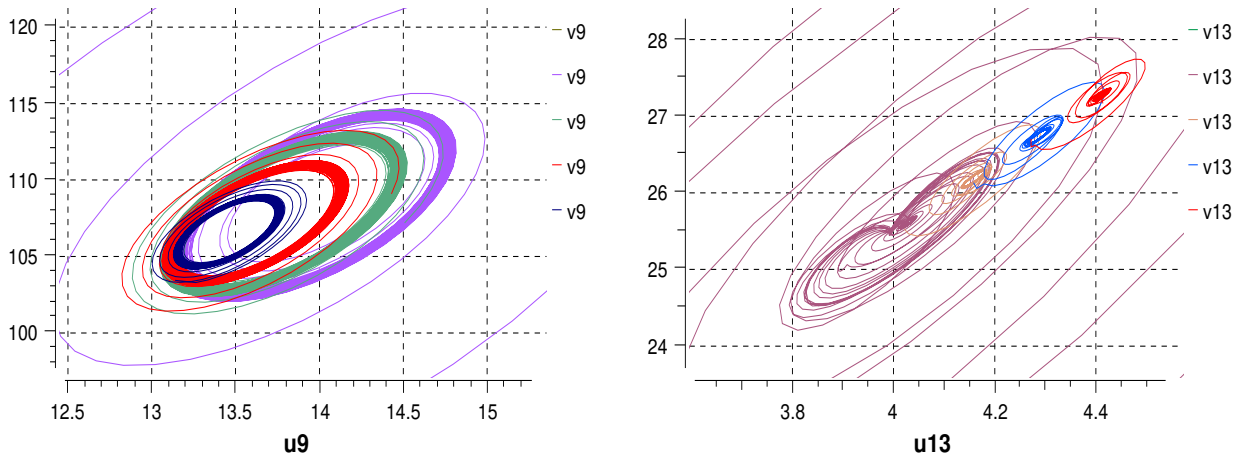

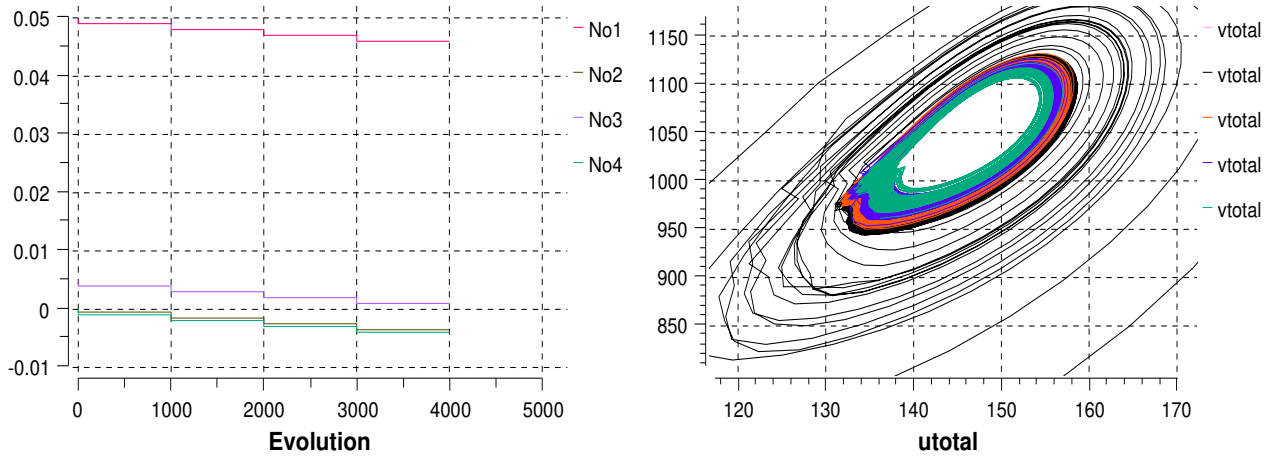

Figure 6.22: Results of experiment 1, showing: response of clusters 3, 4, system response and step functions used to stabilize the system into multiple periodically stable states.

Chapter 7

The Brusselator

7.1 Model Development

This model was developed by Prigogine et. al. in the late 1960's in Brussels, which was a contributing factor to its name. It was developed in order to prove Turing's theory, and show that Turing patterns which follow the rules of chemical kinetics exist. This model represents the interaction between a reactor and an inhibitor. It was selected as it is considered one of the simplest reaction-diffusion systems capable of generating complex spatial patterns [74], this property aligns with the characteristics of the methodology as it is desired to avoid using large scale models of this stage bound by rigorous parameters. It is known for being a model capable of generating a wide range of dynamic behaviours using a relatively simple formulation.

The activator-inhibitor interaction presented by this model is a well-known principle to explain pattern formation in chemical, ecological, physical, and biological systems, this is an important feature for the base models as it is desired for these to be biologically relevant. The model is comprised of two differential equations, including two rate constants and two diffusion coefficients:

$$\frac{dx}{dt} = a - (b+1)x + x^2y + D_x\nabla^2 x \tag{7.1}$$

$$\frac{dy}{dt} = bx - x^2y + D_y\nabla^2 y \tag{7.2}$$

7.1.1 Stability Analysis

The selected parameters for the Brusselator also render the desired behaviour (see figure 7.1), the action of the activator and the inhibitor can be distinguished clearly. As previously mentioned, the complete formulation used for this project is provided in section 7.1.2, where it can be seen that there are more variables to consider once the coupling, and the RCC is implemented in the system. The modification of parameters a and b will also be implemented in order to see if it is possible for the system to maintain the required dynamics and control them accordingly. The works by Kytta [37] and Wang [74]were used in order to define and tune the system parameters for this model.

Behaviour	Parameters and Initial Conditions
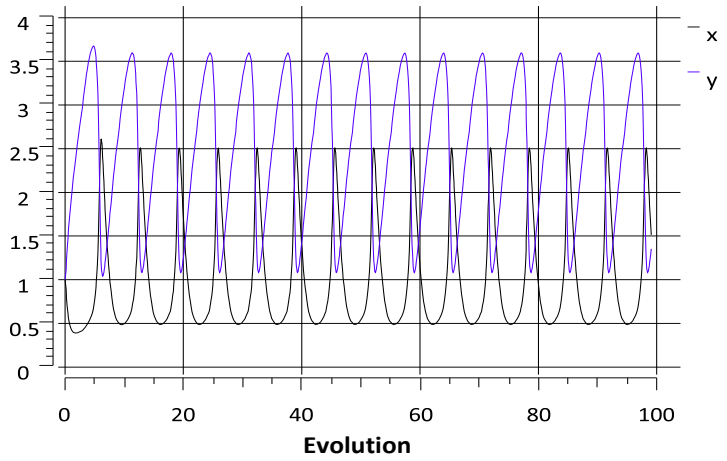	Initial Conditions • x = 1 • y = 1 Parameters • a = 1 • b = 2.5

Figure 7.1: Stability Analysis - Brusselator Model

7.1.2 Model Structure

This system was obtained from [37], the formulation was used in all experiments presented in the following section and is defined as follows:

$$\frac{\partial x_i}{\partial t} = D_x \nabla^2 x_i + \alpha x_i x_j (x_j - x_i) + f(x_i, y_i) \tag{7.3}$$

$$\frac{\partial y_i}{\partial t} = D_y \nabla^2 y_i + \beta y_i y_j (y_j - y_i) + g(x_i, y_i) \tag{7.4}$$

Where:

$$f(x_i, y_i) = a - (b+1)x + \sigma_x(x, y)x^2 y \tag{7.5}$$

and:

$$g(x_i, y_i) = \sigma_y(y)bx - x^2 y \tag{7.6}$$

Where $\nabla^2 = \frac{\partial^2}{\partial z^2}$. In order to differentiate the clusters we have parameters a, b, D_x, D_y, α, and β. The specific values for these are mentioned in the following chapter. RCC is applied on the incremental term x^2y in equation 7.5 denoted as $\sigma_x(x, y)$, and in the incremental term bx in 7.6 denoted as $\sigma_y(y)$. Coupling is given by terms $Dx\nabla^2 x_i$ and $\alpha x_i x_j(x_j - x_i)$ of 7.3, and terms $D_y\nabla^2 y_i$ and $\beta y_i y_j(y_j - y_i)$ in equation 7.4, parameters D_x, D_y, α and β will therefore be useful to control the coupling strength.

7.2 Results

7.2.1 Parameter Tuning to Support Model Structure

The stability analysis assisted in identifying the parameters that would result in the model exhibiting periodic stability. These were taken as reference to build the model following the structure of sixteen coupled oscillators. The parameter values and initial conditions used for the experiment are presented in tables 7.1 and 7.2.

Parameter	Value
a	1
b	2.5
Dx1, Dx2	1.85
Dy1, Dy2	16.66
α	0.1
β	0.1
f_x (RCC)	1
f_y (RCC)	1
ξ_x (RCC)	0.65
ξ_y (RCC)	0.2
μ_x (RCC)	3
μ_y (RCC)	5

Table 7.1: Brusselator Experiment 1 - Parameters

Variable	Initial Value
x_1, x_5, x_9, x_{13}	1
y_1, y_5, y_9, y_{13}	2
x_2, x_6, x_{10}, x_{14}	0.5
y_2, y_6, y_{10}, y_{14}	5
x_3, x_7, x_{11}, x_{15}	1
y_3, y_7, y_{11}, y_{15}	1
x_4, x_8, x_{12}, x_{16}	0.1
y_4, y_8, y_{12}, y_{16}	0.01

Table 7.2: Brusselator Experiment 1 - Initial Conditions

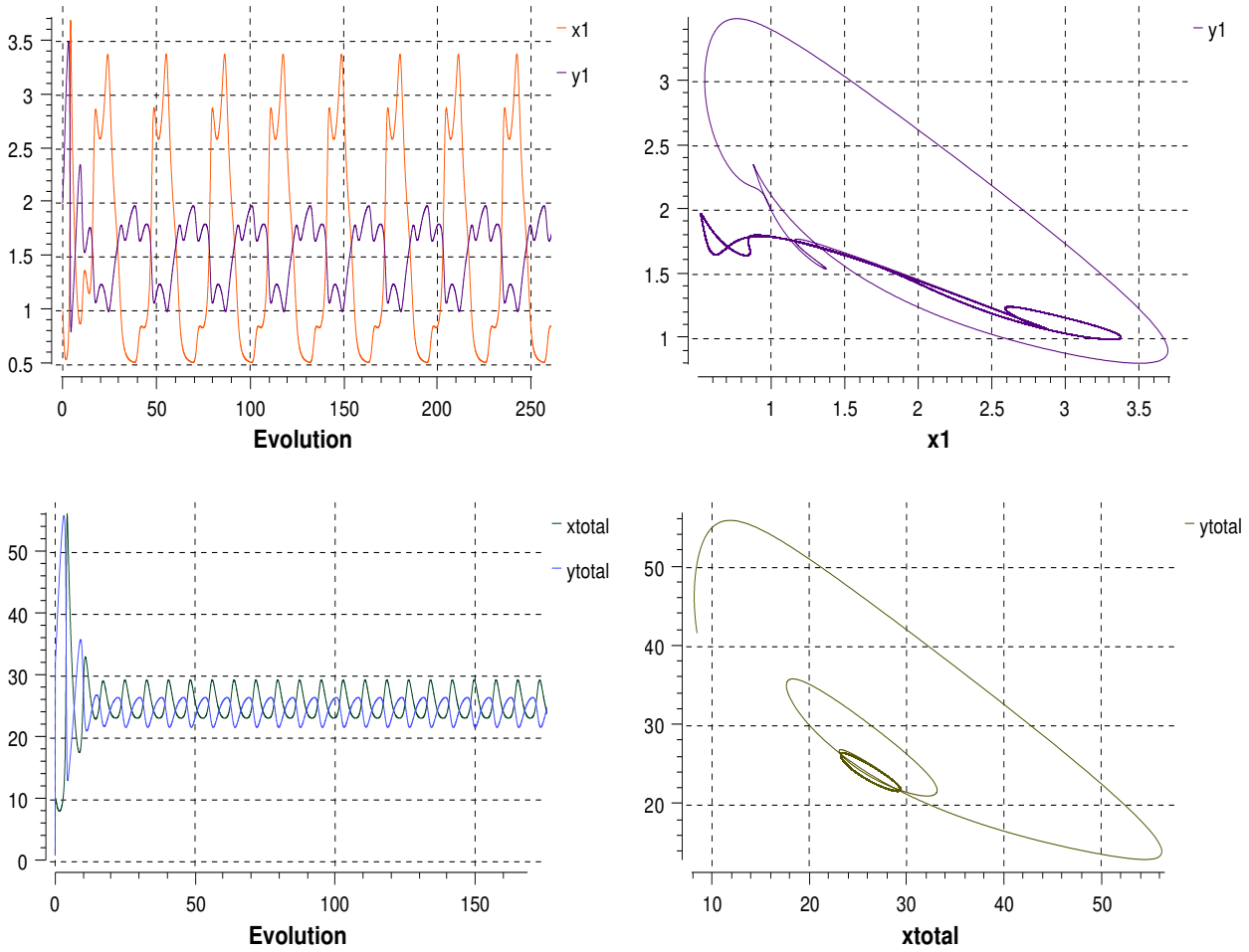

Figure 7.2: Results of Brusselator model. Tables 7.1 and 7.2 shows the parameters used for this experiment, where the initial conditions were used to separate the system into clusters as an initial experiment. Further experiments were conducted once changes in the controller were implemented.

At this stage the system has not been separated into clusters, and the RCC controller has been implemented throughout. When coupling was introduced to the system, given by terms: Dx, Dy, α, and β, it was observed that the system response remained as desired to continue with the development of the model, where the values of the coupling strength and the control strength

were modified to both separate the system into clusters and to observe the overall response. The results of this experiment can be observed in figure 7.2, where [x1,y1] was selected to demonstrate the behaviour of one of the clusters. The total response of the system shows periodical stability.

7.2.2 Response to changes in coupling and control strength in the system

The final form of the Brusselator with the RCC controller used for the following experiments is given by equations 7.7, 7.8, 7.9, and 7.10 where i and j = {1....16}.

$$\frac{\partial x_i}{\partial t} = D_x \nabla^2 x_i + \alpha x_i x_j (x_j - x_i) + a - (b+1)x + \sigma_x(x,y)x^2 y \tag{7.7}$$

$$\frac{\partial y_i}{\partial t} = D_y \nabla^2 y_i + \beta y_i y_j (y_j - y_i) + \sigma_y(y) bx - x^2 y \tag{7.8}$$

Where the control equations are as follows:

$$\sigma(x,y) = f_x e^{\xi_i q_x q_y} \qquad \sigma(y) = f_y e^{\xi_i q_x} \tag{7.9}$$

and:

$$q_x = \frac{x}{x+\mu_x} \qquad q_y = \frac{y}{y+\mu_y} \tag{7.10}$$

For this model, it was not possible to use the system parameters to separate the clusters, therefore the control parameters had to be used, which leaves the final structure as follows:

- Cluster 1:
  - Parameters: No_1, ξ_{x1}, ξ_{y1}.
  - Oscillators: [x1,y1], [x2,y2], [x3,y3], [x4,y4].
- Cluster 2:

  - Parameters: No_2, ξ_{x2}, ξ_{y2}.
  - Oscillators: [x5,y5], [x6,y6], [x7,y7], [x8,y8].

- Cluster 3:
  - Parameters: No_3, ξ_{x3}, ξ_{y3}.
  - Oscillators: [x9,y9], [x10,y10], [x11,y11], [x12,y12].

- Cluster 4:
  - Parameters: No_4, ξ_{x4}, ξ_{y4}.
  - Oscillators: [x13,y13], [x14,y14], [x15,y15], [x16,y16].

The first experiment shown consisted in observing the response of the system to a step input to activate the controller at t = 200. This was relevant to verify the structure reacts well to the implementation of the controller and further experimentation can follow. The parameter values and initial conditions used are shown in tables 7.3 and 7.4. At this stage, only the initial conditions have been used to establish the four clusters. The same was observed as for the Lengyel-Epstein system, where the parameter values could not be used to distinguish the clusters, therefore the following experiments relied on the coupling strength and the control parameters. Figure 7.3 shows the results of the experiment where it is seen that the system responds correctly to the controller. The behaviour of the oscillator mimics that of the system response which is why it was important to continue the experiments to establish differences among the clusters.

Parameter	Value
a	1
b	2.5
Dx1, Dx2	1.85
Dy1, Dy2	16.66
α	0.1
β	0.1
f_x (RCC)	1
f_y (RCC)	1
ξ_x (RCC)	0.65
ξ_y (RCC)	0.2
μ_x (RCC)	3
μ_y (RCC)	5

Table 7.3: Brusselator Experiment 1 - Parameters

Variable	Initial Value
x_1, x_5, x_9, x_{13}	1
y_1, y_5, y_9, y_{13}	2
x_2, x_6, x_{10}, x_{14}	0.5
y_2, y_6, y_{10}, y_{14}	5
x_3, x_7, x_{11}, x_{15}	1
y_3, y_7, y_{11}, y_{15}	1
x_4, x_8, x_{12}, x_{16}	0.1
y_4, y_8, y_{12}, y_{16}	0.01

Table 7.4: Brusselator Experiment 1 - Initial Conditions

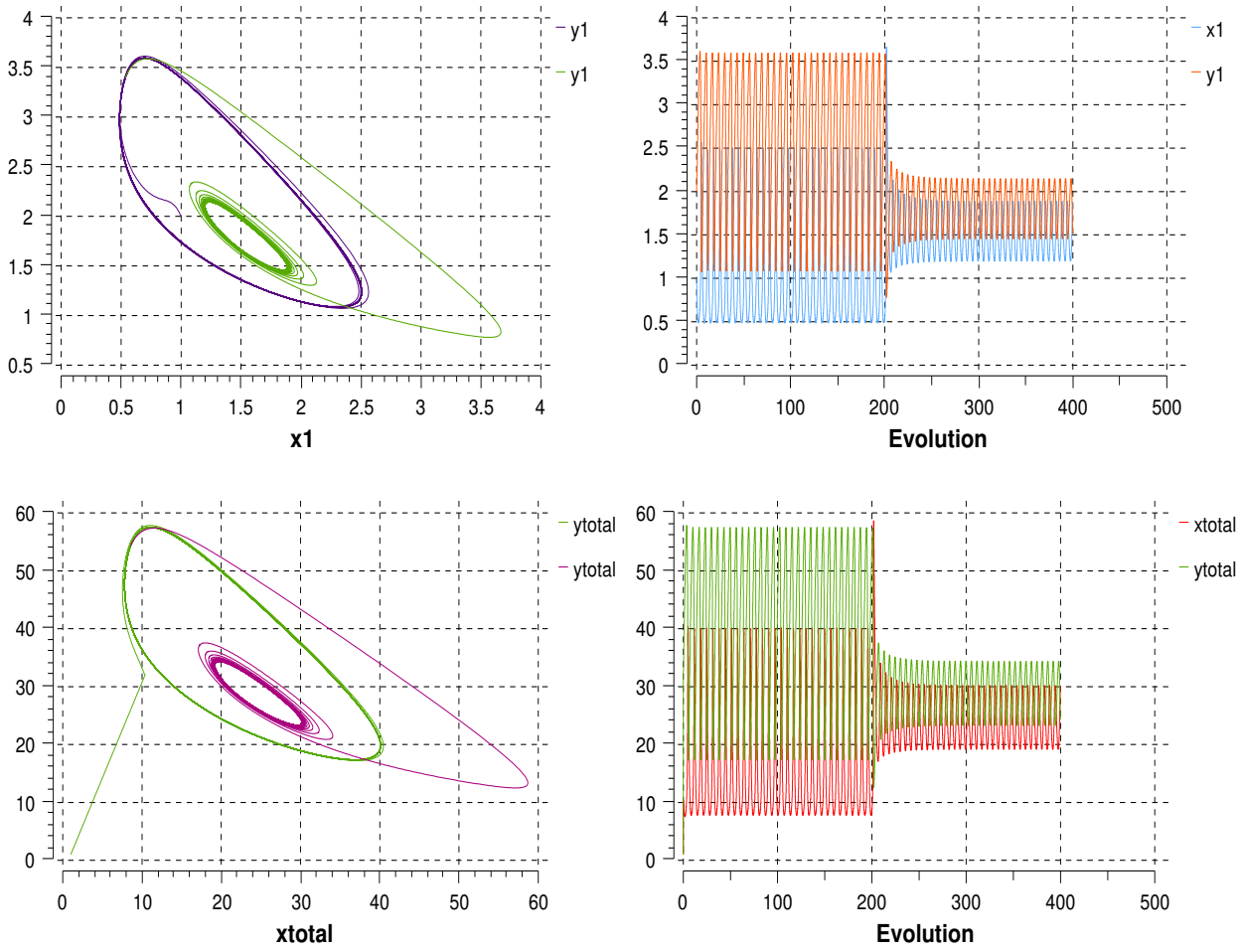

Figure 7.3: Results of the first experiment for the Brusselator with implementation of RCC. The parameters for this experiment are available in tables 7.3 and 7.4. Initial conditions were used to split the system into clusters.

The parameters for the second experiment are shown in tables 7.5 and 7.6, where the parameters for the controller are also included.

Parameter	Value
a	1
b	2.5
Dx1, Dx2	1.85
Dy1, Dy2	16.66
No_1 (step)	0.01
No_2 (step)	0.0001
No_3 (step)	0.001
No_4 (step)	0.00001
f_x, f_y (RCC)	1
μ_x, μ_y (RCC)	3, 5
ξ_{x1}, ξ_{y1} (RCC)	[0.222, 0.296]
ξ_{x2}, ξ_{y2} (RCC)	[0.234, 0.312]
ξ_{x3}, ξ_{y3} (RCC)	[0.228, 0.304]
ξ_{x4}, ξ_{y4} (RCC)	[0.24, 0.32]
Step time	0.1

Table 7.5: Brusselator Experiment 2 - Parameters

Variable	Initial Value
x_1, x_5, x_9, x_{13}	1
y_1, y_5, y_9, y_{13}	2
x_2, x_6, x_{10}, x_{14}	0.5
y_2, y_6, y_{10}, y_{14}	5
x_3, x_7, x_{11}, x_{15}	1
y_3, y_7, y_{11}, y_{15}	1
x_4, x_8, x_{12}, x_{16}	0.1
y_4, y_8, y_{12}, y_{16}	0.01

Table 7.6: Brusselator Experiment 2 - Initial Conditions

Parameters No1, No2, No3, and No4 are step functions set at the specified initial value in the

table. These are used to control the increments in coupling for the model, and along with the initial conditions, assist in separating the system into clusters. For the controller, parameters μ_x and μ_y were selected according to the amplitude of the phase space response of x and y in the stability analysis, and control parameters ξ_1, ξ_2, ξ_3, and ξ_4 have also been used to further distinguish the clusters. In this experiment, a step function was used to activate the controller and to increase the coupling strength of the system. The main reason for carrying out this experiment was to demonstrate the capability of the system to adapt to these changes by switching to different periodically stable states.

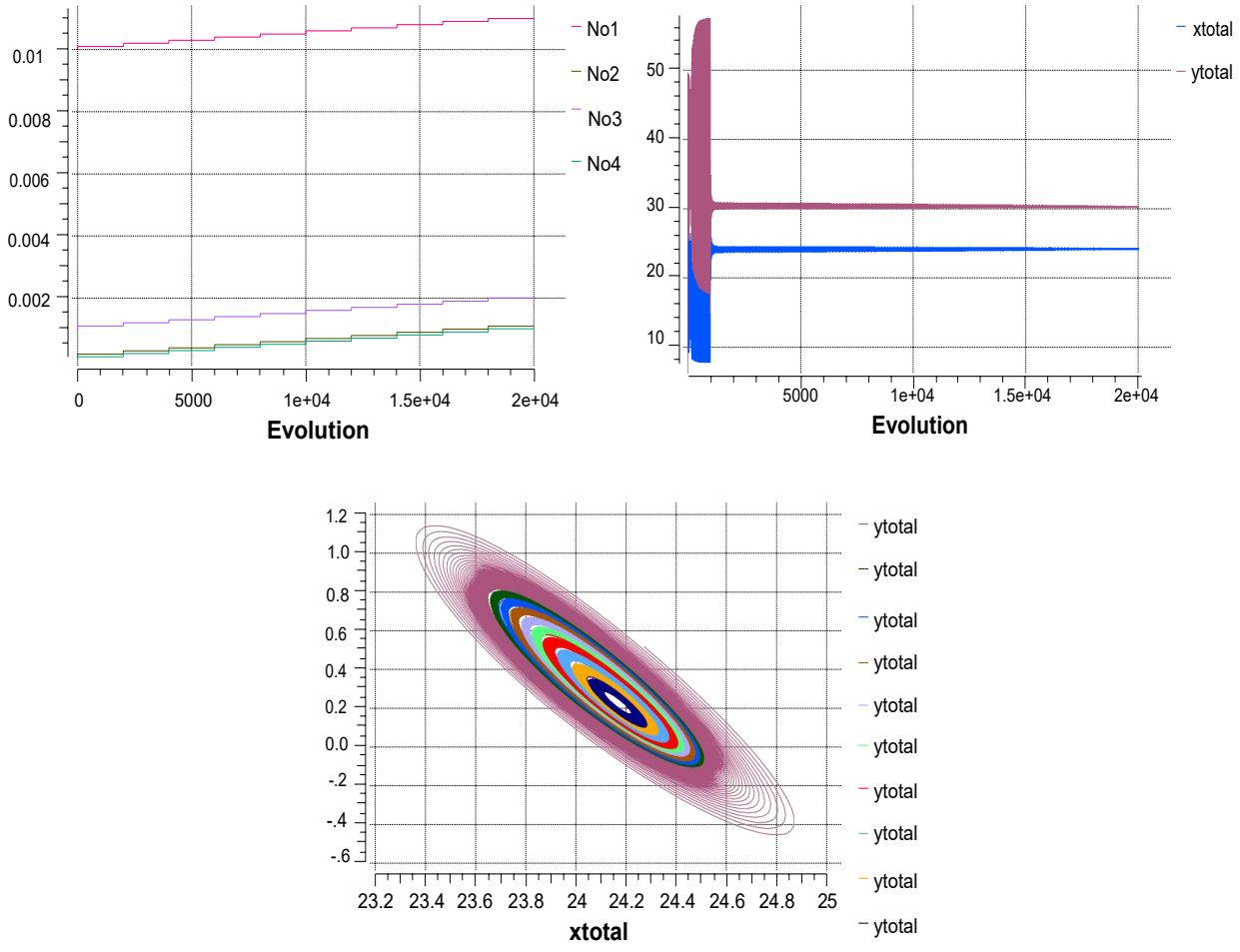

Figure 7.4: Results of the second experiment of the Brusselator with implementation of RCC. Showing the evolution of the step increases for coupling strength [top-left], evolution of the total system response [top-right], complete phase-space plot for system response [bottom-left], and colour coded periodically stable states [bottom-right]. See tables 7.5 and 7.6 for parameters.

The effects can be seen in figure 7.4, the two evolution graphs on top show the different states the system stabilizes into. The bottom image shows the same in the phase space plots of the

system response. Periodically stable states which the system stabilizes to are seen. Figure 7.5 shows the response of oscillators [x1,y1] and [x5,y5] which belong to clusters 1 and 2 respectively. The complete response is shown in the images on the left, and it has been amplified in the images on the right.

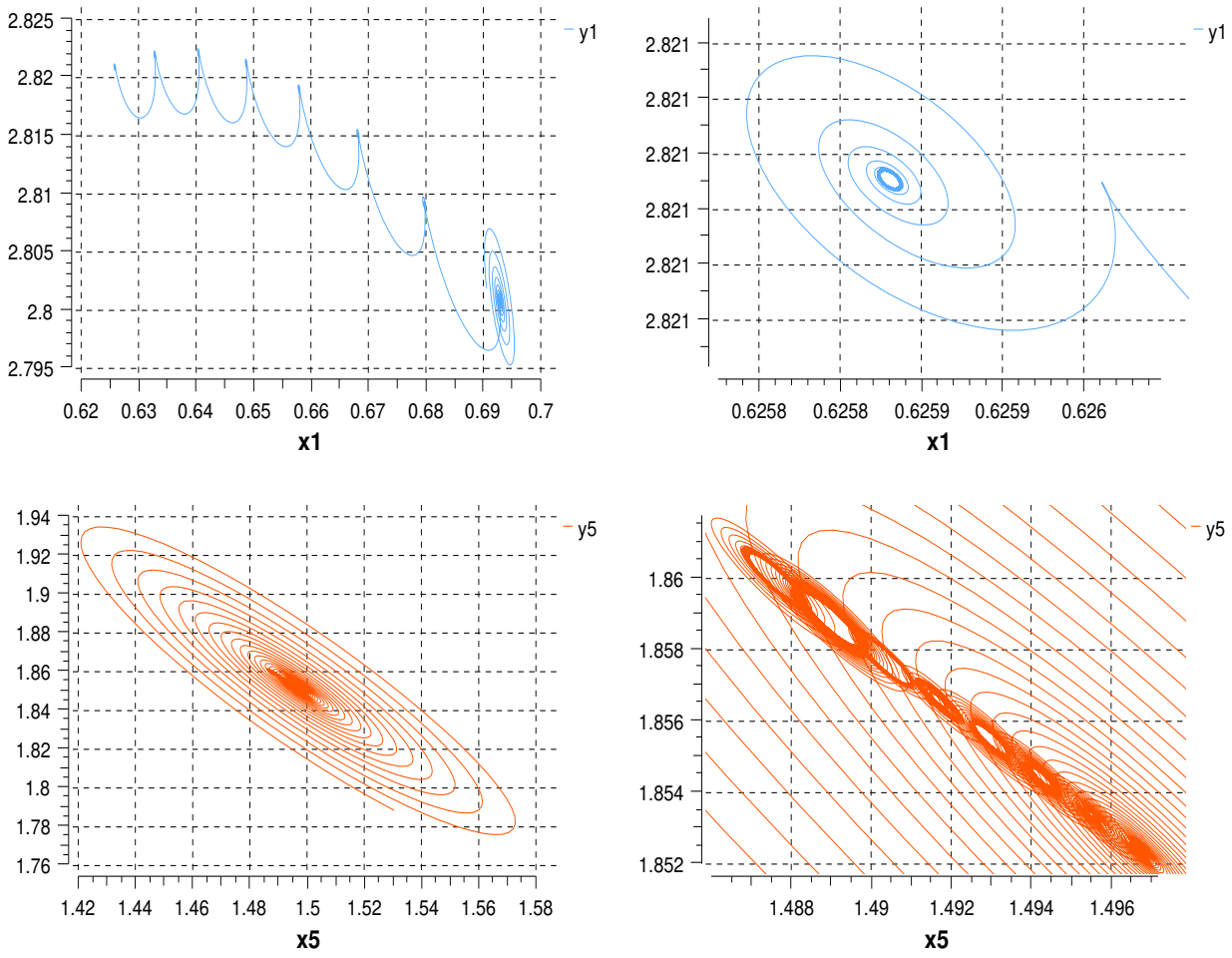

Figure 7.5: Response of oscillators [x1,y1] and [x5,y5]. The complete response is shown on the left and an amplification of the figure is provided on the right. The parameters for this experiment are available in tables 7.5 and 7.6

For the third experiment of the Brusselator, the coupling strength was decreased for every cluster, see tables 7.7 and 7.8. These changes were made to evaluate the case where communication among the clusters was not as strong as in the previous experiment. The expectation is for the system to stabilize periodically into different states as the ones shown in the previous experiment, where the control of the system seemed stronger. The results of this experiment are shown in figure 7.6, which shows the evolution of the coupling strength and the evolution

of the total system variables. The phase space plot of the total system response is shown, where all the periodically stable states are colour coded. The system is robust as it responds appropriately to the increments in coupling strength, the structure of clusters, and the strength of the control signal.

Parameter	Value
a	1
b	2.5
Dx1, Dx2	1.85
Dy1, Dy2	16.66
No_1 (step)	0.009
No_2 (step)	0.00009
No_3 (step)	0.0009
No_4 (step)	0.000009
f_x, f_y (RCC)	1
μ_x, μ_y (RCC)	3, 5
ξ_{x1}, ξ_{y1} (RCC)	[0.222, 0.296]
ξ_{x2}, ξ_{y2} (RCC)	[0.234, 0.312]
ξ_{x3}, ξ_{y3} (RCC)	[0.228, 0.304]
ξ_{x4}, ξ_{y4} (RCC)	[0.24, 0.32]
Step time	0.1

Table 7.7: Brusselator Experiment 3 - Parameters

Variable	Initial Value
x_1, x_5, x_9, x_{13}	1
y_1, y_5, y_9, y_{13}	2
x_2, x_6, x_{10}, x_{14}	0.5
y_2, y_6, y_{10}, y_{14}	5
x_3, x_7, x_{11}, x_{15}	1
y_3, y_7, y_{11}, y_{15}	1
x_4, x_8, x_{12}, x_{16}	0.1
y_4, y_8, y_{12}, y_{16}	0.01

Table 7.8: Brusselator Experiment 3 - Initial Conditions

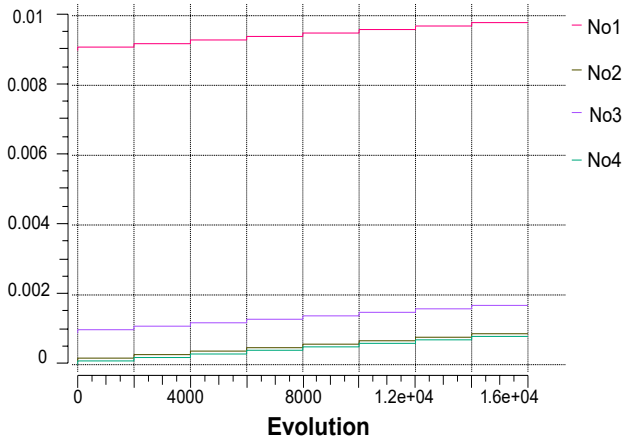

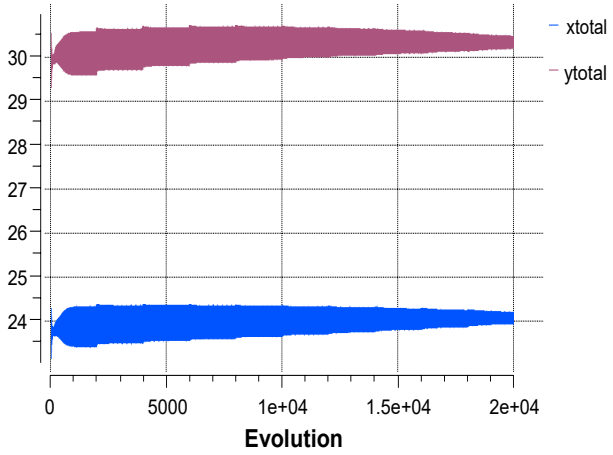

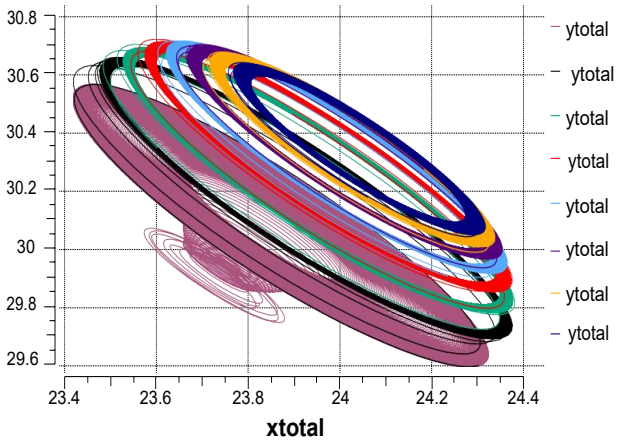

Figure 7.6: Results of the Brusselator with implementation of RCC. The evolution of the step increases for coupling strength is shown, along with the evolution of the total system response. The controlled states can be best seen in the image at the bottom left corner. Initial conditions, coupling strength, and control strength have all been used to separate the network into clusters.

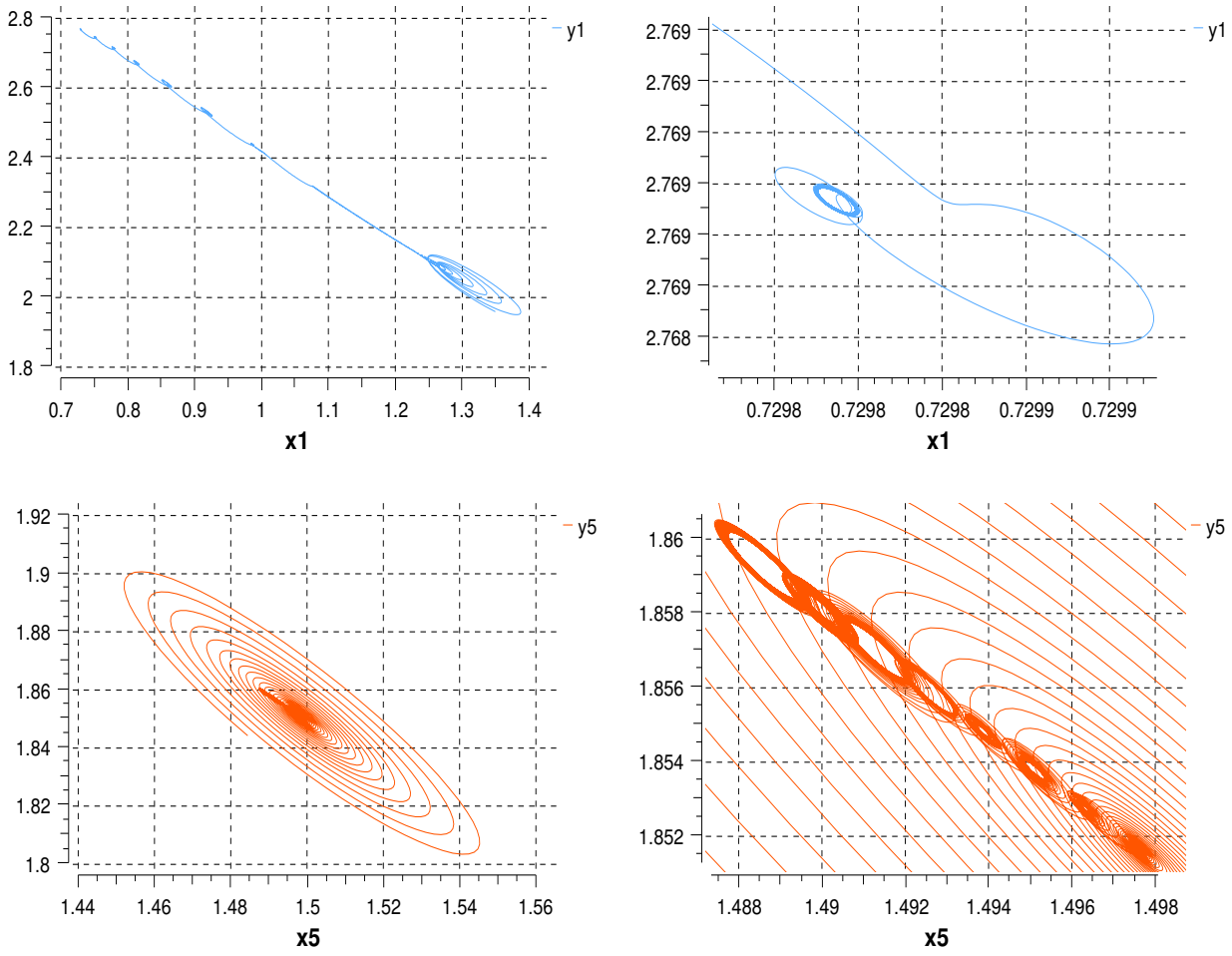

Figure 7.7: Response of oscillators [x1,y1] and [x5,y5]. The complete response is shown on the left and an amplification of the figure is provided on the right. The parameters for this experiment are available in tables 7.7 and 7.8

The aim of the final twoexperiments was to evaluate different values of coupling for the system in order to see an effect onthe response. The periodically stable states are much more defined in the third experiment, which is desired for the system in question.

7.3 Discussion

This section discusses the results obtained for the experiments performed on the Brusselator. The formulation for this model was introduced in section 7.1.2 of this work and was taken from

[37], where the parameter values used in this work are also available. The main advantage of using this formulation is that it contains non-linear coupling, which allows to maintain the system in a dynamic state as desired. Four experiments were conducted on this model, the first one was conducted in order to evaluate the adaptation to the requirement for the model, and to observe if it could be supported with the implementation of the controller. The second experiment was conducted to demonstrate the action of the controller when it was activated with a step function. experiments 3 and 4 were conducted in order to evaluate the response of the system to increments in coupling strength.

7.3.1 Response to modifications to support model structure and implementation of RCC controller

This experiment focused on setting the required parameters to split the model into clusters, implement the controller, and observe the response to determine if the structure could be supported. The initial conditions, and parameter D were used to split the system into clusters initially, and the controller was implemented using different values for x and y. These values are available in tables 7.1 and 7.2. The results are shown in figure 7.2, where the response of oscillator x_1 is shown alongside the results of the system response. These results both demonstrate the structure is supported by the model, and how it is possible to achieve a periodically stable response of the whole system, even when the behaviour at the lower level (of the oscillator) contains highly dynamic components. To continue the experiments, the parameter values were taken into consideration and the coupling strength was modified.

7.3.2 Response to modifications of coupling strength

The first experiment presented in this section uses a step function to activate the controller at t = 200. The parameters used are presented in tables 7.3 and 7.4 and the response is shown

in figure 7.3, where the response of oscillator x_1 is shown alongside the response of the system. For this case, the system response and the response of oscillator x_1 appear to be equal. This prompted the following experiments to consider other parameters to further distinguish the clusters.

For the second experiment presented in section 7.2.2, the coupling strength was modified for each cluster and turned into a step function. The control strength was modified for each cluster. The values used for these parameters are available in tables 7.5 and 7.6 and the responses are available in figures 7.4 and 7.5. Figure 7.4 shows the response of the system, including the step signal used to modify the coupling strength throughout the simulation. The response of the system shows periodical stability in 10 different states, showing changes in amplitude and shift in space. Figure 7.5 shows the amplified response of oscillators x_1 and x_5 which belong to clusters 1 and 2 respectively. The response of both of these clusters also reflects the changes in amplitude and shifts in space.

For the third experiment presented in section 7.2.2, the coupling strength was reduced for each cluster, the values used are available in tables 7.7 and 7.8 and the responses are available in figures 7.6 and 7.7. Figure 7.6 shows the response of the system, including the step signal used to modify the coupling strength throughout the simulation. The response of the system shows periodical stability in 8 different states, showing changes in amplitude and shift in space. Figure 7.7 shows the amplified response of oscillators x_1 and x_5 which belong to clusters 1 and 2 respectively. The response of both of these clusters also reflects the changes in amplitude and shifts in space.

For both experiments it is observed that the response of the clusters operates in a reduced phase space, but the changes in amplitude and shifts in space are relevant to the problem formulation. Overall the best results were observed in experiment 3, where the coupling strength was reduced for all the clusters. All experiments show the model is capable of supporting the struc-

ture and adapt to the modifications in coupling strength, which demonstrates the possibility of tailoring solutions. It was observed that, similar to the Lengyel-Epstein system, this model is limited by its system parameters. Even with these limitations, the response to the controller outperformed the results in comparison with the Lengyel-Epstein system, which could possibly be due to the fact that the formulation used for the Brusselator contains two incremental terms where the controller could be implemented. Figure 7.8 shows the results of experiment 3, which is considered as the most successful experiment. The figure shows the response to the system with the periodically stable states it stabilizes to, the same response is shown for clusters 1 and 2, and the step functions used to modify the coupling strength are also shown. Additionally, figure 7.9 shows the relationship between the coupling strength and the amplitude of the system response, where each state the system stabilizes to is clearly seen in a quasi-linear manner.

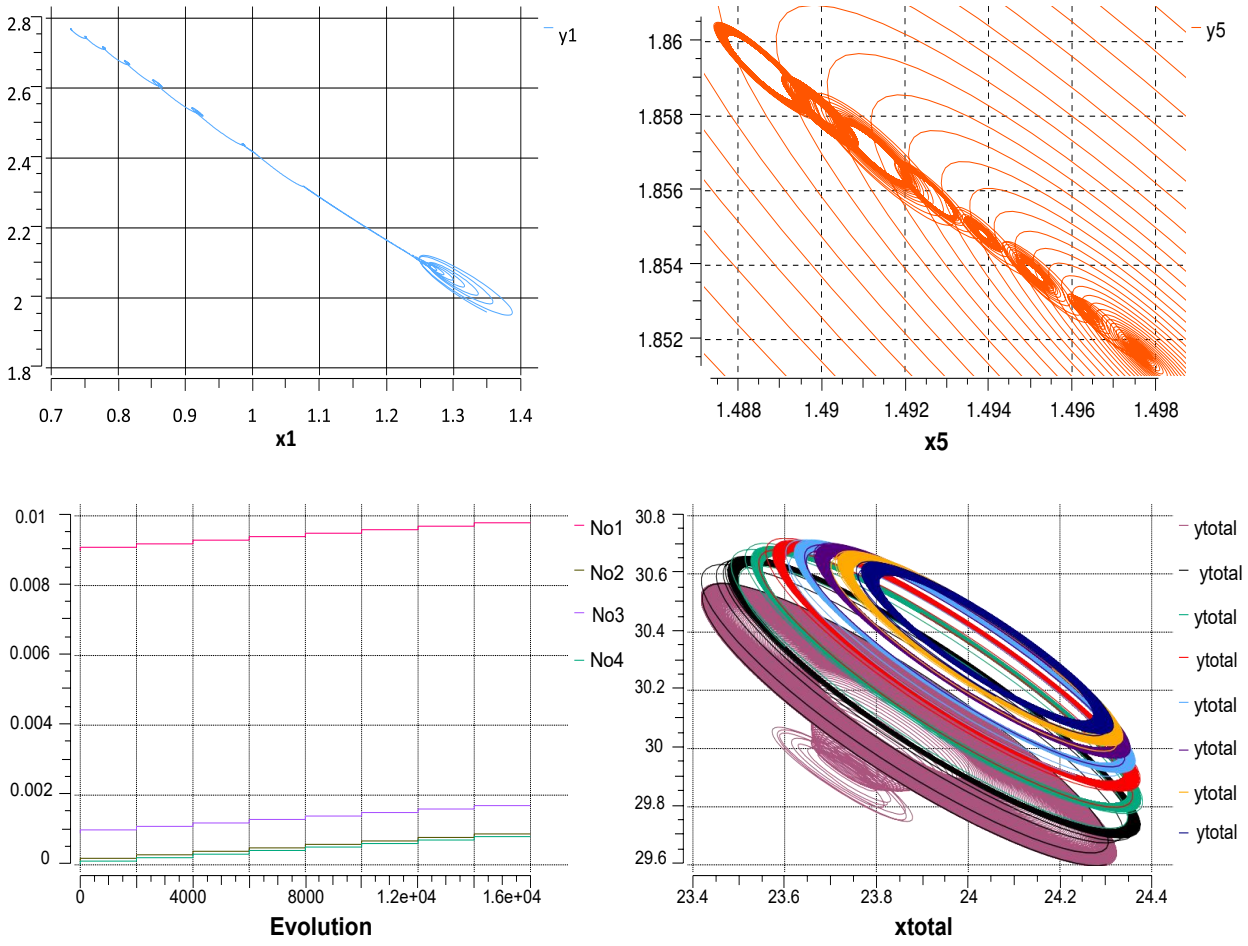

Figure 7.8: Results of experiment 3, including: phase space plots for clusters 1, 2, system response, and step functions to increase coupling strength. This experiment considered different coupling strengths and values for each cluster and the RCC controller was implemented throughout the simulation. The parameters for this experiment are available in tables 7.7 and 7.8.

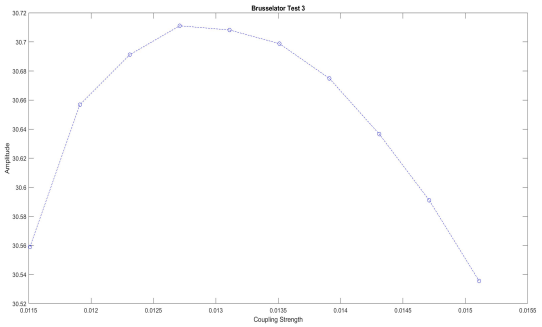

Figure 7.9: Figure showing the relationship between the coupling strength and the amplitude of the system response, each point represents a periodically stable state the system converges to.

Chapter 8

The Gray-Scott System

8.1 Model Development

The Gray-Scott cubic auto-catalysis model, developed by P. Gray, and S.K. Scott. It describes an auto-catalytic chemical reaction of the type described by equations 8.1 and 8.2. This model was chosen as it has been useful to study dynamics such as the interaction between Turing and Hopf bifurcations and the effects of time-delayed feedback control. This model has also been studied in biological systems. It's association is mostly with chemical processes as can be seen from its description of a cubic, auto-catalytic chemical reaction of the type:

$$U + 2V \rightarrow 3V \tag{8.1}$$

$$V \rightarrow P \tag{8.2}$$

This formulation represents the constant supply of U, and the removal of product P. Equation 8.1 corresponds to the auto-catalytic process where two units of V interact with a molecule of U to produce 3V. It was selected due to the wide range of dynamics it can support, especially its capability to represent travelling fronts and pulses, which can be a characteristic that equates to propagation of insulin pulses. To achieve the generation of the wide range of dynamics it

is imperative for the system to maintain far-from-equilibrium conditions [36]. This is achieved by continuously feeding U uniformly into the system. This model can be represented mathematically using the system of equations shown in equations 8.3 and 8.4. These describe three sources of increase and decrease for each of the two chemicals a and b.

$$\frac{\partial a}{\partial t} = \delta \nabla^2 a + \frac{(1-a)}{T_{res}} - a\beta^2 \tag{8.3}$$

$$\frac{\partial b}{\partial t} = \nabla^2 b + \frac{(b_0 - b)}{T_{res}} + ab^2 - k_2 b \tag{8.4}$$

8.1.1 Stability Analysis

The complete formulation for this model is presented in the next section, it contains the inclusion of coupling which was not considered for the analysis. Several combinations were tried for the initial conditions as can be seen from the ranges in figure 8.1, where the response is also shown. The kinetic equations standalone contain parameters b_0, k and T_{res}, and the incorporation of coupling adds δ.

Behaviour	Parameters and Initial Conditions
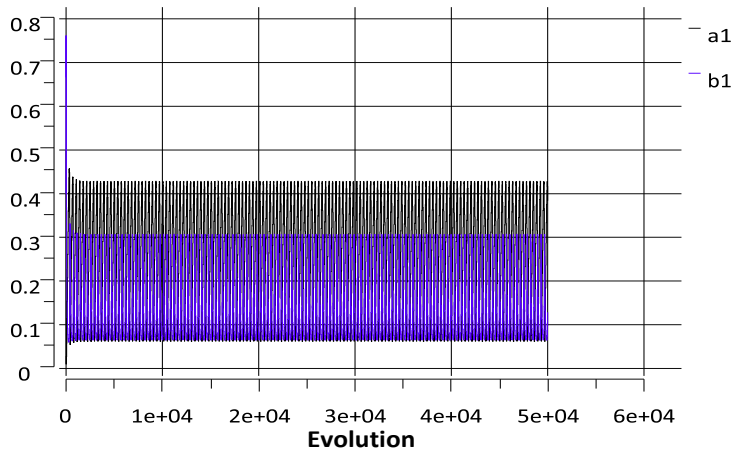	Initial Conditions • a = 0.1 - 0.9 • b = 0.2 - 0.8 Parameters • $b_0 = \frac{1}{15}$ • k = $\frac{1}{40}$ • $T_{res} = 214.5$ • $\delta = 4.6$

Figure 8.1: Stability Analysis - Gray-Scott System

8.1.2 Model Structure

This system and the parameter values to establish the baseline for the model were obtained from [56], the formulation was used in all experiments presented in the following section and is defined as follows:

$$\frac{\partial a_i}{\partial t} = \delta \nabla^2 a_i + \frac{(\sigma_a(a)(1 - a_i))}{T_{res}} - a_i \beta_i^2 \tag{8.5}$$

$$\frac{\partial b_i}{\partial t} = \nabla^2 b_i + \frac{\sigma_b(b)(b_0 - b_i)}{T_{res}} + a_i b_i^2 - k b_i \tag{8.6}$$

Where $\nabla = \frac{\partial^2}{\partial x^2}$. In order to differentiate the clusters we have parameters T_{res}, β, δ, b_0, and k. The specific values for these are mentioned in each experiment. RCC is applied on the incremental term $\frac{1-a_i}{T_{res}}$ in equation 8.5 denoted as $\sigma_a(a)$, and in the incremental term $\frac{b_0-b_i}{T_{res}}$ in 8.6 denoted as $\sigma_b(b)$. Coupling is given by term $\delta \frac{\partial^2}{\partial x^2}$ of equation 8.5, and $\frac{\partial^2}{\partial x^2}$ in equation 8.6, parameter δ will therefore be useful to control the coupling strength. The structure of the clusters including all the terms used for separating the system is defined as follows:

- Cluster 1:
  - Parameters: $T_{res}1$, ξ_1, No_1.
  - Oscillators: [a1,b1], [a2,b2], [a3,b3], [a4,b4].
- Cluster 2:
  - Parameters: $T_{res}2$, ξ_2, No_2.
  - Oscillators: [a5,b5], [a6,b6], [a7,b7], [a8,b8].
- Cluster 3:
  - Parameters: $T_{res}1$, ξ_3, No_3.
  - Oscillators: [a9,b9], [a10,b10], [a11,b11], [a12,b12].
- Cluster 4:

– Parameters: $T_{res}2$, ξ_4, No_4.

– Oscillators: [a13,b13], [a14,b14], [a15,b15], [a16,b16].

8.2 Results

8.2.1 Parameter Tuning to Support Model Structure

The stability analysis of the system is provided in section 8.1.1, where it is first mentioned that the system is capable of responding to a variety of initial conditions. This was a particular consideration along with the modification of parameter T_{res} and coupling parameters G_a and G_b; five experiments were performed. The reference parameters were taken from the work developed by Petrov et. al [56]. The aim of conducting these experiments was to observe the behaviour of the system using 16 coupled oscillators and demonstrating that all instances of the parameter values are supported. This was a necessary step in the process given that it is desired to use these parameter values to separate the system into clusters and modify the values to trigger state-shifting.

Tables 8.1 and 8.2 present the parameters for the first experiment, where parameter T_{res} was set to 240 according to the range established in [56] of $214.8 < T_{res} < 242$, where a Turing pattern with a typical stationary periodic concentration profile is observed. The coupling strength, given by Ga and Gb, was set to 0.005 Figure 8.2 shows the evolution and phase space plots of the total response of the system, and the first oscillator [a6,b6].

Parameter	Value
b_0	$\frac{1}{15}$
k	$\frac{1}{40}$
δ	4.6
T_{res}	240
G_a	0.005
G_b	0.005

Table 8.1: Gray-Scott Experiment 1 - Parameters

Variable	Initial Value
a_1, a_3, a_6, a_7	0.5
b_1, b_2, b_4, b_5, b_8	0.4
a_2	0.6
b_3, b_9	0.3
a_4, a_{10}	0.7
a_5, a_9	0.1
a_8, a_10	0.9
b_6	0.2

Table 8.2: Gray-Scott Experiment 1 - Initial Conditions

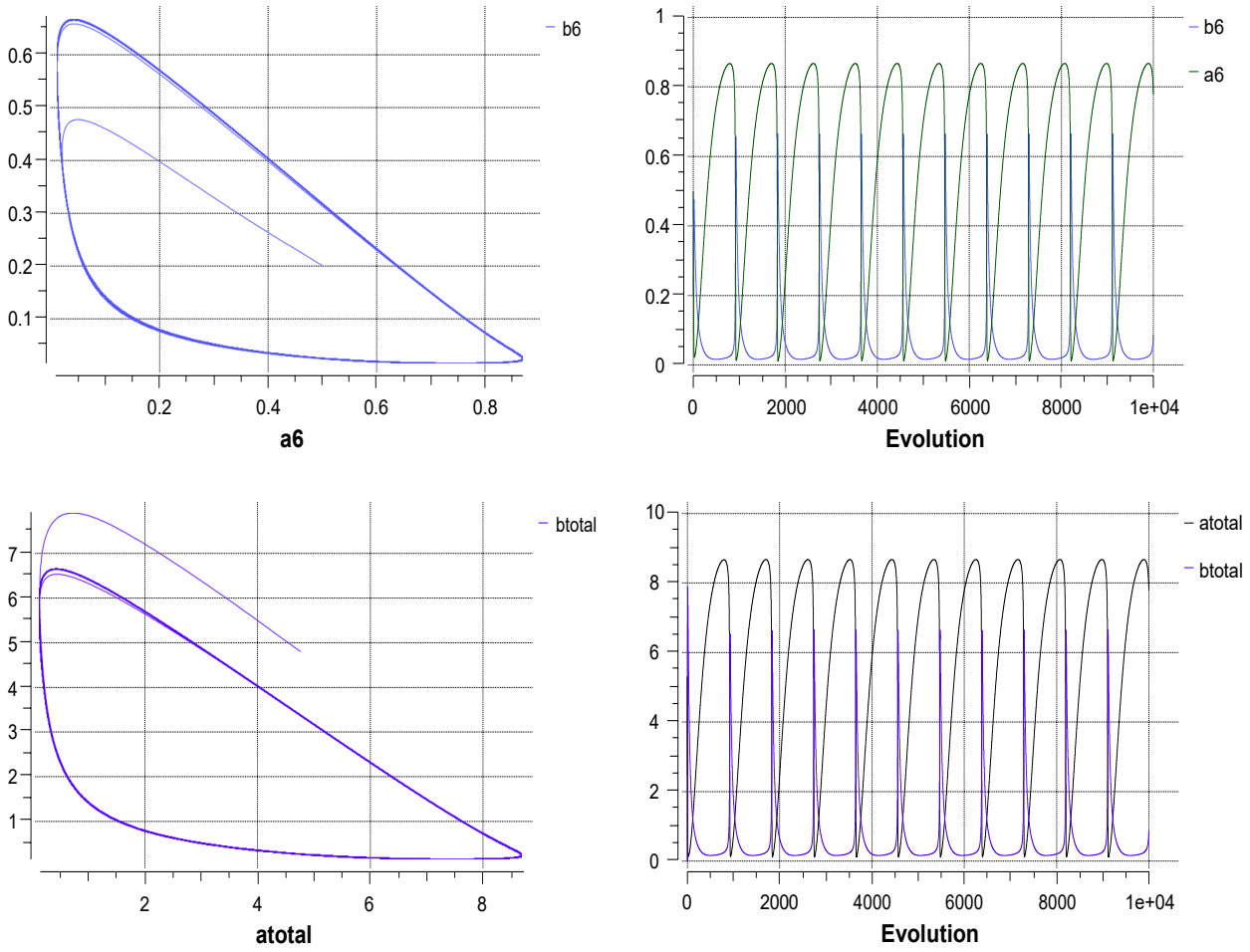

Figure 8.2: Results of the first experiment of the Gray-Scott model, where $T_{res} = 240$ and the coupling strength is set to 0.005. Following the recommendations in [56], the parameter values were set as described in tables 8.1 and 8.2.

Tables 8.3 and 8.4 presents the parameters for the first experiment, where parameter T_{res} was set to 214.5 and the coupling strength remains at Ga = Gb = 0.005. Figure 8.3 shows the evolution and phase space plots of the total response of the system, and one of the oscillators [a6,b6]. The difference in periodic stability between these two experiments is evident and contributed to separating the system into clusters in further stages of development presented in the following section of this chapter. The system behaviour with these two different values is widely different, which increases the biological relevance, where it is expected that all clusters will behave differently according to the instance of local feedback detected, meaning the surrounding level of glucose.

Parameter	Value
b_0	$\frac{1}{15}$
k	$\frac{1}{40}$
δ	4.6
T_{res}	214.5
G_a	0.005
G_b	0.005

Table 8.3: Gray-Scott Experiment 2 - Parameters

Variable	Initial Value
a_1, a_3, a_6, a_7	0.5
b_1, b_2, b_4, b_5, b_8	0.4
a_2	0.6
b_3, b_9	0.3
a_4, a_{10}	0.7
a_5, a_9	0.1
a_8, a_10	0.9
b_6	0.2

Table 8.4: Gray-Scott Experiment 2 - Initial Conditions

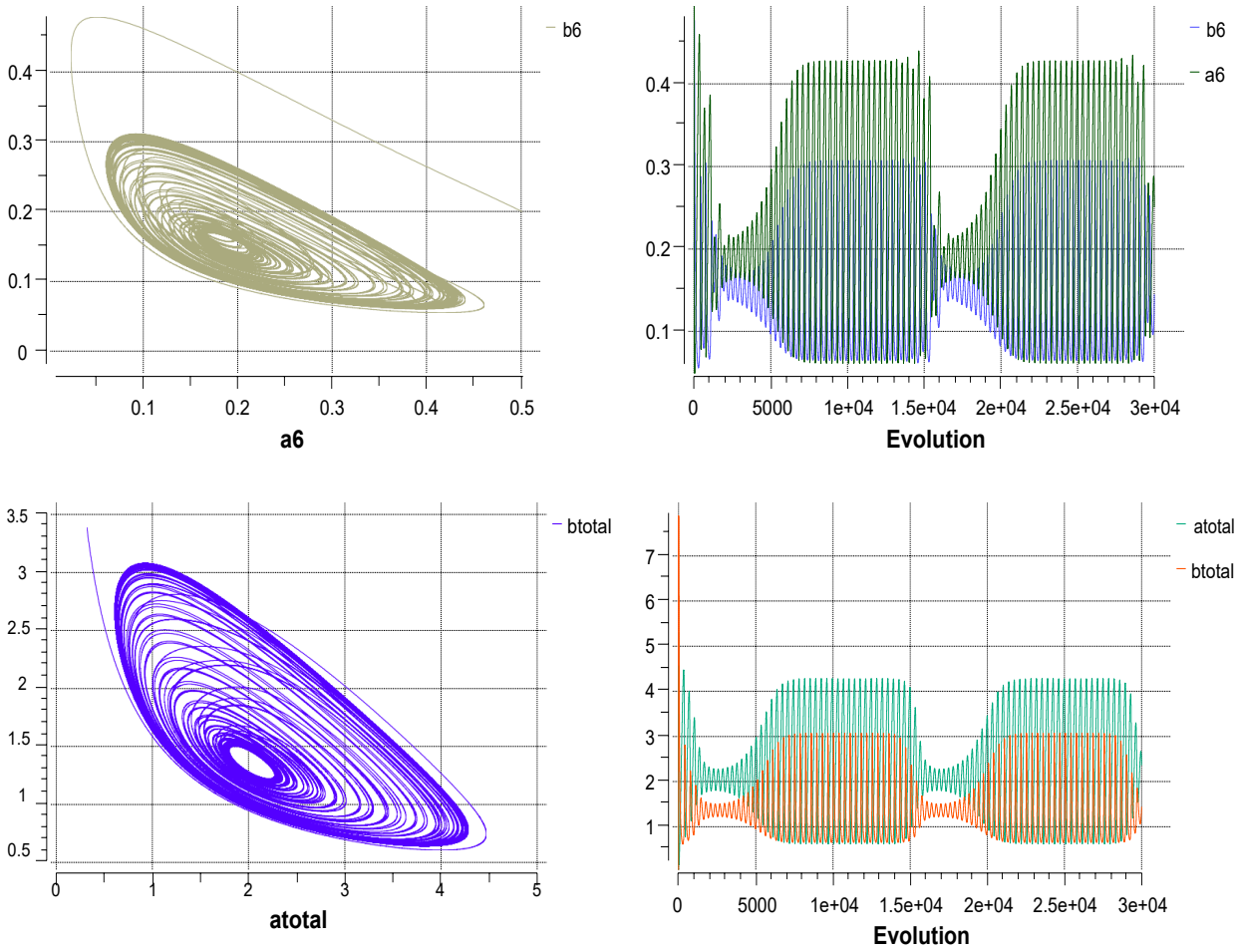

Figure 8.3: Results of the second experiment of the Gray-Scott model, where $T_{res} = 214.5$ and the coupling strength is set to 0.005. Following the recommendations in [56], the parameter values were set as described in tables 8.3 and 8.4.

Experiments 3, 4, and 5 were performed in order to observe the effect of minor changes to the coupling strength to continue establishing the ranges of operation to sustain the desired behaviour. This was needed to determine the ranges that would adapt best to the increments introduced by the step function, the results of which are shown in the following section. Tables 8.5 - 8.10 present the parameter values used for these experiments, where the coupling parameter was set to 0.006 and 0.003, and 0.002 respectively. The results can be observed in figures 8.4 -

8.6. Knowing that the system can tolerate these ranges of values in terms of coupling strength facilitates the implementation of the signals in charge of triggering state-shifting in the model.

Parameter	Value
b_0	$\frac{1}{15}$
k	$\frac{1}{40}$
δ	4.6
T_{res}	214.5
G_a	0.006
G_b	0.006

Table 8.5: Gray-Scott Experiment 3 - Parameters

Variable	Initial Value
a_1, a_3, a_6, a_7	0.5
b_1, b_2, b_4, b_5, b_8	0.4
a_2	0.6
b_3, b_9	0.3
a_4, a_{10}	0.7
a_5, a_9	0.1
a_8, a_10	0.9
b_6	0.2

Table 8.6: Gray-Scott Experiment 3 - Initial Conditions

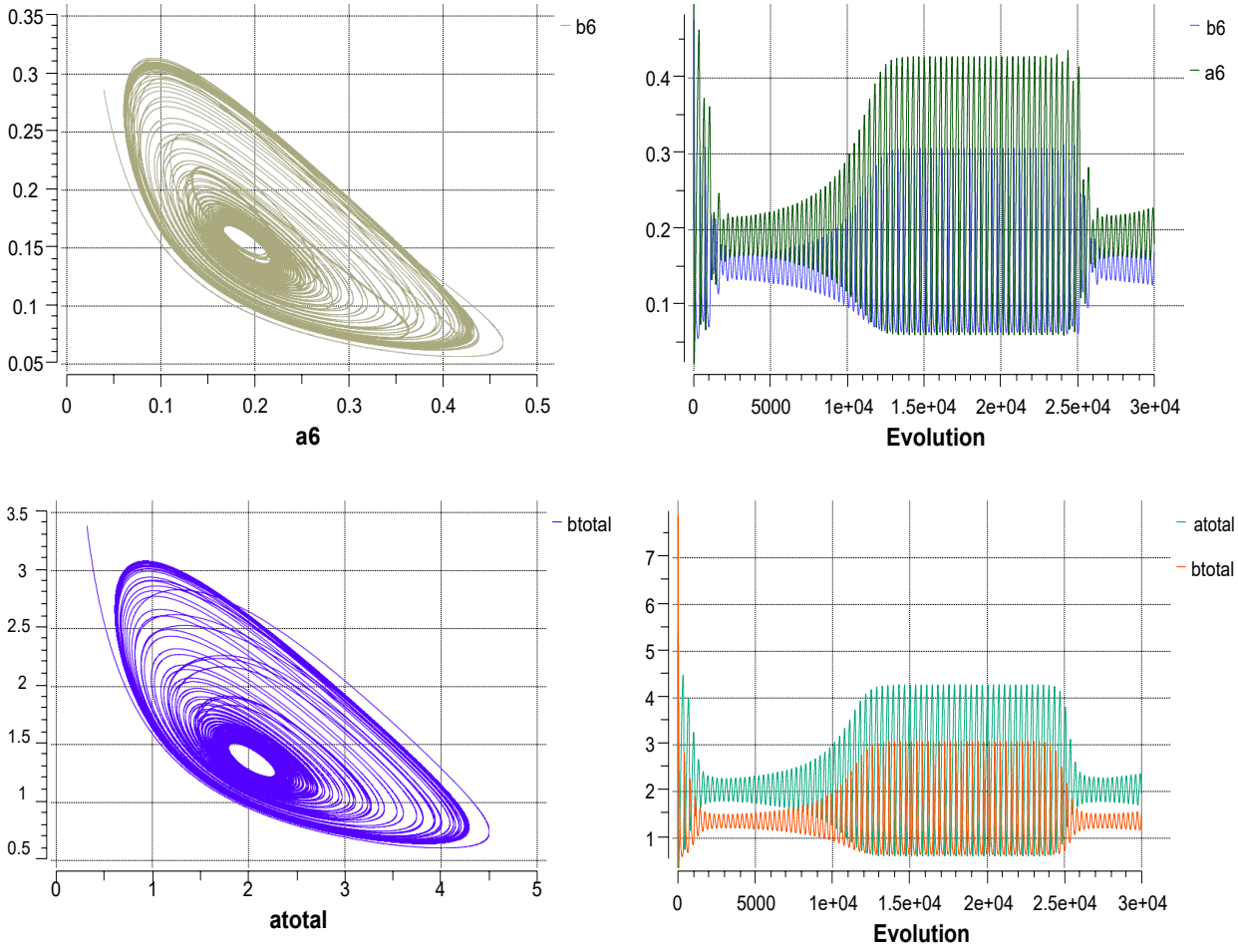

Figure 8.4: Results of the third experiment of the Gray-Scott model, where $T_{res} = 214.5$ and the coupling strength is set to 0.006. Following the recommendations in [56], the parameter values were set as described in tables 8.5 and 8.6.

Parameter	Value
b_0	$\frac{1}{15}$
k	$\frac{1}{40}$
δ	4.6
T_{res}	214.5
G_a	0.003
G_b	0.003

Table 8.7: Gray-Scott Experiment 4 - Parameters

Variable	Initial Value
a_1, a_3, a_6, a_7	0.5
b_1, b_2, b_4, b_5, b_8	0.4
a_2	0.6
b_3, b_9	0.3
a_4, a_{10}	0.7
a_5, a_9	0.1
a_8, a_10	0.9
b_6	0.2

Table 8.8: Gray-Scott Experiment 4 - Initial Conditions

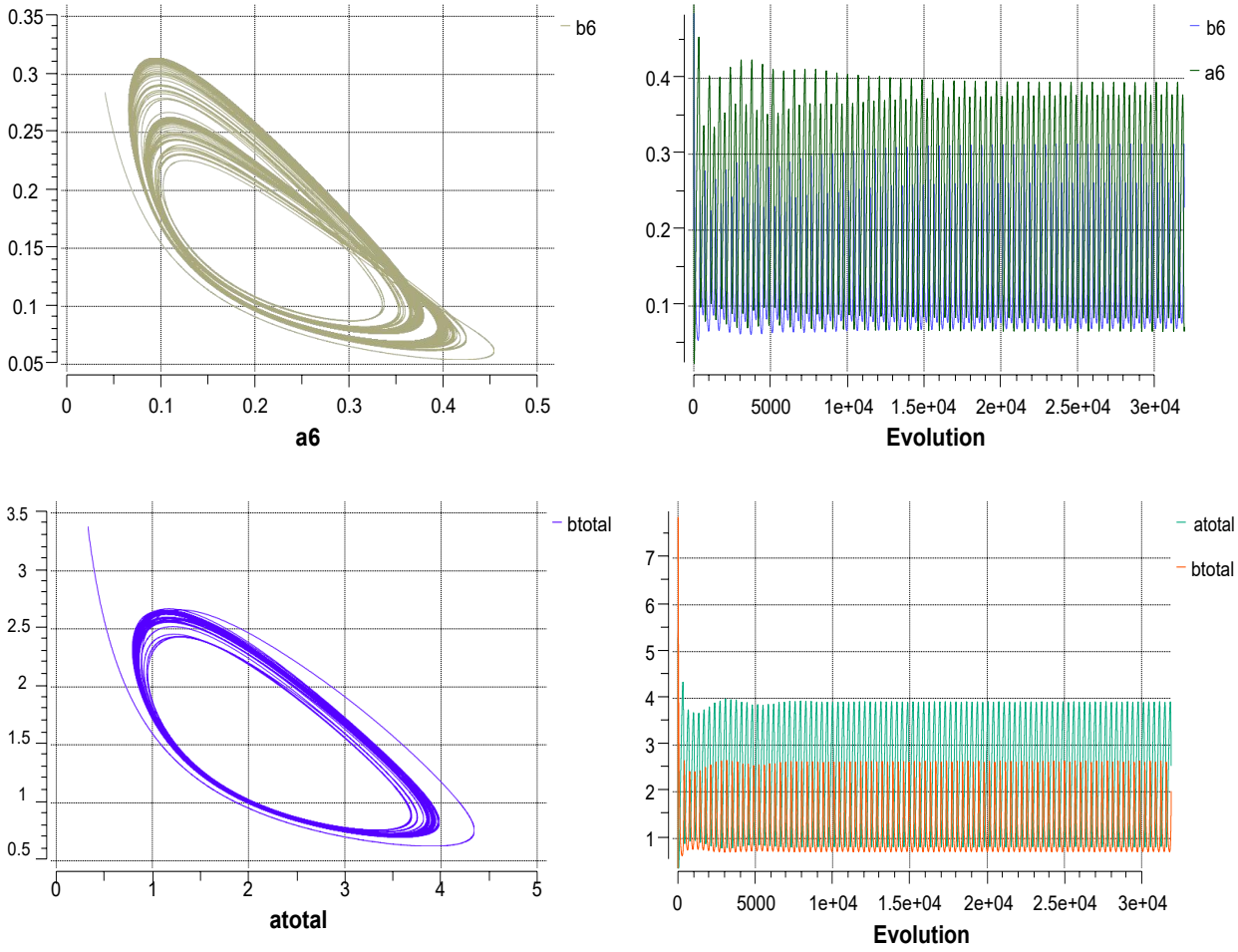

Figure 8.5: Results of the fourth experiment of the Gray-Scott model, where $T_{res} = 214.5$ and the coupling strength is set to 0.003. Following the recommendations in [56], the parameter values were set as described in tables 8.5 and 8.6.

Parameter	Value
b_0	$\frac{1}{15}$
k	$\frac{1}{40}$
δ	4.6
T_{res}	214.5
G_a	0.002
G_b	0.002

Table 8.9: Gray-Scott Experiment 5 - Parameters

Variable	Initial Value
a_1, a_3, a_6, a_7	0.5
b_1, b_2, b_4, b_5, b_8	0.4
a_2	0.6
b_3, b_9	0.3
a_4, a_{10}	0.7
a_5, a_9	0.1
a_8, a_10	0.9
b_6	0.2

Table 8.10: Gray-Scott Experiment 5 - Initial Conditions

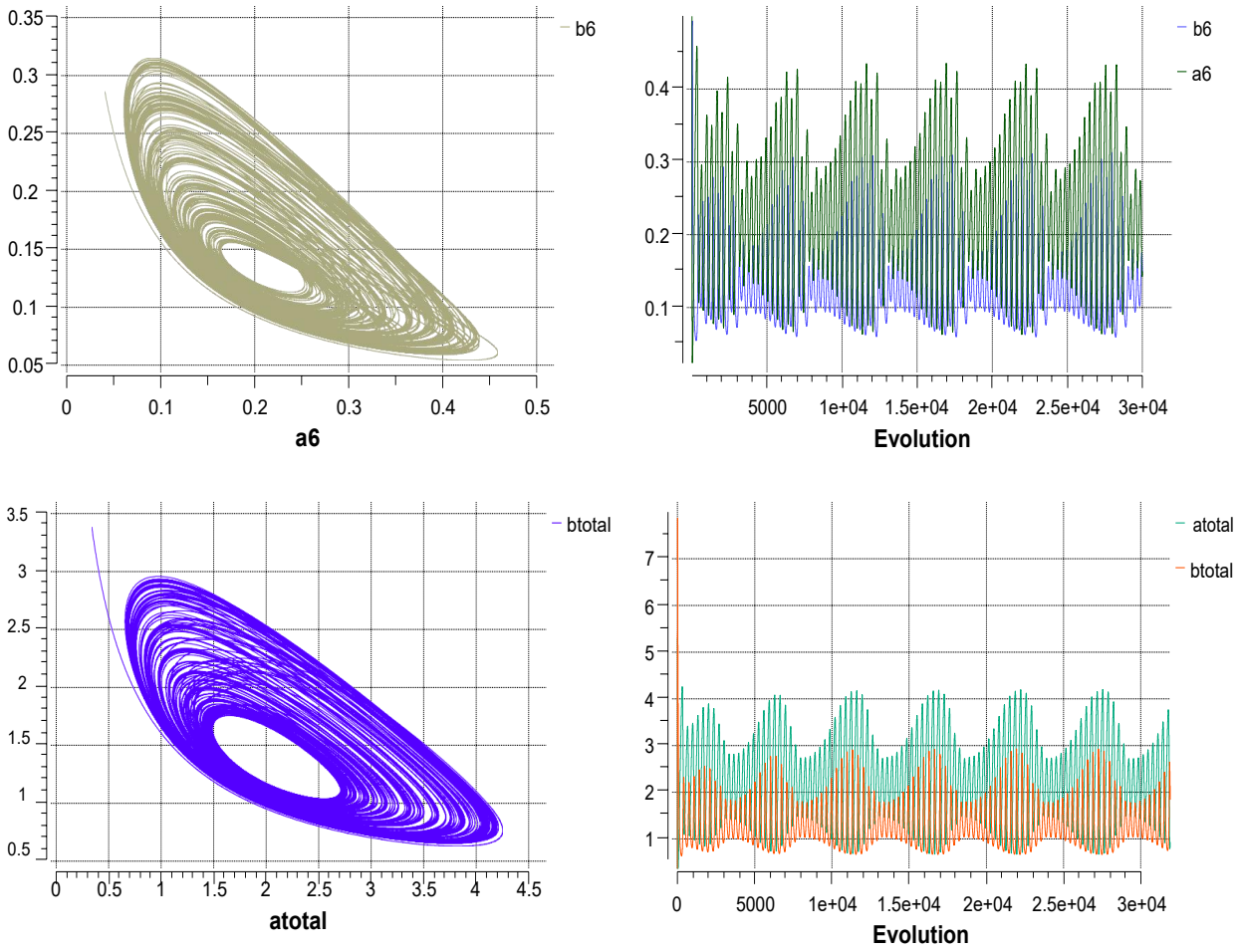

Figure 8.6: Results of the fifth experiment of the Gray-Scott model, where $T_{res} = 214.5$ and the coupling strength is set to 0.002. Following the recommendations in [56], the parameter values were set as described in tables 8.7 and 8.8.

8.2.2 Response to changes in coupling and control strength in the system

The final form of the Gray-Scott system with the RCC controller used for the following experiments is given by equations 8.7, 8.8, 8.9, and 8.10 where i = {1....16}.

$$\frac{\partial a_i}{\partial t} = \delta \nabla^2 a_i + \frac{\sigma_a(a)(1 - a_i)}{T_{res}} - a_i \beta_i^2 \tag{8.7}$$

$$\frac{\partial b_i}{\partial t} = \nabla^2 b_i + \frac{\sigma_b(b)(b_0 - b_i)}{T_{res}} + a_i b_i^2 - k b_i \tag{8.8}$$

Where the control equations are as follows:

$$\sigma(a) = f_a e^{\xi_i q_a} \qquad \sigma(b) = f_b e^{\xi_i q_b} \tag{8.9}$$

and:

$$q_a = \frac{a}{a + \mu_a} \qquad q_b = \frac{b}{b + \mu_b} \tag{8.10}$$

Experiment 1 consisted in observing the response of the controller to different values of parameter T_{res}. This experiment was split into three parts:

1. Experiment 1a: The parameters for this experiment are available in tables 8.11 and 8.12, where it can be seen that T_{res} is set to 240 and the control strength is set to 0.2. Control is applied throughout the simulation and it is observed how the RCC is not strong enough to stabilize the system into periodic orbits. The results are shown in figure 8.2.2.

2. Experiment 1b: The parameters for this experiment are available in tables 8.13 and 8.14, where it can be seen that T_{res} is set to 240 and the control strength is increased to 0.4. For this experiment, a step function is used to activate the controller at t = 25,000. The results are shown in figure 8.2.2, where it is now seen that the system is periodically stable.

3. Experiment 1c: The parameters for this experiment are available in tables 8.15 and 8.16, where it can be seen that T_{res} is set to 214.5 and the control strength is set to 0.2. A step function is used to activate the controller at t = 25,000. The results are shown in figure 8.2.2, for this experiment the controller was strong enough to stabilize the system into periodic orbits.

Parameter	Value
b_0	$\frac{1}{15}$
k	$\frac{1}{40}$
δ	4.6
T_{res}	240
G_a	0.005
G_b	0.005
f_a, f_b (RCC)	1,1
μ_a, μ_b (RCC)	1, 1
ξ_a, ξ_b (RCC)	0.2, 0.2

Table 8.11: Gray-Scott Experiment 1a - Parameters

Variable	Initial Value
a_1, a_3, a_6, a_7, a_{10}, a_{12}, a_{13}, a_{15}	0.5
b_1, b_2, b_4, b_5, b_8, b_{11}, b_{14}, b_{16}	0.4
a_2, a_{11}	0.6
b_3, b_9, b_{13}	0.3
a_4, b_{10}, b_{15}	0.7
a_5, a_9, a_{14}	0.1
a_8, a_16	0.9
b_6, b_12	0.2
b_7	0.8

Table 8.12: Gray-Scott Experiment 1a - Initial Conditions

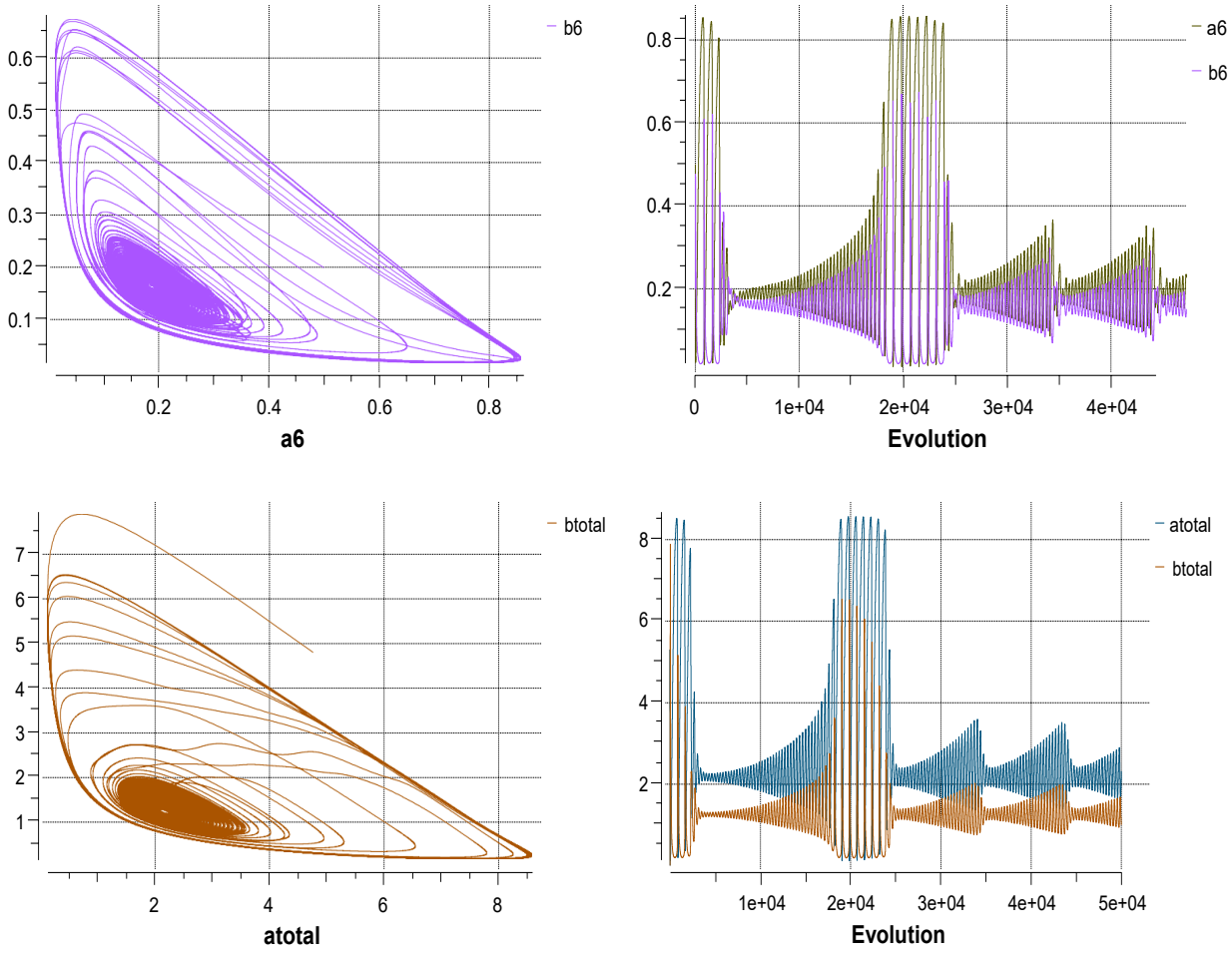

Figure 8.7: Results of experiment 1a with Gray-Scott model, where control is applied on the whole signal. The phase space plots for oscillator [a_6,b_6] and the total response of the system are included. Parameter T_{res} was set to 240

Parameter	Value
b_0	$\frac{1}{15}$
k	$\frac{1}{40}$
δ	4.6
T_{res}	240
G_a	0.005
G_b	0.005
f_a, f_b (RCC)	1, 1
μ_a, μ_b (RCC)	1, 1
ξ_a, ξ_b (RCC)	0.4, 0.4

Table 8.13: Gray-Scott Experiment 1b - Parameters

Variable	Initial Value
a_1, a_3, a_6, a_7, a_{10}, a_{12}, a_{13}, a_{15}	0.5
b_1, b_2, b_4, b_5, b_8, b_{11}, b_{14}, b_{16}	0.4
a_2, a_{11}	0.6
b_3, b_9, b_{13}	0.3
a_4, b_{10}, b_{15}	0.7
a_5, a_9, a_{14}	0.1
a_8, a_16	0.9
b_6, b_12	0.2
b_7	0.8

Table 8.14: Gray-Scott Experiment 1b - Initial Conditions

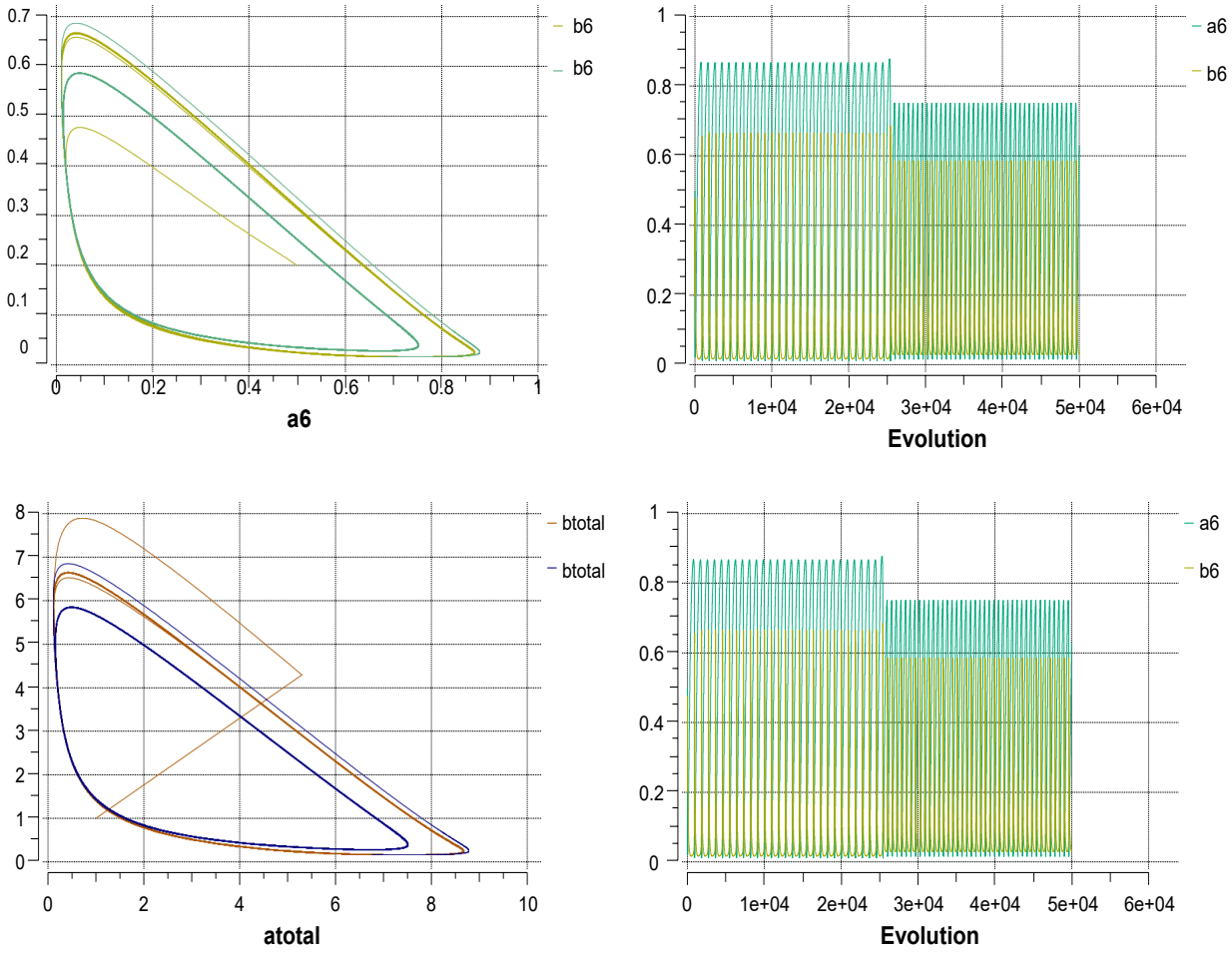

Figure 8.8: Results of experiment 1b with Gray-Scott model. A step function activates the controller at $t = 25,000$. The phase space plots for oscillator [a_6,b_6] and the total response of the system are included. Parameter T_{res} was set to 240

Parameter	Value
b_0	$\frac{1}{15}$
k	$\frac{1}{40}$
δ	4.6
T_{res}	214.5
G_a	0.005
G_b	0.005
f_a, f_b (RCC)	1, 1
μ_a, μ_b (RCC)	1, 1
ξ_a, ξ_b (RCC)	0.2, 0.2

Table 8.15: Gray-Scott Experiment 1c - Parameters

Variable	Initial Value
a_1, a_3, a_6, a_7, a_{10}, a_{12}, a_{13}, a_{15}	0.5
b_1, b_2, b_4, b_5, b_8, b_{11}, b_{14}, b_{16}	0.4
a_2, a_{11}	0.6
b_3, b_9, b_{13}	0.3
a_4, b_{10}, b_{15}	0.7
a_5, a_9, a_{14}	0.1
a_8, a_16	0.9
b_6, b_12	0.2
b_7	0.8

Table 8.16: Gray-Scott Experiment 1c - Initial Conditions

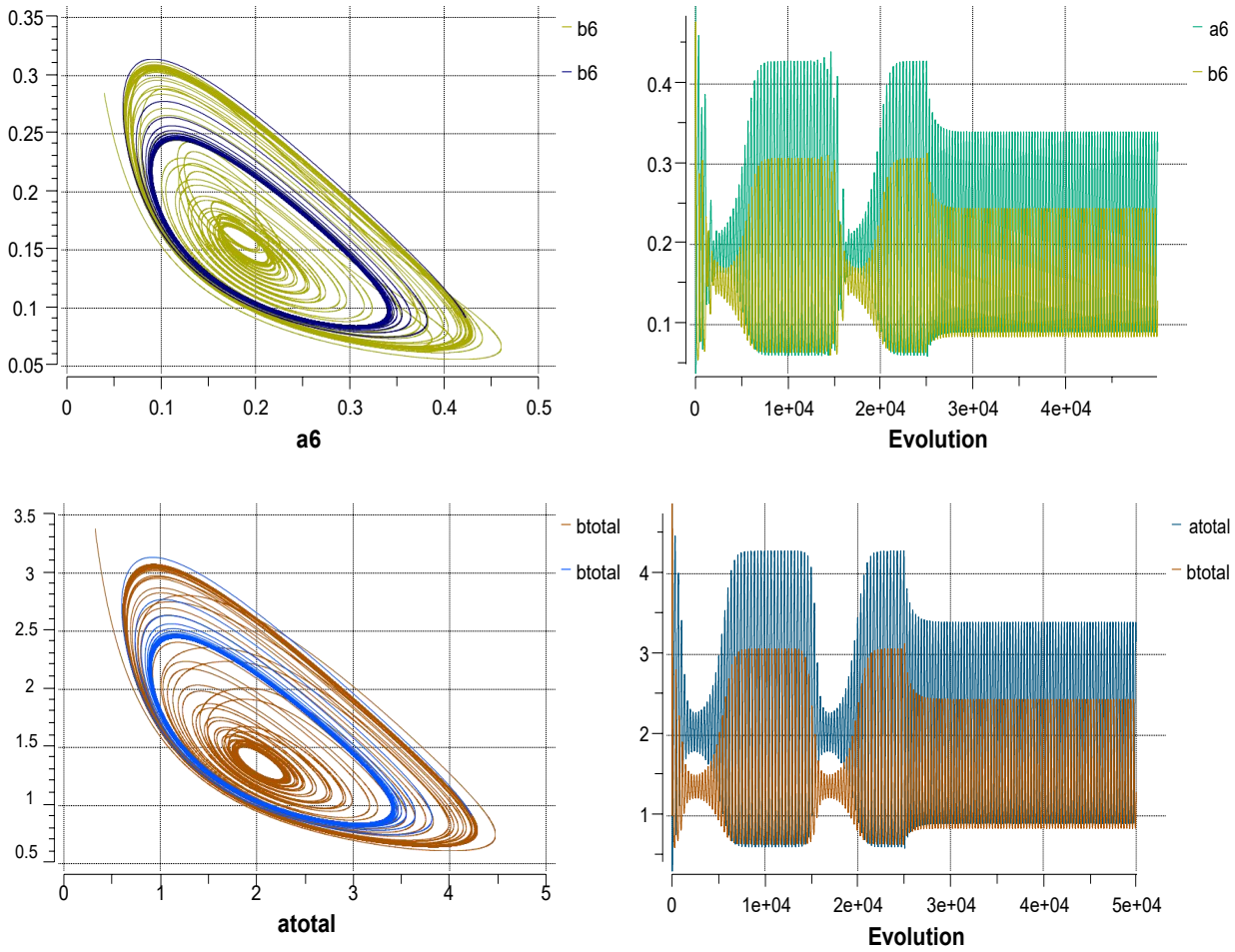

Figure 8.9: Results of experiment 1c with Gray-Scott model. A step function activates the controller at $t = 25,000$. The phase space plots for oscillator [a_6,b_6] and the total response of the system are included. Parameter T_{res} was set to 214.5

The aim of experiment 1 was to continue tuning the system, but with the effect of the controller incorporated. The results assisted in defining the ranges of behaviour for the controller and the effect this would have on the structure. It was proven that the control strength could be modified accordingly, and it was then possible to continue tuning the system with the controller implemented as well as the step input to modify the coupling strength. From the

results described in section 8.2.1 it was observed that the system would provide a wide range of dynamics when the coupling strength was modified. For the following experiment, a step function was used to increment the coupling strength throughout the simulation, with the RCC controller implemented. The aim of conducting this experiment also related to further the tuning of the system, except this time, modifying the coupling strength was the main focus. Tables 8.17 and 8.18 contains the parameter values used for this experiment, where the initial values for the coupling functions are set as 0.009 for cluster 1, 0.0007 for cluster 2, 0.006 for cluster 3, and 0.0005 for cluster 4. For the purpose of this, and further experiments considering a step increase in the coupling/control strength, the variable is referred to as No_i (where i = 1,2,3,4) instead of G_a and G_b. The results are shown in figures 8.10 and 8.11. Figure 8.10 shows the five different states the system exhibits according to the increments in coupling. The evolution of the total system response and the step functions are shown in figure 8.11.

Parameter	Value
b_0	$\frac{1}{15}$
k	$\frac{1}{40}$
δ	4.6
$T_{res}1$	214.5
$T_{res}2$	240
No_1(step)	0.009
No_2(step)	0.0007
No_3(step)	0.006
No_4(step)	0.0005
f_a, f_b (RCC)	1, 1
μ_a, μ_b (RCC)	1, 1
ξ_1, ξ_3 (RCC)	0.2, 0.2
ξ_2, ξ_4 (RCC)	0.4, 0.4

Table 8.17: Coupling Strength Experiment - Parameters

Variable	Initial Value
a_1, a_3, a_6, a_7, a_{10}, a_{12}, a_{13}, a_{15}	0.5
b_1, b_2, b_4, b_5, b_8, b_{11}, b_{14}, b_{16}	0.4
a_2, a_{11}	0.6
b_3, b_9, b_{13}	0.3
a_4, b_{10}, b_{15}	0.7
a_5, a_9, a_{14}	0.1
a_8, a_16	0.9
b_6, b_12	0.2
b_7	0.8

Table 8.18: Coupling Strength Experiment - Initial Conditions

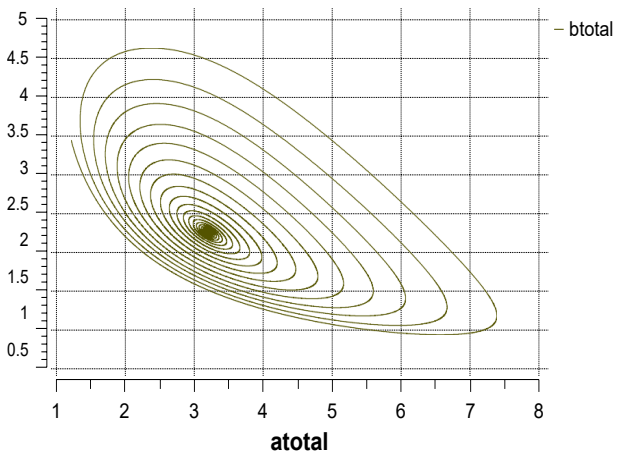

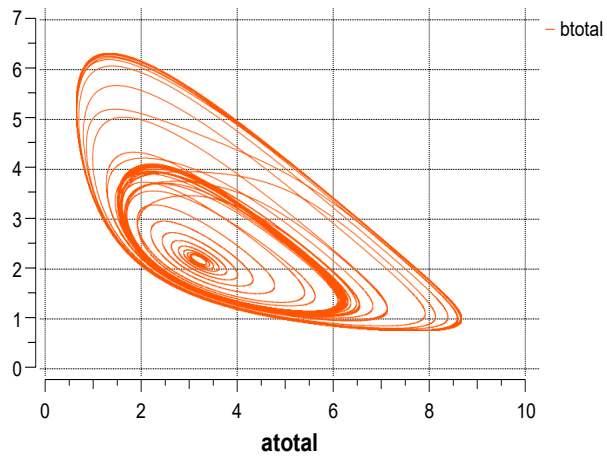

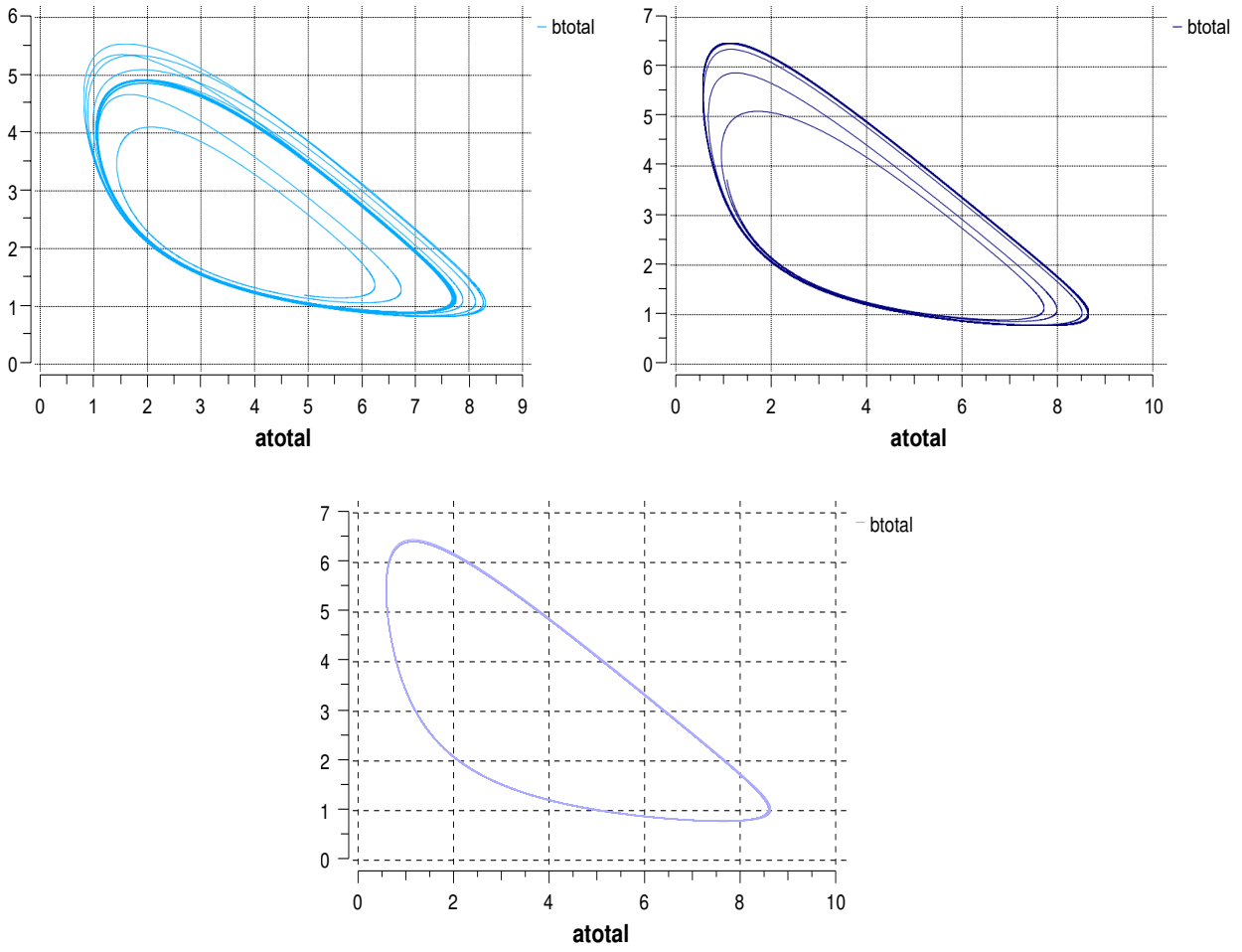

Figure 8.10: Phase space plots of the five different states the system exhibits in response to increments in coupling strength.

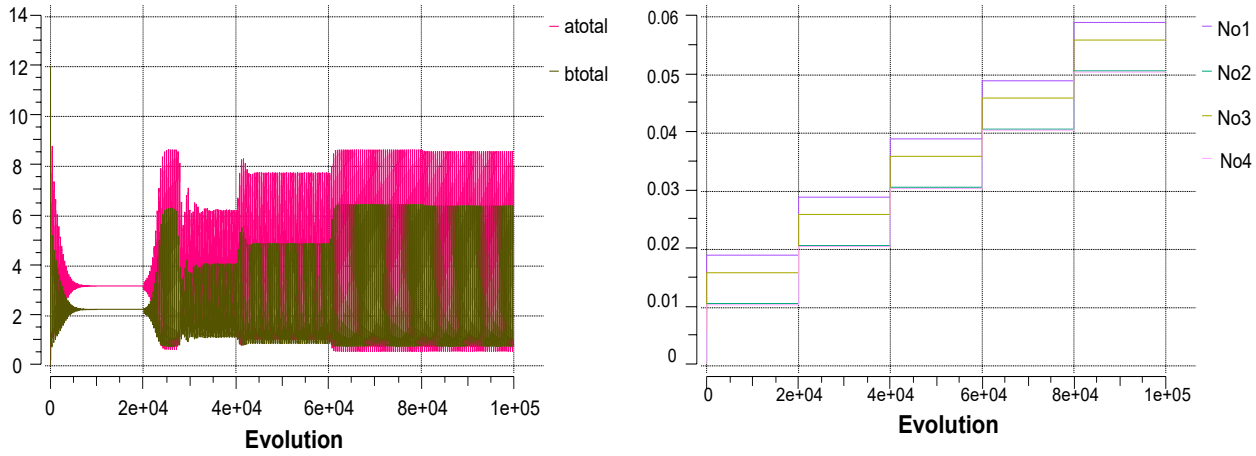

Figure 8.11: Evolution in time of the system response, and the step functions which increase the coupling strength.

Table 8.19 and 8.20 shows the parameters used for the second experiment conducted on the Gray-Scott model after implementing the RCC controller. For this experiment, the control

parameters are equal for all the oscillators and the initial conditions are unique for the same. No_1, No_2, No_3, and No_4 are step functions of the coupling strength implemented in the system. These are used to separate the system into clusters as can be seen by the initial values assigned. For this experiment, control parameter ξ was also modified using a step function. The aim of conducting this experiment was to evaluate the The results are shown in figures 8.12, 8.13, 8.14, and 8.15. Figures 8.12, 8.13, and 8.14 show the phase space plots of oscillators 3, 11, and the total system respectively. The figures on the left show the response before the controller is activated by c_{in}, when the system is only responding to the increments in the coupling strength. The figures on the right show the states the system stabilizes to once the controller is activated. Figure 8.15 shows the evolution of the step functions for the coupling strength and the control strength at the top, and the evolution of the total system response in the bottom, where the different states the system stabilizes into are also visible.

Parameter	Value
b_0	$\frac{1}{15}$
k	$\frac{1}{40}$
δ	4.6
T_{res}	214.5
No_1(step)	0.009
No_2(step)	0.0007
No_3(step)	0.006
No_4(step)	0.0005
f_a, f_b (RCC)	1, 1
μ_a, μ_b (RCC)	1, 1
ξ_1, ξ_3 (RCC)	0.35
ξ_2, ξ_4 (RCC)	0.35

Table 8.19: Gray-Scott Experiment 2 - Parameters

Variable	Initial Value
a_1, a_3, a_6, a_7, a_{10}, a_{12}, a_{13}, a_{15}	0.5
b_1, b_2, b_4, b_5, b_8, b_{11}, b_{14}, b_{16}	0.4
a_2, a_{11}	0.6
b_3, b_9, b_{13}	0.3
a_4, b_{10}, b_{15}	0.7
a_5, a_9, a_{14}	0.1
a_8, a_16	0.9
b_6, b_12	0.2
b_7	0.8

Table 8.20: Gray-Scott Experiment 2 - Initial Conditions

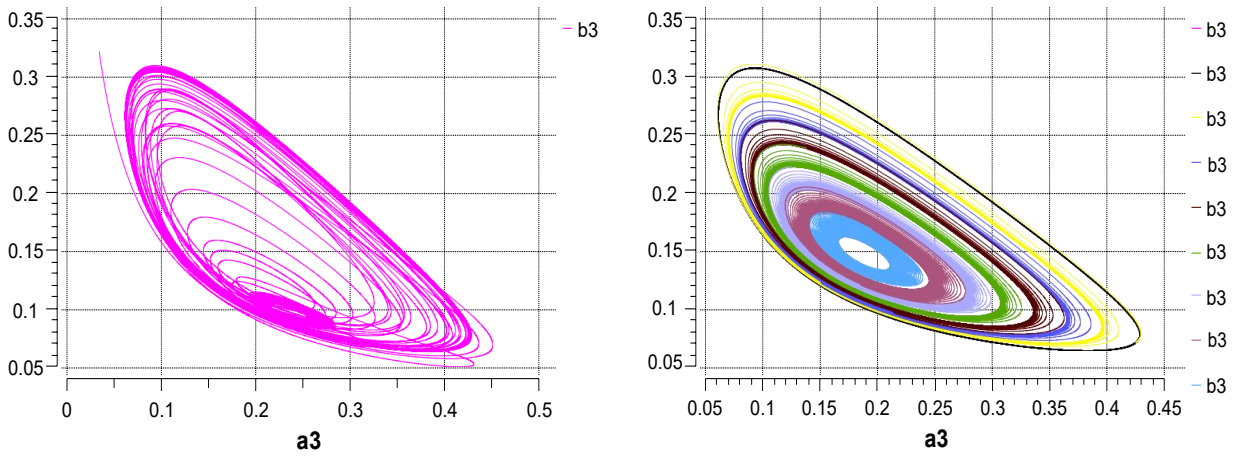

Figure 8.12: Results of the second experiment for the Gray-Scott system. This figure shows the phase space plots for oscillator [a3,b3] before and after the controller stabilizes the system. See tables 8.19 and 8.20 for parameter values.

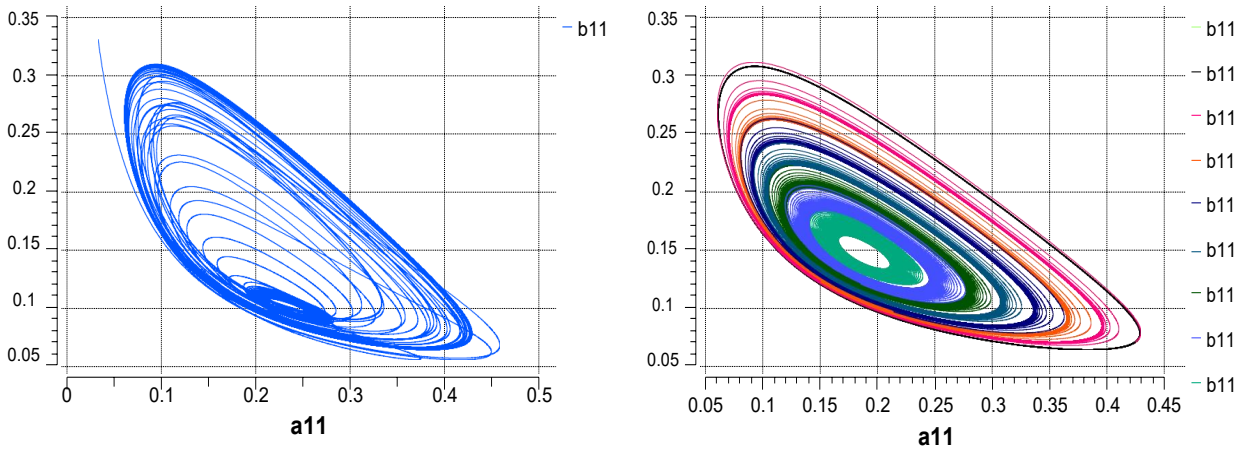

Figure 8.13: Results of the second experiment for the Gray-Scott system. This figure shows the phase space plots for oscillator [a11,b11] before and after the controller stabilizes the system. See tables 8.19 and 8.20 for parameter values.

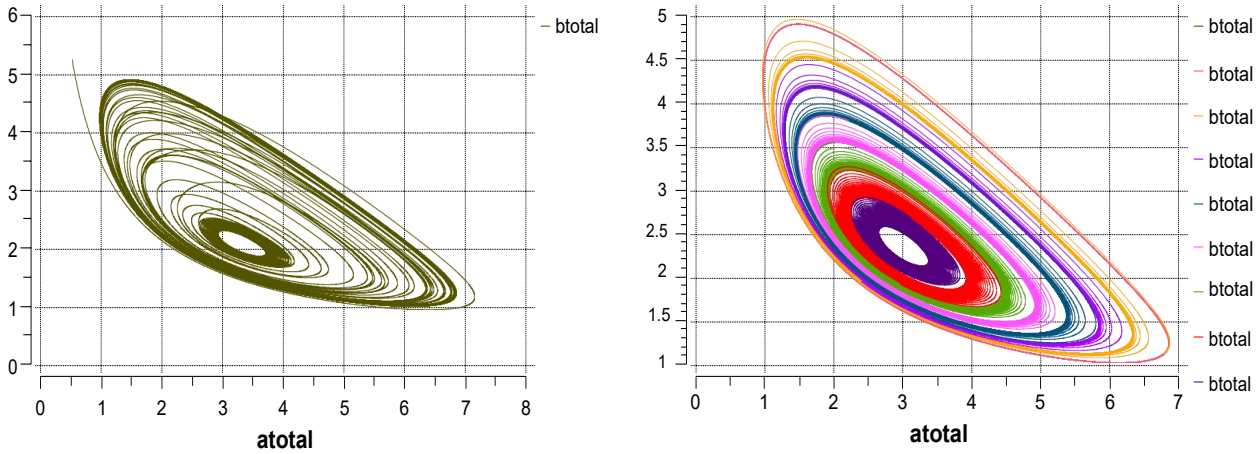

Figure 8.14: Results of the second experiment for the Gray-Scott system. This figure shows the phase space plots for the total system before and after the controller stabilizes the system. See tables 8.19 and 8.20 for parameter values.

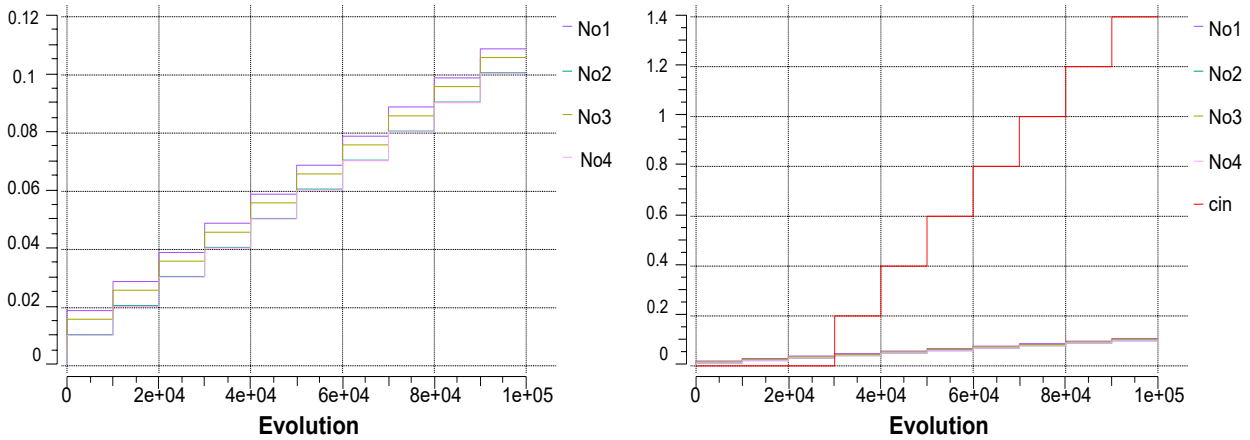

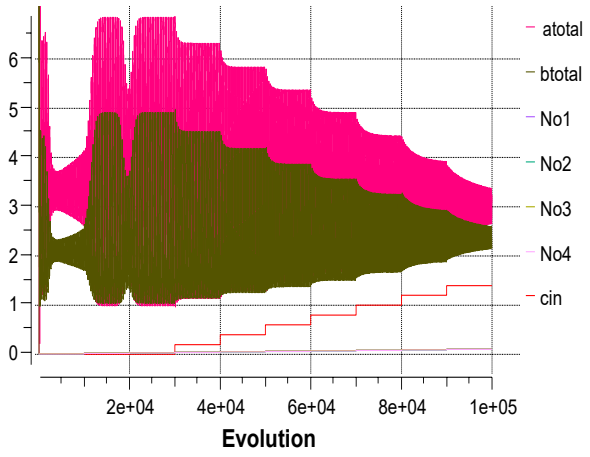

Figure 8.15: Evolution of step functions $No_{1,2,3,4}$ used to increase coupling strength [top-left] and c_{in}, used to increase control strength [top-right]. Evolution of system response [bottom], see tables 8.19 and 8.20 for parameters.

Tables 8.21 and 8.22 shows the parameters used for the third experiment conducted on the Gray-Scott model after implementing the RCC controller. In addition to the step functions for the controller and the coupling strength implemented in the previous experiment, parameter T_{res} was set to 240 for clusters 2 and 4. The results are shown in figures 8.16, 8.17, 8.18, and 8.19. Figures 8.16, 8.17, and 8.18 show the phase space plots of oscillators 3, 11, and the total system respectively. The figures on the left show the response before the controller is activated by c_{in}, when the system is only responding to the increments in the coupling strength. The figures on the right show the states the system stabilizes to once the controller is activated. Figure 8.19 shows the evolution of the step functions for the coupling strength and the control strength at the top, and the evolution of the total system response in the bottom, where the different states the system stabilizes into are also visible. By conducting this experiment, it is verified that the structure is supported, it adapts to the increments in coupling and control strength, and tolerates the singularity provided by modifying the value of T_{res}.

Parameter	Value
b_0	$\frac{1}{15}$
k	$\frac{1}{40}$
δ	4.6
$T_{res}1$	214.5
$T_{res}2$	240
No_1(step)	0.009
No_2(step)	0.0007
No_3(step)	0.006
No_4(step)	0.0005
f_a, f_b (RCC)	1, 1
μ_a, μ_b (RCC)	1, 1
ξ_1, ξ_3 (RCC)	0.35
ξ_2, ξ_4 (RCC)	0.35

Table 8.21: Gray-Scott Experiment 3 - Parameters

Variable	Initial Value
a_1, a_3, a_6, a_7, a_{10}, a_{12}, a_{13}, a_{15}	0.5
b_1, b_2, b_4, b_5, b_8, b_{11}, b_{14}, b_{16}	0.4
a_2, a_{11}	0.6
b_3, b_9, b_{13}	0.3
a_4, b_{10}, b_{15}	0.7
a_5, a_9, a_{14}	0.1
a_8, a_16	0.9
b_6, b_12	0.2
b_7	0.8

Table 8.22: Gray-Scott Experiment 3 - Initial Conditions

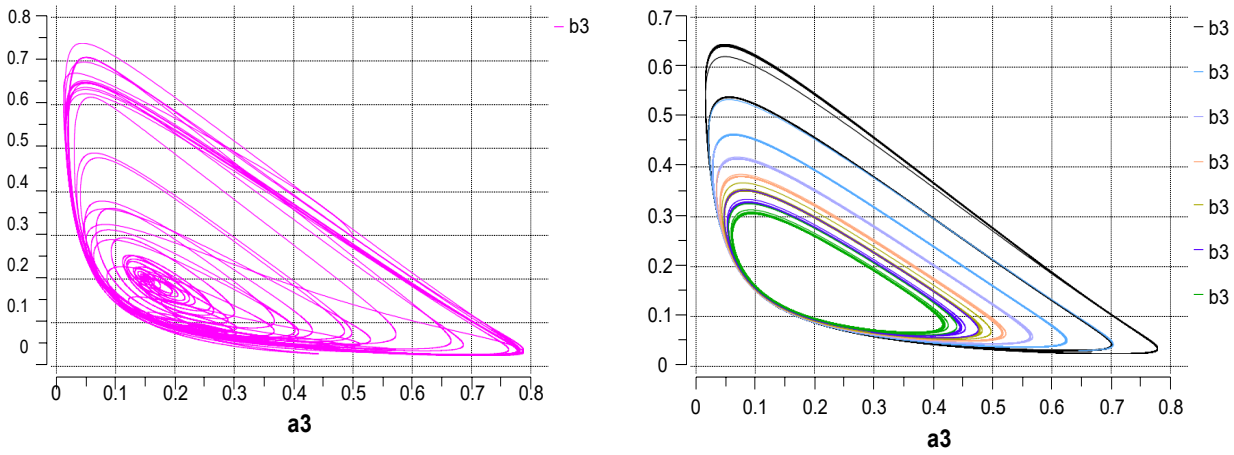

Figure 8.16: Results of the third experiment for the Gray-Scott system. This figure shows the phase space plots for oscillator [a3,b3] before and after the controller stabilizes the system. See tables 8.21 and 8.22 for parameter values.

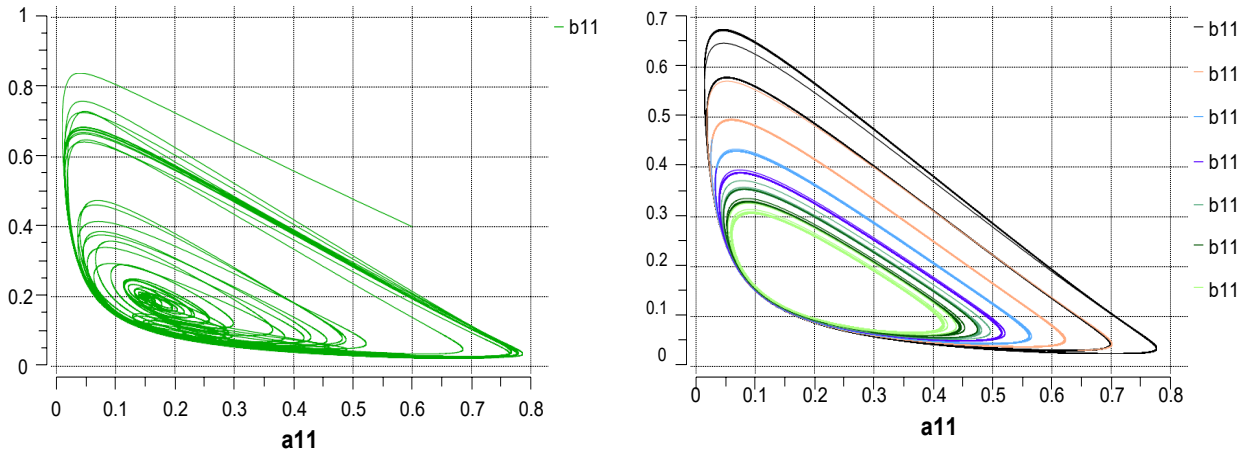

Figure 8.17: Results of the third experiment for the Gray-Scott system. This figure shows the phase space plots for oscillator [a11,b11] before and after the controller stabilizes the system. See tables 8.21 and 8.22 for parameter values.

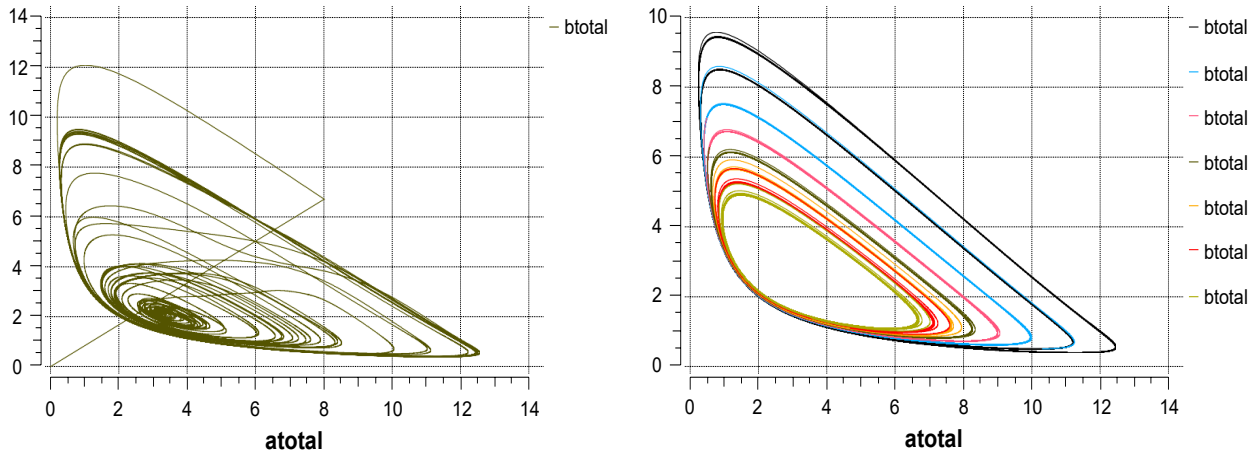

Figure 8.18: Results of the third experiment for the Gray-Scott system. This figure shows the phase space plots for the total system before and after the controller stabilizes the system. See tables 8.21 and 8.22 for parameter values.

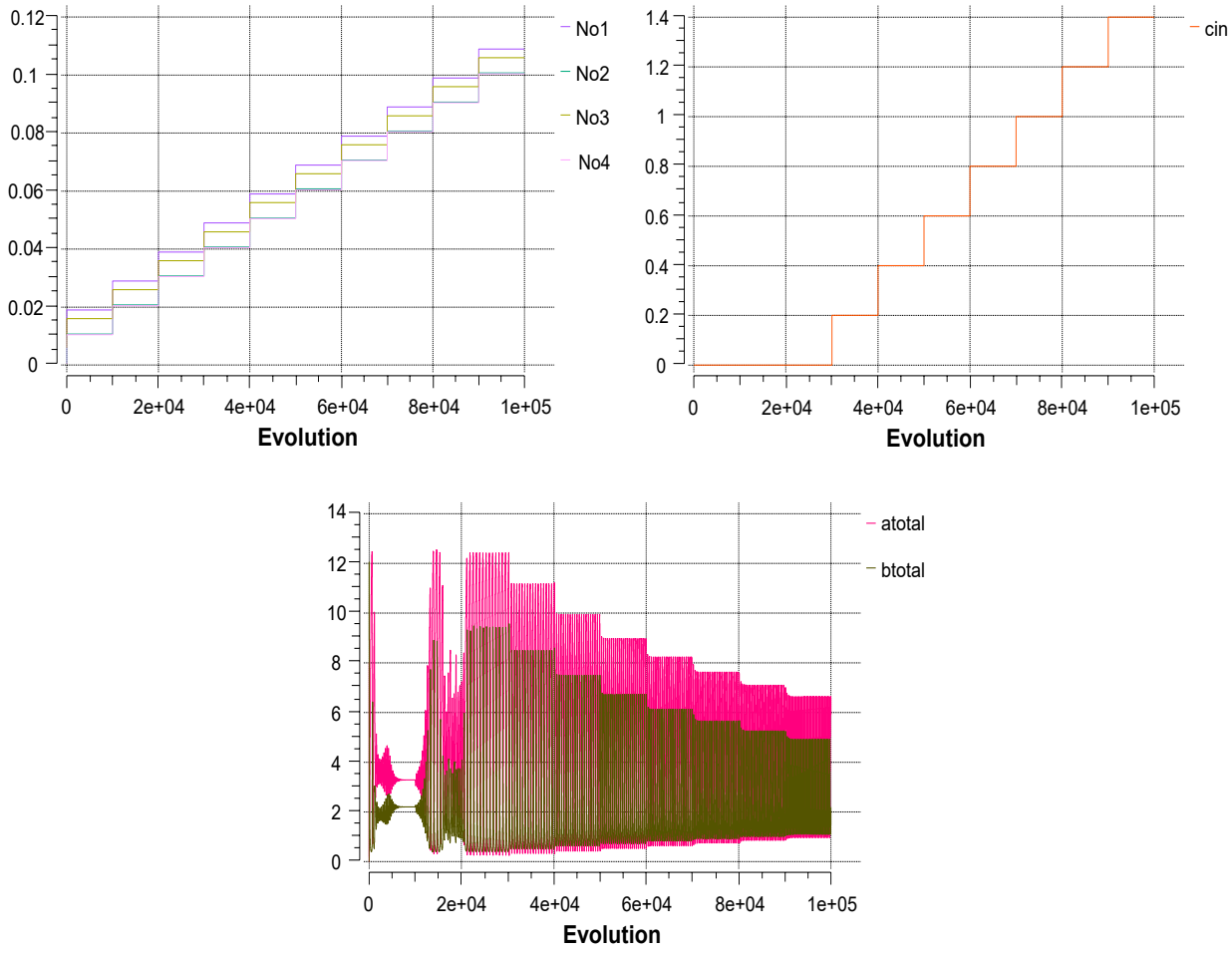

Figure 8.19: Evolution of step functions $No_{1,2,3,4}$ used to increase coupling strength [top-left] and c_{in}, used to increase control strength [top-right]. Evolution of system response [bottom], see tables 8.21 and 8.22 for parameters.

8.3 Discussion

The formulation used for the Gray-Scott system was taken from the work developed by Valery Petrov et. al in [56]. This article served as guidance for the implementation of the model as it provides possible values and ranges for the parameter values. The RCC controller has already been successfully implemented with this model, this work is available in [48]. The experiments conducted on this model for the purpose of this research project are presented in this section, which is divided into two parts. The first part presents the results of the experiments conducted prior to the implementation of the controller and evaluating the possible parameter values to be modified on a network of 10 coupled oscillators. The second part presents the experiments conducted once the full structure of the model was implemented, including the separation into clusters, the RCC controller, and step functions to modify coupling strength and control strength. The results to these experiments were presented in section 8.2 of this chapter.

8.3.1 Response to modifications to support model structure

The results observed from performing the experiments described in this section assisted in determining the ranges of values which can be used to separate the system into clusters. Five experiments were conducted to explore these modifications. The system was modelled as a network of 10 coupled oscillators, and the experiments focused on the modification of two parameters: T_{res} and the coupling strength, referred to as G in this work. The first experiment considered $T_{res} = 240$ and $G = 0.005$. The results of this experiment show periodic stability to a single orbit throughout, similar to the results obtained with the stability analysis. The rest of the parameters used for this experiment are presented in table 8.1 and 8.2, where it is also seen that the initial conditions were assigned in the ranges used for the stability analysis.
For the second experiment, the coupling strength remained the same and T_{res} was set to 214.5, which is at the lower end of the range established for this parameter. This value results in the

behaviour seen on figure 8.3, where it is seen that the system is still periodically stable but exhibiting more complex dynamics. For this reason, the remaining experiments used the same value for T_{res} and only modified the coupling strength to further observe how the dynamics would change.

For the third experiment, the coupling strength was increased to 0.006. The remaining values were left equal to the previous experiment, as seen in tables 8.5 and 8.6. Figure 8.4 4.16 shows the behaviour of the system under these conditions. The dynamics appear to be similar to the results exhibited in experiment 2, with an increase in the periodicity of the signal. This behaviour still remains within the desired level of dynamics. As it is desired for the control strength to remain small, the following two experiments considered smaller values.

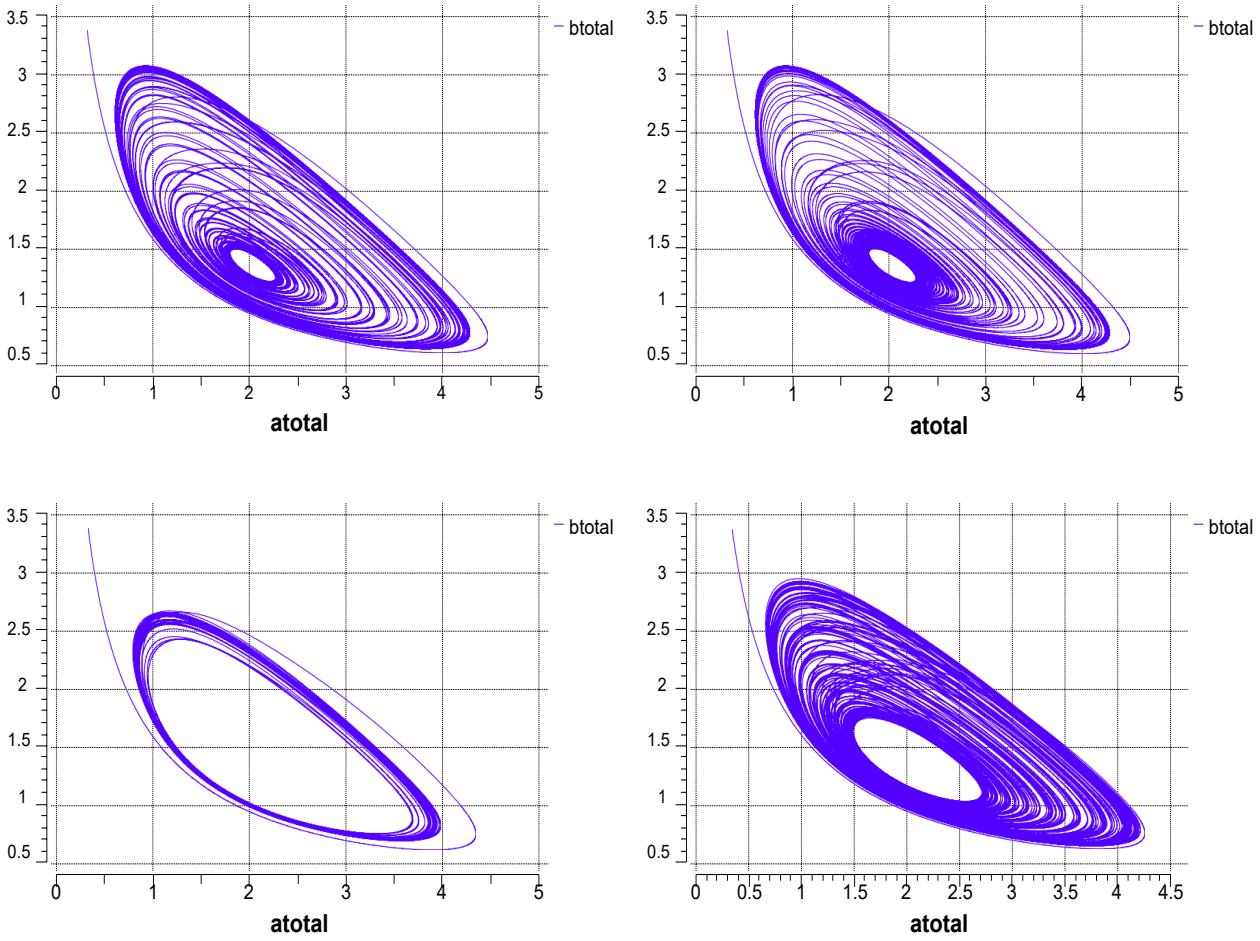

Figure 8.20: Results of the Gray-Scott system using four different values for coupling strength: 0.005 (top-left), 0.006 (top-right), 0.003 (bottom-left), and 0.002 (0.002). For these experiments $T_{res} = 214.5$.

For the fourth experiment, the coupling strength was set to 0.003. The response to this modification is available in figure 8.5. The system exhibits dynamics similar to those obtained with $T_{res} = 240$, with the exception that the response of oscillator 6 appears to stabilize into two periodic orbits. For the final experiment conducted in this section the coupling strength was reduced to 0.002. The response is shown in figure 8.6, where similar periodicity to that of experiments 2 and 3 is exhibited.

8.3.2 Response to implementation of RCC controller and modifications of coupling strength

The experiments presented in this section focused on constructing the sixteen coupled oscillator structure, using the values determined from the results of the previous section. Once the structure was established, the controller was implemented and the parameter values were modified to observe the response of the system. The first experiment was an initial approach to evaluate these modifications. This experiment was divided into three parts. The first part considered the effect of the controller on the whole system, the values used are available in tables 8.11 and 8.12 and the results can be seen in figure 8.7.

The implementation of the controller amplified the dynamics of the system, which indicates that the control strength should be increased. This was considered for the second part of the experiment, where the control strength was increased and a step function was used to activate the controller halfway through the simulation. Tables 8.13 and 8.14 show the values used, and the effect of the controller is shown in figure 8.8. The third part of this experiment consisted in modifying the value of T_{res} to 214.5. For this case, it was observed that a lower value of the controller was sufficient to stabilize the system to a single periodic orbit, as seen in figure 8.9.

After observing these changes, and taking into account the findings from the experiments detailed in section 8.2.1, an additional experiment was performed in order to observe the response of the system to increments in the coupling strength. The values used for this experiment are

available in tables 8.17 and 8.18. For this experiment, the sixteen coupled oscillator structure was completed. This was achieved by using four step functions to modify the coupling strength, two different values for the control strength, and the two different values used previously experimented for T_{res}. The values for the control strength were selected according to the results obtained from experiment 1, where it was seen that lower values for the controller work better for $T_{res} = 214.5$, and higher values of the control strength work better for $T_{res} = 240$. Figure 8.10 shows the phase space plots for the five individual responses to the increments in coupling strength. The system response is shown in figure 8.11, along with the step functions which control the increments in coupling strength. The results of this experiment allowed the observation of the system response to internal modifications under the influence of the controller. The structure defined in this model was used in subsequent experiments, where the control strength was modified.

Experiment 2 considered unique values for T_{res} and the control strength, where $T_{res} = 214.5$ and $xi = 0.35$, as shown in table 8.19 and 8.20. This experiment also included step function c_{in}, which activates the controller at t = 40000 and controls the increments in the control strength. This was done in order to allow the system to respond to the increments in coupling strength for three cycles before the controller is activated. Figures 8.12 and 8.13 show the response of oscillators 3 and 11. The response of the system prior to the activation of the controller is shown on the left, and the response to the increments in control strength is shown on the right. This experiment successfully demonstrates multi-stability in the system in terms of response to the coupling and control strength. The system response is shown in figure 8.14, where it is seen that just like oscillators 3 and 11, the system stabilizes periodically into 9 different states. Figure 8.15 shows the evolution of the step functions involved in controlling the increments in coupling strength and control strength, as well as the evolution of the system response, where the states the system stabilizes into can be easily seen.

For the third experiment the value of T_{res} was changed to 240 for clusters 2 and 4, as shown in tables 8.21 and 8.22. The response to these changes is shown in figures 8.16 - 8.19. The

same protocol was followed as that to the previous experiment, where step functions were used to increase the control strength, and the coupling strength. It is evident by the responses observed that the system responds positively to the modifications to parameter T_{res}. The system stabilizes to the same states as in the previous experiment. The most evident modification is how the transition between states is achieved faster than what was observed for experiment 2. This indicates that the system responds positively to the modification of parameter T_{res}, and that this could be instrumental in tailoring solutions where a faster response or delay may be required. Figures 8.21 and 8.22 show the response of the system for the third experiment, where the best results were achieved in general terms. For this experiment, both the coupling and the control strength were used to modify the system. The effects of these modifications was seen in the phase space plots and it can also be seen in figure 8.23, where the relation between the amplitude and the coupling strength is shown, as well as the relation between the control strength and the amplitude.

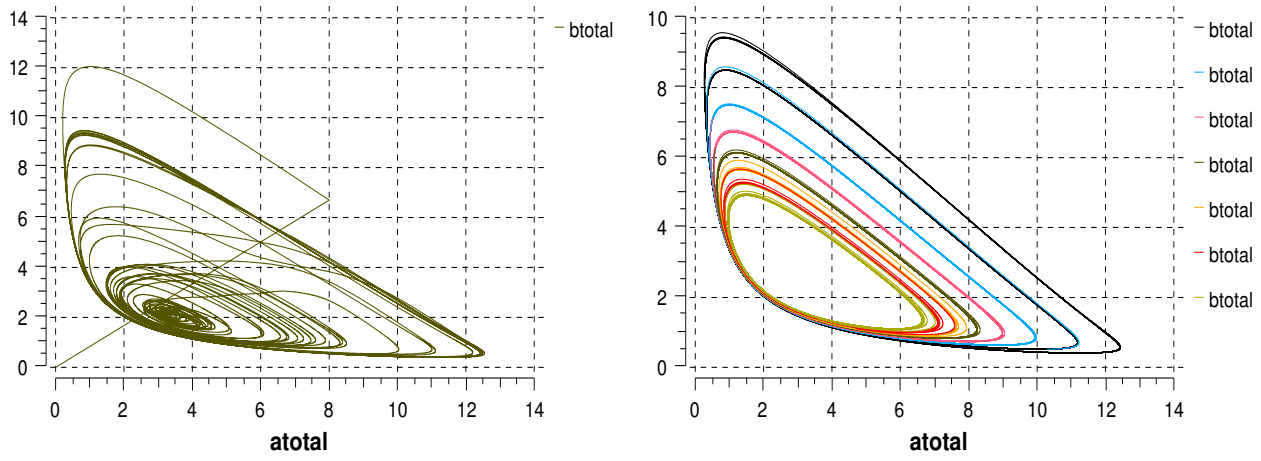

Figure 8.21: Results of the second experiment for the Gray-Scott system. This figure shows the phase space plots for the total system before and after the controller stabilizes the system. See tables 8.21 and 8.22 for parameter values.

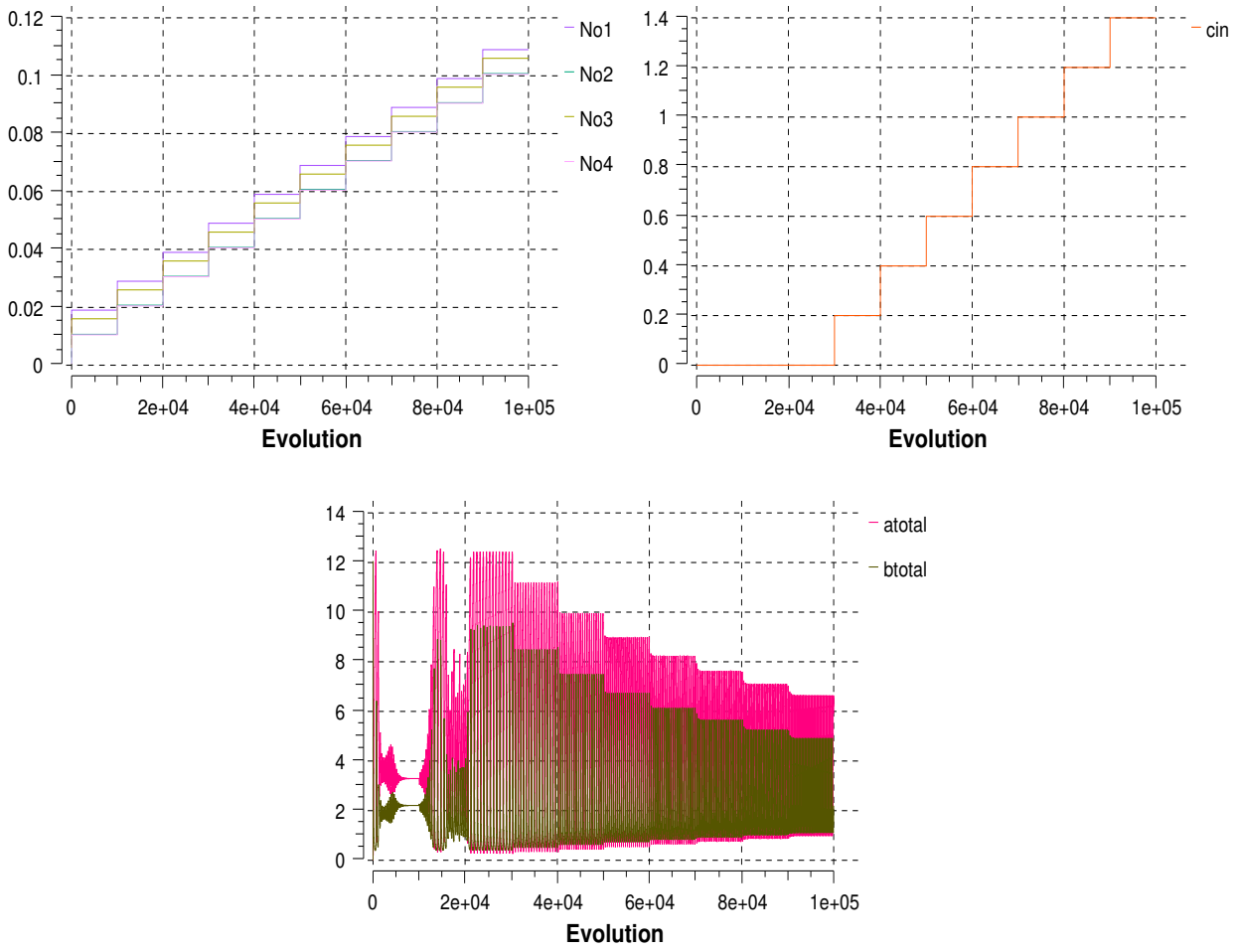

Figure 8.22: Evolution of step functions $No_{1,2,3,4}$ used to increase coupling strength [top-left] and c_{in}, used to increase control strength [top-right]. Evolution of system response [bottom], see tables 8.21 and 8.22 for parameter values.

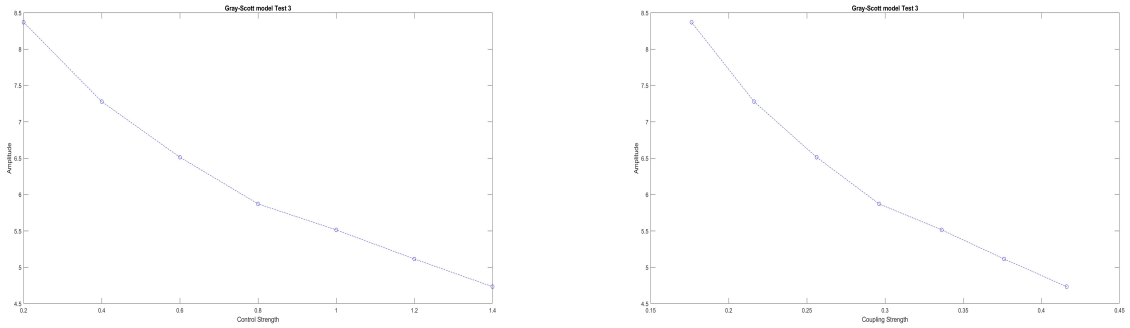

Figure 8.23: Figure showing the relationship between the coupling strength and the amplitude of the system response, each point represents a periodically stable state the system converges to.

Chapter 9

The Berry Model

9.1 Model Development

This model, detailed further in [8], describes the generation, and degradation of proteins in the extracellular matrix. The latter is a collection of molecules on the outside of cells, whose function is to give support structurally, and biochemically. The equations for this model are shown below, and contain a wider range of parameters and variables in comparison to the previous models. Some of these are m, which represents the matrix created at constant rate rim , and p and g represent enzymes, whose production is due to the presence of fragments f. The advantage of using this model was mostly identified through the elaboration of the stability analysis. The morphology of the generated wave-patterns could be of high biological relevance for the purpose of the system it is attempting to simulate in this work.

$$\frac{dm}{dt} = k_g \frac{fg}{K_G + f} - \frac{mp}{1+m} + r_{im_i} \tag{9.1}$$

$$\frac{df}{dt} = -k_g \frac{fg}{K_G + f} + \frac{mp}{1+m} - \frac{fp}{1+f} \tag{9.2}$$

$$\frac{dp}{dt} = \alpha \frac{f^n}{K_R^n + f^n} - k_a p^2 \tag{9.3}$$

$$\frac{dg}{dt} = \beta \frac{f^l}{K_S^l + f^l} - k_{deg} \frac{gp}{K_{deg} + g} \tag{9.4}$$

9.1.1 Stability Analysis

The oscillations in this model differ greatly from the other two models (see figure 9.1), which could be beneficial as the oscillations in our system are not symmetric, as can be seen from figure 3.6; it also provides a wider range of parameters. Both of these properties will allow to tune the system with more flexibility, and represent a more biologically relevant approach. For the stability analysis, parameter r_{im} was set as constant, but this was the parameter used to model the coupling in the final system.

Behaviour	Parameters and Initial Conditions
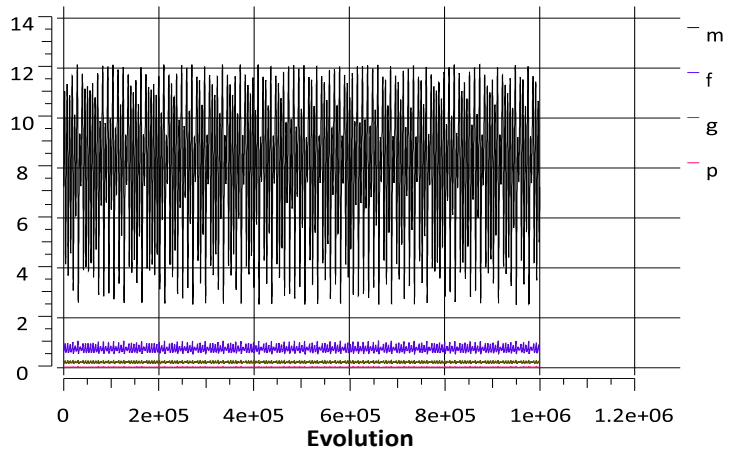	Initial Conditions • p = 0.016 m = 7.26 • f = 0.665 g = 0.177 Parameters • $K_g = 0.1$ $k_g = 0.05$ • $K_s = 1$ $k_a = 0.0455$ • $K_d = 1.1$ $k_d = 0.05$ • $K_r = 4.5$ $\alpha = 0.026$ • $n = 4$ $\beta = 0.00075$ • $I = 4$ $r_{im} = 0.0098$

Figure 9.1: Stability Analysis - Berry Model

9.1.2 Model Structure

This system was obtained from [8], the parameters have been set according to the values specified in the same article; this same work was taken as reference to tune the parameters for the experiments presented in this chapter. The specific values for these are mentioned in each experiment. RCC is applied on the incremental term $\alpha \frac{{f_i}^n}{{K_R}^n + {f_i}^n}$ in equation 9.7 denoted as $\sigma_p(f)$, and in the incremental term $\beta \frac{{f_i}^l}{{K_S}^l + {f_i}^l}$ in 9.8 denoted as $\sigma_g(f)$. Coupling is given by

terms r_{im} of 9.5, this equation was used to separate the system into clusters, as well as the initial conditions of the system.

$$\frac{dm_i}{dt} = k_g \frac{f_i g_i}{K_G + f_i} - \frac{m_i p_i}{1 + m_i} + r_{imi} \tag{9.5}$$

$$\frac{df_i}{dt} = -k_g \frac{f_i g_i}{K_G + f_i} + \frac{m_i p_i}{1 + m_i} - \frac{f_i p_i}{1 + f_i} \tag{9.6}$$

$$\frac{dp_i}{dt} = \sigma_p(f)\alpha \frac{{f_i}^n}{{K_R}^n + {f_i}^n} - k_a {p_i}^2 \tag{9.7}$$

$$\frac{dg_i}{dt} = \sigma_g(f)\beta \frac{{f_i}^l}{{K_S}^l + {f_i}^l} - k_{deg} \frac{g_i p_i}{K_{deg} + g_i} \tag{9.8}$$

9.2 Results

9.2.1 Response to changes in coupling and control strength in the system

The final form of the Berry model with the RCC controller used for the following experiments is given by equations 9.9, 9.10, 9.11, 9.12, 9.13, and 9.14 where i = {1....16}.

$$\frac{dm_i}{dt} = k_g \frac{f_i g_i}{K_G + f_i} - \frac{m_i p_i}{1 + m_i} + r_{imi} \tag{9.9}$$

$$\frac{df_i}{dt} = -k_g \frac{f_i g_i}{K_G + f_i} + \frac{m_i p_i}{1 + m_i} - \frac{f_i p_i}{1 + f_i} \tag{9.10}$$

$$\frac{dp_i}{dt} = \sigma_p(f)\alpha \frac{{f_i}^n}{{K_R}^n + {f_i}^n} - k_a {p_i}^2 \tag{9.11}$$

$$\frac{dg_i}{dt} = \sigma_g(f)\beta \frac{{f_i}^l}{{K_S}^l + {f_i}^l} - k_{deg} \frac{g_i p_i}{K_{deg} + g_i} \tag{9.12}$$

Where the control equations are given as follows:

$$\sigma_p(f) = f_f e^{\xi_i q_f} \qquad \sigma_g(f) = f_f e^{\xi_i q_f} \tag{9.13}$$

and:

$$q_f = \frac{f}{f + \mu_f} \tag{9.14}$$

The structure of the clusters for the final model, including the parameters that were used to split the system is shown below. For this model, only one system parameter was used to split the system. For this reason, step signal No_i was used in the term r_{im} to modify the coupling strength for each cluster. For experiment 4, the initial conditions were also used to provide further singularity to the clusters, the changes are reflected in tables 9.7 and 9.8.

- Cluster 1:
  - Parameters: β_1, No_1.
  - Oscillators: [m1,f1,p1,g1], [m2,f2,p2,g2], [m3,f3,p3,g3], [m4,f4,p4,g4].
- Cluster 2:
  - Parameters: β_2, No_2.
  - Oscillators: [m5,f5,p5,g5], [m6,f6,p6,g6], [m7,f7,p7,g7], [m8,f8,p8,g8].
- Cluster 3:
  - Parameters: β_3, No_3.
  - Oscillators: [m9,f9,p9,g9], [m10,f10,p10,g10], [m11,f11,p11,g11], [m12,f12,p12,g12].
- Cluster 4:
  - Parameters: β_4, No_4.
  - Oscillators: [m13,f13,p13,g13], [m14,f14,p14,g14], [m15,f15,p15,g15], [m16,f16,p16,g16].

For the first and second experiment with this model the parameters were set according to the recommendations in [48] and [8]. This was decided to experiment a model which can be bound by certain parameter values, which is generally the case for most physiological models of the glucose-insulin system. For the first experiment, the system was not separated into clusters,

and for the second one functions No1, No2, No3, and No4 were used to establish the separation. In the first experiment, the step inputs were alternated among the oscillators as established in tables 9.1 and 9.2. The results are shown in figures 9.2 and 9.3. Figure 9.2 shows the phase space plot and the evolution in time of the whole system, and the phase space plots for oscillators 8 and 11. Figure 9.3 shows the evolution of the signals used to tune the coupling strength (r_{im}). This first experiment was carried out in order to establish the initial structure before proceeding with the implementation of modifications to the system.

Parameter	Value
K_g	0.1
K_s	1
K_d	1.1
K_r	4.5
n	4
l	4
k_g	0.05
k_a	0.0455
k_d	0.05
α	0.026
β	0.00075
f_p (RCC)	1
f_g (RCC)	1
μ_f (RCC)	2
ξ_p (RCC)	-3
ξ_g (RCC)	-3

Table 9.1: Berry Experiment 1 - Parameters

Variable	Initial Value
m_i	0.26
f_i	0.465
p_i	0.016
g_i	0.127
$No_{1,5,9,13}$(step)	0.00001
$No_{2,6,10,14}$(step)	0.00002
$No_{3,7,11,15}$(step)	0.00003
$No_{4,8,12,16}$(step)	0.00004

Table 9.2: Berry Experiment 1 - Initial Conditions

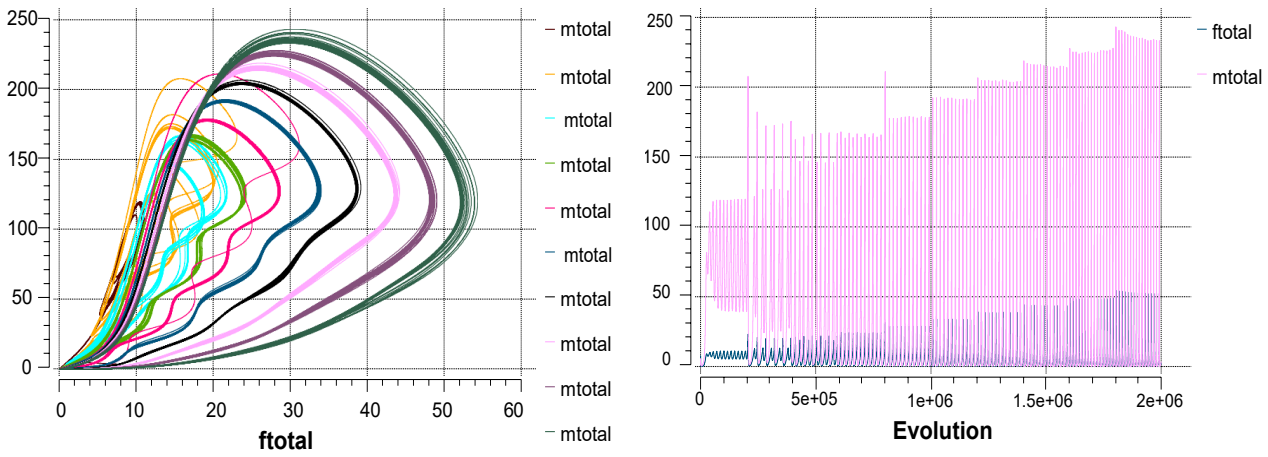

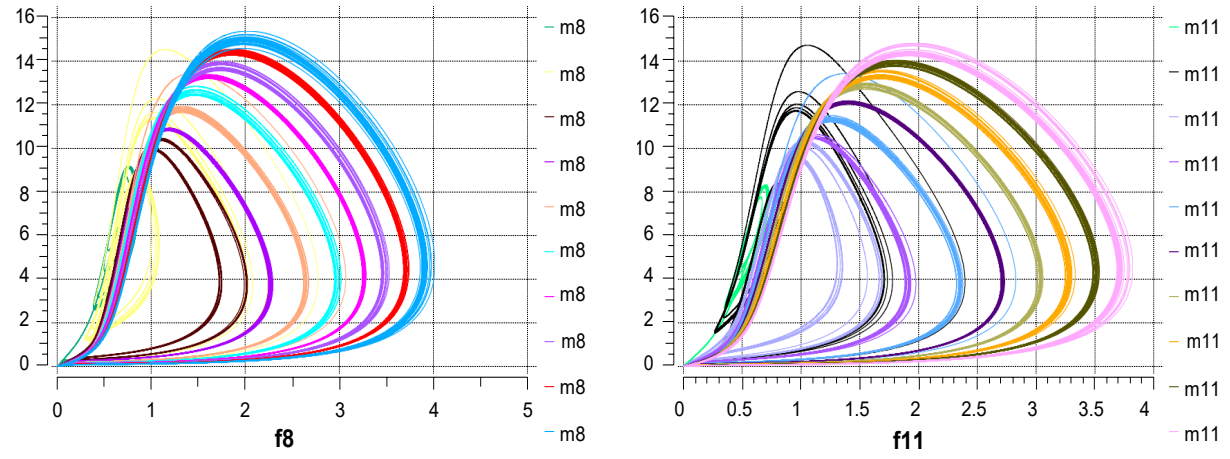

Figure 9.2: Results of the Berry model for the first experiment using the parameters in tables 9.1 and 9.2. This figure shows the total response of the system using the phase space plot [Top-Left] and the evolution in time [Top-Right]. The phase space plots of oscillators 8 and 11 are shown to exemplify the lower-level behaviour of the system.

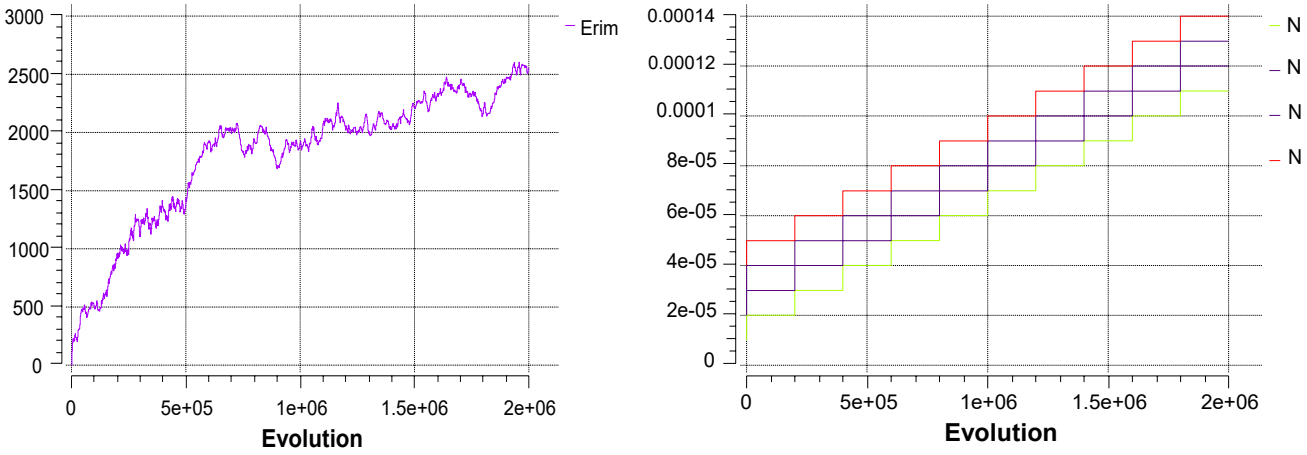

Figure 9.3: Evolution of the signals which control the changes in coupling for the first experiment. From top to bottom: No4, No3, No2, No1.

Tables 9.3 and 9.4 shows the parameters used for the second experiment conducted on the Berry model. For this experiment, the coupling strength was used to establish the separation of the system into clusters using step functions No_1, No_2, No_3, and No_4. The results are shown in figures 9.4 and 9.5. Figure 9.4 shows the phase space plot and the evolution in time of the whole system, and the phase space plots for oscillators 8 and 11. Figure 9.5 shows the evolution of the signals used to tune the coupling strength (r_{im}). The aim of this experiment was to establish an initial separation of the system into four clusters and prove the structure to be supported. The results demonstrate the structure can be supported with minor modifications to the amplitude in the total response of the system.

Parameter	Value
K_g	0.1
K_s	1
K_d	1.1
K_r	4.5
n	4
l	4
k_g	0.05
k_a	0.0455
k_d	0.05
α	0.026
β	0.00075
f_p (RCC)	1
f_g (RCC)	1
μ_f (RCC)	2
ξ_p (RCC)	-3
ξ_g (RCC)	-3

Table 9.3: Berry Experiment 2 - Parameters

Variable	Initial Value
m_i	0.26
f_i	0.465
p_i	0.016
g_i	0.127
No_1(step)	0.00001
No_2(step)	0.00002
No_3(step)	0.00003
No_4(step)	0.00004

Table 9.4: Berry Experiment 2 - Initial Conditions

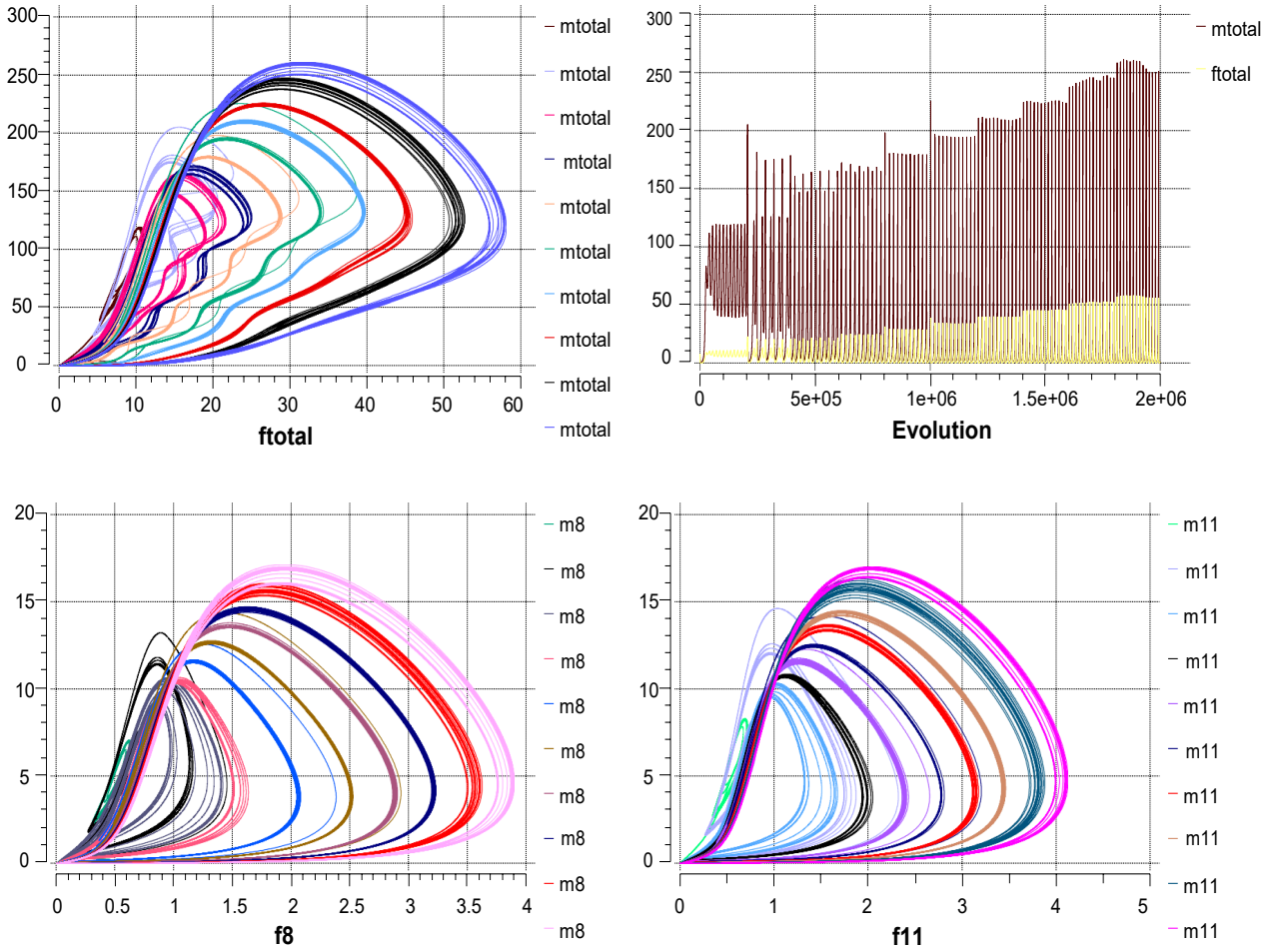

Figure 9.4: Results of the Berry model for the second experiment using the parameters in tables 9.3 and 9.4. This figure shows the total response of the system using the phase space plot [Top-Left] and the evolution in time [Top-Right]. The phase space plots of oscillators 8 and 11 are shown to exemplify the lower-level behaviour of the system.

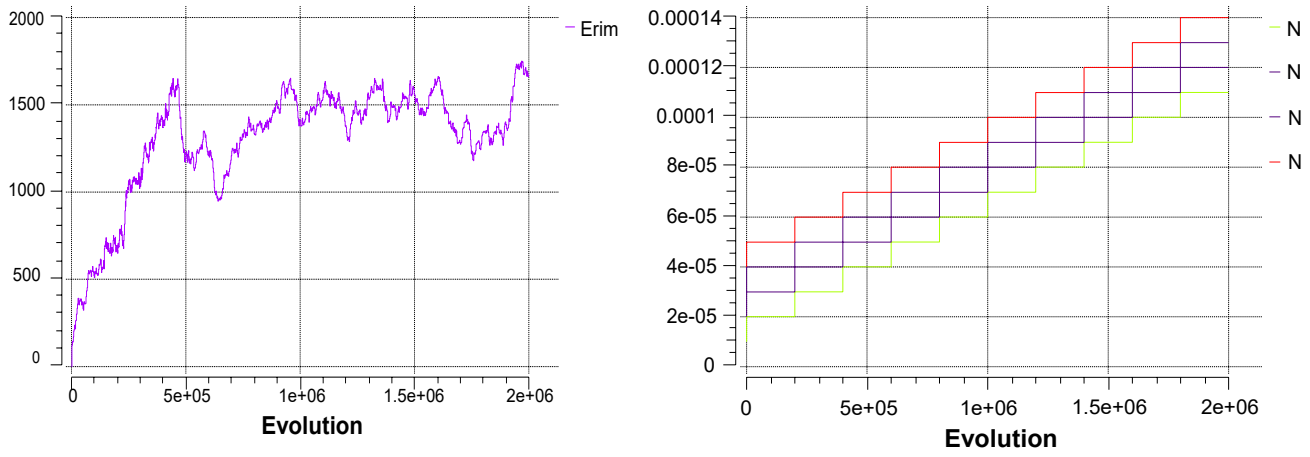

Figure 9.5: Evolution of the signals which control the changes in coupling for the second experiment. From top to bottom: No4, No3, No2, No1. These were used to separate the system into clusters.

For the third and fourth experiments, the aim was to simulate the system using parameter β and the initial conditions of the system variables to further distinguish the clusters. In [8], the author provides a wide range of values for β which can be used depending on the desired behaviour. Figure 9.6 shows the phase-space plots of the system response for four different values of β. These were the values selected to differentiate the clusters for the third experiment, as seen in tables 9.5 and 9.6.

The results from this experiment are shown in figures 9.7 and 9.8. Figure 9.7 shows the phase space plot and the evolution in time of the whole system, and the phase space plots for oscillators 8 and 11. Figure 9.8 shows the evolution of the signals used to tune the coupling strength (r_{im}). It is seen that these minor changes in the clusters are sufficient to modify the response of the system without altering the periodically stable states.

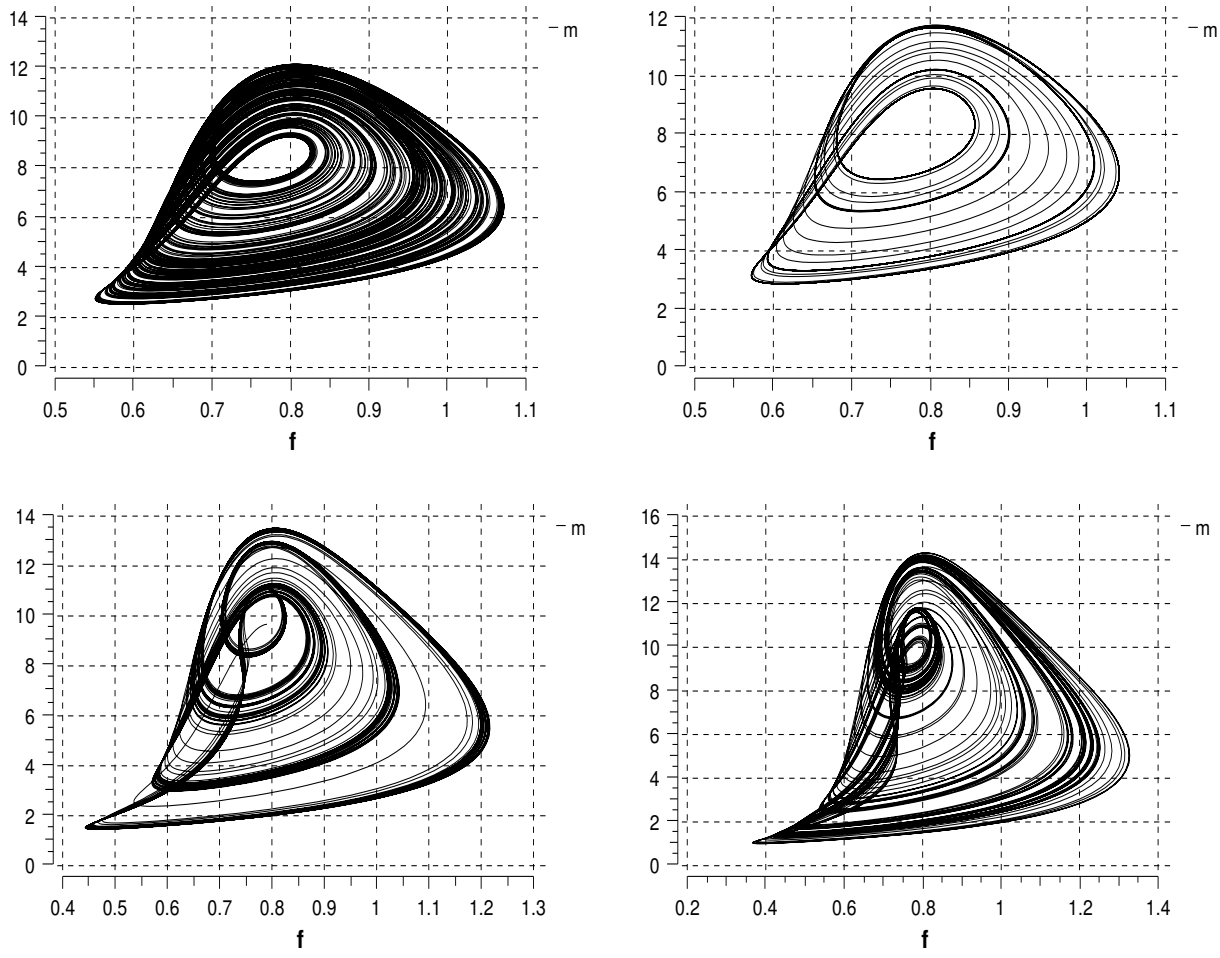

Figure 9.6: Phase space plots for the β values used in experiment 3 for the following values of β: 0.00075 [top-left], 0.0007640 [top-right], 0.000747 [bottom-left], and 0.0007593 [bottom-right].

Parameter	Value
K_g	0.1
K_s	1
K_d	1.1
K_r	4.5
n	4
l	4
k_g	0.05
k_a	0.0455
k_d	0.05
α	0.026
β_1	0.00075
β_2	0.0007640
β_3	0.000747
β_4	0.0007593
f (RCC)	1
μ_f (RCC)	2
ξ (RCC)	-3

Table 9.5: Berry Experiment 3 - Parameters

Variable	Initial Value
m_i	0.26
f_i	0.465
p_i	0.016
g_i	0.127
No_1(step)	0.00001
No_2(step)	0.00002
No_3(step)	0.00003
No_4(step)	0.00004

Table 9.6: Berry Experiment 3 - Initial Conditions

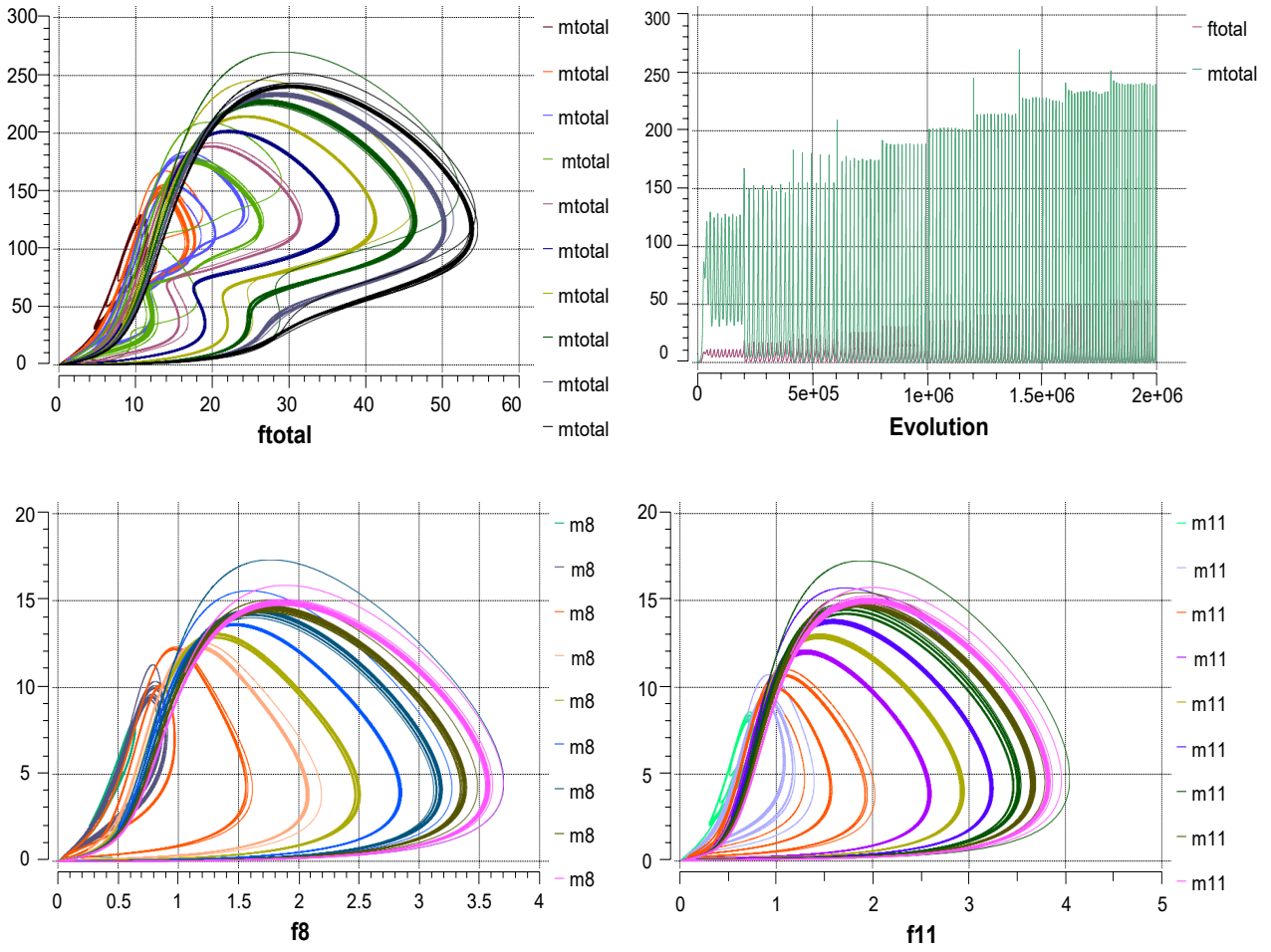

Figure 9.7: Results of the Berry model for the third experiment using the parameters in tables 9.5 and 9.6. This figure shows the total response of the system using the phase space plot [Top-Left] and the evolution in time [Top-Right]. The phase space plots of oscillators 8 and 11 are shown to exemplify the lower-level behaviour of the system.

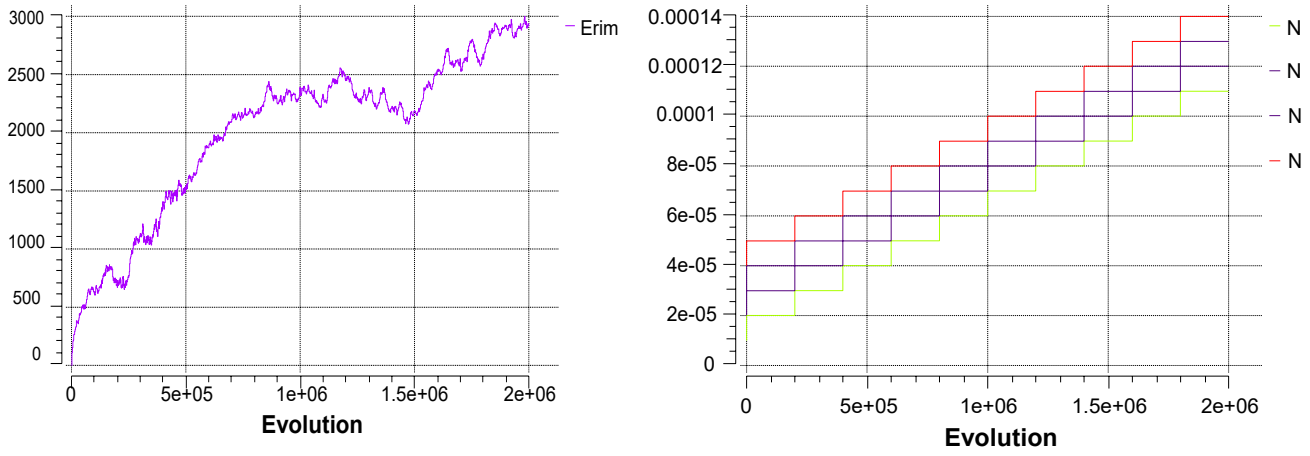

Figure 9.8: Evolution of the signals which control the changes in coupling for the third experiment. From top to bottom: No4, No3, No2, No1. These were used to separate the system into clusters.

For the fourth experiment using the Berry model, aside from the different values of β, the initial

conditions of the system were modified for clusters 2 and 4. The values were modified following the rule provided in [8], where it is stated that the following should be met: m > p, f > g, and f > p. Tables 9.7 and 9.8 shows the parameters used to achieve the results shown in figures 9.9 and 9.10, where it is seen that the system is still capable of representing the desired structure and adapt to the modifications maintaining periodic stability.

Parameter	Value
K_g	0.1
K_s	1
K_d	1.1
K_r	4.5
n	4
l	4
k_g	0.05
k_a	0.0455
k_d	0.05
α	0.026
β_1	0.00075
β_2	0.0007640
β_3	0.000747
β_4	0.0007593
f_p (RCC)	1
f_g (RCC)	1
μ_f (RCC)	2
ξ_p (RCC)	-3
ξ_g (RCC)	-3

Table 9.7: Berry Experiment 4 - Parameters

Variable	Initial Value
$m_{1,3}$, $m_{2,4}$	[0.26, 0.46]
$f_{1,3}$, $f_{2,4}$	[0.465, 0.665]
$p_{1,3}$, $p_{2,4}$	[0.016, 0.036]
$g_{1,3}$, $g_{2,4}$	[0.127, 0.327]
No_1(step)	0.00001
No_2(step)	0.00002
No_3(step)	0.00003
No_4(step)	0.00004

Table 9.8: Berry Experiment 4 - Initial Conditions

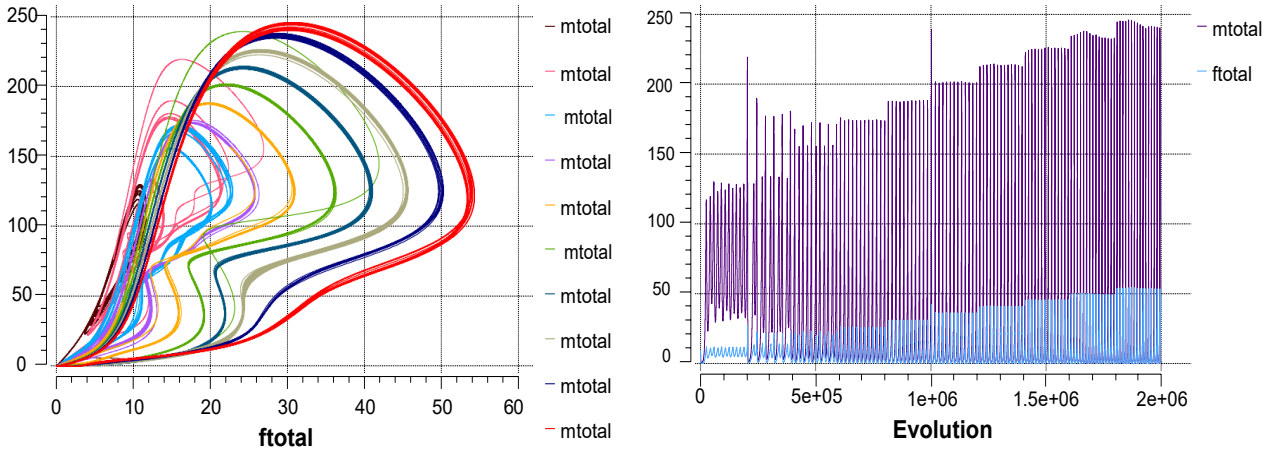

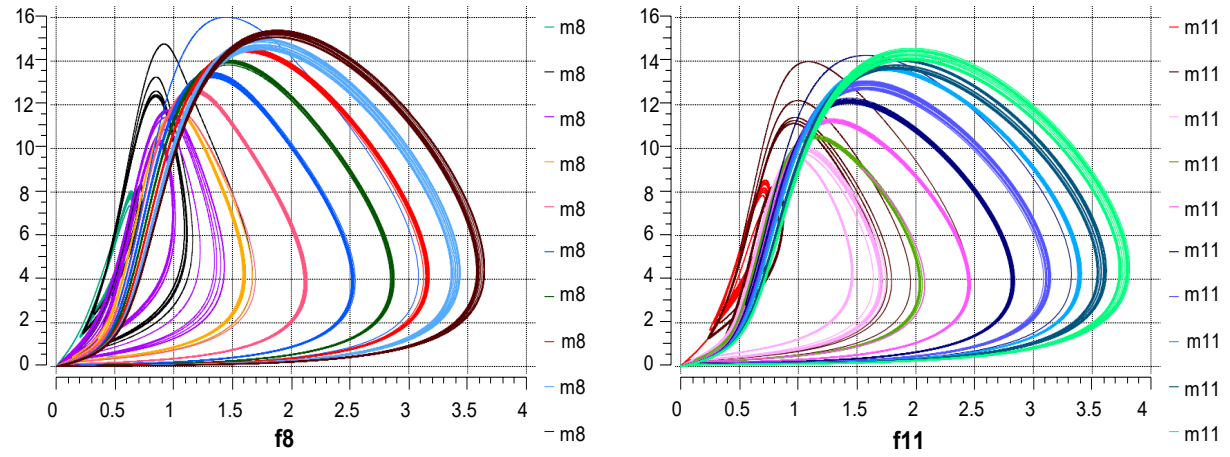

Figure 9.9: Results of the Berry model for the fourth experiment using the parameters in tables 9.7 and 9.8. This figure shows the total response of the system using the phase space plot [Top-Left] and the evolution in time [Top-Right]. The phase space plots of oscillators 8 and 11 are shown to exemplify the lower-level behaviour of the system.

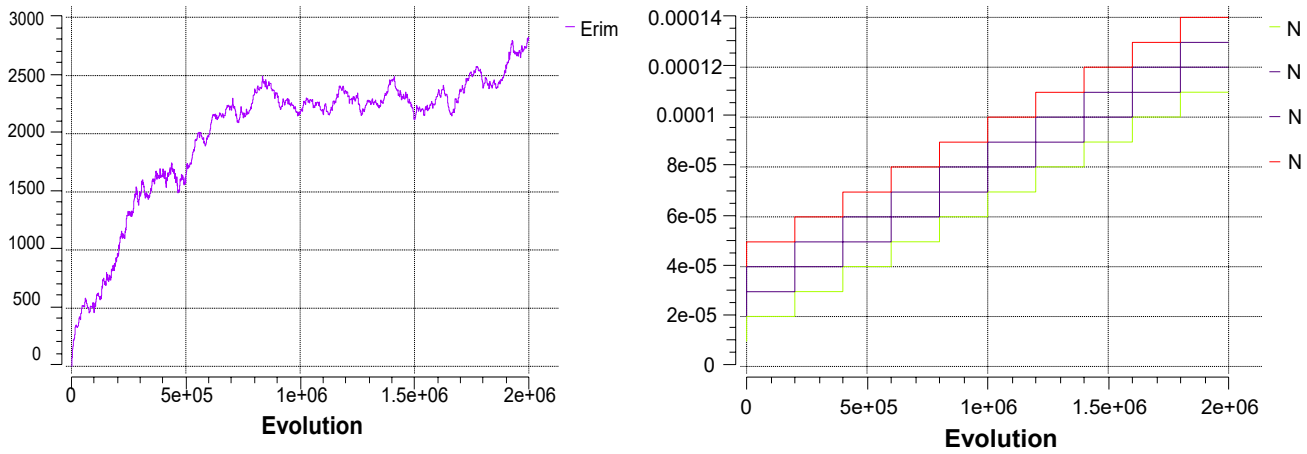

Figure 9.10: Evolution of the signals which control the changes in coupling for the fourth experiment. From top to bottom: No4, No3, No2, No1. These were used to separate the system into clusters.

9.3 Discussion

This model was selected since it has already been proven to work appropriately with the RCC controller, as shown in [48] and [49]. The first few tests conducted on this model consisted in establishing the 16 coupled oscillator structure. As this was already proven to work successfully, the remaining tests focused on defining the clusters using the parameters available and demonstrating it can be supported. A total of four tests are presented in this section, including the parameter values, system response, and the response of two individual oscillators. For all

the tests, the control strength was kept constant and the coupling strength was varied using signal E_{rim}, a scaled random input signal. Further to this, step functions No_1, No_2, No_3, and No_4 were used to modify the coupling strength in the clusters. These signals were used in tests 2 to 4 to distinguish the clusters.

9.3.1 Response to modifications to support model structure, implementation of RCC controller, modifications of coupling strength.

Tests 1 and 2 were conducted in order to construct the structure and implement the controller as described in [48] and [49]. The parameter values were taken from [48], [49], and [8]. The parameters for the first test are available in tables 9.1 and 9.2, and the results are shown in figures 9.2 and 9.3. This first test showed the reproducibility of the model described in [48] and [49]. Figure 9.2 shows the response and evolution in time of the system, and the phase space plots of oscillators 8 and 11. These figures show the system stabilizes into 10 periodically stable states.

In the second test step functions No_1, No_2, No_3, and No_4 were used to provide cluster differentiation. This was an initial test to observe the influence of this minor change on the response of the system. It can be seen from figures 9.4 and 9.5 that the response is modified only slightly. The system still manages to converge to the same 10 periodically stable states. This prompted the development of further tests to continue distinguishing the clusters. The results for these tests are presented in the following section.

9.3.2 Response to modifications of system parameters

Tests 3 and 4 focused on using parameter β, and the initial conditions of the system, to continue distinguishing the clusters and observe the response to these modifications. The work by [8] was used as reference in order to select the values that would work appropriately for the

model. For the third test, parameter β was considered for the modifications. For the fourth test, in addition to the changes in parameter β, the initial conditions were modified for two clusters. To modify these parameters, the work by Berry was considered, where the research pertinent to the wide ranges of dynamics which can be achieved by modifying β is presented. Several of these were tested in order to determine the appropriate ranges that would work on the structure of the model and were then implemented. This same article provides indication of the accepted initial conditions for the model, which was taken into account for the fourth test where these were considered. The tests performed on this model further demonstrated the capacity of the Berry model to work with the RCC controller, and to adapt to modifications in the structure beyond increments in the coupling strength.

The values of β which were chosen for each cluster are: 0.00075 (used for the previous tests) for cluster 1, 0.0007640 for cluster 2, 0.000747 for cluster 3, and 0.0007593 for cluster 4. Figure 9.11 presents the stability analysis of the model using each one of these values, where it is seen that although the differences among the values are minimal, the behaviour of the system is not. Once the stability analysis was concluded, the values were modified in the system and the third test was conducted. The values used for the third test are available in table 9.5 and 9.6, and the results are available in figures 9.7 and 9.8. Once again it can be seen that the system manages to stabilize periodically into 10 states with minimal modifications. This result is the same for oscillators 8 and 11. Figure 9.8 shows the evolution of the signals which were in control of modifying the coupling strength in the system.

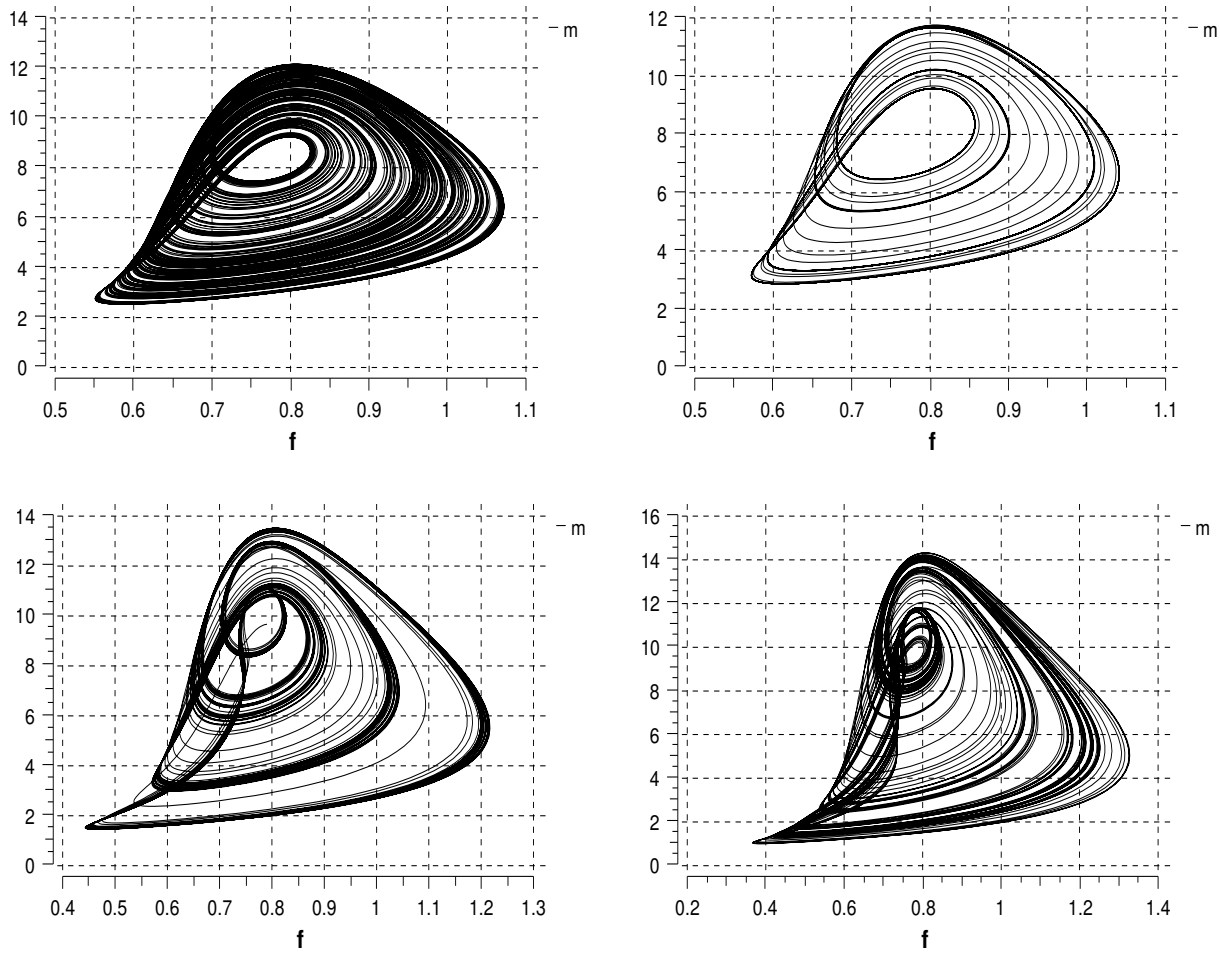

Figure 9.11: Phase space plots for the β values used in Test 3 for the following values of β: 0.00075 [top-left], 0.0007640 [top-right], 0.000747 [bottom-left], and 0.0007593 [bottom-right].

The fourth and final test conducted on the Berry model considered the modification of the initial conditions. The final values chosen are available in tables 9.7 and 9.8. The values were increased by 0.2 for variables m, f, and g, and by 0.02 for p. The values were modified in clusters 2 and 4. The test also considered the values for β which were implemented in test 3. The results are available in figures 9.12 and 9.13. Once again it is seen that the system adapts to the changes with very minimal modification to the general response of the system. The ten periodically stable states can still be distinguished as desired, both for the total response of the system, and the individual responses of oscillators 8 and 11. Figure 9.14 shows the relationship between the coupling strength and the amplitude, where it is possible to seethe 10 periodically stable states the system exhibits.

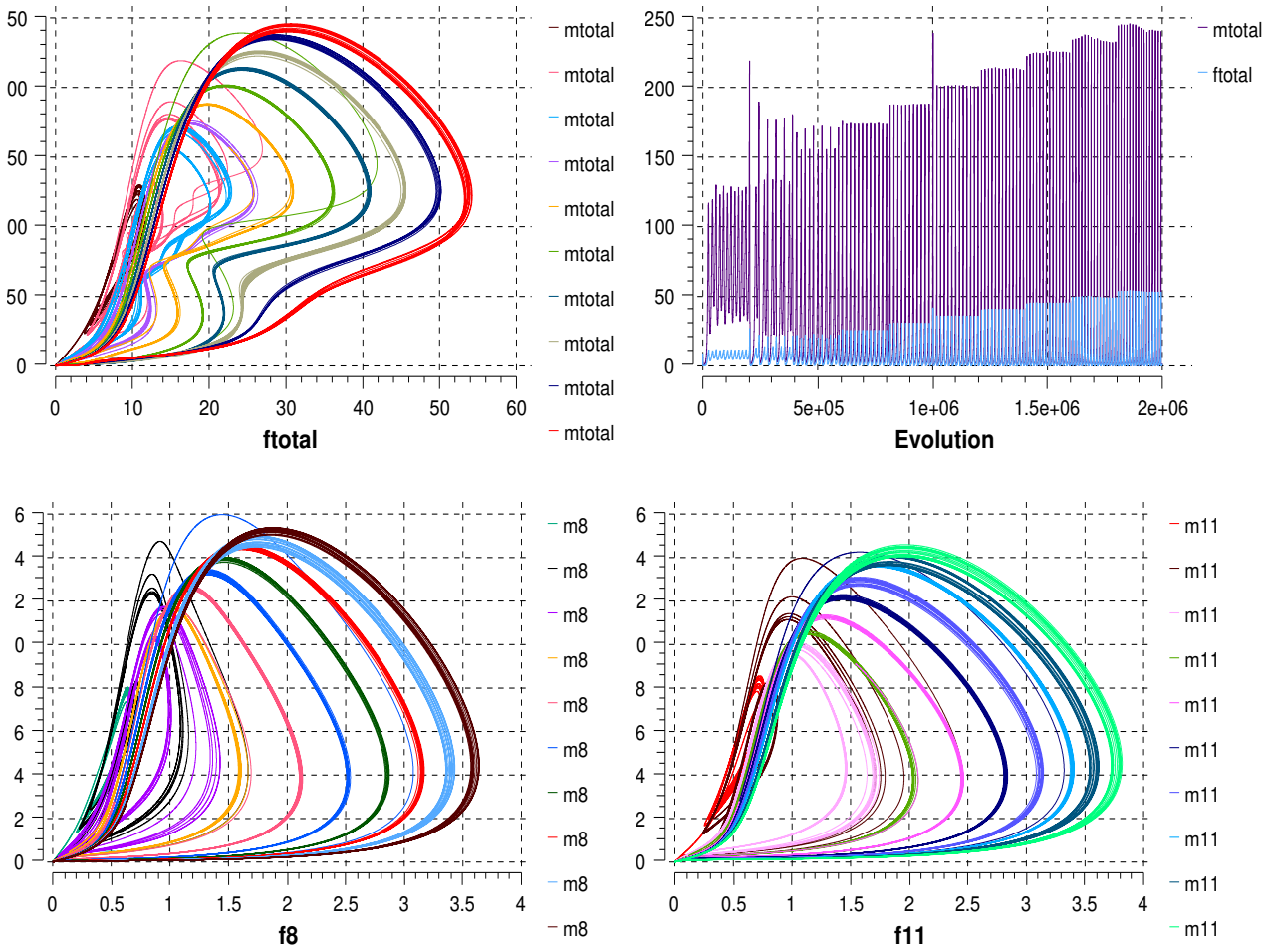

Figure 9.12: Results of the Berry model for the third test using the parameters in tables 9.5 and 9.6. This figure shows the total response of the system using the phase space plot [Top-Left] and the evolution in time [Top-Right]. The phase space plots of oscillators 8 and 11 are shown to exemplify the lower-level behaviour of the system.

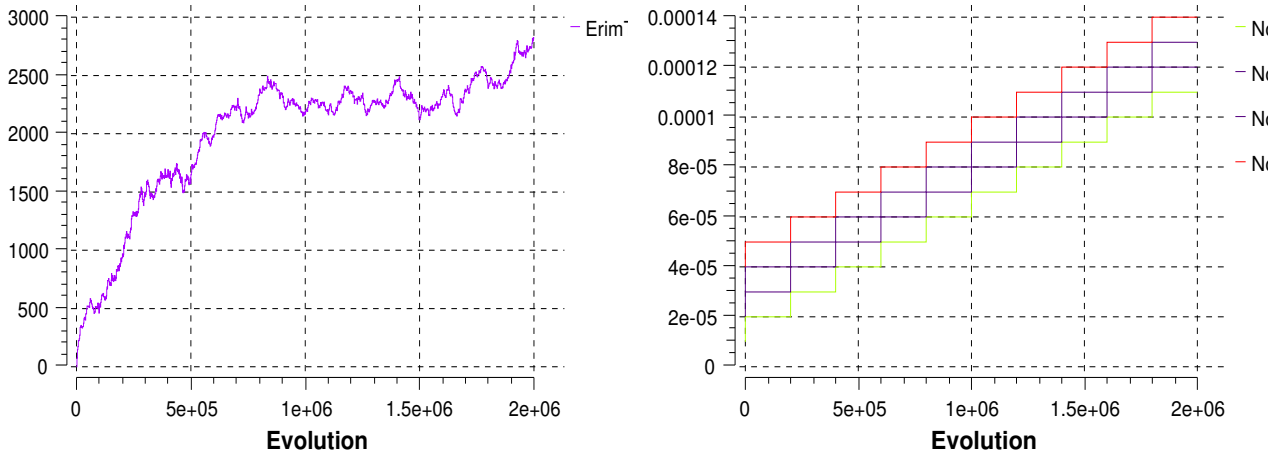

Figure 9.13: Evolution of the signals which control the changes in coupling for the third test. For this test, functions No1, No2, No3, and No4 were used to separate the system into clusters.

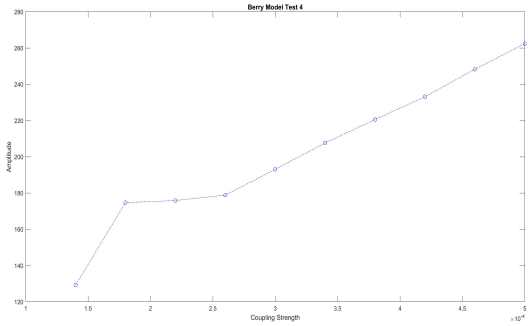

Figure 9.14: Figure showing the relationship between the coupling strength and the amplitude of the system response, each point represents a periodically stable state the system converges to.

Chapter 10

Discussion

Four different reaction-diffusion systems were used as candidates to develop the outcome model associated with this research project. Each of these models was evaluated in its capacity to represent a system of sixteen coupled oscillators (sixteen beta cells, separated into four islets); to tolerate modifications to the system parameters and to adapt to the response of the implemented RCC controller. Two models (Lengyel-Epstein and Brusselator) were selected given their relatively simple formulation which allows a wide range of behaviours according to the literature. The other two models (Berry and Gray-Scott) were chosen as they had already been proven to work with the RCC controller implemented. The tests performed on the models focused on three main aspects. The first was to verify the structure is supported by the model, where it is possible to establish the separation into clusters using the available parameters. The second was to evaluate the response of the system once the controller was implemented. The third was to evaluate the response of the system to modifications in the control strength and the coupling strength. This chapter summarizes the findings detailed in the previous four chapters of this work and presents the model formulation chosen as the best fit to represent the system.

For each model, the tests focused on three main aspects:

- Verifying that the sixteen coupled oscillator and four cluster structure could be supported. This structure represented the base for the model, where each oscillator is representing a β-cell, and each cluster of coupled oscillators represents an islet of Langerhan's. It was necessary to verify that the selected models could be coupled this way since this type of structure was not identified in the literature for all the models.

- Verifying that the system responded appropriately to the controller. The RCC controller had been successfully implemented with the Berry model and the Gray-Scott model, therefore it was only necessary to verify that these models responded positively to the changes in the structure provided by the separation into clusters.

- Verifying that the model structure responded appropriately to modifications of its internal parameters. This refers to the modifications of the parameters to separate the system into the clusters (islets), as well as the step functions used to modify the coupling and control strength.

The Lengyel-Epstein system and the Brusselator were selected given their relatively simple formulation which can yield a wide range of dynamics. The results of the Lengyel-Epstein system show that the system is capable of supporting the structure with a few limitations. The main limitation was observed when the sixteen coupled oscillator was constructed and an initial attempt was made to separate it into four clusters. It was found that the formulation selected was constricted by specific parameter values, which meant there were very reduced options to differentiate the clusters. This restriction reduces biological relevance as it would be preferred to have a range of values that allow singularity in the islets. Additionally, the response of the system exhibits regions of instability. This was thought to be due to the formulation of the controller, but it was found that it is mostly associated with the system parameters. Overall, the system was capable of representing the structure and exhibit periodic multi stability in response to modifications to the coupling strength.

Similar limitations were observed for the Brusselator in terms of the parameter values, where it proved difficult to use these to separate the system into clusters. Even with these limitations the response of the system manages to show periodic stability in multiple states. The model

also responded positively to modifications of the coupling strength, which serves to tailor solutions according to specific requirements. Overall the performance of the model was superior to the Lengyel-Epstein system. This was a positive result and proved that such a structure can be represented using a simple formulation such as the one provided by the Brusselator. The model also responded positively to the modifications in control strength and coupling strength, proving the existence of multiple periodically stable states. In future work, an alternative would be to use the parameters of the controller to provide cluster singularity.

The other two models used, Berry and Gray-Scott, were selected as they had already been proven to work well with the RCC controller. For this reason, the tests focused on observing how they would handle the separation into clusters and adapt to modifications in coupling strength and control strength. The results of the tests discussed in this chapter showed a positive response of the system to changes in coupling strength and control strength. Proper ranges of values accepter for the system parameters were determined with the help of the available literature and implemented in the model, the most notable being parameter T_{res}. Additionally, a wide range of values were identified to respond appropriately for the coupling strength. Similar results were obtained for the tests performed on the Berry model, where parameter β was used to separate the system into clusters. In addition to this, the coupling strength was modified using a scaled random external input function applied to the bifurcation parameter.

10.1 Final Model Selection

After evaluating the methodology on all four candidate models, it was determined that the best fit to represent the structure is the Gray-Scott system. This system performed best in terms of supporting the structure, allowing singularity in the oscillators though the use of the initial conditions, as well as the clusters with the use of two system parameters. The structure was also robust in adapting to increases to coupling and control strength. The equations used,

including the RCC controller, where i = {1....16} are:

$$\frac{\partial a_i}{\partial t} = \delta \nabla^2 a_i + \frac{\sigma_a(a)(1 - a_i)}{T_{res}} - a_i \beta_i^2 \tag{10.1}$$

$$\frac{\partial b_i}{\partial t} = \nabla^2 b_i + \frac{\sigma_b(b)(b_0 - b_i)}{T_{res}} + a_i b_i^2 - k b_i \tag{10.2}$$

Where the control equations are as follows:

$$\sigma(a) = f_a e^{\xi_i q_a} \qquad \sigma(b) = f_b e^{\xi_i q_b} \tag{10.3}$$

and:

$$q_a = \frac{a}{a + \mu_a} \qquad q_b = \frac{b}{b + \mu_b} \tag{10.4}$$

This section presents the results of a final simulation to demonstrate an additional advantage of the model, where delayed coupling is implemented. Biologically, this would account for the case where the clusters are being recruited in accordance to the surrounding level of glucose to control the system. In this scenario, the communication among the clusters would not be synchronous initially but would reach such a state with the implementation of the controller, indicating the level of glucose must be stabilized. The values used for the parameters and initial conditions are available in tables 10.1 and 10.2. Parameter $T_{res}i$ was used to split the system into clusters using two different values. The coupling strength (∇^2) is modified using step inputs No_i which are different for each cluster. The same is true for the control strength (ξ) which is modified using a step input denoted as cin. The complete form of the model used for simulation is included in the appendix (A.4).

The phase space response of the system is shown in figure 10.1, where the relevant stages are individually exhibited. The top-left figure shows the behaviour of the system prior to the implementation of the controller which, as is seen in figure 10.2 [bottom-right], the controller is activated at t = 30000. The controlled states are also shown in figure 10.1 [bottom-right], which are similar in amplitude and frequency to those observed in prior experiments, meaning the system manages to achieve the desired periodical stability. Two intermediary states are

Parameter	Value
b_0	$\frac{1}{15}$
k	$\frac{1}{40}$
δ	4.6
$T_{res}1$, $T_{res}3$	214.5
$T_{res}2$, $T_{res}4$	240
No_1(step)	0.009
No_2(step)	0.0007
No_3(step)	0.006
No_4(step)	0.0005
f_a, f_b (RCC)	1, 1
μ_a, μ_b (RCC)	1, 1
ξ_1 (RCC)	0.55
ξ_2 (RCC)	0.85
ξ_3 (RCC)	0.75
ξ_4 (RCC)	0.65

Table 10.1: Gray-Scott Parameters

Variable	Initial Value
a_1, a_3, a_6, a_7, a_{10}, a_{12}, a_{13}, a_{15}	0.5
b_1, b_2, b_4, b_5, b_8, b_{11}, b_{14}, b_{16}	0.4
a_2, a_{11}	0.6
b_3, b_9, b_{13}	0.3
a_4, b_{10}, b_{15}	0.7
a_5, a_9, a_{14}	0.1
a_8, a_16	0.9
b_6, b_12	0.2
b_7	0.8

Table 10.2: Gray-Scott Initial Conditions

also shown, which are exhibited in the system after the controller is implemented, but before all the clusters are active in their coupling stages. As seen in figure 10.2 [bottom-left], coupling is activated at different stages. All of these stages can be seen in the system evolution shown in 10.2 [top].

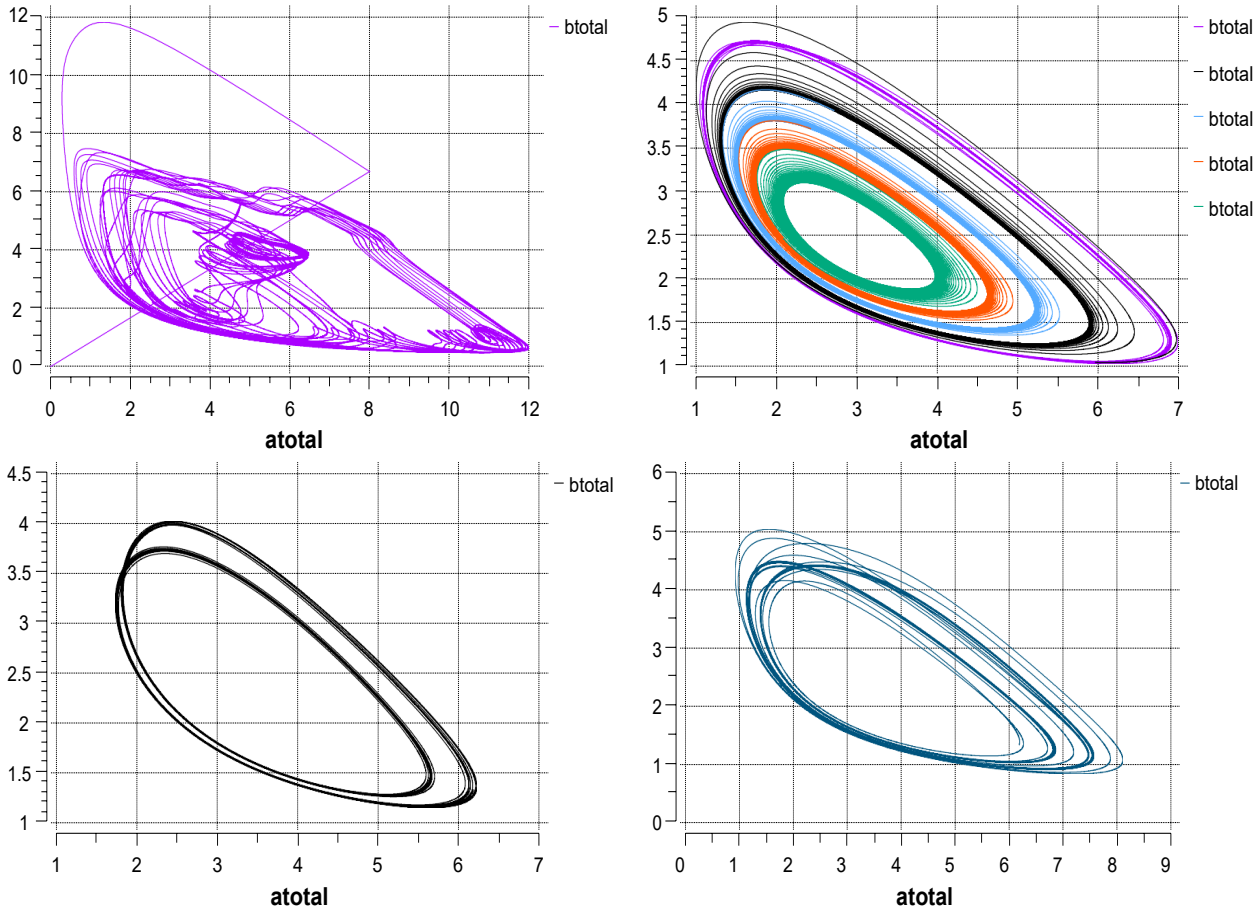

Figure 10.1: Phase-space plots of the total system response. Including the response before the controller is activated [Top-left], The controlled states [Top-Right], and two intermediary states, t = 30000-40000 [Bottom-left], and t = 40000 - 50000 [Bottom-Right]

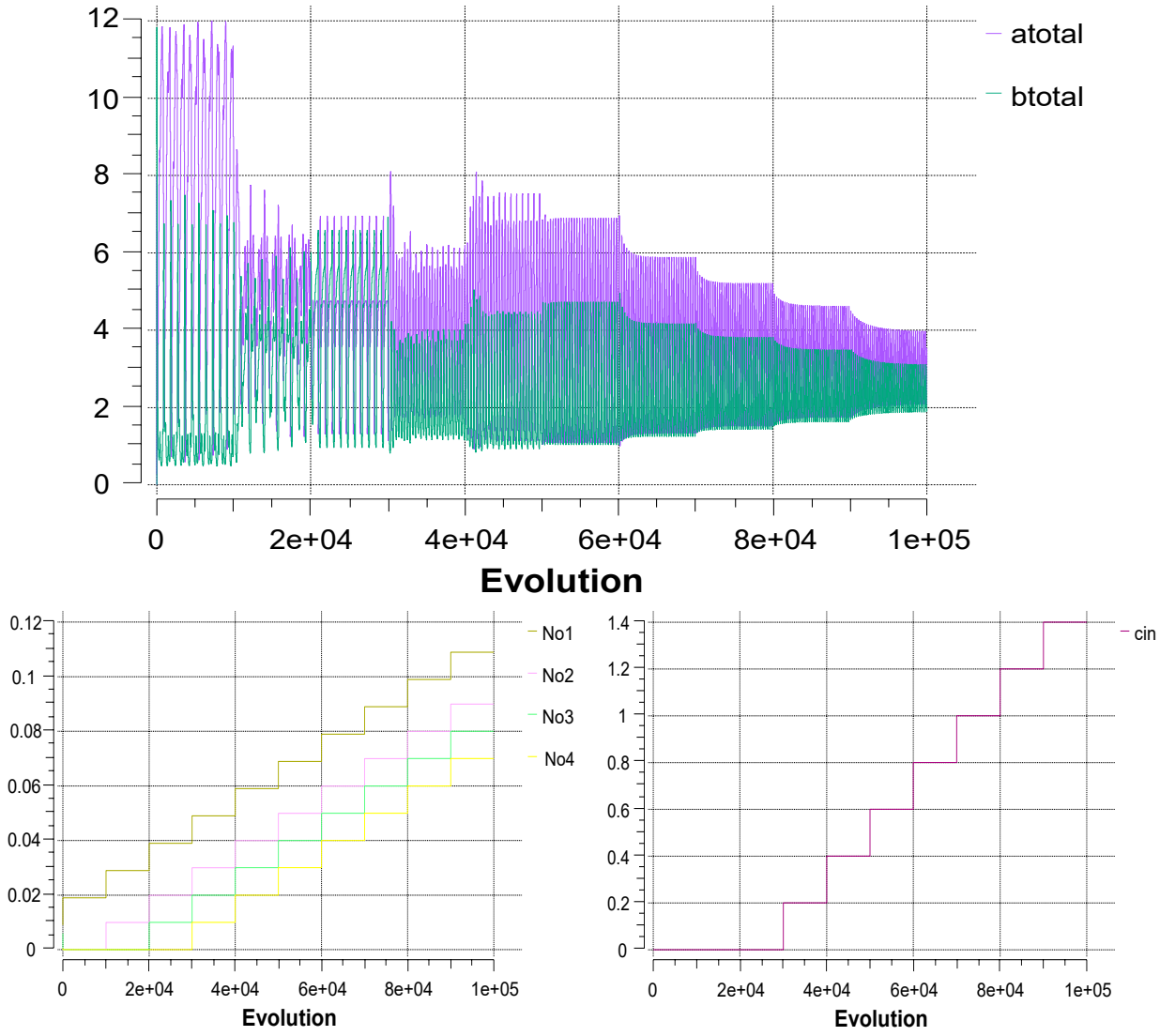

Figure 10.2: Evolution of the total system response [Top], step inputs No_i which control the coupling strength [Bottom-Left], and step input cin which controls the control strength [Bottom-Right]

Relevant differences are seen among the clusters in each stage when taking a more granular look. Figure 10.3 shows the individual phase-space response of each cluster, where the effects of the delayed coupling input become visible. At this stage, the controller has not been activated, and only the coupling strength of cluster 1 is active. The biological relevance of this observation would be the case where the system is in a state where the cells are ready to release insulin, but the required threshold of surrounding glucose has not been surpassed, therefore the response has not been propagated.

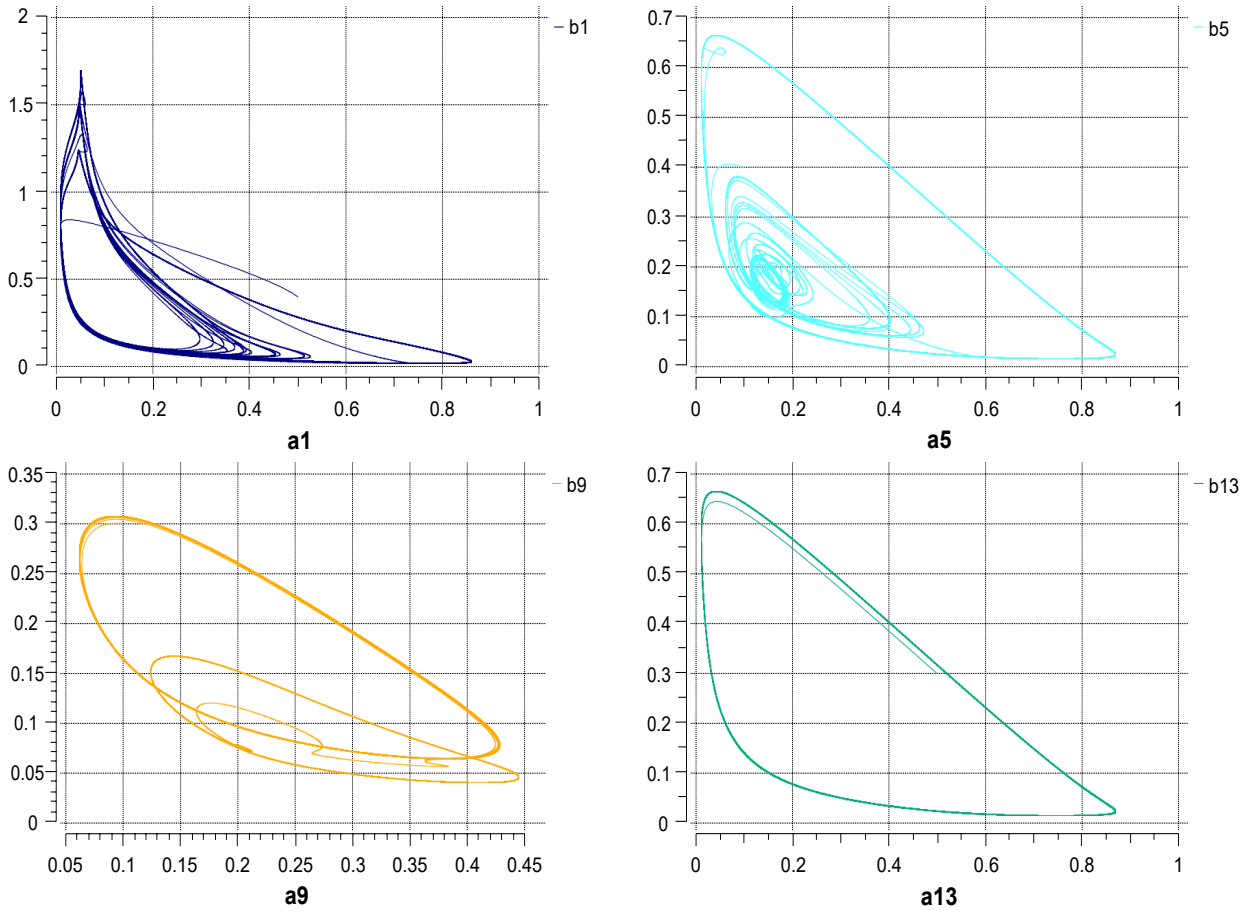

Figure 10.3: Phase-Space response of clusters before the control is activated. Cluster 1 [a1,b1], cluster 2 [a5,b5], cluster 3 [a9,b9], and cluster 4 [a13,b13]

The responses shown in figures 10.4 and 10.5 correspond to the intermediary stages, where the controller has been activated, but the clusters are still propagating the response, meaning the communication among the clusters is periodically being activated. The effect of the controller can be seen, as the behaviour appears more uniform, but not enough to stabilize the total response, as was seen in figures 10.1 and 10.2.

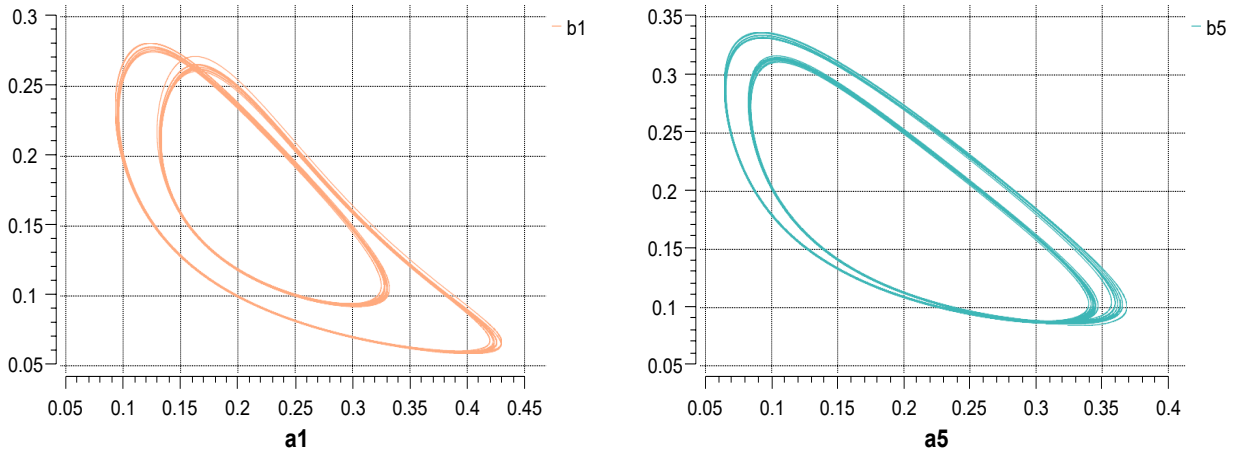

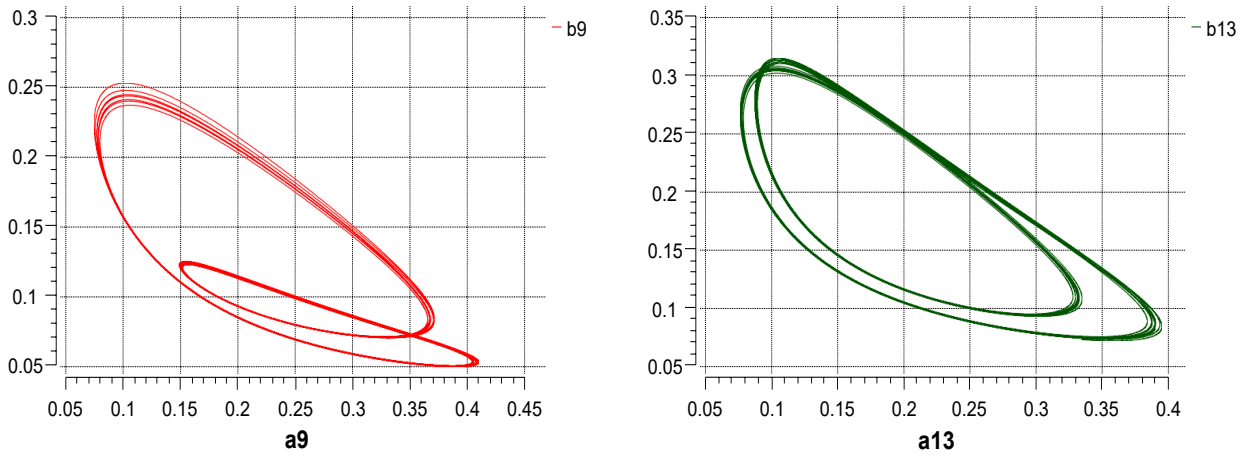

Figure 10.4: Phase-Space response of clusters in the first intermediary state where t = 30000 - 40000. Cluster 1 [a1,b1], cluster 2 [a5,b5], cluster 3 [a9,b9], and cluster 4 [a13,b13]

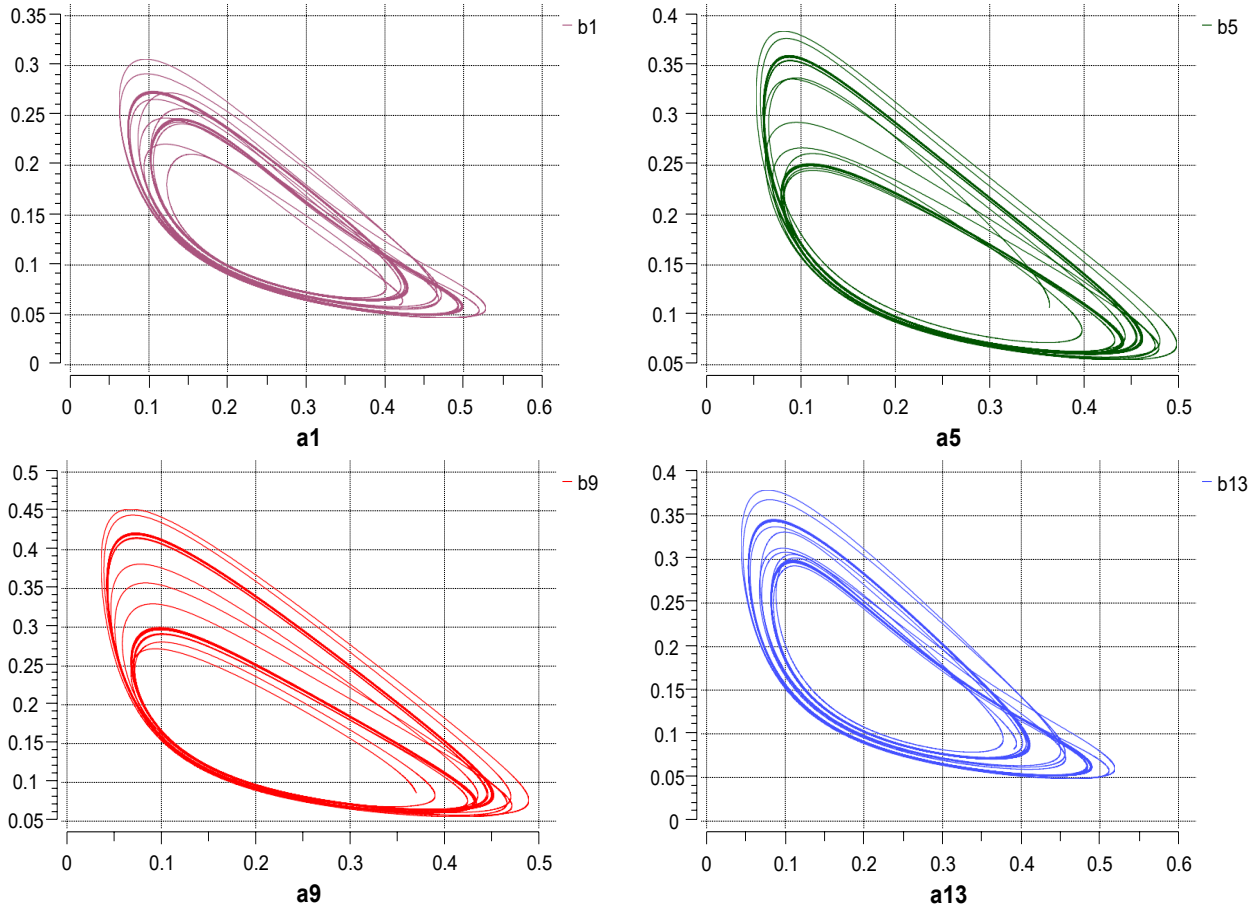

Figure 10.5: Phase-Space response of clusters in the first intermediary state where t = 40000 - 50000. Cluster 1 [a1,b1], cluster 2 [a5,b5], cluster 3 [a9,b9], and cluster 4 [a13,b13]

Figure 10.6 shows the phase-space response of the controlled states in the clusters, at this stage the controller is active, as is the coupling strength of all the clusters, meaning the response has been fully propagated, recruiting all the clusters to control the system. As the coupling

strength continues to increase, along with the control strength. The controlled states continue to decrease in amplitude, reducing the need for the controlled output. Figure 10.7 shows the evolution in time of the individual clusters, where all the states are visible.

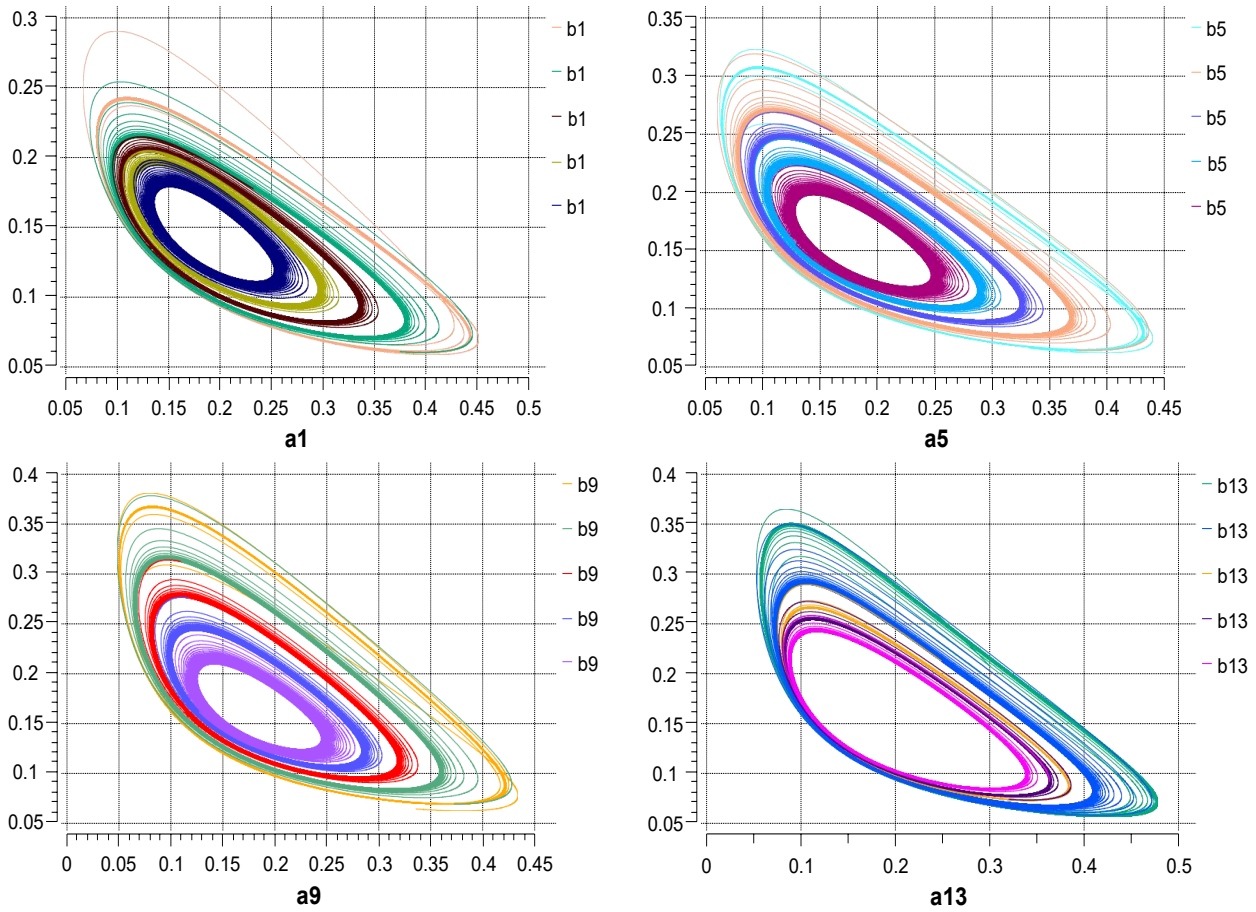

Figure 10.6: Phase-Space response of the controlled states. Cluster 1 [a1,b1], cluster 2 [a5,b5], cluster 3 [a9,b9], and cluster 4 [a13,b13]

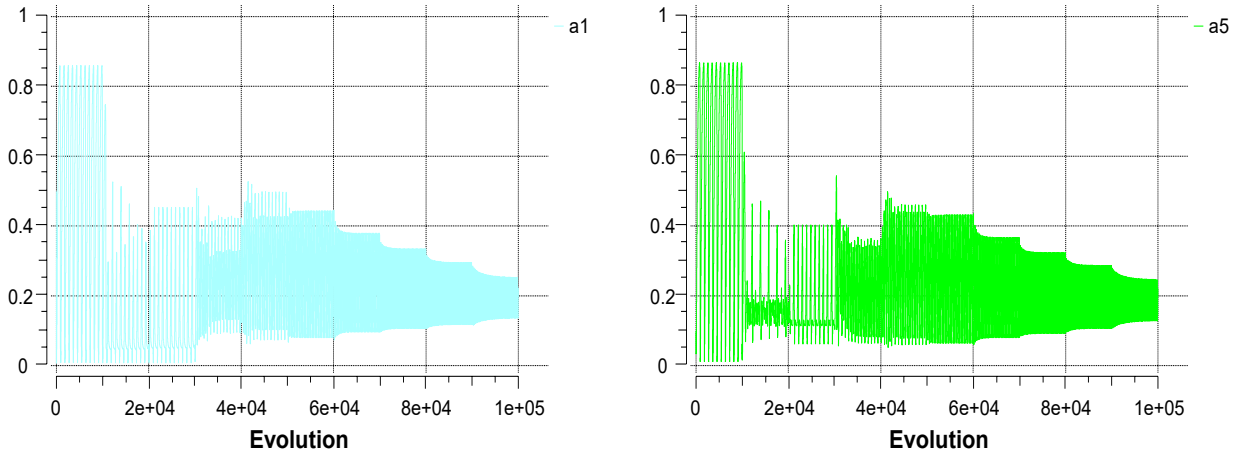

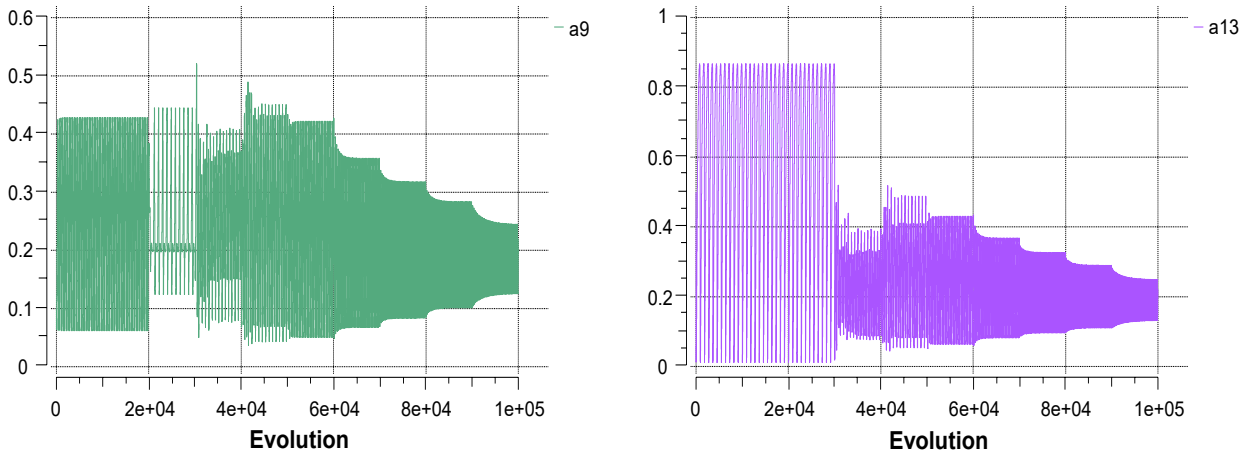

Figure 10.7: Evolution in time of each cluster. Cluster 1 [a1], cluster 2 [a5], cluster 3 [a9], and cluster 4 [a13]

10.2 Final considerations

This final experiment emphasizes the advantages of the structure, which encompasses the use of the RCC controller, the use of coupled oscillators, and the advantages of using the Gray-Scott system, which provides an adaptable formulation that can represent pulsatile insulin secretion. The model studied by Pu et. al. is one of the few available examples of progression in studying a system of coupled oscillators in relation to the glucose-insulin system. In [57], the authors use the model developed by Bertram et al in [9] to represent a structure of coupled β -cells. The author uses a 3D hexagonal lattice to represent the system and assumes the coupling is always present from the beginning of the simulation for the scaled structure. The aim of the study by Pu et al is to use the model to evaluate the effect of unhealthy cells on synchronized insulin secretion, and the authors report that insulin secretion will be destroyed once the number of unhealthy cells surpasses a threshold of 20%.

The model used is a deterministic model made up of four components: a glycolytic component, a mitochondrial metabolism component, a cytoplasmic intermediate, and a plasma membrane component. The differential equations and parameters of the referenced model are available in [9], these are not included in this work as the formulation includes 31 equations and 61 parameters for all components. Taking a closer look at the model it is found that it is an extension

of a previous model developed by the authors. It is a simplified model of mitochondrial ATP production initially developed by Smolen [65] based on data from muscle extracts [9] combined with the mitochondrial metabolism component originally developed by Keizer and Magnus [35] using a minimal description and a third model previously developed by the authors. This results in a top-down approach based model of rigorous enzymatic reactions with established parameters. From the literature review, and the objective definition established for this thesis, it was determined that this methodology is likely to be limited in it's capacity to represent the Glucose-Insulin system, which is why this, and other glycolytic oscillators were not considered as candidates to build the model.

The scope of the study performed by Pu et al does not cover studying the system under the effect of a controller, observing the effects of modifying the coupling strength, or studying a structure of clusters. Such a system is not found in the literature and it can be inferred that this would prove a difficult task using the model by Bertram et al given its scale and structural limitations. Throughout the literature review stage of this research project it was established that a bottom-up approach, based on properties of the system and using a base model capable of generating periodically stable behaviour yields a favourable approach to representing the glucose-insulin system.

From the experimental work presented in this chapter, it is seen that the structure proposed in this research work provides the advantages desired. The resulting model represents a system of coupled oscillators, split into clusters by providing singularity given by system parameters as well as control parameters. It adapts to modifications to coupling strength and control strength, and responds appropriately to delayed input of coupling strength. All these properties increase it's biological relevance and allow further experimentation to be conducted on it due to the flexibility seen in it's parameter values. Additionally, the structure is scalable as it has been proven to work on the Berry model with as many as 96 coupled oscillators.

Overall, the results obtained from developing the model, representing the structure, and modifying the system parameters, prove that the proposed model structure can be represented, multi-stability is demonstrated in all the models tested, and the solutions can be tailored according to the requirements of the simulation. The following chapter elaborates further on the conclusions reached and what this means for the representation of the glucose-insulin system. Special focus is given to each aspect tested and the characteristics that were established in the first chapter of this work.

Chapter 11

Conclusion

This chapter summarizes the results and achievements of this research. The chapter is the final one of this thesis and is divided into three sections, the first focuses on highlighting the main aspects that contributed to the results of this research. The second section presents the possible applications and future work associated with the findings, and the third section presents the statement of originality of this thesis.

11.1 Summary of Thesis Achievements

During the initial stages of development of this project, a review of physiological models of the glucose-insulin system was conducted. The review focused on exploring the models which marked the most representative milestones in the development of the representation of the system. The aim of this review was to obtain the key characteristics of the system which needed to be represented in the model, focusing particularly on the dynamic aspects around them. Once these results were obtained, a second review was performed to explore computational models, to determine which ones could represent the desired properties. Four models were selected, including the Lengyel-Epstein system, the Brusselator auto-catalytic system, the Gray-Scott model, and the Berry model.

There is no evidence suggesting that the aforementioned models have ever been used to represent the phenomenological aspects of insulin release in the pancreas. A major advantage of using these models was their capability of explaining complex dynamical systems using a flexible mathematical approach given the range of parameter values that can be used, a key element to assess biological relevance. Implementing this novel methodology assisted in filling in one major gap in physiological modelling, the inclusion of the dynamic behaviour present in the system, which was achieved by following a bottom-up approach. The aspects that contributed to the successful implementation of the model, and the results presented and discussed in chapters 4 and 5 are highlighted below. These are based on the characteristics of the system introduced in chapter 2 (section 2.2), and described in chapter 3 (section 5.1).

11.1.1 Coupled oscillator structure

This was one of the most relevant aspects to represent given the bottom-up approach desired, and the fact that it would represent the base of the model. The structure desired consists on a set of sixteen coupled oscillators, where each oscillator represents a β cell. Further to this, the structure is separated into four clusters, where each cluster represents a Langerhans islet. It had already been proven that the sixteen coupled oscillator structure worked for the Berry model and the Gray-Scott model (see [48] and [49]). For these to models what remained to be implemented was the separation of the structure into clusters, which was successful for both models using the coupling strength and specific system parameters. For the Gray-Scott system in particular, the structure showed greater flexibility given the possible parameter values, one of the main reasons it was chosen as the best performer.

In the case of the Brusselator and Lengyel-Epstein, no evidence was found on the representation of the structure, especially using more than two oscillators. The structure was successfully implemented on the Brusselator with a few limitations on the parameters. For the case of the Lengyel-Epstein system, the structure was eventually achieved, but the performance and

response of the system to changes in coupling and control strength was limited. Overall it was proven that the structure can be represented, both in terms of the size and the separation into clusters. Additionally, three out of the four candidate models tested were capable of achieving positive results in terms of changes to the coupling and control strength.

11.1.2 Coupling Strength

Coupling strength in this model represents the connectivity of the cells. This was the initial factor to modify in the model to achieve separation of the clusters. This was taken as the starting point to represent how the cells in each islet share a common connectivity which differs from the connectivity in other clusters. This represents the property of the propagation of the response. β cells will release a packet of insulin once a threshold is surpassed after sensing the neighbouring concentration of glucose. This indicates that the cells and islets are operating in states and will increase their connectivity strength when the requirement for insulin increases at a local level according to what they sense in their neighbouring cells and islets.

This property was successfully implemented in all four of the candidate models selected. For the Brusselator and the Lengyel-Epstein system higher variations among the clusters were used as this structure had not been implemented for these systems in the literature. This proved advantageous as it demonstrates the capability of representing a system with high variability in the connection of its cells which still manages to respond to the changes appropriately and maintains global periodic stability. For the case of the Brusselator, an additional advantage was the implementation of non-linear coupling, which maintains the dynamical aspects of the system throughout. The structure was also successful for the Berry model and Gray-Scott. One particular aspect of the Gray-Scott system was the fact that minor changes in the coupling strength would cause significant changes. To address this, several tests were performed in order to establish the ranges of operation that would suit this model. This wide range of coupling strength values made this candidate model the optimal one to represent the system, as

it allows for relevant longitudinal experimentation and is tolerant of modifications to intra-islet coupling changes, particularly for the case where the coupling is set to 0

11.1.3 Implementation of RCC controller

The implementation of the RCC controller was essential to maintain the structure in a periodically stable state and contributed to the state changes in the system which represent the propagation of the response to modifications to the system parameters or disturbances. The implementation of this controller was different for each of the models given that it is applied on the incremental terms of the equations. A limitation was observed for the Lengyel-Epstein system, where there is only one available incremental term where the controller could be implemented. For the other three models, there was more flexibility as there were more incremental terms where the controller was successfully implemented. For these three models, the controller contributed in great measure to allow the system to switch states.

This is an important characteristic to replicate in our model as it represents the capability of the system to respond to disturbances (meal, exercise, stress, etc.) and shift to states where the output of insulin increases or decreases accordingly. Implementing this type of controller provides an additional advantage over other controllers normally implemented, as it stabilizes the system into periodically stable states. Having this dynamic behaviour represented was one of the other main objectives of this research project, as it tends to be overlooked to avoid system complexity. The other representative aspect that contributed to the representation of the dynamic components of the system given their inherent capability to represent it.

11.1.4 Use of system parameters

When the models used for this project were introduced in chapter 3, their parameters were also introduced. Using these system parameters was useful and played a key part in both tuning the

system to maintain the dynamical behaviour, and in providing additional elements to separate the system into clusters. This is to maintain biological relevance, in the sense that each cluster behaves in accordance to the cells that it is composed of. In order to achieve this is was necessary for the models to have flexible parameter values. For the Lengyel-Epstein system this property was challenging to represent as the parameter values were limited for the formulation chosen. This made it particularly difficult to achieve state shifting in the structure with this particular model. Although the changes in state were evident for individual cells, they could hardly be visible when looking at the global response. A similar limitation was observed for the Brusselator, where the parameter values were limited, which is why for this model it was decided to use the control strength to increase singularity in the clusters.

The Berry model and the Gray-Scott system, parameters β and T_{res} respectively were modified to add singularity to the clusters, as well as the initial conditions. The effects of implementing these modifications could be seen in the response of the individual oscillators and maintained the global response as desired. This helped assess the performance of the models as it is desired to use a base model whose parameters can represent biologically relevant features. It was therefore determined that Gray-Scott and Berry are more biologically relevant for the purpose of representing the glucose-insulin system.

11.1.5 Closing Statement

The first chapter of this work introduced the research question to be answered through the development of this project:

Can we simulate the relationship between glucose and insulin secretion at cellular level by developing a dynamical, biologically-inspired phenomenological model?

The discussion presented in this section described the main aspects that contributed to successfully answering this question. It was found that this relationship can be represented and

three out of the four models selected were highly successful in doing so. Using these models provides an advantage over the physiological models explored given the flexibility observed in their parameter values and their inherent capacity to generate the desired dynamic behaviour. This makes them biologically relevant as it is known that biological systems also operate within ranges and will display particular features accordingly. These models were also seen to be dynamically relevant as they were able to converge to multiple periodically-stable states.
Using this structure also provided the advantage of representing singularity in clusters, which is another relevant aspect for biological relevance, where it is known that no two cells, or cell clusters, will behave in the exact same way. The model assessed this matter by using a structure where each of the cells are represented by an oscillator with flexible parameter values. Another important feature of this work was the implementation of the RCC controller, which assisted in tuning the system behaviour to achieve the desired dynamics, and provided additional parameters to add singularity to the clusters and cells. The following sections present the relevant future work to be considered for this research project, and the originality statement of this thesis.

11.2 Future Work

It was found that three out of the four selected base models were capable of representing all the characteristics established for the system. Of the three models which successfully represented the system, two were determined to be more appropriate in terms of biological relevance, the Berry model and the Gray-Scott system. The model that renders the best results altogether, also when considering computational cost, and adaptability to delayed coupling, is the Gray-Scott system. This result was obtained from the observation that the parameters of these models have the capability of operating in ranges which both maintain the desired dynamics of the system, and allow the establishment of singularity in the clusters of the system. Although the focus of this research was to represent the system under non-pathological conditions, the development of this methodology and these models opens up avenues to represent other prop-

erties of the system, especially the ones present under pathological conditions, specifically type-2 diabetes. An example of properties that can be explored are the malfunctioning of the cells/clusters, and the response of the system under these circumstances.

This thesis intended to demonstrate that the behaviour of the system could be represented using reaction-diffusion systems with a dynamically relevant formulation that generates the desired behaviour. Additionally, it was intended to use models which had not been fitted from physiological data, which is a common trend of physiological models of the glucose-insulin system. The results of this project showed that the Gray-Scott system provides the best outcome in terms of cluster parameter flexibility and biological relevance.
After observing that the candidate base models chosen were capable of representing the desired behaviour, it opens up avenues to explore the use of other reaction-diffusion systems to continue assessing the matter of biological relevance. A possible candidate model which can be explored is the Morris - Lecar model [38], or the variation to it developed by Tsaneva - Atanasova et. al. in [71]. The Morris - Lecar model was developed by Catherine Morris and Harold Lecar an it presents a model to represent the behaviour exhibited by barnacle muscle fibres. It was developed after observing the oscillating behaviour caused by the interaction of calcium and potassium in the fibres. The variation presented by Tsaneva - Atanasova et al in [71] is also used to study the diffusion of calcium. The reason this model was not included in the scope of this project was because of its consideration of calcium oscillations. Although there is overwhelming evidence on the link between calcium oscillations and glucose oscillations, this is not a relationship that has been studied in depth and would require further research to successfully implement it using the structure presented in this work. Some work has been done on the morphology of these oscillations [66], but the formulations are complex, and based on experimental data which subjects them to strict parameter values, which strays from the proposed approach in this thesis.

For this research, the system's response was evaluated by using step functions to increase the coupling strength and the control strength. It was important for the model to respond pos-

itively to these changes and adapt the global response appropriately to multiple states. For further research it would be appropriate to test the system response to other inputs which resemble inputs of meal intake. This will allow to continue tuning the system and to observe the response to a more biologically accurate input. The model should also be validated using data from real patients, however, which are the most appropriate datasets or signals should be studied. A possibility would be to explore the data that can be provided using the Type 2 diabetes simulator developed by Dalla Man, Rizza, and Cobelli, available in [17].

11.3 Statement of Originality

The development of physiological models of the glucose-insulin system has undergone three major waves of development. The trend has shifted from early models which followed a compartmental approach, going through maximal and minimal models,and arriving to the current trend where the oscillations in the system are being studied. This observation, and the identification of all the properties identified in the system due to the development of all the models motivated the development of this research project.

It had been mentioned in the literature how little work has been done on detailed modelling of insulin secretion, this is one of the main aspects which were assessed in this project. The model developed is bio-inspired, as it was developed following characteristics identified from the study and development of models of insulin-release. The characteristics desired were strictly related to lower-level mechanisms involved in the release of insulin. The model also followed a bottom-up approach development, which strays from the traditional top-down approach. Another important aspect which was represented was the dynamic behaviour of the system, characterized by the presence of oscillations. This is one of the aspects that a lot of physiological models tend to overlook or simplify.

The key aspect to the positive results achieved in this model was the use of reaction diffusion models as a base. It is common practice to use these types of models and analyse their behaviour under the effects of coupling. The contribution of this work was to adapt the structure

to represent a low-scale pancreas, and it was possible to prove the existence of multiple periodically stable states under the influence of the RCC controller. Such a structure has not been used before to represent the behaviour of the glucose-insulin release system. The resulting structure uses the Gray-Scott system, which is capable of generating periodically stable behaviour and tolerate delayed coupling. The model successfully adapts to the implementation and increments of coupling and control strength even when these are incorporated at different times in the simulation, this renders different periodically stable states at the local and global level, a property of the Glucose-Insulin system. And finally, the model incorporates singularity provided by parameter values to establish clusters.

References

[1] Abdelmalek S and Bendoukha S. "The Lengyel – Epstein Reaction Diffusion System". 2019 https://doi.org/10.1007/978-3-319-99918-0

[2] Adams CL and Lasseigne DG. "An extensible mathematical model of glucose metabolism. Part I: the basic glucose-insulin-glucagon model, basal conditions and basic dynamics". *Letters in Biomathematics*,2018, 5(1), 70-90.

[3] Aly S. "Bifurcation in the Lengyel – Epstein system for the coupled reactors with diffusion". *Journal of the Egyptian Mathematical Society*, 2016, 24(1), 25-29.

[4] Bak P, Tang C, and Wiesenfeld K. "Self-organized criticality: An explanation of the 1/f noise". *Physical Review Letters*. 1987, 59(4), 381-384.

[5] Berg JM, Tymoczko JL, Stryer L. "The Michaelis-Menten Model Accounts for the Kinetic Properties of Many Enzymes". *Biochemistry*. 5th edition. New York: W H Freeman; 2002. Section 8.4, Available from: https://www.ncbi.nlm.nih.gov/books/NBK22430/

[6] Bergman RN, Ider YZ, Bowden CR and Cobelli C. "Quantitative estimation of insulin sensitivity". *American Journal of Physiology* 1979;236:E667–E677.

[7] Bergman RN, Phillips LS and Cobelli C. "Physiologic evaluation of factors controlling glucose tolerance in man: measurement of insulin sensitivity and beta-cell glucose sensitivity from the response to intravenous glucose". *The Journal of Clinical Investigation*, 1981, 68(6), 1456-1467.

[8] Berry H. "Chaos in a bienzymatic cyclic model with two autocatalytic loops". *Chaos, Solitons and Fractals*, 2003, 18(5), 1001-1014.

[9] Bertram R, Satin LS, Pedersen MG, Luciani DS and Sherman A. "Interaction of glycolysis and mitochondrial respiration in metabolic oscillations of pancreatic islets". *Biophysical Journal*, 2007, 92(5), 1544-1555.

[10] Brun JF, Fedou C, and Mercier J. "Postprandial Reactive Hypoglycemia". *Diabetes & Metabolism (Paris)*, 2000, 26, 337-351.

[11] Cantu L, Sanchez IY, Garza-Castañón L, and Martinez SO. "Feedforward compensation of exercise in diabetes". *18th Mediterranean Conference on Control and Automation, MED'10 - Conference Proceedings*, 2010, 1335-1340.

[12] Chappell M, and Payne S. *Physiology for Engineers* 2016, 13.

[13] Cobelli C, Caumo A and Omenetto M. "Minimal model SG overestimation and SI underestimation: improved accuracy by a Bayesian two-compartment model". *The American Journal of Physiology*, 1999, 277(3 Pt 1), E481-E488.

[14] Cobelli C, Man CD, Sparacino G, Magni L, De Nicolao G, and Kovatchev BP, "Diabetes : Models , Signals , and Control," 2009, vol. 2, pp. 54-96.

[15] Cobelli C, Renard E, and Kovatchev B, "Artificial pancreas : Past, present, future". *Diabetes* 2011, vol. 60, no. 11, pp. 2672-2682.

[16] Dalla Man C, Raimondo DM, Rizza RA, and Cobelli C, "GIM, Simulation Software of Meal Glucose-Insulin Model". *Journal of diabetes science and technology (Online)*, 2007, vol. 1, no. 3, pp. 323-30.

[17] Dalla Man C, Rizza RA, and Cobelli C, "Meal simulation model of the glucose-insulin system". *IEEE Trans. on Biomedical Eng.*, 2007, vol. 54, no. 10, pp. 1740-1749.

[18] Dassau E, Zisser H, Harvey R, Percival M, Grosman B, Bevier W, Atlas E, Miller S, Nimri R, Jovanovic L, and Doyle F. "Clinical Evaluation of a Personalized Artificial Pancreas". *Diabetes Care*. 2013 Apr; 36(4): 801-809.

[19] De Kepper P, Castets V, Dulos E and Boissonade J. "Turing-type chemical patterns in the chlorite-iodide-malonic acid reaction". *Physica D*, 1991, 49, 161-169.

[20] Demirel Y. "Michaelis-Menten Equation". *Nonequilibrium Thermodynamics (Second Edition)*. 2007.

[21] Devi A, Kalita R and Ghosh A. "A Mathematical Model of Glucose-Insulin regulation under the influence of externally ingested glucose (G-I-E model)". *International Journal of Mathematics and Statistics Invention (IJMSI) Www.Ijmsi.Org*, 2016, 4(5), 54-58.

[22] Derouich M and Boutayeb A. "The effect of physical exercise on the dynamics of glucose and insulin". *Journal of Biomechanics*, 2002, 35, 911-917.

[23] Dua P, Doyle 3rd FJ and Pistikopoulos EN. "Model-based blood glucose control for Type 1 diabetes via parametric programming". *IEEE Transactions on Bio-Medical Engineering*, 2006, 53(8), 1478-1491.

[24] Enderle JD, and Bronzino JD. *Introduction To Biomedical Engineering* . 3rd ed. London: Academic Press, 2011. pp. 127-131.

[25] García-Jaramillo M, Calm R, Bondia J, Tarín C, and Vehí J. "Computing the risk of postprandial hypo- and hyperglycemia in type 1 diabetes mellitus considering intrapatient variability and other sources of uncertainty". *Journal of Diabetes Science and Technology*, 2009, 3(4), 895-902.

[26] Gilon P, Ravier MA, Jonas JC, and Henquin JC. "Control Mechanisms of the Oscillations of Insulin Secretion In Vitro and In Vivo". *Diabetes*, 2002, 51(1), 144-151.

[27] Herman MA and Kahn BB. "Glucose transport and sensing in the maintenance of glucose homeostasis and metabolic harmony". *Journal of Clinical Investigation*, 2006, 116(7), 1767-1775.

[28] Hesse J and Gross T. "Self-organized criticality as a fundamental property of neural systems". *Frontiers in Systems Neuroscience*, 2014, 8(September), 1-14.

[29] Hovorka R, Elleri D, Thabit H, Allen JM, Leelarathna L, El-khairi R, Wilinska ME, et al. "Overnight Closed-Loop Insulin Delivery in Young People With Type 1 Diabetes : A Free-Living, Randomized Clinical Trial". 2014, 37(May), 1204-1211.

[30] Hovorka R, Shojaee-Moradie F, Carroll PV, Chassin LJ, Gowrie IJ, Jackson NC ... Jones RH. "Partitioning glucose distribution/transport, disposal, and endogenous production during IVGTT". *American Journal of Physiology. Endocrinology and Metabolism*, 2002, 282(5), E992-E1007.

[31] Ji L and Li QS, "Turing pattern formation in coupled reaction-diffusion systems: Effects of sub-environment and external influence," *Chemical Physics Letters*, 2006, vol. 424, no. 4-6, pp. 432-436.

[32] Ji L and Li QS. Li, "Effect of local feedback on Turing pattern formation," *Chemical Physics Letters*, 2004, vol. 391, no. 1-3, pp. 176-180.

[33] Jonkers FC, and Henquin JC, "Measurements of cytoplasmic $Ca2^{+}$ in islet cell clusters show that glucose rapidly recruits β-cells and gradually increases the individual cell response", *Diabetes*, 2001, vol. 50, no. 3, pp. 540-550.

[34] Kovatchev BP, Breton M, Dalla Man C, and Cobelli C, "In Silico Preclinical Trials: A Proof of Concept in Closed-Loop Control of Type 1 Diabetes". *Journal of Diabetes Science and Technology*, 2009, vol. 3, no. 1, pp. 44-55.

[35] Keizer J and Magnus G. "The ATP-sensitive potassium channel and bursting in the pancreatic b-cell". *Biophys. J.*.1989. 56:229–242

[36] Kyrychko YN, Blyuss KB, Hogan SJ, and Schöll E, "Control of spatiotemporal patterns in the Gray-Scott model". *Chaos*, 2009, vol. 19, no. 4, pp. 1-7.

[37] Kyttä K, Kaski K, and Barrio RA, "Complex turing patterns in non-linearly coupled systems". *Physica A: Statistical Mechanics and its Applications*, 2007, vol. 385, no. 1, pp. 105-114.

[38] Lecar H and Morris C. "Voltage oscillations in the barnacle giant muscle fibre". *Biophysical Journal*, 1981, 35(1), 193-213.

[39] Lee B, Song T, Lee K, Kim J, Han S, Berggren PO, ... Jo J. "Phase modulation of insulin pulses enhances glucose regulation and enables inter-islet synchronization". *PLoS ONE*, 2017 12(2), 1-15.

[40] Lenart PJ, and Parker RS. "Modeling exercise effects in type I diabetic patients". *IFAC Proceedings Volumes (IFAC-PapersOnline)*, 2002.

[41] Lengyel I and Epstein IR. "A chemical approach to designing Turing patterns in reaction-diffusion systems". *Proceedings of the National Academy of Sciences of the United States of America*, 1992, 89(9), 3977-3979.

[42] Lengyel I and Epstein IR, "Modeling of Turing structures in the chlorite–iodide–malonic Acid–starch reaction system." *Science*, 1991, vol. 251, no. 4994, pp. 650-652.

[43] Marković D, and Gros C. "Power laws and self-organized criticality in theory and nature". *Physics Reports*, 2014, 536(2), 41-74.

[44] Montani S, Magni P, Bellazzi R, Larizza C, Roudsari AV, and Carson ER. "Integrating model-based decision support in a multi-modal reasoning system for managing type 1 diabetic patients". *Artificial Intelligence in Medicine*, 2003, 29(1-2), 131-151.

[45] Mora T and Bialek W, "Are Biological Systems Poised at Criticality?". *Journal of Statistical Physics*, 2011, vol. 144, no. 2, pp. 268-302.

[46] Ni WM and Tang M. "Turing Patterns in the Lengyel-Epstein System for the Cima Reaction Author". *Transactions of the American Mathematical Society*, 2015, Vol . 357 , No . 10 (Oct, 2005), Published by: American Mathematical Society Sta. 2019, 357(10), 3953-3969.

[47] Nucci G and Cobelli C. "Models of subcutaneous insulin kinetics. A critical review." *Comput Methods Programs Biomed*, 2000, vol. 62, no. 3, pp. 249-257.

[48] olde Scheper TV. "Why metabolic systems are rarely chaotic". *BioSystems*, 2008, vol. 94, no. 1-2, pp. 145-152.

[49] olde Scheper TV. "Biologically Inspired Rate Control of Chaos". *Chaos: An Interdisciplinary Journal of Nonlinear Science*, 2017, 27(10).

[50] Oley NH, Broekhuyse HM, Nelson JD, Zinman B and Albisser AM. "Papers Comparison of Algorithms for the Closed-Loop Control of Blood Glucose Using the Artificial Beta Cell" *IEEE Transactions on Biomedical Engineering*, 1981, BME-28(10), 678-687.

[51] Pagkalos I, Herrero P, and Georgiou P, "An analogue implementation of the beta cell insulin release model". *Proceedings - IEEE International Symposium on Circuits and Systems*, 2013, pp. 2489-2492.

[52] Palumbo P, Ditlevsen S, Bertuzzi A, and De Gaetano A. "Mathematical modeling of the glucose-insulin system: A review". *Mathematical Biosciences*, 2013, 244(2), 69-81.

[53] Pedersen MG, Bertram R and Sherman A. "Intra- and Inter-Islet Synchronization of Metabolically Driven Insulin Secretion". *Biophysical Journal*, 2005, 89(1), 107-119.

[54] Pedersen MG, Corradin A, Toffolo GM, and Cobelli C, "A subcellular model of glucose-stimulated pancreatic insulin secretion". *Philosophical transactions. Series A, Mathematical, physical, and engineering sciences*, 2008, vol. 366, no. 1880, pp. 3525-43.

[55] Pedersen MG, Toffolo GM, and Cobelli C, "Cellular modeling: insight into oral minimal models of insulin secretion". *American journal of physiology. Endocrinology and metabolism*, 2010, vol. 298, no. 3, pp. E597-601.

[56] Petrov V, Metens S, Borckmans P, Dewel G and Showalter K. "Tracking unstable turing patterns through mixed-mode spatiotemporal chaos". *Physical Review Letters*, 1995, 75(15), 2895-2898.

[57] Pu Y, Lee S, Samuels DC, Watson LT and Cao Y. "The effect of unhealthy β - cells in synchronized insulin secretion". *Proceedings - 2012 IEEE International Conference on Bioinformatics and Biomedicine, BIBM 2012*, 2012, 416-419.

[58] Rajeswari AM, Sidhika MS, Kalaivani M and Deisy C. "Prediction of Pre-diabetes using Fuzzy Logic based Association Classification". *Proceedings of the International Conference on Inventive Communication and Computational Technologies, ICICCT 2018*, 2018, 782-787.

[59] Reddy M, Herrero P, El Sharkawy M, Pesl P, Jugnee N, Thomson H, ... Oliver N. "Feasibility Study of a Bio-inspired Artificial Pancreas in Adults with Type 1 Diabetes". *Diabetes Technology & Therapeutics*, 2014, 16(9), 10-17.

[60] Roy A and Parker RS. "Dynamic modeling of exercise effects on plasma glucose and insulin levels". *Journal of diabetes science and technology*, 2007, vol. 1, no. 3, pp. 338-347.

[61] R*ü*diger S, Nicola EM, Casademunt J, and Kramer L, "Theory of pattern forming systems under traveling-wave forcing". *Physics Reports*, 2007, vol. 447, no. 3-6, pp. 73-111.

[62] Saunders PT, Koeslag JH, and Wessels JA. "Integral rein control in physiology". *Journal of Theoretical Biology*, 1998, 194(2), 163-173.

[63] Simon C and Brandenberger G. "Ultradian oscillations of insulin secretion in humans". *Diabetes*,2002, vol 51, pp. 3-6.

[64] Smith JW, Everhart JE, Dickson WC, Knowler WC, and Johannes RS. "Using the ADAP Learning Algorithm to Forecast the Onset of Diabetes Mellitus". *Proceedings of the Symposium on Computer Applications and Medical Care*, 1988, 261-265.

[65] Smolen P. "A model for glycolytic oscillations based on skeletal muscle phosphofructokinase kinetics". *Journal of Theoretical Biology*. 1995. 174:137–148.

[66] Sneyd J, Han J M, Wang L, Chen J, Yang X, Tanimura A., ... Yule D I. "On the dynamical structure of calcium oscillations". *Proceedings of the National Academy of Sciences of the United States of America*, (2017) 114(7), 1456–1461.

[67] Sorensen, J.T. (1985). "A Physiologic Model of Glucose Metabolism in Man and its Use to Design and Assess Improved Insulin Therapies for Diabetes." Ph.D. Dissertation. Department of Chemical Engineering, MIT. Cambridge, Massachusets.

[68] Steil GM, Rebrin K, Darwin C, Hariri F, and Saad MF. "Feasibility of automating insulin delivery for the treatment of type 1 diabetes." *Diabetes*, 2006, vol. 55, no. 12, pp. 3344-3350.

[69] Stumpf MPH, and Porter MA. "Critical Truths About Power Laws". *Science*, 2012, 335(6069), 665-666.

[70] Tolić IM, Mosekilde E, and Sturis J. "Modeling the insulin-glucose feedback system: The significance of pulsatile insulin secretion". *Journal of Theoretical Biology*, 2000, 207(3), 361-375.

[71] Tsaneva-Atanasova K, Zimliki CL, Bertram R, and Sherman A. "Diffusion of Calcium and Metabolites in Pancreatic Islets: Killing Oscillations with a Pitchfork". *Biophysical Journal*, 2006, 90(10), 3434-3446.

[72] Toffolo G, Bergman R, Finegood D, Bowden C and Cobelli C. "Quantitative estimation of beta cell sensitivity to glucose in the intact organism: A minimal model of insulin kinetics in the dog". *Diabetes*, 1980, 29, 979-990.

[73] Visentin R, Man CD, Kudva YC, Basu A, and Cobelli C, "Circadian Variability of Insulin Sensitivity : Physiological Input for In Silico Artificial Pancreas", 2015, vol. 17, no. 1.

[74] Wang K, Steyn-Ross ML, Steyn-Ross DA, Wilson MT, Sleigh JW, and Shiraishi Y. "Simulations of pattern dynamics for reaction-diffusion systems via SIMULINK". *BMC Systems Biology*, 2014, vol. 8, no. 1, p. 45.

[75] Wilinska ME, Chassin LJ, Schaller HC, Schaupp L, Pieber TR, and Hovorka R. "Insulin kinetics in type-1 diabetes: Continuous and bolus delivery of rapid acting insulin". *IEEE Transactions on Biomedical Engineering*, 2005, 52(1), 3-12.

[76] Yao NK, Chang LW, Lin BJ, Kuo TS. "Dynamic aspects for inter-islet synchronization of oscillatory insulin secretions". *American Journal of Physiology*, 1997, 272(6 Pt 1):E981–8. PMID: 9227441 20.

Appendix A

Scripts

This appendix contains the scripts that were used to run the models of this research project. They were run on the software EuNeurone, developed by Tjeerd V. olde Scheper.

A.1 Brusselator

<Name >

Brusselator 16.C.RCC

<Description >

<Parameters >

a=1

b=2.5

Dx = 1.85

Dy = 16.66

fx=1

fy=1

scx= 3

ppx1 = 0.222

ppx2 = 0.234

ppx3 = 0.228

ppx4 = 0.24

scy= 5

ppy1 = 0.296

ppy2 = 0.312

ppy3 = 0.304

ppy4 = 0.32

toglow=1000

toghigh=20000

bcx = 0.06

bcy= 0.08

swlen = 2000

ersw=0.0001

<Equation >

st=pulse(t,toglow,toghigh)

sw = step(t,swlen,0.1)

No1 = abs(No1+sw*ersw)

No2 = abs(No2+sw*ersw)

No3 = abs(No3+sw*ersw)

```
No4 = abs(No4+sw*ersw)
qx1=x1/(x1+scx)
qy1=y1/(y1+scy)
sx1=fx*exp(st*ppx1*qx1*qy1*bcx)
sy1=fy*exp(st*ppy1*qx1*bcy)
qx2=x2/(x2+scx)
qy2=y2/(y2+scy)
sx2=fx*exp(st*ppx1*qx2*qy2*bcx)
sy2=fy*exp(st*ppy1*qx2*bcy)
qx3=x3/(x3+scx)
qy3=y3/(y3+scy)
sx3=fx*exp(st*ppx1*qx3*qy3*bcx)
sy3=fy*exp(st*ppy1*qx3*bcy)
qx4=x4/(x4+scx)
qy4=y4/(y4+scy)
sx4=fx*exp(st*ppx1*qx4*qy4*bcx)
sy4=fy*exp(st*ppy1*qx4*bcy)
qx5=x5/(x5+scx)
qy5=y5/(y5+scy)
sx5=fx*exp(st*ppx2*qx5*qy5*bcx)
sy5=fy*exp(st*ppy2*qx5*bcy)
qx6=x6/(x6+scx)
qy6=y6/(y6+scy)
sx6=fx*exp(st*ppx2*qx6*qy6*bcx)
sy6=fy*exp(st*ppy2*qx6*bcy)
qx7=x7/(x7+scx)
qy7=y7/(y7+scy)
sx7=fx*exp(st*ppx2*qx7*qy7*bcx)
sy7=fy*exp(st*ppy2*qx7*bcy)
```

```
qx8=x8/(x8+scx)
qy8=y8/(y8+scy)
sx8=fx*exp(st*ppx2*qx8*qy8*bcx)
sy8=fy*exp(st*ppy2*qx8*bcy)
qx9=x9/(x9+scx)
qy9=y9/(y9+scy)
sx9=fx*exp(st*ppx3*qx9*qy9*bcx)
sy9=fy*exp(st*ppy3*qx9*bcy)
qx10=x10/(x10+scx)
qy10=y10/(y10+scy)
sx10=fx*exp(st*ppx3*qx10*qy10*bcx)
sy10=fy*exp(st*ppy3*qx10*bcy)
qx11=x11/(x11+scx)
qy11=y11/(y11+scy)
sx11=fx*exp(st*ppx3*qx11*qy11*bcx)
sy11=fy*exp(st*ppy3*qx11*bcy)
qx12=x12/(x12+scx)
qy12=y12/(y12+scy)
sx12=fx*exp(st*ppx3*qx12*qy12*bcx)
sy12=fy*exp(st*ppy3*qx12*bcy)
qx13=x13/(x13+scx)
qy13=y13/(y13+scy)
sx13=fx*exp(st*ppx4*qx13*qy13*bcx)
sy13=fy*exp(st*ppy4*qx13*bcy)
qx14=x14/(x14+scx)
qy14=y14/(y14+scy)
sx14=fx*exp(st*ppx4*qx14*qy14*bcx)
sy14=fy*exp(st*ppy4*qx14*bcy)
qx15=x15/(x15+scx)
```

qy15=y15/(y15+scy)

sx15=fx*exp(st*ppx4*qx15*qy15*bcx)

sy15=fy*exp(st*ppy4*qx15*bcy)

qx16=x16/(x16+scx)

qy16=y16/(y16+scy)

sx16=fx*exp(st*ppx4*qx16*qy16*bcx)

sy16=fy*exp(st*ppy4*qx16*bcy)

xtotal=x1+x2+x3+x4+x5+x6+x7+x8+x9+x10+x11+x12+x13+x14+x15+x16

ytotal=y1+y2+y3+y4+y5+y6+y7+y8+y9+y10+y11+y12+y13+y14+y15+y16

x1' = Dx * (No1 * (x16-x1) + No1 * (x2-x1)) + a - (b+1) * x1 + sx1 * (x1^2) * y1 + (No1*x16*x1) * (x16-x1)

y1' = Dy * (No1 * (y16-y1) + No1 * (y2-y1)) + sy1 * (b * x1) - x1^2 * y1 + (No1 * y16 * y1) * (y16 - y1)

x2' = Dx * (No1 * (x1-x2) + No1 * (x3-x2)) + a - (b+1) * x2 + sx2 * (x2^2) * y2 + (No1*x1*x2) * (x1-x2)

y2' = Dy * (No1 * (y1-y2) + No1 * (y3-y2)) + sy2 * (b * x2) - x2^2 * y2 + (No1*y1*y2) * (y1-y2)

x3' = Dx * (No1 * (x2-x3) + No1 * (x4-x3)) + a - (b+1) * x3 + sx3 * (x3^2) * y3 + (No1*x2*x3) * (x2-x3)

y3' = Dy * (No1 * (y2-y3) + No1 * (y4-y3)) + sy3 * (b * x3) - x3^2 * y3 + (No1*y2*y3) * (y2 - y3)

x4' = Dx * (No1 * (x3-x4) + No1 * (x5-x4)) + a - (b+1) * x4 + sx4 * (x4^2) * y4 + (No1*x3*x4) * (x3-x4)

y4' = Dy * (No1 * (y3-y4) + No1 * (y5-y4)) + sy4 * (b * x4) - x4^2 * y4 + (No1*y3*y4) * (y3-y4)

x5' = Dx * (No2 * (x4-x5) + No2 * (x6-x5)) + a - (b+1) * x5 + sx5 * (x5^2) * y5 + (No2*x4*x5) * (x4-x5)

y5' = Dy * (No2 * (y4-y5) + No2 * (y6-y5)) + sy5 * (b * x5) - x5^2 * y5 + (No2*y4*y5) * (y4 - y5)

x6' = Dx * (No2 * (x5-x6) + No2 * (x7-x6)) + a - (b+1) * x6 + sx6 * (x6^2) * y6 + (No2*x5*x6) * (x5-x6)

y6' = Dy * (No2 * (y5-y6) + No2 * (y7-y6)) + sy6 * (b * x6) - x6^2 * y6 + (No2*y5*y6) * (y5 - y6)

x7' = Dx * (No2 * (x6-x7) + No2 * (x8-x7)) + a - (b+1) * x7 + sx7 * (x7^2) * y7 + (No2*x6*x7) * (x6*x7)

y7' = Dy * (No2 * (y6-y7) + No2 * (y8-y7)) + sy7 * (b * x7) - x7^2 * y7 + (No2*y6*y7) * (y6 - y7)

x8' = Dx * (No2 * (x7-x8) + No2 * (x9-x8)) + a - (b+1) * x8 + sx8 * (x8^2) * y8 + (No2*x7*x8) * (x7-x8)

y8' = Dy * (No2 * (y7-y8) + No2 * (y9-y8)) + sy8 * (b * x8) - x8^2 * y8 + (No2*y7*y8) * (y7 - y8)

x9' = Dx * (No3 * (x8-x9) + No3 * (x10-x9)) + a - (b+1) * x9 + sx9 * (x9^2) * y9 + (No3*x8*x9) * (x8-x9)

y9' = Dy * (No3 * (y8-y9) + No3 * (y10-y9)) + sy9 * (b * x9) - x9^2 * y9 + (No3*y8*y9) * (y8 - y9)

x10' = Dx * (No3 * (x9-x10) + No3 * (x11-x10)) + a - (b+1) * x10 + sx10 * (x10^2) * y10 + (No3*x9*x10) * (x9-x10)

y10' = Dy * (No3 * (y9-y10) + No3 * (y11-y10)) + sy10 * (b * x10) - x10^2 * y10 + (No3*y9*y10) * (y9-y10)

x11' = Dx * (No3 * (x10-x11) + No3 * (x12-x11)) + a - (b+1) * x11 + sx11 * (x11^2) * y11 + (No3*x10*x11) * (x10-x11)

y11' = Dy * (No3 * (y10-y11) + No3 * (y12-y11)) + sy11 * (b * x11) - x11^2 * y11 + (No3*y10*y11) * (y10 - y11)

x12' = Dx * (No3 * (x11-x12) + No3 * (x13-x12)) + a - (b+1) * x12 + sx12 * (x12^2) * y12 + (No3*x11*x12) * (x11-x12)

y12' = Dy * (No3 * (y11-y12) + No3 * (y13-y12)) + sy12 * (b * x12) - x12^2 * y12 + (No3*y11*y12) * (y11 - y12)

x13' = Dx * (No4 * (x12-x13) + No4 * (x14-x13)) + a - (b+1) * x13 + sx13 * (x13^2) * y13

+ (No4*x12*x13) * (x12-x13)

y13' = Dy * (No4 * (y12-y13) + No4 * (y14-y13)) + sy13 * (b * x13) - x13^2 * y13 + (No4*y12*y13) * (y12 - y13)

x14' = Dx * (No4 * (x13-x14) + No4 * (x15-x14)) + a - (b+1) * x14 + sx14 * (x14^2) * y14 + (No4*x13*x14) * (x13-x14)

y14' = Dy * (No4 * (y13-y14) + No4 * (y15-y14)) + sy14 * (b * x14) - x14^2 * y14 + (No4*y13*y14) * (y13 - y14)

x15' = Dx * (No4 * (x14-x15) + No4 * (x16-x15)) + a - (b+1) * x15 + sx15*(x15^2)*y15 + (No4*x14*x15)*(x14-x15)

y15' = Dy * (No4 * (y14-y15) + No4 * (y16-y15)) + sy15 * (b * x15) - x15^2 * y15 + (No4*y14*y15) * (y14 - y15)

x16' = Dx * (No4 * (x15-x16) + No4 * (x1-x16)) + a - (b+1) * x16 + sx16 * (x16^2) * y16 + (No4*x15*x16) * (x15-x16)

y16' = Dy * (No4 * (y15-y16) + No4 * (y1-y16)) + sy16 * (b * x16) - x16^2 * y16 + (No4*y15*y16) * (y15 - y16)

t' = 1

<Initial >

x1 = 1

y1 = 2

x2 = 0.5

y2 = 5

x3 = 1

y3 = 1

x4 = 0.1

y4 = 0.01

x5 = 1

y5 = 2

x6 = 0.5

y6 = 5

x7 = 1

y7 = 1

x8 = 0.1

y8 = 0.01

x9 = 1

y9 = 2

x10 = 0.5

y10 = 5

x11 = 1

y11 = 1

x12 = 0.1

y12 = 0.01

x13 = 1

y13 = 2

x14 = 0.5

y14 = 5

x15 = 1

y15 = 1

x16 = 0.1

y16 = 0.01

xtotal = 1

ytotal = 1

sx1=1

sy1=1

sx2=1

sy2=1

sx3=1

sy3=1

sx4=1

sy4=1

sx5=1

sy5=1

sx6=1

sy6=1

sx7=1

sy7=1

sx8=1

sy8=1

sx9=1

sy9=1

sx10=1

sy10=1

sx11=1

sy11=1

sx12=1

sy12=1

sx13=1

sy13=1

sx14=1

sy14=1

sx15=1

sy15=1

sx16=1

sy16=1

st=0

sw=0

No1=0.01

No2=0.0001

No3=0.001

No4=0.00001

t = 0

<Options >

Integrator=Runge-Kutta

Step=0.1

Duration=20000

Output=3000

Graph=Evolution,xtotal,ytotal

Graph=xtotal,ytotal

Logfile=brusselator.1.4.log

A.2 Lengyel-Epstein

A.2.1 Coupling Tests

<Name >

Lengyel-Epstein model <Description >

<Parameters >

a1 = 21

a2 = 16

a3 = 20

a4 = 15

b1=1.3375

b2=1.3475

b3=1.3375

b4=1.3475

sigma=8

d1 = 0.005

d2 = 0.005

d3 = 0.05

d4 = 0.05

d5 = 0.5

d6 = 0.5

d7 = 0.0005

d8 = 0.0005

scu = 6

ppv = 1.5

toglow=50

toghigh=50

fv=1.5

adu=0

<Equation >

```
tog=pulse(t,toglow,toghigh)


utotal=u1+u2+u3+u4+u5+u6+u7+u8+u9+u10+u11+u12+u13+u14+u15+u16
vtotal=v1+v2+v3+v4+v5+v6+v7+v8+v9+v10+v11+v12+v13+v14+v15+v16


qu1=u1/(u1+scu)
sv1=fv*exp(ppv*qu1)
qu2=u2/(u2+scu)
sv2=fv*exp(ppv*qu2)
qu3=u3/(u3+scu)
sv3=fv*exp(ppv*qu3)
qu4=u4/(u4+scu)
sv4=fv*exp(ppv*qu4)
qu5=u5/(u5+scu)
sv5=fv*exp(ppv*qu5)
qu6=u6/(u6+scu)
sv6=fv*exp(ppv*qu6)
qu7=u7/(u7+scu)
sv7=fv*exp(ppv*qu7)
qu8=u8/(u8+scu)
sv8=fv*exp(ppv*qu8)
qu9=u9/(u9+scu)
sv9=fv*exp(ppv*qu9)
qu10=u10/(u10+scu)
sv10=fv*exp(ppv*qu10)
qu11=u11/(u11+scu)
sv11=fv*exp(ppv*qu11)
qu12=u12/(u12+scu)
sv12=fv*exp(ppv*qu12)
```

qu13=u13/(u13+scu)

sv13=fv*exp(ppv*qu13)

qu14=u14/(u14+scu)

sv14=fv*exp(ppv*qu14)

qu15=u15/(u15+scu)

sv15=fv*exp(ppv*qu15)

qu16=u16/(u16+scu)

sv16=fv*exp(ppv*qu16)

u1' = a1-u1-4*(u1*v1)/(1+u1^2) + d1*(u16-u1)

v1' = sigma*b1*(u1-(u1*v1)/(1+u1^2)) +d2*(v16-v1)

u2' = a1-u2-4*(u2*v2)/(1+u2^2) + d1*(u1-u2)

v2' = sigma*b1*(u2-(u2*v2)/(1+u2^2)) + d2*(v1-v2)

u3' = a1-u3-4*(u3*v3)/(1+u3^2) + d1*(u2-u3)

v3' = sigma*b1*(u3-(u3*v3)/(1+u3^2)) +d2*(v2-v3)

u4' = a1-u4-4*(u4*v4)/(1+u4^2) + d1*(u3-u4)

v4' = sigma*b1*(u4-(u4*v4)/(1+u4^2)) + d2*(v3-v4)

u5' = a2-u5-4*(u5*v5)/(1+u5^2) + d3*(u4-u5)

v5' = sigma*b2*(u5-(u5*v5)/(1+u5^2)) +d4*(v4-v5)

u6' = a2-u6-4*(u6*v6)/(1+u6^2) + d3*(u5-u6)

v6' = sigma*b2*(u6-(u6*v6)/(1+u6^2)) + d4*(v5-v6)

u7' = a2-u7-4*(u7*v7)/(1+u7^2) + d3*(u6-u7)

v7' = sigma*b2*(u7-(u7*v7)/(1+u7^2)) +d4*(v6-v7)

u8' = a2-u8-4*(u8*v8)/(1+u8^2) + d3*(u7-u8)

v8' = sigma*b2*(u8-(u8*v8)/(1+u8^2)) + d4*(v7-v8)

u9' = a3-u9-4*(u9*v9)/(1+u9^2) + d5*(u8-u9)

v9' = sigma*b3*(u9-(u9*v9)/(1+u9^2)) +d6*(v8-v9)

u10' = a3-u10-4*(u10*v10)/(1+u10^2) + d5*(u9-u10)

v10' = sigma*b3*(u10-(u10*v10)/(1+u10^2)) + d6*(v9-v10)

u11' = a3-u11-4*(u11*v11)/(1+u11^2) + d5*(u10-u11)

v11' = sigma*b3*(u11-(u11*v11)/(1+u11^2)) +d6*(v10-v11)

u12' = a3-u12-4*(u12*v12)/(1+u12^2) + d5*(u11-u12)

v12' = sigma*b3*(u12-(u12*v12)/(1+u12^2)) + d6*(v11-v12)

u13' = a4-u13-4*(u13*v13)/(1+u13^2) + d7*(u12-u13)

v13' = sigma*b4*(u13-(u13*v13)/(1+u13^2)) +d8*(v12-v13)

u14' = a4-u14-4*(u14*v14)/(1+u14^2) + d7*(u13-u14)

v14' = sigma*b4*(u14-(u14*v14)/(1+u14^2)) + d8*(v13-v14)

u15' = a4-u15-4*(u15*v15)/(1+u15^2) + d7*(u14-u15)

v15' = sigma*b4*(u15-(u15*v15)/(1+u15^2)) +d8*(v14-v15)

u16' = a4-u16-4*(u16*v16)/(1+u16^2) + d7*(u15-u16)

v16' = sigma*b4*(u16-(u16*v16)/(1+u16^2)) + d8*(v15-v16)

t' = 1

<Initial>

u1 = 3.3

v1 = 10.5

u2 = 2

v2 = 5

u3 = 3.3

v3 = 5

u4 = 3.8

v4 = 16.8

u5 = 3.3

v5 = 10.5

u6 = 2

v6 = 5

u7 = 3.3

v7 = 5

u8 = 3.8

v8 = 16.8

u9 = 3.3

v9 = 10.5

u10= 2

v10= 5

u11= 3.3

v11= 5

u12= 3.8

v12= 16.8

u13= 3.3

v13= 10.5

u14= 2

v14= 5

u15= 3.3

v15= 5

u16= 3.8

v16= 16.8

utotal=1

vtotal=1

sv1=1

sv2=1

sv3=1

sv4=1

t=0

<Options>

Integrator=Fehlberg-RK

Step=0.1

Duration=99

Output=3000

Graph=Evolution,u1,u5,u9,u13

Graph=utotal,vtotal

Graph=u1,v1

Graph=u5,v5

Graph=u9,v9

Graph=u13,v13

Logfile=lengepstein.1.16.log

A.2.2 Control Tests

<Name>

Lengyel-Epstein model <Description >

<Parameters >

a1=50

a2=33

a3=50

a4=33

b=2.5

sigma=8

du1 = 0.00007

dv1 = 0.00007

du2 = 0.0005

dv2 = 0.0005

du3 = 0.00009

dv3 = 0.00009

du4 = 0.0003

dv4 = 0.0003

phi1 = 5

phi2 = 5

phi3 = 5

phi4 = 5

D1 = 1.2

D2 = 1.2

D3 = 1.2

D4 = 1.2

scu1 = 8

scu2 = 16

scu3 = 8

scu4 = 16

scu5 = 8

scu6 = 16

scu7 = 8

scu8 = 16

scu9 = 8

scu10 = 16

scu11 = 8

scu12 = 16

scu13 = 8

scu14 = 16

scu15 = 8

scu16 = 16

ppv1 = -0.6

ppv2 = -0.6

ppv3 = -0.6

ppv4 = -0.6

toglow=100

toghigh=4000

bv= 1.9

fv=1

adu=0

swlen=1000

ersw=0.001

<Equation>

tog=pulse(t,toglow,toghigh)

st = step(t,swlen,0.1)

No1 = No1-st*ersw

No2 = No2-st*ersw

No3 = No3-st*ersw

No4 = No4-st*ersw

utotal=u1+u2+u3+u4+u5+u6+u7+u8+u9+u10+u11+u12+u13+u14+u15+u16

vtotal=v1+v2+v3+v4+v5+v6+v7+v8+v9+v10+v11+v12+v13+v14+v15+v16

qu1=u1/(u1+scu1)

sv1=fv*exp(tog*ppv1*(qu1+bv))

qu2=u2/(u2+scu2)

sv2=fv*exp(tog*ppv1*(qu2+bv))

qu3=u3/(u3+scu3)

sv3=fv*exp(tog*ppv1*(qu3+bv))

qu4=u4/(u4+scu4)

sv4=fv*exp(tog*ppv1*(qu4+bv))

qu5=u5/(u5+scu5)

sv5=fv*exp(tog*ppv2*(qu5+bv))

qu6=u6/(u6+scu6)

sv6=fv*exp(tog*ppv2*(qu6+bv))

qu7=u7/(u7+scu7)

sv7=fv*exp(tog*ppv2*(qu7+bv))

qu8=u8/(u8+scu8)

sv8=fv*exp(tog*ppv2*(qu8+bv))

qu9=u9/(u9+scu9)

sv9=fv*exp(tog*ppv3*(qu9+bv))

qu10=u10/(u10+scu10)

sv10=fv*exp(tog*ppv3*(qu10+bv))

qu11=u11/(u11+scu11)

sv11=fv*exp(tog*ppv3*(qu11+bv))

qu12=u12/(u12+scu12)

sv12=fv*exp(tog*ppv3*(qu12+bv))

qu13=u13/(u13+scu13)

sv13=fv*exp(tog*ppv4*(qu13+bv))

qu14=u14/(u14+scu14)

sv14=fv*exp(tog*ppv4*(qu14+bv))

qu15=u15/(u15+scu15)

sv15=fv*exp(tog*ppv4*(qu15+bv))

qu16=u16/(u16+scu16)

sv16=fv*exp(tog*ppv4*(qu16+bv))

u1' = a1-u1-4*((u1*v1)/(1+u1^2)) - phi1 + (No1*(u16-u1)+No1*(u2-u1)) + No1*(u16 - u1)

v1' = sigma * (b*(sv1*u1-((u1*v1) / (1+u1^2)) + phi1) + D1 * (No1 * (v16-v1) + No1*(v2-v1)) + No1 * (v16-v1))

u2' = a1-u2-4*((u2*v2)/(1+u2^2)) - phi2 + (No1*(u1-u2)+No1*(u3-u2)) + No1*(u1-u2)

v2' = sigma * (b*(sv2*u2-((u2*v2) / (1+u2^2)) + phi2) + D2 * (No1 * (v1-v2) + No1*(v3-v2)) + No1 * (v1-v2))

u3' = a1-u3-4*((u3*v3)/(1+u3^2)) -phi3 + (No1*(u2-u3)+No1*(u4-u3)) + No1*(u2 - u3)

v3' = sigma * (b*(sv3*u3-((u3*v3) / (1+u3^2)) + phi3) + D3 * (No1 * (v2-v3) + No1*(v4-v3)) + No1 * (v2-v3))

u4' = a1-u4-4*((u4*v4)/(1+u4^2)) - phi4 + (No1*(u3-u4)+No1*(u5-u4))+ No1*(u3-u4)

v4' = sigma * (b*(sv4*u4-((u4*v4) / (1+u4^2)) + phi4) + D4 * (No1*(v3-v4) + No1 * (v5-v4)) + No1 * (v3-v4))

u5' = a2-u5-4*((u5*v5)/(1+u5^2)) - phi1 + (No2*(u4-u5)+No2*(u6-u5)) + No2*(u4 - u5)

v5' = sigma * (b*(sv5*u5-((u5*v5) / (1+u5^2)) + phi1) + D1 * (No2*(v4-v5) + No2*(v6-v5)) + No2 * (v4-v5))

u6' = a2-u6-4*((u6*v6)/(1+u6^2)) - phi2 + (No2*(u5-u6)+No2*(u7-u6)) + No2*(u5-u6)

v6' = sigma * (b*(sv6*u6-((u6*v6) / (1+u6^2)) + phi2) + D2 * (No2*(v5-v6) + No2*(v7-v6)) + No2 * (v5-v6))

u7' = a2-u7-4*((u7*v7)/(1+u7^2)) -phi3 + (No2*(u6-u7)+No2*(u8-u7)) + No2*(u6 - u7)

v7' = sigma * (b*(sv7*u7-((u7*v7) / (1+u7^2)) + phi3) + D3 * (No2*(v6-v7) + No2*(v8-v7)) + No2 * (v6-v7))

u8' = a2-u8-4*((u8*v8)/(1+u8^2)) - phi4 + (No2*(u7-u8)+No2*(u9-u8))+ No2*(u7-u8)

v8' = sigma * (b*(sv8*u8-((u8*v8) / (1+u8^2)) + phi4) + D4 * (No2*(v7-v8) + No2*(v9-v8)) + No2 * (v7-v8))

u9' = a3-u9-4*((u9*v9)/(1+u9^2)) - phi1 + (No3*(u8-u9)+No3*(u10-u9)) + No3*(u8 - u9)

v9' = sigma * (b*(sv9*u9-((u9*v9) / (1+u9^2)) + phi1) + D1 * (No3*(v8-v9) + No3*(v10-v9)) + No3 * (v8-v9))

u10' = a3-u10-4*((u10*v10)/(1+u10^2)) - phi2 + (No3*(u9-u10)+No3*(u11-u10)) + No3*(u9-u10)

v10' = sigma * (b*(sv10*u10-((u10*v10) / (1+u10^2)) + phi2) + D2 * (No3*(v9-v10) + No3*(v11-v10)) + No3 * (v9-v10))

u11' = a3-u11-4*((u11*v11)/(1+u11^2)) -phi3 + (No3*(u10-u11)+No3*(u12-u11)) + No3*(u10 - u11)

v11' = sigma * (b*(sv11*u11-((u11*v11) / (1+u11^2)) + phi3) + D3 * (No3*(v10-v11) + No3*(v12-v11)) + No3 * (v10-v11))

u12' = a3-u12-4*((u12*v12)/(1+u12^2)) - phi4 + (No3*(u11-u12)+No3*(u13-u12))+ No3*(u11-u12)

v12' = sigma * (b*(sv12*u12-((u12*v12) / (1+u12^2)) + phi4) + D4 * (No3*(v11-v12) + No3*(v13-v12)) + No3 * (v11-v12))

u13' = a4-u13-4*((u13*v13)/(1+u13^2)) - phi1 + (No4*(u12-u13)+No4*(u14-u13)) + No4*(u12 - u13)

v13' = sigma * (b*(sv13*u13-((u13*v13) / (1+u13^2)) + phi1) + D1 * (No4*(v12-v13) + No4*(v14-v13)) + No4 * (v12-v13))

u14' = a4-u14-4*((u14*v14)/(1+u14^2)) - phi2 + (No4*(u13-u14)+No4*(u15-u14)) + No4*(u13-

u14)

v14' = sigma * (b*(sv14*u14-((u14*v14) / (1+u14^2)) + phi2) + D2 * (No4*(v13-v14) + No4*(v15-v14)) + No4 * (v13-v14))

u15' = a4-u15-4*((u15*v15)/(1+u15^2)) -phi3 + (No4*(u14-u15)+No4*(u16-u15)) + No4*(u14 - u15)

v15' = sigma * (b*(sv15*u15-((u15*v15) / (1+u15^2)) + phi3) + D3 * (No4*(v14-v15) + No4*(v16-v15)) + No4 * (v14-v15))

u16' = a4-u16-4*((u16*v16)/(1+u16^2)) - phi4 + (No4*(u15-u16)+No4*(u1-u16))+ No4*(u15-u16)

v16' = sigma * (b*(sv16*u16-((u16*v16) / (1+u16^2)) + phi4) + D4 * (No4*(v15-v16) + No4*(v1-v16)) + No4 * (v15-v16))

t' = 1

<Initial>

u1 = 3.8

v1 = 15.44

u2 = 2

v2 = 5

u3 = 3.8

v3 = 15.44

u4 = 2

v4 = 5

u5 = 3.8

v5 = 15.44

u6 = 2

v6 = 5

u7 = 3.8

v7 = 15.44

u8 = 2

v8 = 5

u9 = 3.8

v9 = 15.44

u10 = 2

v10 = 5

u11 = 3.8

v11 = 15.44

u12 = 2

v12 = 5

u13 = 3.8

v13 = 15.44

u14 = 2

v14 = 5

u15 = 3.8

v15 = 15.44

u16 = 2

v16 = 5

utotal=1

vtotal=1

sv1=1

sv2=1

sv3=1

sv4=1

sv5=1

sv6=1

sv7=1

sv8=1

sv9=1

sv10=1

sv11=1

sv12=1

sv13=1

sv14=1

sv15=1

sv16=1

No1 = 0.05

No2 = 0.0005

No3 = 0.005

No4 = 0.00005

t=0

st=0

<Options>

Integrator=Runge-Kutta

Step=0.1

Duration=4000

Output=3000

Graph=Evolution,u1,u2,u3,u4

Graph=Evolution,v1,v2,v3,v4

Graph=u1,v1

Graph=u2,v2

Graph=Evolution,utotal

Graph=Evolution,sv1,sv2,sv3,sv4

Graph=Evolution,No1,No2,No3,No4

Graph=utotal,vtotal

Graph=Evolution,st

Logfile=lengepstein.1.2.log

A.3 Berry Model

<Name >

Berry4.12newb.eq <Description >

<Parameters >

Kg=0.1

Kd=1.1

kg=0.05

kd=0.05

ka=0.0455

Kr=4.5

Ks=1

alpha=0.026

beta1=0.00075

beta2=0.0007640

beta3=0.000747

beta4=0.0007593

n=4

l=4

scm=20

scf=2

ppp1=-3

ppp2=-3

ppp3=-3

ppp4=-3

ppp5=-3

ppp6=-3

ppp7=-3

ppp8=-3

ppp9=-3

ppp10=-3

ppp11=-3

ppp12=-3

ppp13=-3

ppp14=-3

ppp15=-3

ppp16=-3

fp=1

adp=0

ppg1=-3

ppg2=-3

ppg3=-3

ppg4=-3

ppg5=-3

ppg6=-3

ppg7=-3

ppg8=-3

ppg9=-3

ppg10=-3

ppg11=-3

ppg12=-3

ppg13=-3

ppg14=-3

ppg15=-3

ppg16=-3

fg=1

adg=0

swlen=200000

ersw=0.00001

ersc=10

rlow=-1

rhigh=1

stscalar=0.000001

toglow=2000

toghigh=1

<Equation>

st=pulse(t,toglow,toghigh)

sw=step(t,swlen,0.05)

Erim1=abs(Erim1+st*ersc*random(rlow,rhigh))

Erim2=abs(Erim2+st*ersc*random(rlow,rhigh))

Erim3=abs(Erim3+st*ersc*random(rlow,rhigh))

Erim4=abs(Erim4+st*ersc*random(rlow,rhigh))

```
Erim5=abs(Erim5+st*ersc*random(rlow,rhigh))
Erim6=abs(Erim6+st*ersc*random(rlow,rhigh))
Erim7=abs(Erim7+st*ersc*random(rlow,rhigh))
Erim8=abs(Erim8+st*ersc*random(rlow,rhigh))
Erim9=abs(Erim9+st*ersc*random(rlow,rhigh))
Erim10=abs(Erim10+st*ersc*random(rlow,rhigh))
Erim11=abs(Erim11+st*ersc*random(rlow,rhigh))
Erim12=abs(Erim12+st*ersc*random(rlow,rhigh))
Erim13=abs(Erim13+st*ersc*random(rlow,rhigh))
Erim14=abs(Erim14+st*ersc*random(rlow,rhigh))
Erim15=abs(Erim15+st*ersc*random(rlow,rhigh))
Erim16=abs(Erim16+st*ersc*random(rlow,rhigh))


No1=abs(No1+sw*ersw)
No2=abs(No2+sw*ersw)
No3=abs(No3+sw*ersw)
No4=abs(No4+sw*ersw)


qf1=f1/(f1+scf)
qf2=f2/(f2+scf)
qf3=f3/(f3+scf)
qf4=f4/(f4+scf)
qf5=f5/(f5+scf)
qf6=f6/(f6+scf)
qf7=f7/(f7+scf)
qf8=f8/(f8+scf)
qf9=f9/(f9+scf)
qf10=f10/(f10+scf)
qf11=f11/(f11+scf)
```

qf12=f12/(f12+scf)

qf13=f13/(f13+scf)

qf14=f14/(f14+scf)

qf15=f15/(f15+scf)

qf16=f16/(f16+scf)

ftotal=f1+f2+f3+f4+f5+f6+f7+f8+f9+f10+f11+f12+f13+f14+f15+f16

mtotal=m1+m2+m3+m4+m5+m6+m7+m8+m9+m10+m11+m12+m13+m14+m15+m16

ErimTotal=Erim1+Erim2+Erim3+Erim4+Erim5+Erim6+Erim7+Erim8+Erim9

+Erim10+Erim11+Erim12+Erim13+Erim14+Erim15+Erim16

qpp1=qf1+adp

sp1=fp*exp(ppp1*qpp1)

qpg1=qf1+adg

sg1=fg*exp(ppg1*qpg1)

qpp2=qf2+adp

sp2=fp*exp(ppp2*qpp2)

qpg2=qf2+adg

sg2=fg*exp(ppg2*qpg2)

qpp3=qf3+adp

sp3=fp*exp(ppp3*qpp3)

qpg3=qf3+adg

sg3=fg*exp(ppg3*qpg3)

qpp4=qf4+adp

sp4=fp*exp(ppp4*qpp4)

qpg4=qf4+adg

sg4=fg*exp(ppg4*qpg4)

qpp5=qf5+adp

sp5=fp*exp(ppp5*qpp5)

```
qpg5=qf5+adg
sg5=fg*exp(ppg5*qpg5)
qpp6=qf6+adp
sp6=fp*exp(ppp6*qpp6)
qpg6=qf6+adg
sg6=fg*exp(ppg6*qpg6)
qpp7=qf7+adp
sp7=fp*exp(ppp7*qpp7)
qpg7=qf7+adg
sg7=fg*exp(ppg7*qpg7)
qpp8=qf8+adp
sp8=fp*exp(ppp8*qpp8)
qpg8=qf8+adg
sg8=fg*exp(ppg8*qpg8)
qpp9=qf9+adp
sp9=fp*exp(ppp9*qpp9)
qpg9=qf9+adg
sg9=fg*exp(ppg9*qpg9)
qpp10=qf10+adp
sp10=fp*exp(ppp10*qpp10)
qpg10=qf10+adg
sg10=fg*exp(ppg10*qpg10)
qpp11=qf11+adp
sp11=fp*exp(ppp11*qpp11)
qpg11=qf11+adg
sg11=fg*exp(ppg11*qpg11)
qpp12=qf12+adp
sp12=fp*exp(ppp12*qpp12)
qpg12=qf12+adg
```

sg12=fg*exp(ppg12*qpg12)

qpp13=qf13+adp

sp13=fp*exp(ppp13*qpp13)

qpg13=qf13+adg

sg13=fg*exp(ppg13*qpg13)

qpp14=qf14+adp

sp14=fp*exp(ppp14*qpp14)

qpg14=qf14+adg

sg14=fg*exp(ppg14*qpg14)

qpp15=qf15+adp

sp15=fp*exp(ppp15*qpp15)

qpg15=qf15+adg

sg15=fg*exp(ppg15*qpg15)

qpp16=qf16+adp

sp16=fp*exp(ppp16*qpp16)

qpg16=qf16+adg

sg16=fg*exp(ppg16*qpg16)

rim1=No1*(m2+m3+m4+m5+m6+m7+m8+m9+m10+m11+m12+m13+m14+m15+m16)
+Erim1*stscalar

rim2=No1*(m1+m3+m4+m5+m6+m7+m8+m9+m10+m11+m12+m13+m14+m15+m16)
+Erim2*stscalar

rim3=No1*(m1+m2+m4+m5+m6+m7+m8+m9+m10+m11+m12+m13+m14+m15+m16)
+Erim3*stscalar

rim4=No1*(m1+m2+m3+m5+m6+m7+m8+m9+m10+m11+m12+m13+m14+m15+m16)
+Erim4*stscalar

rim5=No2*(m1+m2+m3+m4+m6+m7+m8+m9+m10+m11+m12+m13+m14+m15+m16)
+Erim5*stscalar

rim6=No2*(m1+m2+m3+m4+m5+m7+m8+m9+m10+m11+m12+m13+m14+m15+m16)

```
+Erim6*stscalar
rim7=No2*(m1+m2+m3+m4+m5+m6+m8+m9+m10+m11+m12+m13+m14+m15+m16)
+Erim7*stscalar
rim8=No2*(m1+m2+m3+m4+m5+m6+m7+m9+m10+m11+m12+m13+m14+m15+m16)
+Erim8*stscalar
rim9=No3*(m1+m2+m3+m4+m5+m6+m7+m8+m10+m11+m12+m13+m14+m15+m16)
+Erim9*stscalar
rim10=No3*(m1+m2+m3+m4+m5+m6+m7+m8+m9+m11+m12+m13+m14+m15+m16)
+Erim10*stscalar
rim11=No3*(m1+m2+m3+m4+m5+m6+m7+m8+m9+m10+m12+m13+m14+m15+m16)
+Erim11*stscalar
rim12=No3*(m1+m2+m3+m4+m5+m6+m7+m8+m9+m10+m11+m13+m14+m15+m16)
+Erim12*stscalar
rim13=No4*(m1+m2+m3+m4+m5+m6+m7+m8+m9+m10+m11+m12+m14+m15+m16)
+Erim13*stscalar
rim14=No4*(m1+m2+m3+m4+m5+m6+m7+m8+m9+m10+m11+m12+m13+m15+m16)
+Erim14*stscalar
rim15=No4*(m1+m2+m3+m4+m5+m6+m7+m8+m9+m10+m11+m12+m13+m14+m16)
+Erim15*stscalar
rim16=No4*(m1+m2+m3+m4+m5+m6+m7+m8+m9+m10+m11+m12+m13+m14+m15)
+Erim16*stscalar


m1'=kg*(f1*g1)/(Kg+f1)-(m1*p1)/(1+m1)+rim1
f1'=-kg*(f1*g1)/(Kg+f1)+(m1*p1)/(1+m1)-(f1*p1)/(1+f1)
p1'=sp1*alpha*(f1^n)/(Kr^n+f1^n)-ka*p1^2
g1'=sg1*beta1*(f1^l)/(Ks^l+f1^l)-kd*(g1*p1)/(Kd+g1)
m2'=kg*(f2*g2)/(Kg+f2)-(m2*p2)/(1+m2)+rim2
f2'=-kg*(f2*g2)/(Kg+f2)+(m2*p2)/(1+m2)-(f2*p2)/(1+f2)
p2'=sp2*alpha*(f2^n)/(Kr^n+f2^n)-ka*p2^2
```

g2'=sg2*beta1*(f2^l)/(Ks^l+f2^l)-kd*(g2*p2)/(Kd+g2)

m3'=kg*(f3*g3)/(Kg+f3)-(m3*p3)/(1+m3)+rim3

f3'=-kg*(f3*g3)/(Kg+f3)+(m3*p3)/(1+m3)-(f3*p3)/(1+f3)

p3'=sp3*alpha*(f3^n)/(Kr^n+f3^n)-ka*p3^2

g3'=sg3*beta1*(f3^l)/(Ks^l+f3^l)-kd*(g3*p3)/(Kd+g3)

m4'=kg*(f4*g4)/(Kg+f4)-(m4*p4)/(1+m4)+rim4

f4'=-kg*(f4*g4)/(Kg+f4)+(m4*p4)/(1+m4)-(f4*p4)/(1+f4)

p4'=sp4*alpha*(f4^n)/(Kr^n+f4^n)-ka*p4^2

g4'=sg4*beta1*(f4^l)/(Ks^l+f4^l)-kd*(g4*p4)/(Kd+g4)

m5'=kg*(f5*g5)/(Kg+f5)-(m5*p5)/(1+m5)+rim5

f5'=-kg*(f5*g5)/(Kg+f5)+(m5*p5)/(1+m5)-(f5*p5)/(1+f5)

p5'=sp5*alpha*(f5^n)/(Kr^n+f5^n)-ka*p5^2

g5'=sg5*beta2*(f5^l)/(Ks^l+f5^l)-kd*(g5*p5)/(Kd+g5)

m6'=kg*(f6*g6)/(Kg+f6)-(m6*p6)/(1+m6)+rim6

f6'=-kg*(f6*g6)/(Kg+f6)+(m6*p6)/(1+m6)-(f6*p6)/(1+f6)

p6'=sp6*alpha*(f6^n)/(Kr^n+f6^n)-ka*p6^2

g6'=sg6*beta2*(f6^l)/(Ks^l+f6^l)-kd*(g6*p6)/(Kd+g6)

m7'=kg*(f7*g7)/(Kg+f7)-(m7*p7)/(1+m7)+rim7

f7'=-kg*(f7*g7)/(Kg+f7)+(m7*p7)/(1+m7)-(f7*p7)/(1+f7)

p7'=sp7*alpha*(f7^n)/(Kr^n+f7^n)-ka*p7^2

g7'=sg7*beta2*(f7^l)/(Ks^l+f7^l)-kd*(g7*p7)/(Kd+g7)

m8'=kg*(f8*g8)/(Kg+f8)-(m8*p8)/(1+m8)+rim8

f8'=-kg*(f8*g8)/(Kg+f8)+(m8*p8)/(1+m8)-(f8*p8)/(1+f8)

p8'=sp8*alpha*(f8^n)/(Kr^n+f8^n)-ka*p8^2

g8'=sg8*beta2*(f8^l)/(Ks^l+f8^l)-kd*(g8*p8)/(Kd+g8)

m9'=kg*(f9*g9)/(Kg+f9)-(m9*p9)/(1+m9)+rim9

f9'=-kg*(f9*g9)/(Kg+f9)+(m9*p9)/(1+m9)-(f9*p9)/(1+f9)

p9'=sp9*alpha*(f9^n)/(Kr^n+f9^n)-ka*p9^2

g9'=sg9*beta3*(f9^l)/(Ks^l+f9^l)-kd*(g9*p9)/(Kd+g9)

```
m10'=kg*(f10*g10)/(Kg+f10)-(m10*p10)/(1+m10)+rim10
f10'=-kg*(f10*g10)/(Kg+f10)+(m10*p10)/(1+m10)-(f10*p10)/(1+f10)
p10'=sp10*alpha*(f10^n)/(Kr^n+f10^n)-ka*p10^2
g10'=sg10*beta3*(f10^l)/(Ks^l+f10^l)-kd*(g10*p10)/(Kd+g10)
m11'=kg*(f11*g11)/(Kg+f11)-(m11*p11)/(1+m11)+rim11
f11'=-kg*(f11*g11)/(Kg+f11)+(m11*p11)/(1+m11)-(f11*p11)/(1+f11)
p11'=sp11*alpha*(f11^n)/(Kr^n+f11^n)-ka*p11^2
g11'=sg11*beta3*(f11^l)/(Ks^l+f11^l)-kd*(g11*p11)/(Kd+g11)
m12'=kg*(f12*g12)/(Kg+f12)-(m12*p12)/(1+m12)+rim12
f12'=-kg*(f12*g12)/(Kg+f12)+(m12*p12)/(1+m12)-(f12*p12)/(1+f12)
p12'=sp12*alpha*(f12^n)/(Kr^n+f12^n)-ka*p12^2
g12'=sg12*beta3*(f12^l)/(Ks^l+f12^l)-kd*(g12*p12)/(Kd+g12)
m13'=kg*(f13*g13)/(Kg+f13)-(m13*p13)/(1+m13)+rim13
f13'=-kg*(f13*g13)/(Kg+f13)+(m13*p13)/(1+m13)-(f13*p13)/(1+f13)
p13'=sp13*alpha*(f13^n)/(Kr^n+f13^n)-ka*p13^2
g13'=sg13*beta4*(f13^l)/(Ks^l+f13^l)-kd*(g13*p13)/(Kd+g13)
m14'=kg*(f14*g14)/(Kg+f14)-(m14*p14)/(1+m14)+rim14
f14'=-kg*(f14*g14)/(Kg+f14)+(m14*p14)/(1+m14)-(f14*p14)/(1+f14)
p14'=sp14*alpha*(f14^n)/(Kr^n+f14^n)-ka*p14^2
g14'=sg14*beta4*(f14^l)/(Ks^l+f14^l)-kd*(g14*p14)/(Kd+g14)
m15'=kg*(f15*g15)/(Kg+f15)-(m15*p15)/(1+m15)+rim15
f15'=-kg*(f15*g15)/(Kg+f15)+(m15*p15)/(1+m15)-(f15*p15)/(1+f15)
p15'=sp15*alpha*(f15^n)/(Kr^n+f15^n)-ka*p15^2
g15'=sg15*beta4*(f15^l)/(Ks^l+f15^l)-kd*(g15*p15)/(Kd+g15)
m16'=kg*(f16*g16)/(Kg+f16)-(m16*p16)/(1+m16)+rim16
f16'=-kg*(f16*g16)/(Kg+f16)+(m16*p16)/(1+m16)-(f16*p16)/(1+f16)
p16'=sp16*alpha*(f16^n)/(Kr^n+f16^n)-ka*p16^2
g16'=sg16*beta4*(f16^l)/(Ks^l+f16^l)-kd*(g16*p16)/(Kd+g16)
```

t'=1

<Initial>

m1=0.26

m2=0.26

m3=0.26

m4=0.26

m5=0.46

m6=0.46

m7=0.46

m8=0.46

m9=0.26

m10=0.26

m11=0.26

m12=0.26

m13=0.46

m14=0.46

m15=0.46

m16=0.46

mtotal=1

f1=0.465

f2=0.465

f3=0.465

f4=0.465

f5=0.665

f6=0.665

f7=0.665

f8=0.665

f9=0.465

f10=0.465

f11=0.465

f12=0.465

f13=0.665

f14=0.665

f15=0.665

f16=0.665

ftotal=1

p1=0.016

g1=0.127

p2=0.016

g2=0.127

p3=0.016

g3=0.127

p4=0.016

g4=0.127

p5=0.036

g5=0.327

p6=0.036

g6=0.327

p7=0.036

g7=0.327

p8=0.036

g8=0.327

p9=0.016

g9=0.127

p10=0.016

g10=0.127

p11=0.016

g11=0.127

p12=0.016

g12=0.127

p13=0.036

g13=0.327

p14=0.036

g14=0.327

p15=0.036

g15=0.327

p16=0.036

g16=0.327

qpp1=0

sp1=1

qpg1=0

sg1=1

qpp2=0

sp2=1

qpg2=0

sg2=1

qpp3=0

sp3=1

qpg3=0

sg3=1

qpp4=0

sp4=1

qpg4=0

sg4=1

qpp5=0

sp5=1

qpg5=0

sg5=1

qpp6=0

sp6=1

qpg6=0

sg6=1

qpp7=0

sp7=1

qpg7=0

sg7=1

qpp8=0

sp8=1

qpg8=0

sg8=1

qpp9=0

sp9=1

qpg9=0

sg9=1

qpp10=0

sp10=1

qpg10=0

sg10=1

qpp11=0

sp11=1

qpg11=0

sg11=1

qpp12=0

sp12=1

qpg12=0

sg12=1

qpp13=0

sp13=1

qpg13=0

sg13=1

qpp14=0

sp14=1

qpg14=0

sg14=1

qpp15=0

sp15=1

qpg15=0

sg15=1

qpp16=0

sp16=1

qpg16=0

sg16=1

st=0

sw=0

No1=0.00001

No2=0.00002

No3=0.00003

No4=0.00004

t=0

<Options>

Integrator=Fehlberg-RK

Step=0.5

Duration=1999999

Output=3000

Graph=Evolution,ErimTotal

Graph=Evolution,m5,m16

Graph=Evolution,Erim16

Graph=Evolution,No1,No2,No3,No4

Graph=Evolution,mtotal

Graph=Evolution,ftotal

Graph=ftotal,mtotal

Lyapunov=false

Statistics=false

Logfile=berry4.8.log

A.4 Gray-Scott system

<Name>

Turing pattern from Gray-Scott model

<Description>

<Parameters>

b0=1/15

k=1/40

delta=4.6

Tres1=214.5

Tres2 = 240

sca=1

scb=1

ppa=0.35

ppb=0.35

fa=1

fb=1

toglow=25000

toghigh=100000

swlen = 10000

stlen = 10000

ersw=0.01

ercw=0.2

<Equation >

tog=pulse(t,toglow,toghigh)

sw=step(t,swlen,0.1)

atotal = a1+a2+a3+a4+a5+a6+a7+a8+a9+a10+a11+a12+a13+a14+a15+a16

btotal = b1+b2+b3+b4+b5+b6+b7+b8+b9+b10+b11+b12+b13+b14+b15+b16

No1 = abs(No1+sw*ersw)

No2 = abs(No2+sw*ersw)

```
No3 = abs(No3+sw*ersw)
No4 = abs(No4+sw*ersw)


st = step(t,stlen,0.1)
cin = tog*(abs(cin+st*ercw))


qa1=a1/(a1+sca)
qb1=b1/(b1+scb)
sa1=fa*exp(cin*qa1*ppa)
sb1=fb*exp(cin*qb1*ppb)
qa2=a2/(a2+sca)
qb2=b2/(b2+scb)
sa2=fa*exp(cin*qa2*ppa)
sb2=fb*exp(cin*qb2*ppb)
qa3=a3/(a3+sca)
qb3=b3/(b3+scb)
sa3=fa*exp(cin*qa3*ppa)
sb3=fb*exp(cin*qb3*ppb)
qa4=a4/(a4+sca)
qb4=b4/(b4+scb)
sa4=fa*exp(cin*qa4*ppa)
sb4=fb*exp(cin*qb4*ppb)
qa5=a5/(a5+sca)
qb5=b5/(b5+scb)
sa5=fa*exp(cin*qa5*ppa)
sb5=fb*exp(cin*qb5*ppb)
qa6=a6/(a6+sca)
qb6=b6/(b6+scb)
sa6=fa*exp(cin*qa6*ppa)
```

```
sb6=fb*exp(cin*qb6*ppb)
qa7=a7/(a7+sca)
qb7=b7/(b7+scb)
sa7=fa*exp(cin*qa7*ppa)
sb7=fb*exp(cin*qb7*ppb)
qa8=a8/(a8+sca)
qb8=b8/(b8+scb)
sa8=fa*exp(cin*qa8*ppa)
sb8=fb*exp(cin*qb8*ppb)
qa9=a9/(a9+sca)
qb9=b9/(b9+scb)
sa9=fa*exp(cin*qa9*ppa)
sb9=fb*exp(cin*qb9*ppb)
qa10=a10/(a10+sca)
qb10=b10/(b10+scb)
sa10=fa*exp(cin*qa10*ppa)
sb10=fb*exp(cin*qb10*ppb)
qa11=a11/(a11+sca)
qb11=b11/(b11+scb)
sa11=fa*exp(cin*qa11*ppa)
sb11=fb*exp(cin*qb11*ppb)
qa12=a12/(a12+sca)
qb12=b12/(b12+scb)
sa12=fa*exp(cin*qa12*ppa)
sb12=fb*exp(cin*qb12*ppb)
qa13=a13/(a13+sca)
qb13=b13/(b13+scb)
sa13=fa*exp(cin*qa13*ppa)
sb13=fb*exp(cin*qb13*ppb)
```

qa14=a14/(a14+sca)

qb14=b14/(b14+scb)

sa14=fa*exp(cin*qa14*ppa)

sb14=fb*exp(cin*qb14*ppb)

qa15=a15/(a15+sca)

qb15=b15/(b15+scb)

sa15=fa*exp(cin*qa15*ppa)

sb15=fb*exp(cin*qb15*ppb)

qa16=a16/(a16+sca)

qb16=b16/(b16+scb)

sa16=fa*exp(cin*qa16*ppa)

sb16=fb*exp(cin*qb16*ppb)

a1'=delta*(No1*(a16-a1)+No1*(a2-a1))+sa1*(1-a1)/Tres1-a1*b1*b1

b1'=(No1*(b16-b1)+No1*(b2-b1))+sb1*(b0-b1)/Tres1+a1*b1*b1-k*b1

a2'=delta*(No1*(a1-a2)+No1*(a3-a2))+sa2*(1-a2)/Tres1-a2*b2*b2

b2'=(No1*(b1-b2)+No1*(b3-b2))+sb2*(b0-b2)/Tres1+a2*b2*b2-k*b2

a3'=delta*(No1*(a2-a3)+No1*(a4-a3))+sa3*(1-a3)/Tres1-a3*b3*b3

b3'=(No1*(b2-b3)+No1*(b4-b3))+sb3*(b0-b3)/Tres1+a3*b3*b3-k*b3

a4'=delta*(No1*(a3-a4)+No1*(a5-a4))+sa4*(1-a4)/Tres1-a4*b4*b4

b4'=(No1*(b3-b4)+No1*(b5-b4))+sb4*(b0-b4)/Tres1+a4*b4*b4-k*b4

a5'=delta*(No2*(a4-a5)+No2*(a6-a5))+sa5*(1-a5)/Tres2-a5*b5*b5

b5'=(No2*(b4-b5)+No2*(b6-b5))+sb5*(b0-b5)/Tres2+a5*b5*b5-k*b5

a6'=delta*(No2*(a5-a6)+No2*(a7-a6))+sa6*(1-a6)/Tres2-a6*b6*b6

b6'=(No2*(b5-b6)+No2*(b7-b6))+sb6*(b0-b6)/Tres2+a6*b6*b6-k*b6

a7'=delta*(No2*(a6-a7)+No2*(a8-a7))+sa7*(1-a7)/Tres2-a7*b7*b7

b7'=(No2*(b6-b7)+No2*(b8-b7))+sb7*(b0-b7)/Tres2+a7*b7*b7-k*b7

a8'=delta*(No2*(a7-a8)+No2*(a9-a8))+sa8*(1-a8)/Tres2-a8*b8*b8

b8'=(No2*(b7-b8)+No2*(b9-b8))+sb8*(b0-b8)/Tres2+a8*b8*b8-k*b8

a9'=delta*(No3*(a8-a9)+No3*(a10-a9))+sa9*(1-a9)/Tres1-a9*b9*b9

b9'=(No3*(b8-b9)+No3*(b10-b9))+sb9*(b0-b9)/Tres1+a9*b9*b9-k*b9

a10'=delta*(No3*(a9-a10)+No3*(a11-a10))+sa10*(1-a10)/Tres1-a10*b10*b10

b10'=(No3*(b9-b10)+No3*(b11-b10))+sb10*(b0-b10)/Tres1+a10*b10*b10-k*b10

a11'=delta*(No3*(a10-a11)+No3*(a12-a11))+sa11*(1-a11)/Tres1-a11*b11*b11

b11'=(No3*(b10-b11)+No3*(b12-b11))+sb11*(b0-b11)/Tres1+a11*b11*b11-k*b11

a12'=delta*(No3*(a11-a12)+No3*(a13-a12))+sa12*(1-a12)/Tres1-a12*b12*b12

b12'=(No3*(b11-b12)+No3*(b13-b12))+sb12*(b0-b12)/Tres1+a12*b12*b12-k*b12

a13'=delta*(No4*(a12-a13)+No4*(a14-a13))+sa13*(1-a13)/Tres2-a13*b13*b13

b13'=(No4*(b12-b13)+No4*(b14-b13))+sb13*(b0-b13)/Tres2+a13*b13*b13-k*b13

a14'=delta*(No4*(a13-a14)+No4*(a15-a14))+sa14*(1-a14)/Tres2-a14*b14*b14

b14'=(No4*(b13-b14)+No4*(b15-b14))+sb14*(b0-b14)/Tres2+a14*b14*b14-k*b14

a15'=delta*(No4*(a14-a15)+No4*(a16-a15))+sa15*(1-a15)/Tres2-a15*b15*b15

b15'=(No4*(b14-b15)+No4*(b16-b15))+sb15*(b0-b15)/Tres2+a15*b15*b15-k*b15

a16'=delta*(No4*(a15-a16)+No4*(a1-a16))+sa16*(1-a16)/Tres2-a16*b16*b16

b16'=(No4*(b15-b16)+No4*(b1-b16))+sb16*(b0-b16)/Tres2+a16*b16*b16-k*b16

t'=1

<Initial >

a1=0.5

b1=0.4

a2=0.6

b2=0.4

a3=0.5

b3=0.3

a4=0.7

b4=0.4

a5=0.1

b5=0.4

a6=0.5

b6=0.2

a7=0.5

b7=0.8

a8=0.9

b8=0.4

a9=0.1

b9=0.3

a10=0.5

b10=0.7

a11=0.6

b11=0.4

a12=0.5

b12=0.2

a13=0.5

b13=0.3

a14=0.1

b14=0.4

a15=0.5

b15=0.7

a16=0.9

b16=0.4

sa1=1

sa2=1

sa3=1

sa4=1

sa5=1

sa6=1

sa7=1

sa8=1

sa9=1

sa10=1

sb1=1

sb2=1

sb3=1

sb4=1

sb5=1

sb6=1

sb7=1

sb8=1

sb9=1

sb10=1

t=0

cin = 0

No1 = 0.009

No2 = 0.0007

No3 = 0.006

No4 = 0.0005

<Options>

Integrator=Fehlberg-RK

Step=0.1

Duration=100000

Output=1000

Graph = Evolution,atotal,btotal

Graph = atotal,btotal

Graph = Evolution,cin

Graph = Evolution,No1,No2,No3,No4

Lyapunov=false

Statistics=false

Logfile=petrov.3.log